

McLeish Distribution: Performance of Digital Communications over Additive White McLeish Noise (AWMN) Channels

Ferkan Yilmaz, *Member, IEEE,*

Abstract—The objective of this article is to statistically characterize and describe a more general additive noise distribution, termed as McLeish distribution, whose random nature can model different impulsive noise environments often encountered in practice and provides a robust alternative to Gaussian distribution. Accordingly, we develop circularly and elliptically symmetric multivariate McLeish distribution and introduce additive white McLeish noise (AWMN) channels. In particular, we propose novel analytical and closed-form expressions for the symbol error rate (SER) performance of coherent/non-coherent signaling using various digital modulation techniques over AWMN channels. In that context, we illustrate some novel expressions by some selected numerical examples and verify them by some well chosen computer-based simulations.

Index Terms—Additive white McLeish noise channels, Coherent/non-coherent signaling, Conditional symbol error probability, McLeish distribution, McLeish Q-function, Multivariate McLeish distribution, and non-Gaussian noise.

LIST OF ACRONYMS

ASE	Amplified Spontaneous Emission
ASK	Amplitude Shift Keying
AWGN	Additive White Gaussian Noise
AWLN	Additive White Laplacian Noise
AWMN	Additive White McLeish Noise
BER	Bit Error Rate
BDPSK	Binary Differential Phase Shift Keying
BFSK	Binary Frequency Shift Keying
BPSK	Binary Phase Shift Keying
CDMA	Code Division Multiple Access
CR	Cognitive Radio
CS	Circularly Symmetric
CSI	Channel-Side Information
C²DF	Complementary CDF
CCS	Complex and Circularly Symmetric
CDF	Cumulative Distribution Function
CES	Complex and Elliptically Symmetric
CLT	Central Limit Theorem
DPSK	Differential Phase Shift Keying
DS	Direct Sequence
DSL	Digital Subscriber Line
ES	Elliptically Symmetric

FSO	Free-Space Optical Communications
ILT	Inverse Laplace Transform
IQR	Inphase-to-Quadrature Ratio
M-ASK	M-ary Amplitude Shift Keying
M-DPSK	M-ary Differential Phase Shift Keying
M-PSK	M-ary Phase Shift Keying
M-QAM	M-ary Quadrature Amplitude Modulation
MAI	Multiple Access Interference
MAP	Maximum A Posteriori Decision
MGF	Moment-Generating Function
ML	Maximum Likelihood Decision
MUI	Multiple User Interference
MOM	Method of Moments Estimation
OOK	On-Off Keying
PDF	Probability Density Function
PLC	Power-Line Communications
PMF	Probability Mass Function
Q-function	Quantile-function
QPSK	Quadrature Phase Shift Keying
RF	Radio Frequency
SER	Symbol Error Rate
SNR	Signal-to-Noise Ratio
WSS	Wide Sense Stationary

I. INTRODUCTION

THE ADDITIVE WHITE NOISE in communication systems [1]–[4, and references therein] can be widely defined as any arbitrarily varying undesired signal that additively corrupts signal transmission over communication channels. In the last few decades, many modern techniques have been developed to address the challenges of reliable transmission over noisy communication channels. These developments consist of both information theoretical and experimental results on source/channel coding and modulation schemes. Accordingly, their performances have been evaluated and judged for various communication channels in order to bring together the information theory and practice behind the reliable transmission over noisy channels. In many noisy channels, it is widely agreed to have signal transmission corrupted additively by thermal noise, and the most significant property of the thermal noise is that it is abstracted by a complex Gaussian distribution as a result of the central limit theorem (CLT) application on the composite effect of infinitely small noise sources [3]–[6]. While the resulting Gaussian abstraction of the additive noise, which is usually called the additive Gaussian noise, provides

Paper approved by ?. ????, the Editor for ??????. Manuscript received ??????? ??, ?????, ??????? ?????????? ??, ????.

Ferkan Yilmaz is with Yildiz Technical University, Faculty of Electrical & Electronics Engineering, Department of Computer Engineering, 34220 Esenler, Istanbul, Turkey (e-mail: ferkan@yildiz.edu.tr).

This work was supported partially by Yildiz Technical University.

an insight into the underlying behavior of communication channels, it ignores some other impairments which are common in nature occurring in diverse of communication channels. For instance, rather than the thermal noise, the presence of undesirable interference signals, which arise in the form of random bursts for a short period of time, induces random fluctuations in the power of the additive noise. Such additive noise with random power fluctuations is called additive non-Gaussian noise, sometimes termed as impulsive additive noise and is of concern in many communication systems.

From the experimental point of view, there are many communication channels that exhibit additive non-Gaussian noise. In digital subscriber line (DSL) networks, the random noise-power fluctuations caused by electromagnetic interference due to physical phenomena, electrical switches and home appliances are example sources of non-Gaussian noise [7]–[10]. Power-line communications (PLC) is intrinsically the other type of communication system suffering from additive non-Gaussian noise. As such, the impulsive additive noise is inherently formed in PLC systems due to switching transients among different appliances and devices [11]–[16]. Even if signal transmission over PLC networks has been verified as a good technique, the impulsive nature of non-Gaussian noise is often observed as a hindrance for more efficient PLC-based transmission [16]–[18]. Additive non-Gaussian noise is also experienced in underwater acoustics channels, which results from interference and malicious jamming [19]–[26]. Other types of communication channels, where signal transmission is subjected to additive non-Gaussian noise, include wireless fading channels, such as urban and indoor radio channels [27]–[33], ultra-wide band communications (UWB) [34]–[36], frequency/time-hopping with jamming [37], [38], millimeter-wave (around 60 GHz or higher) radio channels [39]–[41], wireless chip-to-chip communications (WCC) [42]–[46], and wireless transmissions under strong interference conditions [35], [47]–[52]. Further, some impulsive scenarios, such as engine ignition, rotating machinery, lighting, as well as some impulsive multi-user interference and multi-path propagation, can also produce additive non-Gaussian noise in wireless channels [28], [29], [31], [53]–[57]. Impulsive effects that introduces additive non-Gaussian noise can also be found in cognitive radio (CR) [58]–[64] due to the simultaneous spectrum access under miss-detection events [65]–[68]. The miss-detection event occurs when a cognitive user fails to detect an active primary user. In this event, collisions happens and generates additive non-Gaussian noise in the signal transmission, which considerably strikes the performance of the cognitive links. In addition, the impulsive nature of the additive noise in free-space optical communications (FSO) has received much attention in recent years [69]–[71, and references therein]. An essential aspect of optical communications is the amplified spontaneous emission (ASE) noise [72], [73]. It has been experimentally shown in [74] and theoretically predicted in [75]–[78] that the ASE noise follows a non-Gaussian distribution. It is also worth mentioning that, in wireless-powered communications (WPC) [79]–[83], we typically observe that wireless power transmission causes some random fluctuations in the supply voltage of the analog parts

of wireless powered radio circuits, which arbitrarily shifts the optimum circuit operating point. Therefore, the additive noise to which the wireless-powered signal transmission typically follows a non-Gaussian distribution. Consequently, we could justly remark that additive non-Gaussian noise is supremely and widely prevalent in communication channels. It hence makes more challenging the performance evaluation of different coherent/non-coherent modulation schemes over additive non-Gaussian noise channels in order to properly design different communication technologies and protocols.

A. Non-Gaussian Noise Distributions

From the theoretical point of view, it is worth noting that the additive noise following Gaussian distribution has been shown in [84], [85] and operational justified in [86] to be the worst-case noise distribution for communication channels since minimizing the capacity of signal transmission subject to a noise variance constraint. Hence, in communication channels, the nature of additive non-Gaussian noise has impulsive effects. For an additive noise distribution, the impulsive effects can be properly characterized by its excess-Kurtosis [87], where the excess-Kurtosis for the Gaussian noise distribution is 0. A noise distribution with a positive excess-Kurtosis is identified as a non-Gaussian distribution since having a heavier tail than the Gaussian distribution. In order to accurately model the impulsive effects, many statistical noise distributions are available in literature. The so-called non-Gaussian distributions such as Bernoulli-Gaussian, Middleton Class-A, Class-B and Class-C, Laplacian, symmetric α -stable ($S\alpha S$), and generalized Gaussian distributions, each of which captures different impulsive noise effects, have attracted the interest of the research community due to their mathematical tractability that makes it possible not only to perform many performance computations explicitly but also to present closed-form results for a reliable transmission in a simple manner.

In literature, Bernoulli-Gaussian distribution has been used as an approximation of impulsive noise in communication channels [10], [88]–[93]. The distributions of Middleton Class-A, Class-B and Class-C [57] distinguishes impulsive noise according to the frequency range occupied by the impulsive effects compared to the receiver bandwidth, and has been extensively studied and utilised in the literature [94], [95]. Laplacian distribution is the other non-Gaussian distribution commonly used to model the additive impulsive noise effects in signal processing/detection and communication studies [50], [71], [96]–[105]. In addition, another popular non-Gaussian distribution, which provides a considerably accurate model for impulsive noise, is the $S\alpha S$ distribution [55], [106]–[111]. On the top of Laplacian and $S\alpha S$ distributions, the generalized Gaussian distribution is one of the most versatile non-Gaussian distributions in the literature, and it is commonly used to model noises in several digital communication systems [112]–[114]. It is worth noting that each one of the non-Gaussian noise distributions mentioned above is proposed as an alternative to the Gaussian noise distribution, but cannot be properly interpreted as a sum of a large number of small and almost independent and identically distributed

(*i.i.d.*) impulsive noise sources. From the experimental point of view, unlike Gaussian distribution, non-Gaussian distributions have heavy tail behavior modeled by positive excess-Kurtosis, which causes some statistical moments to be infinite, and hence make it impossible to fit many real-world phenomena. For instance, the variance of $S_{\alpha}S$ distribution is infinite for all $\alpha < 2$. The lack of characterizing the real-world phenomena of impulsive noise sources from Gaussian distribution to non-Gaussian distribution is the crucial weakness of the non-Gaussian noise distributions mentioned above. Within this context, McLeish has suggested in [115], [116] a non-Gaussian distribution as a robust alternative to Gaussian distribution. As such, this distribution closely resembles that of the Gaussian distribution; it is symmetric and unimodal, and it has support the whole real line. More importantly, it has all moments finite and its Kurtosis is greater than or equal to that of the Gaussian distribution. As such, these features makes this distribution useful in modelling impulsive noise phenomena with somewhat heavier tails than the Gaussian distribution. In spite of the fact that it appears physically and rationally justifiable to capture the wide range of impulsive noise effects ranging from non-Gaussian distribution to Gaussian distribution, the laws of McLeish distribution has so far not attracted the attention of researchers and practitioners working in the field of wireless communication systems.

Trending toward the design and analysis of transmissions technologies results in widely exploitation of complex Gaussian distributions to model random fluctuations in wireless radio frequency (RF) communications [1]–[4] and wireless optical communications [75]. It is often assumed and usually experimentally verified that these complex Gaussian distributions are either circularly symmetric (CS) with equal variance or elliptically symmetric (ES) with unequal variance in their real and imaginary parts. This pervasive property attracts the attention of many researchers and practitioners and leads to an active research area for reliable transmission over noisy channels. In this context, we typically reckon two dimensional signaling and hence consider a more general non-Gaussian distribution, i.e., complex CS /complex ES (CCS/CES) non-Gaussian distribution for signal transmission in which the CS and ES dependence structure known from a standard CCS/CES Gaussian distribution are desirable, but for which we strive to accurately model heavy tailed distributions. This fact motivates us to attain the CCS/CES extension of McLeish distribution. To the best of our knowledge, the CCS/CES McLeish distribution has so far not been well established for a reliable transmission over additive McLeish noise channels.

B. McLeish Noise Distribution

Suggested in [115], [116] as a robust alternative distribution to the Gaussian distribution is the generalization of Laplace distribution and therefore inherently called generalized Laplacian distribution [117]–[123]. However, in literature, generalized Gaussian distribution is also called generalized Laplacian distribution [122, Sec. 4.4.2], [124, Sec. 6], [125]–[137]. In order to avoid this confusion and in honor of D. L. McLeish for

his excellent paper [115] and his technical report [116], it has been recently named by us as McLeish distribution in [138] and by Marichev and Trott in Wolfram’s blog posts [139]. More particularly, McLeish distribution is a versatile additive noise distribution [115], [116], [138]–[140], whose statistical description is typically defined on two key observations, one of which is that the additive noise is naturally observed as the sum of numerous impulsive noise sources at low power, where each impulsive noise source is found to be properly characterized by a Laplacian distribution. The other observation is that, according to the CLT [141], the distribution of the composite additive noise certainly converges to Gaussian distribution as the limit case of that the number of impulsive noise sources infinitely increases. Therefore, McLeish distribution is found to be a noise model capturing different impulsive noise environments [140], and provides a superior fit to both Gaussian and non-Gaussian distributions [138]. Its impulsive nature is implicitly parameterized in such a more convenient and more nature-inspired manner to be transformed from Gaussian distribution into non-Gaussian distribution; especially while in comparison with those of Laplacian, $S_{\alpha}S$ and generalized Gaussian distributions. As such, different impulsive noises are of all special cases or approximations of McLeish distribution. For communication channels, the impulsive noise is one of the performance limiting factors in communication systems. In the last decade, considerable efforts have been devoted to the information-theoretic research on impulsive noise channels, as well as explicit source/channel coding and modulation schemes over impulsive noisy channels. Despite remarkable advancements in the theory of reliable signal transmission, such noisy channels are not fully understood. The problem of determining the fundamental limits of signal transmission subjected to the impulsive noise is hence more challenging but has so far not been explored using McLeish noise distribution.

C. Our Motivations and Contributions

One major concern in reliable signal transmission through communication channels is undoubtedly the additive noise. For the purpose of efficiency, reliability, and cost-effectiveness, we have to analyze and synthesize the impairments originated from the impulsive nature of the additive noise since we typically need to have almost error-free information transmission while the additive impulsive noise is common in all communication channels. Therefore, we critically need some statistical tools to mitigate the impulsive effects and some theoretical results to estimate the probability of signal transmission error. Furthermore, the other important fact is that the impulsive noise-effects causes random fluctuations in the power of the additive noise and yields heavy-tailed non-Gaussian noise distribution. While considering all available non-Gaussian distributions for a compatible analysis and synthesis of the impulsive effects, we need to use a more compact and mathematically more tractable non-Gaussian distribution in which the properties of a standard Gaussian distribution are desirable. This strong piece of evidence motivates us to introduce McLeish distribution in Section III-A as a mathematically tractable non-Gaussian distribution for modeling impulsive

additive noise in communication channels, and accordingly to present the basic statistical principles behind the laws of McLeish distribution. In particular, Dirac's distribution, Laplacian distribution, and Gaussian distribution are shown to be the special cases of the McLeish distribution. Further, any additive noise distribution or additive noise data is pointed out to be accurately approximated or modeled as a McLeish distribution using Kurtosis based on moments. Accordingly, after defining in Section III-A McLeish's quantile-function (Q-function) as a tail distribution function of the McLeish distribution, the statistical laws of McLeish distribution have been demonstrated by deriving closed-form expressions for the moments, cumulative distribution function (CDF), complementary CDF (C^2DF), and moment-generating function (MGF) and then by investigating their special cases on the purpose of analytical accuracy and completeness with the literature.

Additionally, worth mentioning that many situations arise in reliable signal transmission through communication channels, where the additive noise can be typically explored to be the sums of noise distributions. The most important ones of these situations are the diversity combining and the cooperative communications [1]–[3]. Thus, we demand some results about the statistical properties of the sums of McLeish distributions, which highly motivates us to present in Section III the laws of McLeish distribution starting with the univariate case and continuing through to the complex multivariate case. In particular, we investigate in Section III-B the distribution of the sums of independent McLeish distributions, where our contributions are summarized as the closed-form expressions for the probability density function (PDF), CDF, MGF and moments of the sums of the independent McLeish distributions, each of which is typically derived for arbitrary parameters on the purpose of statistical characterization.

Another essential point to reasonably consider is that the statistical behavior of the additive noise both in RF communications [2]–[4] and optical communications [142]–[144] is well represented by a complex Gaussian distribution whose real and imaginary parts are jointly Gaussian distribution. From this point of view and our motivation from the fact that the complex (bivariate) McLeish distribution allow for modeling non-Gaussian noise with a simple linear correlation structure known from the complex Gaussian distribution, our other contribution is to achieve the complex extensions, i.e., the CCS McLeish distribution in Section III-C and the CES McLeish distribution in Section III-D. We define McLeish's bivariate Q-function and derive the exact closed-form expressions for the PDF, CDF, MGF and moments of the CCS/CES McLeish distribution. As noted previously, the use of multi-dimensional signaling makes the multivariate extension of the non-Gaussian distributions attractive to model the additive impulsive noise in multi-dimensional communication channels. Our other motivation is therefore to achieve in Section III-E the extension of the standard McLeish distribution to vectors, and then to propose CS and ES multivariate McLeish distributions. Their joint PDF, CDF, C^2DF , MGF and moments are also among our contributions. We also treat marginal and conditional distributions of CS/ES multivariate McLeish distributed random vectors. At this point, we contribute in Section III-F

by generalizing the CS/ES multivariate McLeish distribution to the CCS/CES multivariate McLeish distribution, where our closed-form expressions for the joint PDF, CDF, C^2DF , MGF and moments are to be exercised in the following sections within the scope of analysis of detection and modulation schemes in additive white McLeish noise (AWMN) channels.

Our extensive work mentioned above definitely serves as a primary motivation for acknowledging the presence of AWMN in signal transmission. Accordingly, in Section IV, we consider signal transmission over complex vector channels. For the first time in the literature, we introduce the complex AWMN vector channels, where the complex noise vector is accurately modeled as a CCS/CES multivariate McLeish distribution due to random fluctuations in the total variance of the additive noise, thereby investigating in Section IV-A the existence of non-Gaussian noise distributions, where the coherence of the fluctuations, i.e., the uncertainty in the total variance of the additive noise vector is one of our contributions by utilizing Allan's variance. We properly classify the impulsive noise channels as *i*) constant variance, *ii*) slow variance-uncertainty, *iii*) fast variance-uncertainty. Both from theoretical view points and experimental conclusions, we provide in Section IV-B some of the most common examples (i.e., Johnson noise in Section IV-B1, and multiple access interference (MAI)/multiple user interference (MUI) in Section IV-B2, and the versatility of McLeish distribution in Section IV-B3) of our motivation for modeling the additive non-Gaussian noise existing in modern communication technologies as an additive McLeish noise.

In the literature, despite the ubiquity and apparent importance of analysing the various effects of additive impulsive noise in reliable signal transmission, only a few publications have been devoted to the bit error rate (BER)/symbol error rate (SER) performance of detection and modulation schemes over additive impulsive noise channels. In Section V, in consideration of impulsive noise effects, we present the definition of correlated complex AWMN vector channels. This motivates us to consider in Section V-A the optimum receivers (i.e., maximum a posteriori decision (MAP) and maximum likelihood decision (ML) rules) for coherent signaling over AWMN channels. Specifically, closed-form BER/SER expressions for the modulation schemes such as binary keying modulation, M-ary amplitude shift keying (M-ASK), M-ary quadrature amplitude modulation (M-QAM), and M-ary phase shift keying (M-PSK) are a few of our contributions. We are also motivated to investigate in Section V-B the BER/SER performance of non-coherent signaling over complex AWMN channels, specifically that of non-coherent orthogonal signaling in Section V-B0a and that of non-coherent differential phase shift keying (DPSK) in Section V-B0b. The exactness and numerical accuracy of all closed-form expressions derived in this article have been demonstrated either by the presence of their special cases or Monte-Carlo simulations.

D. Article Organization

The rest is organized as follows. In Section II, we introduce the notation and statistical definitions used throughout this

article. In Section III, we establish the laws of McLeish distribution starting with the univariate case and continuing through to the multivariate case either in real domains or complex domains. In Section IV, we study the variance-uncertainty of additive noise and then introduce AWMN channels with existence examples in the communication technologies. After presenting the complex AWMN vector channels in Section V, we study the BER/SER performance of modulation schemes in Section V-A for coherent signaling and in Section V-B for non-coherent signaling over AWMN channels. Finally, We finally offer some concluding results in the last section.

II. PRELIMINARIES

In this section, we introduce the notations used in this article and present some special functions and statistical definitions.

A. Notations

The following notations are used in this article. In general, scalar numbers such as integer, real and complex numbers are denoted by lowercase letters, e.g. n, x, z . Let \mathbb{N} denote the set of natural numbers, \mathbb{R} the set of real numbers. As such, \mathbb{R}_+ and \mathbb{R}_- denote the sets of positive and negative real numbers, respectively. Appropriately, the set of complex numbers, denoted by \mathbb{C} , is the plane $\mathbb{R} \times \mathbb{R} \triangleq \mathbb{R}^2$ equipped with complex addition, complex multiplication, yielding complex space. The complex conjugate of $z \triangleq (x, y) = x + jy \in \mathbb{C}$ is denoted by $z^* \triangleq (x, -y) = x - jy$, where $x, y \in \mathbb{R}$, and where $j \triangleq \sqrt{-1}$ denotes the imaginary number. Further, the inphase $x = \Re\{z\}$ and the quadrature $y = \Im\{z\}$, where $\Re\{\cdot\}$ and $\Im\{\cdot\}$ give the real part and imaginary part of a given complex number, respectively. Any non-zero complex number has a polar representation $z \triangleq |z| \exp(j\theta)$, where $\theta \triangleq \arg(z) \in [-\pi, \pi)$ is called the *argument* of z , and $|z| \triangleq d(z, 0)$ denotes the (L_2 -norm) *modulus* of z , where $d^2(\cdot, \cdot): \mathbb{C} \times \mathbb{C} \rightarrow \mathbb{R}$ denotes the Euclidean squared-distance between $z_k = x_k + jy_k \in \mathbb{C}$ and $z_\ell = x_\ell + jy_\ell \in \mathbb{C}$, defined as

$$d^2(z_k, z_\ell) \triangleq \langle z_k - z_\ell, z_k - z_\ell \rangle, \quad (1)$$

where $\langle \cdot, \cdot \rangle: \mathbb{C} \times \mathbb{C} \rightarrow \mathbb{R}$ denotes the Euclidean inner product in complex space, defined as

$$\langle z_k, z_\ell \rangle \triangleq \Re\{z_k^* z_\ell\} = \frac{1}{2} z_k^* z_\ell + \frac{1}{2} z_k z_\ell^* = x_k x_\ell + y_k y_\ell. \quad (2)$$

Further, the inphase and quadrature of any $z \in \mathbb{C}$ are given by $\Re\{z\} \triangleq \langle 1, z \rangle$, and $\Im\{z\} \triangleq \langle j, z \rangle$, respectively. Also, the modulus is given by $|z| \triangleq \sqrt{\langle z, z \rangle}$. When the inphase and quadrature numbers of a complex space are correlated by $\rho \neq 0$, the distance between $z_k = x_k + jy_k \in \mathbb{C}$ and $z_\ell = x_\ell + jy_\ell \in \mathbb{C}$ is obtained by Mahalanobis squared-distance, that is

$$d^2(z_k, z_\ell) \triangleq \langle z_k - z_\ell, z_k - z_\ell \rangle_\rho, \quad (3)$$

where $\rho \in [-1, 1]$ denotes the correlation between the inphase and quadrature numbers, and $\langle \cdot, \cdot \rangle_\rho: \mathbb{C} \times \mathbb{C} \rightarrow \mathbb{R}$ denotes the Mahalanobis inner product in complex space, defined as

$$\langle z_k, z_\ell \rangle_\rho \triangleq (x_k x_\ell + y_k y_\ell - \rho x_k y_\ell - \rho y_k x_\ell) / (1 - \rho^2), \quad (4)$$

in correlated (i.e. $\rho \neq 0$) complex space. The modulus of z is given by $|z|_\rho \triangleq \sqrt{\langle z, z \rangle_\rho}$. Setting $\rho = 0$ in (4) yields (2), i.e., $\langle z_k, z_\ell \rangle_0 = \langle z_k, z_\ell \rangle$. Thus, $|z|_0 = |z|$.

For simplicity in case of higher dimensions, column vectors are denoted by boldfaced lowercase letters, e.g. $\mathbf{z} \triangleq \mathbf{x} + j\mathbf{y} \in \mathbb{C}^m$, where $\mathbf{x} = [x_1, x_2, \dots, x_m] \in \mathbb{R}^m$ and $\mathbf{y} = [y_1, y_2, \dots, y_m] \in \mathbb{R}^m$. Similarly, matrices are also denoted by boldfaced uppercase non-italic letters, e.g. $\mathbf{Z} \triangleq \mathbf{X} + j\mathbf{Y} \in \mathbb{C}^{m \times n}$, where $\mathbf{X}, \mathbf{Y} \in \mathbb{R}^{m \times n}$. Moreover, the identity matrix of size $m \times m$ is fixedly denoted by \mathbf{I}_m , and both zero vector of size m and zero matrix of size $m \times m$ are also fixedly denoted by $\mathbf{0}_m$. Further, transpose and hermitian (conjugate) transpose are denoted by $(\cdot)^T$ and $(\cdot)^H$, respectively. $\det(\cdot)$, $(\cdot)^{-1}$ and $\text{Tr}(\cdot)$ denote the determinant, inverse and trace matrix operations, respectively. $\text{diag}(\cdot)$ yields a square diagonal matrix whose diagonal is formed from an vector. In higher dimensional space whose dimensions are correlated, the Mahalanobis squared-distance between $\mathbf{x} \in \mathbb{R}^m$ and $\mathbf{y} \in \mathbb{R}^m$ is given by

$$d^2(\mathbf{x}, \mathbf{y}) = \langle \mathbf{x} - \mathbf{y}, \mathbf{x} - \mathbf{y} \rangle_{\mathbf{P}} \quad (5)$$

with the correlation matrix $\mathbf{P} \triangleq [\rho_{jk}]_{m \times m}$, where $\rho_{jj} = 1$, $\rho_{jk} = \rho_{kj}$ and $-1 \leq \rho_{j,k} \leq 1$ for all $1 \leq j, k \leq m$. Note that \mathbf{P} must be symmetric and positive definite (i.e., $\mathbf{x}^T \mathbf{P} \mathbf{x} > 0$ for all $\mathbf{x} \in \mathbb{R}^m$). Moreover, in (5), $\langle \cdot, \cdot \rangle_{\mathbf{P}}: \mathbb{R}^m \times \mathbb{R}^m \rightarrow \mathbb{R}$ denotes the Mahalanobis inner product in higher dimensional space, and is typically defined as

$$\langle \mathbf{x}, \mathbf{y} \rangle_{\mathbf{P}} \triangleq \mathbf{x}^T \mathbf{P}^{-1} \mathbf{y}. \quad (6)$$

Herewith, the norm of \mathbf{x} , defined as $\|\mathbf{x}\|_{\mathbf{P}} \triangleq d(\mathbf{x}, \mathbf{0})$, is written as $\|\mathbf{x}\|_{\mathbf{P}} \triangleq \sqrt{\langle \mathbf{x}, \mathbf{x} \rangle_{\mathbf{P}}} = \|\mathbf{P}^{-1/2} \mathbf{x}\|$. In case of no correlation, we have $\mathbf{P} = \mathbf{I}$, and hence reduce (6) to the well-known Euclidean inner product in higher dimensional space, that is

$$\langle \mathbf{x}, \mathbf{y} \rangle \triangleq \mathbf{x}^T \mathbf{y}, \quad (7)$$

and the norm of \mathbf{x} to $\|\mathbf{x}\| \triangleq \sqrt{\langle \mathbf{x}, \mathbf{x} \rangle}$. In multi-dimensional complex spaces, similar notations also exist but treat Hermitian instead of transpose operation. For example, for $\mathbf{z}, \mathbf{w} \in \mathbb{C}^m$ and $\mathbf{\Sigma} \in \mathbb{C}^{m \times m}$, we have

$$\langle \mathbf{z}, \mathbf{w} \rangle_{\mathbf{\Sigma}} \triangleq \mathbf{z}^H \mathbf{\Sigma}^{-1} \mathbf{w}, \quad (8)$$

Moreover, when $\mathbf{\Sigma} = \mathbf{I}$, it simplifies more to $\langle \mathbf{z}, \mathbf{w} \rangle \triangleq \mathbf{z}^H \mathbf{w}$. Appropriately, the norm of \mathbf{z} is written as $\|\mathbf{z}\|_{\mathbf{\Sigma}} \triangleq \sqrt{\langle \mathbf{z}, \mathbf{z} \rangle_{\mathbf{\Sigma}}} = \|\mathbf{\Sigma}^{-1/2} \mathbf{z}\|$. Further, in case of $\mathbf{\Sigma} = \mathbf{I}$, it reduces more to $\|\mathbf{z}\| \triangleq \sqrt{\langle \mathbf{z}, \mathbf{z} \rangle}$ as expected.

In order to make the accomplishments of probability and statistics concise and comprehensible, $\Pr\{A\}$ and $\Pr\{A|B\}$ will denote the probability of event A , the probability of event A given event B , respectively. Random distributions will be denoted by uppercase letters, e.g. X, Y, Z . Random vectors and random matrices will be denoted by calligraphic boldfaced uppercase letters, e.g. $\mathbf{X}, \mathbf{Y}, \mathbf{Z}$. Let X be a random distribution, then its PDF is defined by

$$f_X(x) \triangleq \mathbb{E}[\delta(x - X)], \quad (9)$$

where $\mathbb{E}[\cdot]$ denotes the expectation operator, and $\delta(\cdot)$ denotes the Dirac's delta function [145, Eq. (1.8.1)]. Besides, its CDF is defined by

$$F_X(x) \triangleq \mathbb{E}[\theta(x - X)], \quad (10)$$

where $\theta(\cdot)$ is the Heaviside's theta function [145, Eq. (1.8.3)]. Furthermore, the conditional PDF and CDF of X given G will also be denoted by $f_{X|G}(x|g)$ and $F_{X|G}(x|g)$, respectively. Denote by $\mathbf{Z} \triangleq [X, Y]^T$ a real random vector formed of the real and imaginary parts of complex random distribution $Z \triangleq X + jY$, where X and Y are two real random distributions whose joint PDF $f_{\mathbf{Z}}(x, y)$ is

$$f_{\mathbf{Z}}(x, y) \triangleq \mathbb{E}[\delta(x - X)\delta(y - Y)], \quad (11)$$

Therefore, since $Z \triangleq X + jY$ as a linear combination of X and Y [146], the PDF of Z is given by $f_Z(z) = f_{\mathbf{Z}}(\Re\{z\}, \Im\{z\})$. Similarly, the joint CDF of X and Y is

$$F_{\mathbf{Z}}(x, y) \triangleq \mathbb{E}[\theta(x - X)\theta(y - Y)]. \quad (12)$$

The CDF of Z is readily given by $F_Z(z) = F_{\mathbf{Z}}(\Re\{z\}, \Im\{z\})$. In addition, upon considering Z as a linear combination of X and Y , the MGF is useful for finding the PDF and CDF of Z . The MGF of Z , defined as $M_Z(s) \triangleq \mathbb{E}[\exp(-\langle s, Z \rangle)]$ for $s = s_X + js_Y \in \mathbb{C}$ and $s_X, s_Y \in \mathbb{R}$, is equivalent to the joint MGF of \mathbf{Z} , that is

$$M_{\mathbf{Z}}(s_X, s_Y) \triangleq \mathbb{E}[\exp(-s_X X - s_Y Y)], \quad (13)$$

which is finite in $s \in \mathbb{D} \subset \mathbb{C}^2$, thus $M_Z(s) = M_{\mathbf{Z}}(\Re\{s\}, \Im\{s\})$ exploiting complex notations. Similarly, the MGFs of X and Y are respectively denoted by $M_X(s) \triangleq \mathbb{E}[\exp(-sX)]$ and $M_Y(s) \triangleq \mathbb{E}[\exp(-sY)]$. In statistical analyses, $\text{Var}[\cdot]$, $\text{PVar}[\cdot]$, $\text{Cov}[\cdot, \cdot]$, $\text{Skew}[\cdot]$ and $\text{Kurt}[\cdot]$ will represent variance, pseudovariance, covariance, skewness and Kurtosis operators, respectively. Consequently, $\mathbb{E}[Z]$ is written as $\mathbb{E}[Z] = \mathbb{E}[X] + j\mathbb{E}[Y]$. Besides, $\text{Var}[Z] \triangleq \mathbb{E}[|Z - \mathbb{E}[Z]|^2]$ is written as

$$\text{Var}[Z] = \text{Var}[X] + \text{Var}[Y] \quad (14)$$

which does not possess any information about $\text{Cov}[X, Y] \triangleq \mathbb{E}[(X - \mathbb{E}[X])(Y - \mathbb{E}[Y])]$. However, the pseudovariance of Z , defined as $\text{PVar}[Z] \triangleq \mathbb{E}[(Z - \mathbb{E}[Z])^2]$, contains it, that is

$$\text{PVar}[Z] = \text{Var}[X] - \text{Var}[Y] + j2\text{Cov}[X, Y]. \quad (15)$$

In addition, for shorthand notations of random distributions, $\mathcal{N}(\mu, \sigma^2)$, $\mathcal{L}(\mu, \sigma^2)$, and $\mathcal{M}_{\nu}(\mu, \sigma^2)$ denote a Gaussian distribution, a Laplacian distribution, and a McLeish distribution, respectively, with ν normality, μ mean and σ^2 variance. Their CCS distributions are denoted by $\mathcal{CN}(\mu, \sigma^2)$, $\mathcal{CL}(\mu, \sigma^2)$, and $\mathcal{CM}_{\nu}(\mu, \sigma^2)$, respectively. Similarly, their CES distributions for a correlation $\rho \in [-1, 1]$ are similarly denoted by $\mathcal{EN}(\mu, \sigma^2, \rho)$, $\mathcal{EL}(\mu, \sigma^2, \rho)$, and $\mathcal{EM}_{\nu}(\mu, \sigma^2, \rho)$, respectively. Further, $\mathcal{E}(\Omega)$ and $\mathcal{G}(m, \Omega)$ denote an exponential distribution and a Gamma distribution, where $\Omega \in \mathbb{R}_+$ denotes the average power and $m \in \mathbb{R}_+$ denotes the fading figure describing the amount of spread from the average power Ω . In addition, the symbol \sim stands for "distributed as", e.g., $X \sim \mathcal{M}_{\nu}(\mu, \sigma^2)$.

In accordance with previously described notation of random matrices, the joint PDF and CDF of the real random vector $\mathbf{X} \in \mathbb{R}^m$ are respectively expressed by $f_{\mathbf{X}}: \mathbb{R}^m \rightarrow \mathbb{R}_+$ and $F_{\mathbf{X}}: \mathbb{R}^m \rightarrow [0, 1]$, and are respectively defined by

$$f_{\mathbf{X}}(\mathbf{x}) \triangleq \mathbb{E}[\delta(\mathbf{x} - \mathbf{X})], \quad (16)$$

$$F_{\mathbf{X}}(\mathbf{x}) \triangleq \mathbb{E}[\theta(\mathbf{x} - \mathbf{X})], \quad (17)$$

for $\mathbf{x} \in \mathbb{R}^m$, where $\forall \mathbf{y} \in \mathbb{R}^m$, we have $\delta(\mathbf{y}) = \prod_{k=1}^m \delta(y_k)$ and $\theta(\mathbf{y}) = \prod_{k=1}^m \theta(y_k)$. Moreover, the MGF of \mathbf{X} is expressed as $M_{\mathbf{X}}: \mathbb{R}^m \rightarrow [0, 1]$ and defined by

$$M_{\mathbf{X}}(\mathbf{s}) \triangleq \mathbb{E}[\exp(-\langle \mathbf{s}, \mathbf{X} \rangle)] = \mathbb{E}[\exp(-\mathbf{s}^T \mathbf{X})], \quad (18)$$

where $\mathbf{s} \in \mathbb{R}^m$. For simplicity, the mean vector of $\mathbf{X} \in \mathbb{R}^m$ is defined by

$$\boldsymbol{\mu} \triangleq \mathbb{E}[\mathbf{X}] = [\mu_1, \mu_2, \dots, \mu_m]^T, \quad (19)$$

where $\mu_i \triangleq \mathbb{E}[X_i]$, $1 \leq i \leq m$. The covariance matrix of \mathbf{X} is defined in multi-dimensional real space by $\boldsymbol{\Sigma} \in \mathbb{R}^{m \times m}$, that is

$$\boldsymbol{\Sigma} \triangleq \mathbb{E}[(\mathbf{X} - \boldsymbol{\mu})(\mathbf{X} - \boldsymbol{\mu})^T], \quad (20a)$$

$$= \mathbb{E}[\mathbf{X}\mathbf{X}^T] - \boldsymbol{\mu}\boldsymbol{\mu}^T, \quad (20b)$$

$$= [\sigma_{ij}]_{1 \leq i, j \leq m}, \quad (20c)$$

where $\sigma_{ij} \triangleq \text{Cov}[X_i, X_j]$, $1 \leq i, j \leq m$. There is no restriction on $\boldsymbol{\mu}$, but $\boldsymbol{\Sigma}$ must be real, symmetric, full rank, invertible, and hence positive definite (i.e., $\mathbf{x}^T \boldsymbol{\Sigma} \mathbf{x} > 0$ for all $\mathbf{x} \in \mathbb{R}^m$). For the shorthand notations of random vectors, $\mathcal{N}(\boldsymbol{\mu}, \boldsymbol{\Sigma})$, $\mathcal{L}^m(\boldsymbol{\mu}, \boldsymbol{\Sigma})$, and $\mathcal{M}_{\nu}^m(\boldsymbol{\mu}, \boldsymbol{\Sigma})$ denote an m -dimensional Gaussian random vector, an m -dimensional Laplacian random vector, and an m -dimensional McLeish random vector, respectively, with ν normality, $\boldsymbol{\mu}$ mean vector and $\boldsymbol{\Sigma}$ covariance matrix.

In multi-dimensional complex space, the joint PDF and CDF of the complex random vector $\mathbf{Z} \in \mathbb{C}^m$ are respectively expressed by $f_{\mathbf{Z}}: \mathbb{C}^m \rightarrow \mathbb{R}_+$ and $F_{\mathbf{Z}}: \mathbb{C}^m \rightarrow [0, 1]$, and are respectively defined by

$$f_{\mathbf{Z}}(\mathbf{z}) \triangleq \mathbb{E}[\delta(\mathbf{z} - \mathbf{Z})], \quad (21)$$

$$F_{\mathbf{Z}}(\mathbf{z}) \triangleq \mathbb{E}[\theta(\mathbf{z} - \mathbf{Z})], \quad (22)$$

for $\mathbf{z} \in \mathbb{C}^m$ and $\mathbf{s} \in \mathbb{C}^m$, where, for all $\mathbf{z} = \mathbf{x} + j\mathbf{y} \in \mathbb{C}^m$ with $\mathbf{x}, \mathbf{y} \in \mathbb{R}^m$, we have $\delta(\mathbf{z}) = \delta(\mathbf{x})\delta(\mathbf{y})$ and $\theta(\mathbf{z}) = \theta(\mathbf{x})\theta(\mathbf{y})$. Further, the MGF of \mathbf{Z} is expressed as $M_{\mathbf{Z}}: \mathbb{C}^m \rightarrow [0, 1]$ and defined by

$$M_{\mathbf{Z}}(\mathbf{s}) \triangleq \mathbb{E}[\exp(-\langle \mathbf{s}, \mathbf{Z} \rangle)] = \mathbb{E}[\exp(-\mathbf{s}^H \mathbf{Z})], \quad (23)$$

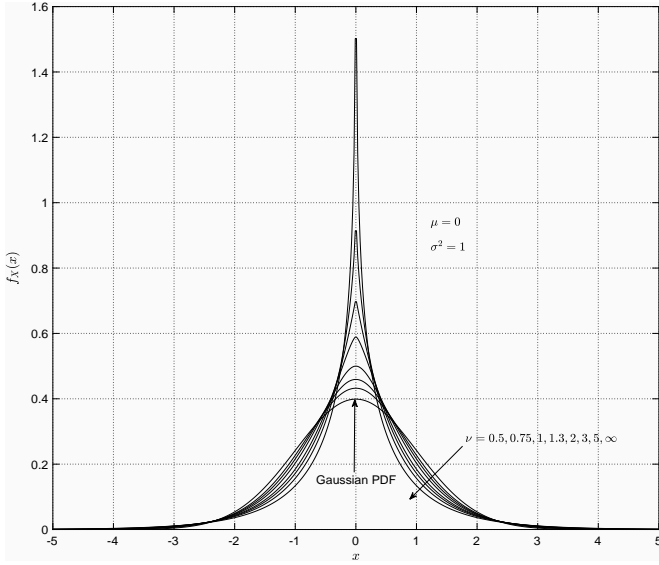
where $\mathbf{s} \in \mathbb{C}^m$. The mean vector of \mathbf{Z} is given by $\boldsymbol{\mu} = \mathbb{E}[\mathbf{Z}]$. In distinction from (20), the covariance matrix of \mathbf{Z} is defined in multi-dimensional complex space $\boldsymbol{\Sigma} \in \mathbb{C}^{m \times m}$, that is

$$\boldsymbol{\Sigma} \triangleq \mathbb{E}[(\mathbf{Z} - \boldsymbol{\mu})(\mathbf{Z} - \boldsymbol{\mu})^H], \quad (24a)$$

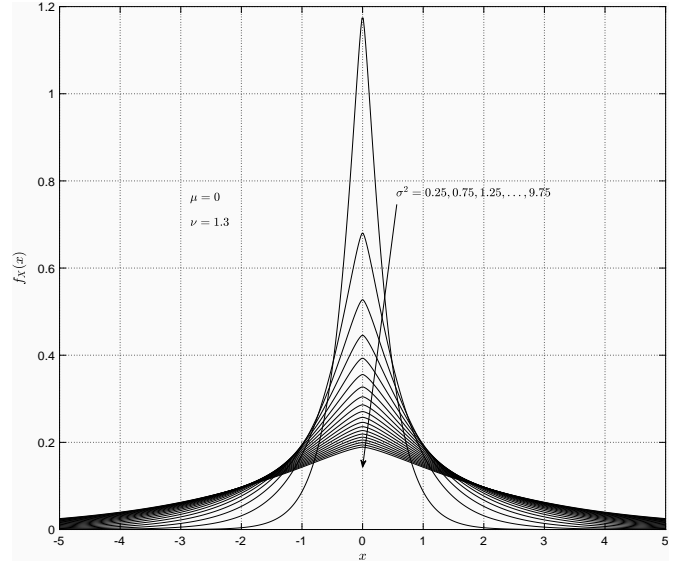
$$= \mathbb{E}[\mathbf{Z}\mathbf{Z}^H] - \boldsymbol{\mu}\boldsymbol{\mu}^H, \quad (24b)$$

$$= [\sigma_{ij}], \quad (24c)$$

where $\sigma_{ij} \triangleq \text{Cov}[Z_i, Z_j]$, $1 \leq i, j \leq m$. For the shorthand notations of random vectors, $\mathcal{CN}^m(\boldsymbol{\mu}, \boldsymbol{\Sigma})$, $\mathcal{CL}^m(\boldsymbol{\mu}, \boldsymbol{\Sigma})$, and $\mathcal{CM}_{\nu}^m(\boldsymbol{\mu}, \boldsymbol{\Sigma})$ denote an m -dimensional CCS Gaussian random vector, an m -dimensional CCS Laplacian random vector, and an m -dimensional CCS McLeish random vector, respectively, with ν normality, $\boldsymbol{\mu}$ mean vector and $\boldsymbol{\Sigma}$ covariance matrix. Further, $\mathcal{EN}^m(\boldsymbol{\mu}, \boldsymbol{\Sigma})$, $\mathcal{EL}^m(\boldsymbol{\mu}, \boldsymbol{\Sigma})$, and $\mathcal{EM}_{\nu}^m(\boldsymbol{\mu}, \boldsymbol{\Sigma})$ denote an m -dimensional CES Gaussian random vector, an m -dimensional CES Laplacian random vector, and an m -dimensional CES McLeish random vector.



(a) With respect to normality.



(b) With respect to variance.

 Fig. 1: The PDF of $\mathcal{M}_\nu(0, \sigma^2)$ with zero mean (i.e., the illustration of (25) for $\mu=0$).

III. STATISTICAL BACKGROUND

A. McLish Distribution

Let X be $\mathcal{M}_\nu(\mu, \sigma^2)$ whose PDF is given by [115, Eq. (3)]

$$f_X(x) = \frac{2}{\sqrt{\pi}} \frac{|x - \mu|^{\nu - \frac{1}{2}}}{\Gamma(\nu) \lambda^{\nu + \frac{1}{2}}} K_{\nu - \frac{1}{2}} \left(\frac{2|x - \mu|}{\lambda} \right), \quad (25)$$

defined over $x \in \mathbb{R}$, where $\nu \in \mathbb{R}_+$ and $\sigma^2 \in \mathbb{R}_+$ denote the normality and variance, respectively, and $\lambda = \sigma \lambda_0 = \sqrt{2\sigma^2/\nu}$ denotes the component deviation (power normalizing) factor. Further, $\Gamma(x) \triangleq \int_0^\infty u^{x-1} \exp(-u) du$ is the Gamma function [147, Eq. (6.1.1)], and $K_n(x) \triangleq \int_0^\infty e^{-x \cosh(u)} \cosh(nu) du$ is the modified Bessel function of the second kind [147, Eq. (9.6.2)]. In order to illustrate the versatility and heavy-tail behaviour of $\mathcal{M}_\nu(\mu, \sigma^2)$, the PDF, given in (25), is aptly illustrated with respect to $\nu \in \mathbb{R}_+$ and $\sigma^2 \in \mathbb{R}_+$ for a certain $\mu \in \mathbb{R}$ in Fig. 1 on the next page.

The special cases of $\mathcal{M}_\nu(\mu, \sigma^2)$ consist of Dirac, Laplacian and Gaussian distributions. In more details, as $\nu \rightarrow 0$, (25) reduces to

$$f_X(x) = \delta(x - \mu), \quad (26)$$

which is the PDF of Dirac's distribution, where $\delta(\cdot)$ denotes the Dirac's delta function [145, Eq. (1.8.1)]. Further, substituting $\nu=1$ into (25) and then utilizing [147, Eq. (9.7.8)] yields the PDF of $\mathcal{L}(\mu, \sigma^2)$, that is

$$f_X(x) = \frac{1}{\sqrt{2\sigma^2}} \exp(-\sqrt{2/\sigma^2} |x - \mu|), \quad (27)$$

Besides, limiting $\nu \rightarrow \infty$ in (25) and using [147, Eq. (9.7.8)] yields

$$f_X(x) = \frac{1}{\sqrt{2\pi\sigma^2}} \exp\left(-\frac{(x - \mu)^2}{2\sigma^2}\right), \quad (28)$$

which is the PDF of $X \sim \mathcal{N}(\mu, \sigma^2)$. In addition, $\mathcal{M}_\nu(\mu, \sigma^2)$ demonstrates a superior fit to different impulsive noise characteristics with respect to $\nu \in \mathbb{R}_+$, and therefore it is reasonably

fit to any noise distribution, especially by estimating ν , μ , and σ^2 with the aid of method of moments estimation (MOM) in which sample moments are equated with theoretical moments of $\mathcal{M}_\nu(\mu, \sigma^2)$, that is

$$\hat{\mu} \triangleq \mathbb{E}[X], \quad \hat{\sigma}^2 \triangleq \text{Var}[X], \quad \text{and} \quad \hat{\nu} \triangleq \frac{3}{\text{Kurt}[X] - 3}. \quad (29)$$

For that purpose, the higher-order moments of $\mathcal{M}_\nu(\mu, \sigma^2)$ are given in the following theorem.

Theorem 1. *The moments of $X \sim \mathcal{M}_\nu(\mu, \sigma^2)$ is given by*

$$\mathbb{E}[X^n] = \mu^n \sum_{k=0}^n \binom{n}{k} \frac{\Gamma(\nu + k/2) \Gamma(1/2 + k/2)}{\Gamma(\nu) \Gamma(1/2)} \left(\frac{\lambda}{\mu}\right)^k \text{en}(k) \quad (30)$$

defined for $n \in \mathbb{N}$, where $\text{en}(k)$ returns 1 if k is an even number, otherwise returns 0.

Proof. Note that X is readily expressed as $X \triangleq \mu + W$, where $W \sim \mathcal{M}_\nu(0, \sigma^2)$. Thus, $\mathbb{E}[X^n] \triangleq \mathbb{E}[(\mu + W)^n]$ can be written using binomial expansion as follows

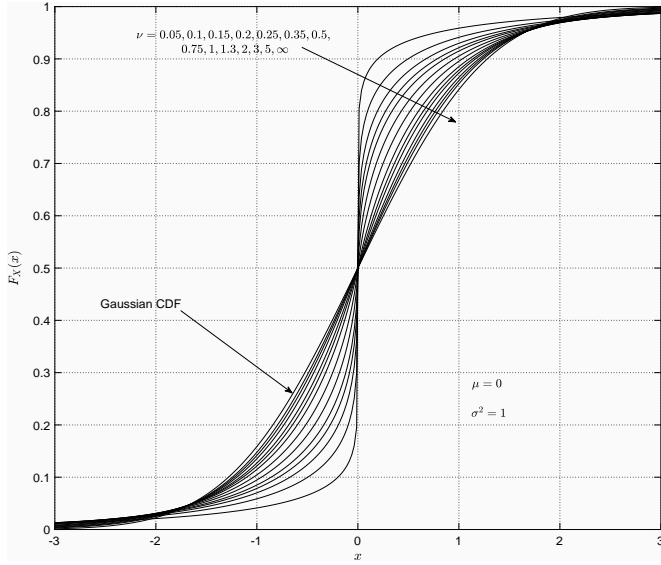
$$\mathbb{E}[X^n] = \mu^n \sum_{k=0}^n \binom{n}{k} \frac{\mathbb{E}[W^k]}{\mu^k}, \quad (31)$$

where the binomial coefficient [148, Eq. (1.1.1)] is defined as

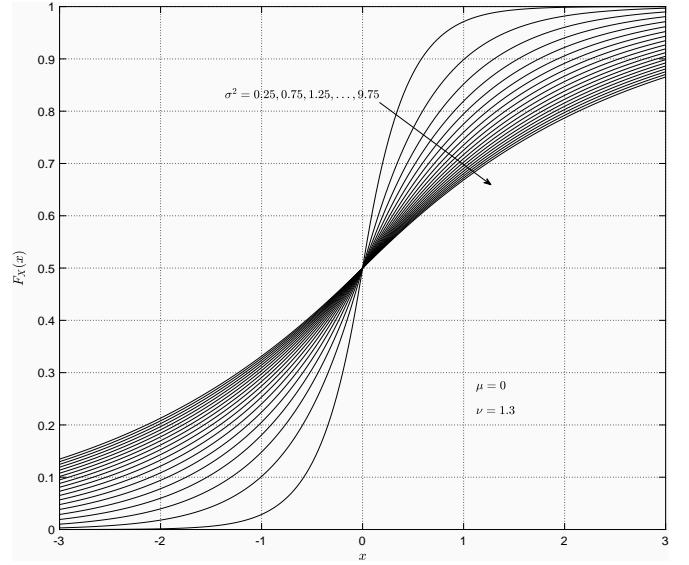
$$\binom{n}{k} \triangleq \frac{n!}{(n-k)! k!} = \frac{(n+1)^k}{k!} \prod_{j=1}^k \left(1 - \frac{j}{n+1}\right). \quad (32)$$

With the aid of utilizing $K_n(x) \triangleq G_{0,2}^{2,0} \left[x^2/2 \mid \overline{\frac{-}{n/2, -n/2}} \right]$ [149, Eq. (03.04.26.0008.01)], where $G_{p,q}^{m,n}[\cdot]$ denotes the Meijer's G function [150, Eq. (8.2.1/1)], the PDF of W can be given in terms of the Meijer's G function. After endorsing $\mu=0$ and applying [151, Eqs. (2.9.1) and (2.9.19)] on (25), $\mathbb{E}[W^n]$ is then expressed for $k \in \mathbb{N}$ as follows

$$\mathbb{E}[W^k] = \int_{-\infty}^{\infty} w^k \frac{1}{\sqrt{\pi\lambda}\Gamma(\nu)} G_{0,2}^{2,0} \left[\frac{w^2}{\lambda} \mid \overline{\frac{-}{0, \nu - \frac{1}{2}}} \right] dw, \quad (33)$$



(a) With respect to normality.



(b) With respect to variance.

 Fig. 2: The CDF of $\mathcal{M}_\nu(0, \sigma^2)$ with zero mean (i.e., the illustration of (37) for $\mu=0$).

where \emptyset denotes the empty coefficient set. Immediately afterwards, in (33), changing the variable $x^2 \rightarrow y$ and employing [151, Eqs. (2.5.1) and (2.9.1)] results in

$$\mathbb{E}[W^k] = \frac{\Gamma(\nu + k/2)}{\Gamma(\nu)} \frac{\Gamma(1/2 + k/2)}{\Gamma(1/2)} \lambda^k \text{en}(k), \quad (34)$$

where $\text{en}(k)$ returns 1 if k is an even number, otherwise returns 0. Finally, substituting (34) into (33) readily results in (30), which completes the proof of Theorem 1. ■

Definition 1 (McLeish's Quantile). *The McLeish's Q-function is defined by*

$$Q_\nu(x) = \int_x^\infty \frac{2}{\sqrt{\pi}} \frac{|w|^{\nu-1/2}}{\Gamma(\nu) \lambda_0^{\nu+1/2}} K_{\nu-1/2} \left(\frac{2|w|}{\lambda_0} \right) dw, \quad (35)$$

for $x \in \mathbb{R}$. Alternatively, it is given for $x \geq 0$ by

$$Q_\nu(x) = \frac{2^{1-\nu}}{\pi \Gamma(\nu)} \int_0^{\frac{\pi}{2}} \left(\frac{2x}{\lambda_0 \sin(\theta)} \right)^\nu K_\nu \left(\frac{2x}{\lambda_0 \sin(\theta)} \right) d\theta, \quad (36a)$$

and given for $x < 0$ by

$$Q_\nu(x) = 1 - Q_\nu(|x|). \quad (36b)$$

In wireless communications [1]–[3, and references therein], the CDF of the additive noise is used as a quantile function to compare different systems in the context of channel reliability. In this connection, the CDF of $X \sim \mathcal{M}_\nu(\mu, \sigma^2)$, i.e., $F_X(x) \triangleq \Pr\{X \leq x\}$ for $x \in \mathbb{R}$ is obtained in the following.

Theorem 2. *The CDF of $X \sim \mathcal{M}_\nu(\mu, \sigma^2)$, which is defined as $F_X(x) \triangleq \Pr\{X \leq x\}$, is given by*

$$F_X(x) = 1 - Q_\nu \left(\frac{x - \mu}{\sigma} \right), \quad (37)$$

where $Q_\nu(\cdot)$ denotes the McLeish's Q-function defined in (36).

Proof. Let us define a new random variable, $W \triangleq (X - \mu)/\sigma$, where $W \sim \mathcal{M}_\nu(0, 1)$, whose PDF is given, using (25), by

$$f_W(w) = \frac{2}{\sqrt{\pi}} \frac{|w|^{\nu-1/2}}{\Gamma(\nu) \lambda_0^{\nu+1/2}} K_{\nu-1/2} \left(\frac{2|w|}{\lambda_0} \right). \quad (38)$$

whose distributional symmetry around 0 consequences that the CDF $F_W(w) \triangleq \Pr\{W \leq w\} = \int_{-\infty}^w f_W(w) dw$ can be rewritten as $F_W(w) = 1 - F_W(|w|)$ for $w \in \mathbb{R}^-$. But for $w \in \mathbb{R}^+$, $F_W(w)$ is written as $F_W(w) = 1 - \int_w^\infty \frac{1}{\sqrt{2w}} f_W(\sqrt{w}) dw$. After some algebraic manipulations, it is rewritten as

$$F_W(w) = 1 - \frac{2^{1-\nu}}{\pi \Gamma(\nu)} \int_0^1 \frac{1}{\sqrt{1-w^2}} \left(\frac{2}{w\lambda_0} \right)^\nu K_\nu \left(\frac{2}{w\lambda_0} \right) dw,$$

where changing the variable as $w \rightarrow \sin(\theta)$ and utilizing (36) results in $F_W(w) = 1 - Q_\nu(w)$. Accordingly, the CDF of X can be readily given as in (37), which proves Theorem 2. ■

The CDF of $X \sim \mathcal{M}_\nu(\mu, \sigma^2)$ is described in Fig. 2 in detail using (37). It is therefore worth for the consistency and validity of the McLeish's Q-function to mention that (36) reduces for $\nu \rightarrow \infty$ to the well-known result, that is

$$\lim_{\nu \rightarrow \infty} Q_\nu(x) = Q(x) \quad (39)$$

where $Q(x) = \frac{1}{\sqrt{2\pi}} \int_x^\infty e^{-\frac{1}{2}u^2} du$ denotes the standard Gaussian Q-function [3, Eq. (2.3-10)]. Further, following are some of the fundamental properties of McLeish's Q-function:

$$Q_\nu(-x) = 1 - Q_\nu(x) \quad \text{and} \quad Q_\nu(\pm\infty) = \frac{1}{2}(1 \mp 1), \quad (40a)$$

$$Q_\nu(0) = \frac{1}{2} \quad \text{and} \quad Q_0(x) \rightarrow 0^+, \quad (40b)$$

In addition, It is worth examining not only the special cases of McLeish's Q-function for the special non-extreme finite values of the normality ν , but also for lower and upper bounds.

Accordingly, setting $\nu = 1$ reduces McLeish's Q-function to the Laplacian Q-function, that is

$$LQ(x) \triangleq \begin{cases} \frac{1}{2} \exp(-2\sqrt{2}x), & \text{if } x \geq 0, \\ 1 - LQ(|x|), & \text{if } x < 0. \end{cases} \quad (41)$$

As seen in the following sections, the McLeish's Q-function is often used in the BER/SER analysis of the signaling using modulation schemes over AWMN channels. The McLeish's Q-function can be tabulated, or implemented as a built-in functions in mathematical software tools. However, in many cases it is useful to have closed-form bounds or approximations instead of the exact expression. In fact, these approximations are particularly useful in evaluating the BER/SER in many problems of the communication theory. For that purpose, the lower and upper bounds of the McLeish's Q-function are found to be obtained for $x > 0$ using Taylor series expansion under some simplification, that is

$$Q_\nu^{\text{LB}}(x) \leq Q_\nu(x) \leq Q_\nu^{\text{UB}}(x), \text{ for } x > 0, \quad (42)$$

where the lower bound approximation $Q_\nu^{\text{LB}}(x)$ is given by

$$Q_\nu^{\text{LB}}(x) = \frac{1}{\sqrt{\pi}\Gamma(\nu)} \left(\frac{x}{\lambda_0}\right)^{\nu-\frac{1}{2}} \times \left(K_{\nu+\frac{1}{2}}\left(\frac{2x}{\lambda_0}\right) - \frac{\lambda_0}{2x} K_{\nu+\frac{3}{2}}\left(\frac{2x}{\lambda_0}\right)\right), \quad (43)$$

and the upper bound approximation $Q_\nu^{\text{UB}}(x)$ is given by

$$Q_\nu^{\text{UB}}(x) = \frac{1}{\sqrt{\pi}\Gamma(\nu)} \left(\frac{x}{\lambda_0}\right)^{\nu-\frac{1}{2}} K_{\nu+\frac{1}{2}}\left(\frac{2x}{\lambda_0}\right). \quad (44)$$

Then, the gap between $Q_\nu^{\text{LB}}(x)$ and $Q_\nu^{\text{UB}}(x)$ is given by

$$Q_\nu^{\text{UB}}(x) - Q_\nu^{\text{LB}}(x) = \frac{1}{2\sqrt{\pi}\Gamma(\nu)} \left(\frac{x}{\lambda_0}\right)^{\nu-\frac{3}{2}} K_{\nu+\frac{3}{2}}\left(\frac{2x}{\lambda_0}\right). \quad (45)$$

Note that H-transforms, also known as Mellin-Barnes integrals¹ are the integral kernels involving Meijer's G and Fox's H functions that have found many applications in such fields as physics, statistics, and engineering [151]. In the literature of wireless communications, H-transforms have been gained some attention to find closed-form expressions for averaged performance analysis, and also Fox's H function has recently started to be used as a possible fading distribution, commonly referred as the Fox's H distribution [152]. It is thus useful to express McLeish's Q-function in terms of Meijer's G and Fox's H functions. Such expressions allow the use of Mellin-Barnes integrals to obtain new closed-form expressions.

Theorem 3. *McLeish's Q-function can be alternatively expressed in terms of Fox's H function as follows*

$$Q_\nu(x) = \begin{cases} \frac{1}{\Gamma(\nu)} H_{1,2}^{2,0} \left[2\nu x^2 \left| \begin{matrix} (1,1) \\ (0,2), (\nu,1) \end{matrix} \right. \right], & \text{if } x \geq 0, \\ 1 - Q_\nu(|x|), & \text{if } x < 0, \end{cases} \quad (46)$$

where $H_{p,q}^{m,n}[\cdot]$ is the Fox's H function [150, Eq.(8.3.1/1)], [151, Eq.(1.1.1)]; or in terms of Meijer's G function as follows

$$Q_\nu(x) = \begin{cases} \frac{1}{2\sqrt{\pi}\Gamma(\nu)} G_{1,3}^{3,0} \left[2\nu x^2 \left| \begin{matrix} 1 \\ 0, 1/2, \nu \end{matrix} \right. \right], & \text{if } x \geq 0, \\ 1 - Q_\nu(|x|), & \text{if } x < 0. \end{cases} \quad (47)$$

Proof. Note that in (36a), taking place of the modified Bessel function of the second by [151, Eq.(2.9.19)] and then performing some algebraic manipulations yields

$$Q_\nu(x) = \frac{1}{\pi\Gamma(\nu)} \int_0^{\frac{\pi}{2}} H_{0,2}^{2,0} \left[\frac{x^2}{\lambda_0^2 \sin^2(\theta)} \left| \begin{matrix} - \\ (0,1), (\nu,1) \end{matrix} \right. \right] d\theta, \quad (48)$$

where employing [151, Eq.(1.1.1)] results in Mellin-Barnes contour integral in which changing the order of integrals and performing manipulations using [148, Eq.(3.621/1)]

$$\int_0^{\pi/2} \sin^{2s}(\theta) d\theta = \frac{\sqrt{\pi}\Gamma(\frac{1}{2}+s)}{2\Gamma(1+s)} \quad (49)$$

for $\Re\{s\} > -\frac{1}{2}$ yields (46), which readily proves the first step of Theorem 46. Then, using [150, Eq.(8.3.2/22)], (46) reduces to (47), which completes the proof of Theorem 3. ■

Immediately after we examine the results provided in [1]–[3], [153], we readily recognize that Craig's partial Q-function, defined as $Q(x, \phi) \triangleq \frac{1}{2\pi} \int_0^\phi \exp(-x^2/\sin^2(\theta)) d\theta$, is widely exploited in the SER analysis of M-ary modulation and 2-dimensional modulation schemes, for example in [153], and [1, Eqs.(4.9), (4.16), (4.17), (4.18), (4.19) and (5.77)]. Analogously, we can define the McLeish's partial Q-function as it is shown in the following.

Definition 2 (McLeish's Partial Quantile). *For a certain $\phi \in [0, \pi/2]$, McLeish's partial Q-function is defined as*

$$Q_\nu(x, \phi) = \frac{2^{1-\nu}}{\pi\Gamma(\nu)} \int_0^\phi \left(\frac{2x}{\lambda_0 \sin(\theta)}\right)^\nu K_\nu\left(\frac{2x}{\lambda_0 \sin(\theta)}\right) d\theta \quad (50a)$$

for $x \geq 0$;

$$Q_\nu(x, \phi) = 1 - Q_\nu(|x|, \phi), \quad (50b)$$

for $x < 0$; such that $Q_\nu(x) = Q_\nu(x, \pi/2)$.

In wireless communications [1]–[3, and references therein], the C^2 DF of the additive noise is used as a quantile function to compare different systems in the context of BER or SER. In this connection, the C^2 DF of $X \sim \mathcal{M}_\nu(\mu, \sigma^2)$ is obtained in the following.

Theorem 4. *The C^2 DF of $X \sim \mathcal{M}_\nu(\mu, \sigma^2)$, which is defined as $\hat{F}_X(x) \triangleq \Pr\{X > x\}$, is given by*

$$\hat{F}_X(x) = Q_\nu\left(\frac{x-\mu}{\sigma}\right). \quad (51)$$

Proof. Note that $\hat{F}_X(x) = 1 - F_X(x)$ since $\Pr\{X > x\} = 1 - \Pr\{X \leq x\}$. The proof is thus obvious using Theorem 2. ■

As mentioned in [1], [154]–[156], the MGF is an efficient mathematical instrument not only to derive inequalities on tail probabilities of distributions but to achieve their statistical characterisations, and therefore is extremely common in performance results for communication problems related to

¹For further details about both H-transforms and Fox's H functions, readers are referred to [151, and references therein].

partially coherent, differentially coherent, and non-coherent communications and is very useful in statistics. We derive the MGF of McLeish distribution as it is given in the following.

Theorem 5. *The MGF of $X \sim \mathcal{M}_\nu(\mu, \sigma^2)$ is given by*

$$M_X(s) = e^{-s\mu} \left(1 - \frac{\lambda^2}{4} s^2\right)^{-\nu} \quad (52)$$

with the existence region $-S_0 < \Re\{s\} < S_0$, where $S_0 \in \mathbb{R}_+$ is given by $S_0 = 2/\lambda$.

Proof. Note that $M_X(s) \triangleq \mathbb{E}[\exp(-sX)]$ can be expressed as $M_X(s) = s \int_{-\infty}^{\infty} \exp(-sx) F_X(x) dx$, where using (37) yields

$$M_X(s) = s \int_{-\infty}^{\infty} \exp(-sx) Q_\nu\left(\frac{x-\mu}{\sigma}\right) dx. \quad (53)$$

which can be divided two integration, i.e., $M_X(s) = sI_+(s) + sI_-(s)$, where $I_\pm(s)$ is written as

$$I_\pm(s) = \pm \int_0^{\infty} \exp(\mp sx) Q_\nu\left(\frac{\pm x - \mu}{\sigma}\right) dx, \quad (54)$$

Subsequently, substituting (46) in (54) and then using both $\exp(-x) = G_{0,1}^{1,0}\left[x \left| \frac{\cdot}{0} \right.\right]$ [150, Eq. (8.4.3/1)], and $\exp(x) = \frac{\pi}{\sin(\pi c)} G_{1,2}^{1,0}\left[x \left| \frac{1-c}{0, 1-c} \right.\right]$ [150, Eq. (8.4.3/5)] results in a Mellin-Barnes integration [151, Theorem 2.9] that readily reduces to

$$I_\pm(s) = e^{-s\mu} \left(1 - \frac{\lambda^2}{4} s^2\right)^{-\nu} \left(\frac{1}{2s} \pm \frac{\lambda}{4\pi} \sin(\pi\nu) \left(\frac{1}{2}\right)_\nu G_{2,2}^{1,2}\left[-\frac{\lambda^2}{4} s^2 \left| \frac{1/2, \nu}{0, -1/2} \right.\right]\right) \quad (55)$$

within the convergence region $-2/\lambda \leq \Re\{s\} \leq 2/\lambda$, where $(a)_n \triangleq \Gamma(a+n)/\Gamma(a)$ denotes Pochhammer's symbol [149, Eq. (1.2.6)]. Consequently, $M_X(s) = sI_+(s) + sI_-(s)$ simplifies to (52), which completes the proof of Theorem 5. ■

For consistency, letting $\nu \rightarrow 0$ in (52) results in $\exp(-s\mu)$, which is the MGF of the Dirac's distribution with mean μ . For $\nu = 1$, (52) simplifies to the MGF of $\mathcal{L}(\mu, \sigma^2)$, that is $M_X(s) = e^{-s\mu} (1 - \sigma^2 s^2/2)^{-1}$ [122], [157]–[159]. In addition, when letting $\nu \rightarrow \infty$ and then using $\lim_{n \rightarrow \infty} (1 + \frac{x}{n})^n \triangleq \exp(x)$ [149, Eq. (01.03.09.0001.01)], (52) simplifies to $M_X(s) = \exp(-s\mu + \sigma^2 s^2/2)$ [3], [157]–[159] which is the well-known MGF of $\mathcal{N}(\mu, \sigma^2)$. Notice that the MGF is also used to derive the moments [141]. Hence, the analytical correctness of (52) can also be checked using (30). Using [150, Eq. (8.4.2/5)], we can express (52) in terms of Meijer's G function as

$$M_X(s) = \frac{e^{-s\mu}}{\Gamma(\nu)} G_{1,1}^{1,1}\left[\frac{\lambda^2}{4} s^2 \left| \frac{1-\nu}{0} \right.\right], \quad (56)$$

whose n th derivation with respect to s , i.e. $(\partial/\partial s)^n M_X(s)$ can be attained using Leibniz's rule [148, Eq. (0.42)] and [150, Eqs. (8.3.2/21) and (8.3.2/21)], and therein setting $s \rightarrow 0$ yields (30) as expected. It is also worth mentioning that the MGFs are very useful for the analysis of sums of the McLeish distributions as exemplified in the following.

B. Sum of McLeish Distributions

Let $X_\ell \sim \mathcal{M}_{\nu_\ell}(\mu_\ell, \sigma_\ell^2)$, $\ell = 1, 2, \dots, L$ be L independent and non-identically distributed (*i.n.i.d.*) distributions. Then, their sum is written as

$$X_\Sigma \triangleq \sum_{\ell=1}^L X_\ell, \quad (57)$$

whose statistically characterization is given in the following.

Theorem 6. *The MGF of (57) is given by*

$$M_{X_\Sigma}(s) = e^{-s \sum_{\ell=1}^L \mu_\ell} \prod_{\ell=1}^L \left(1 - \frac{\lambda_\ell^2}{4} s^2\right)^{-\nu_\ell} \quad (58)$$

with the existence region $-S_0 < \Re\{s\} < S_0$, where $S_0 \in \mathbb{R}_+$ is given by $S_0 = 2/\max_{\ell \in \{1..L\}} \lambda_\ell$.

Proof. Since the McLeish distributions $\{X_\ell\}_{\ell=1}^L$ are independent, the MGF of X_Σ is defined as the product of their MGFs, that is $M_{X_\Sigma}(s) \triangleq \mathbb{E}[\exp(-s \sum_{\ell=1}^L X_\ell)] = \prod_{\ell=1}^L M_{X_\ell}(s)$, where using (52) yields (58), which proves Theorem 6. ■

Let us now consider some special cases of (58). In case of $\nu_\ell \in \mathbb{Z}^+$ and $\lambda_\ell \neq \lambda_m$ for all $\ell \neq m$, X_Σ follows a hyper McLeish distribution, which is also called a mixture McLeish distribution, whose MGF is obtained by simplifying (58) using pole factorization as follows

$$M_{X_\Sigma}(s) = e^{-s \sum_{\ell=1}^L \mu_\ell} \sum_{\ell=1}^L \sum_{m=0}^{\nu_\ell-1} w_{\ell m} \left(1 - \frac{\lambda_\ell^2}{4} s^2\right)^{m-\nu_\ell}, \quad (59)$$

where the weight coefficients $\{w_{\ell m}\}$, which certainly support that $\sum_{\ell=1}^L \sum_{m=0}^{\nu_\ell-1} w_{\ell m} = 1$, are defined as

$$w_{\ell m} = \frac{4^m}{\lambda_\ell^{2m} m!} \left(\frac{\partial}{\partial s}\right)^m \prod_{j=1, j \neq \ell}^L \left(1 - \frac{\lambda_j^2}{\lambda_\ell^2} + \frac{\lambda_j^2}{4} s^2\right)^{-\nu_j} \Big|_{s \rightarrow 0}, \quad (60)$$

where the m th order derivative can be mathematically defined in several ways [160]–[162, and references therein]. We find the Grünwald-Letnikov derivative to be convenient for its numerical computation. In addition, the other special case of (58) is obtained when $\lambda_\ell = \lambda_\Sigma$ with distinct σ_ℓ^2 for $\ell = 1, 2, \dots, n$; X_Σ follows a McLeish distribution, i.e., $X_\Sigma \sim \mathcal{M}_{\nu_\Sigma}(\mu_\Sigma, \sigma_\Sigma^2)$, whose MGF is readily deduced similar to (52), that is

$$M_{X_\Sigma}(s) = e^{-s\mu_\Sigma} \left(1 - \frac{\lambda_\Sigma^2}{4} s^2\right)^{-\nu_\Sigma}, \quad (61)$$

where the normality $\nu_\Sigma \triangleq \sum_{\ell=1}^n \nu_\ell$, the mean $\mu_\Sigma \triangleq \sum_{\ell=1}^n \mu_\ell$ and the variance $\sigma_\Sigma^2 \triangleq \nu_\Sigma \lambda_\Sigma^2/2$. In addition, the other special cases can be deduced for certain normalities $\nu_\ell \rightarrow 0$, $\nu_\ell \rightarrow 1$ and $\nu_\ell \rightarrow \infty$ in (58). Specifically, when $\forall \nu_\ell \rightarrow 0$, (58) and (59) reduces to $M_{X_\Sigma}(s) = e^{-s\mu_\Sigma}$, which is the MGF of the Dirac's distribution. Further, when $\forall \nu_\ell \rightarrow 1$, (58) turns to the MGF of sum of *i.n.i.d.* Laplace distributions, that is [163, Sec. 10.4]

$$M_{X_\Sigma}(s) = e^{-s \sum_{\ell=1}^L \mu_\ell} \prod_{\ell=1}^L \left(1 - \frac{\sigma_\ell^2}{2} s^2\right)^{-1}. \quad (62)$$

In addition, when $\forall \nu_\ell \rightarrow \infty$, (58) turns to the MGF of sum of *i.n.i.d.* Gaussian distributions, that is [163, Sec. 34.5]

$$M_{X_\Sigma}(s) = \exp\left(-s\mu_\Sigma + \frac{s^2}{2} \sigma_\Sigma^2\right). \quad (63)$$

Speaking of statistically characterization, we efficiently exploit the MGF to find the PDF of the sums of independent random distributions [141]. Accordingly, the PDF of X_Σ is obtained in the following.

Theorem 7. *The PDF of (57) is given by*

$$f_{X_\Sigma}(x) = I_{2L,2L}^{L,L} \left[\frac{\exp(-x)}{\exp(-\mu_\Sigma)} \left| \begin{array}{c} \Xi_L^{(1)}, \Xi_L^{(3)} \\ \Xi_L^{(2)}, \Xi_L^{(0)} \end{array} \right. \right] \quad (64)$$

with mean $\mu_\Sigma \triangleq \mu_1 + \mu_2 + \dots + \mu_L$, where the coefficient set $\Xi_n^{(\alpha)}$, consisting of 3-tuples of size n , is defined as

$$\Xi_n^{(\alpha)} = (\alpha - 1, \frac{\lambda_1}{2}, \nu_1), \dots, (\alpha - 1, \frac{\lambda_n}{2}, \nu_n), \quad (65)$$

for $n \in \mathbb{N}$ and $\alpha \in \mathbb{R}$. Moreover in (64), $I_{p,q}^{m,n}[\cdot]$ denotes Fox's I function [164, Eq. (3.1)].

Proof. For $\ell \in \{1, 2, \dots, n\}$, the MGF of X_ℓ , i.e., $M_{X_\ell}(s) \triangleq \mathbb{E}[\exp(-sX_\ell)]$ can be rewritten as

$$M_{X_\ell}(s) = e^{-s\mu_\ell} \left(1 - \frac{\lambda_\ell}{2}s\right)^{-\nu_\ell} \left(1 + \frac{\lambda_\ell}{2}s\right)^{-\nu_\ell}$$

by utilizing $1 - x^2 = (1-x)(1+x)$ on (52). Then, exploiting the relation $\Gamma(1+x) = x\Gamma(x)$ [145], [147], [151], $M_{X_\Sigma}(s)$ has been already obtained in (58) and can be rewritten as

$$M_{X_\Sigma}(s) = e^{-s\sum_{\ell=1}^L \mu_\ell} \prod_{\ell=1}^L \frac{\Gamma^{\nu_\ell} \left(1 + \frac{\lambda_\ell}{2}s\right) \Gamma^{\nu_\ell} \left(1 - \frac{\lambda_\ell}{2}s\right)}{\Gamma^{\nu_\ell} \left(2 + \frac{\lambda_\ell}{2}s\right) \Gamma^{\nu_\ell} \left(2 - \frac{\lambda_\ell}{2}s\right)}. \quad (66)$$

Note that by means of (66), we express the PDF of X_Σ via the inverse Laplace transform (ILT) [165], [166, Chap. 3] as

$$f_{X_\Sigma}(x) = \frac{1}{2\pi j} \int_{c-j\infty}^{c+j\infty} M_{X_\Sigma}(s) \exp(sx) ds \quad (67)$$

within the existence region $-S_0 < \Re\{s\} < S_0$, where $S_0 \in \mathbb{R}_+$ is defined by $S_0 = 2 / \max_{\ell \in \{1..n\}} \lambda_\ell$. Finally, substituting (66) into (67) and then using the mathematical formalism given in [164, Eq. (3.1)] results in (64), which proves Theorem 7. ■

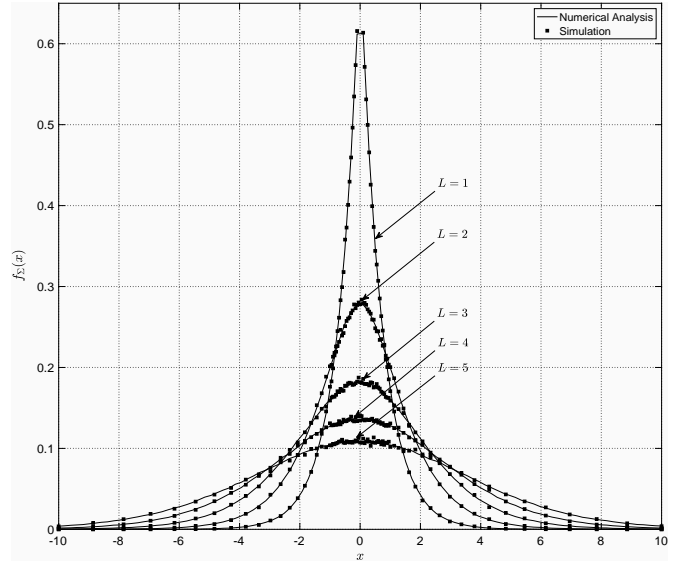
The PDF of X_Σ is depicted in Fig. 3a for different number of variables. In connection with Theorem 7, some special cases are given for consistency in the following. In case of $\nu_\ell \in \mathbb{Z}^+$ and $\lambda_\ell \neq \lambda_m$ for all $\ell \neq m$, (57) follows a hyper McLeish distribution whose PDF can be deduced from Theorem 7 as

$$f_{X_\Sigma}(x) = \sum_{\ell=1}^L \sum_{m=0}^{\nu_\ell-1} \frac{2w_{\ell m}}{\sqrt{\pi}\Gamma(\nu_\ell - m)} \times \frac{|x - \mu_\Sigma|^{\nu_\ell - \frac{1}{2}}}{\lambda^{\nu_\ell - m + \frac{1}{2}}} K_{\nu_\ell - m - \frac{1}{2}} \left(\frac{2|x - \mu_\Sigma|}{\lambda} \right), \quad (68)$$

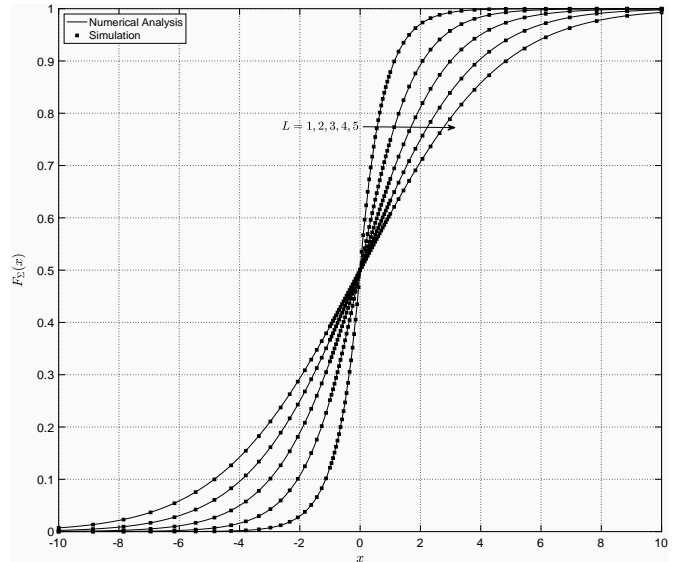
Further, when $\lambda_\ell = \lambda_\Sigma$ with distinct σ_ℓ^2 for $\ell = 1, 2, \dots, n$, (57) certainly follows $\mathcal{M}_{\nu_\Sigma}(\mu_\Sigma, \sigma_\Sigma^2)$, whose PDF has been already given in (25), that is

$$f_{X_\Sigma}(x) = \frac{2|x - \mu_\Sigma|^{\nu_\Sigma - \frac{1}{2}}}{\sqrt{\pi}\Gamma(\nu_\Sigma) \lambda_\Sigma^{\nu_\Sigma + \frac{1}{2}}} K_{\nu_\Sigma - \frac{1}{2}} \left(\frac{2|x - \mu_\Sigma|}{\lambda_\Sigma} \right). \quad (69)$$

Additionally, the other special cases can be deduced for certain normalities $\nu_\ell \rightarrow 0$, $\nu_\ell \rightarrow 1$ and $\nu_\ell \rightarrow \infty$ in (64). Accordingly, setting $\forall \nu_\ell \rightarrow 0$ in (67) and using $I_{0,0}^{0,0}[\exp(-x) | \text{---}] = \delta(x)$ with the aid of [164, Eq. (2.1)] and [145, Eq. (1.8.1/8)], we



(a) PDF.



(b) CDF.

Fig. 3: The PDF and CDF of sum of L McLeish distributions with means $\mu_\ell = 0$, and normalities $\nu_\ell = \ell$, and variances $\sigma_\ell^2 = L - \ell + 1$ for all $1 \leq \ell \leq L$.

readily notice that (64) evolves into $f_{X_\Sigma}(x) = \delta(x - \mu_\Sigma)$. Further, setting $\forall \nu_\ell \rightarrow 1$, (64) simplifies to the PDF of the sum of *i.n.i.d.* Laplace distributions, that is

$$f_{X_\Sigma}(x) = \frac{2^L}{\prod_{\ell=1}^L \sigma_\ell^2} G_{2L,2L}^{L,L} \left[\frac{\exp(-x)}{\exp(-\mu_\Sigma)} \left| \begin{array}{c} \Phi_L^{(1)}, \Phi_L^{(3)} \\ \Phi_L^{(2)}, \Phi_L^{(0)} \end{array} \right. \right], \quad (70)$$

where the coefficient set $\Phi_n^{(\alpha)}$ is given by

$$\Phi_n^{(\alpha)} = \sqrt{2}(\alpha - 1)/\sigma_1^2, \dots, \sqrt{2}(\alpha - 1)/\sigma_n^2. \quad (71)$$

In addition, when we choose all normalities to be infinity (i.e., while having $\forall \ell \in \{1, 2, \dots, L\}, \nu_\ell \rightarrow \infty$), we readily deduce $M_{X_\ell}(s) = \exp(-s\mu_\Sigma + s^2\sigma_\Sigma^2/2)$ and accordingly reduce (64) to the PDF of $\mathcal{N}(\mu_\Sigma, \sigma_\Sigma^2)$ as expected.

Theorem 8. *The CDF of (57) is given by*

$$F_{X_\Sigma}(x) = \mathbb{I}_{2n+1, 2n}^{n+1, n} \left[\frac{\exp(-x)}{\exp(-\mu_\Sigma)} \left| \begin{matrix} \Xi_n^{(1)}, \Xi_n^{(3)}, (1, 1, 1) \\ (0, 1, 1), \Xi_n^{(2)}, \Xi_n^{(0)} \end{matrix} \right. \right]. \quad (72)$$

Proof. Note that $F_{X_\Sigma}(x) \triangleq \Pr(X_\Sigma < x)$ is readily computed by using $F_{X_\Sigma}(x) = \int_{-\infty}^x p_{X_\Sigma}(u) du$, where utilizing (67) yields

$$F_{X_\Sigma}(x) = \frac{1}{2\pi j} \int_{c-j\infty}^{c+j\infty} \left\{ \int_{-\infty}^x e^{su} du \right\} M_{X_\Sigma}(s) ds \quad (73)$$

within the existence region $-S_0 < \Re\{s\} < S_0$. Accordingly, using $\int_{-\infty}^x e^{su} du = e^{sx}/s$ for $\Re\{s\} > 0$ [148, Eq. (3.310)], (73) can be easily rewritten as

$$F_{X_\Sigma}(x) = \frac{1}{2\pi j} \int_{c-j\infty}^{c+j\infty} \frac{\Gamma(s)}{\Gamma(1+s)} M_{X_\Sigma}(s) ds \quad (74)$$

within the existence region $0 < \Re\{s\} < S_0$. Finally, using the mathematical formalism given in [164, Eq. (3.1)] results in (72), which proves Theorem 8. ■

The CDF of X_Σ is depicted in Fig. 3b for different number of variables. Note that for $\nu_\ell \in \mathbb{Z}^+$ and $\lambda_\ell \neq \lambda_m$ for all $\ell \neq m$, (72) reduces by using (68) with Theorem 2 as follows

$$F_{X_\Sigma}(x) = \sum_{\ell=1}^L \sum_{m=0}^{\nu_\ell-1} w_{\ell m} Q_{\nu_\ell-m} \left(\frac{x - \mu_\Sigma}{\sigma_\Sigma} \right). \quad (75)$$

For $\lambda_\ell = \lambda$ with distinct ν_ℓ and σ_ℓ^2 for $\ell = 1, 2, \dots, n$, (57) certainly follows a McLeish distribution whose PDF is already obtained in (69), and whose CDF is then deduced as

$$F_{X_\Sigma}(x) = Q_{\nu_\Sigma} \left(\frac{x - \mu_\Sigma}{\sigma_\Sigma} \right). \quad (76)$$

Further, the other special cases for $\nu_\ell \rightarrow 0$, $\nu_\ell \rightarrow 1$ and $\nu_\ell \rightarrow \infty$ are herein ignored since being well-predicted utilizing the results that are previously obtained above.

Theorem 9. *The n th moment of (57) is given by*

$$\mathbb{E}[X_\Sigma^n] = \sum_{k_1+k_2+\dots+k_L=n} \frac{n!}{\prod_{\ell=1}^L k_\ell!} \prod_{\ell=1}^L \mathbb{E}[X_\ell^{k_\ell}], \quad (77)$$

where $\mathbb{E}[X_\ell^n]$ is given in (30)

Proof. The proof is obvious by applying multinomial expansion [147, Eq. (24.1.2)] on $\mathbb{E}[X_\Sigma^n] = \mathbb{E}[(\sum_{\ell=1}^n X_\ell)^n]$. ■

For the statistical characterization of a McLeish distribution, such as its central tendency, dispersion, skewness and Kurtosis, (77) can be easily used, and its special cases can be obtained by setting its parameters.

C. Complex and Circularly-Symmetric McLeish Distribution

Let $Z \sim \mathcal{CM}_\nu(\mu, \sigma^2)$ be a CCS distribution, defined as

$$Z \triangleq X_1 + jX_2, \quad (78)$$

which is also, as mentioned before, deduced as a vector $\mathbf{Z} \triangleq [X_1, X_2]^T$, where $X_1 \sim \mathcal{M}_{\nu_1}(\mu_1, \sigma^2)$ and $X_2 \sim \mathcal{M}_{\nu_2}(\mu_2, \sigma^2)$ are, without loss of generality, such two mutually correlated and identically distributed (*c.i.d.*) distributions that $\mu \triangleq \mu_1 + j\mu_2$ and $\nu \triangleq \nu_1 = \nu_2$.

Theorem 10. *Under the condition of being CCS, the definition of $Z \sim \mathcal{CM}_\nu(\mu, \sigma^2)$ can be decomposed as*

$$Z \triangleq \sqrt{G}Z_0 + \mu = \sqrt{G}(X_0 + jY_0) + \mu, \quad (79)$$

where $Z_0 \sim \mathcal{CN}(0, \sigma^2)$, $X_0 \sim \mathcal{N}(0, \sigma^2)$, $Y_0 \sim \mathcal{N}(0, \sigma^2)$, and $G \sim \mathcal{G}(\nu, 1)$.

Proof. By the definition of CCS random distributions [167], both $(Z - \mu)$ and $e^{j\phi}(Z - \mu)$ follow the same distribution for any rotation $\phi \in [-\pi, \pi)$. Accordingly, we affirm that the phase of Z around its mean μ is typically given by

$$\Phi \triangleq \arctan(X_1 - \mu_1, X_2 - \mu_2), \quad (80)$$

where $\arctan(\cdot, \cdot)$ denotes the two-argument inverse tangent function [149, Eq. (01.15.02.0001.01)], and Φ is uniformly distributed over $[-\pi, \pi)$ and independent of both X and Y (i.e., $\text{Cov}[\Phi, X_1] = 0$ and $\text{Cov}[\Phi, X_2] = 0$). Therefore, $W \triangleq \tan(\Phi)$ follows a zero-mean Cauchy distribution whose PDF is given by $f_W(w) = \pi^{-1}(1+w^2)^{-1}$ over $w \in \mathbb{R}$ [157], [159], [168]. Upon $Z_0 = X_0 + jY_0$, where $X_0 \sim \mathcal{N}(0, \sigma_Z^2/2)$ and $Y_0 \sim \mathcal{N}(0, \sigma_Z^2/2)$, Y_0/X_0 follows a Cauchy distribution with zero mean and unit variance. Accordingly, W is rewritten as

$$W = \frac{X_2 - \mu_2}{X_1 - \mu_1} = \frac{\sqrt{G}Y_0}{\sqrt{G}X_0}, \quad (81)$$

where without loss of generality, G will follow a non-negative distribution characterized by

$$\sqrt{G} = \frac{|X_1 - \mu_1|}{|X_0|} = \frac{|X_2 - \mu_2|}{|Y_0|}. \quad (82)$$

Utilizing [151, Eq. (2.9.19)] after performing absolute-value transformation on (25), we can deduce the PDF of $|X_1 - \mu_1|$ in terms of Fox's H function as follows

$$f_{|X_1 - \mu_1|}(x) = \frac{1}{\sqrt{\pi}\Gamma(\nu)} \text{H}_{0,2}^{2,0} \left[\frac{2x^2}{\lambda^2} \left| \begin{matrix} \text{---} \\ (0, 1), (\nu - \frac{1}{2}, 1) \end{matrix} \right. \right] \quad (83)$$

defined over $x \in \mathbb{R}_+$. Similarly, using [151, Eq. (2.9.4)], we can also deduce the PDF of $|X_0|$, that is

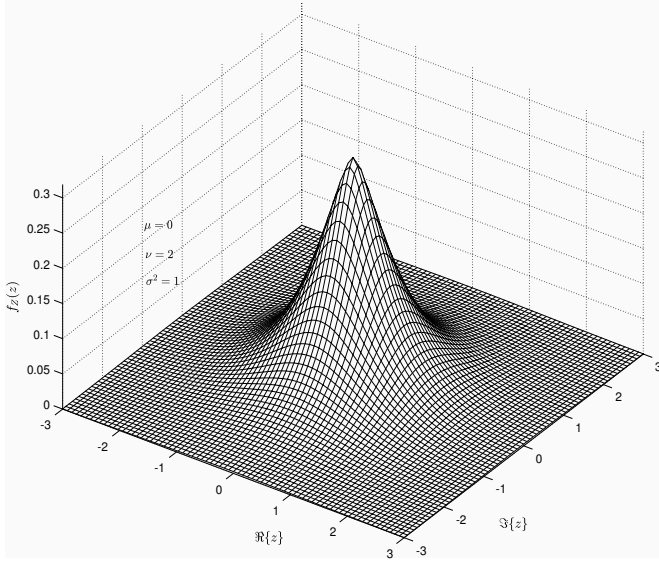
$$f_{|X_0|}(x) = \sqrt{\frac{2}{\pi\sigma^2}} \text{H}_{0,1}^{1,0} \left[\frac{x^2}{\sigma^2} \left| \begin{matrix} \text{---} \\ (0, 1) \end{matrix} \right. \right] \quad (84)$$

defined over $x \in \mathbb{R}_+$. Immediately, embedding both (83) and (84) within [169, Theorem 4.3] and thereon exercising [151, Eqs. (2.1.1), (2.1.4) and (2.1.4)], we derive the PDF of G as

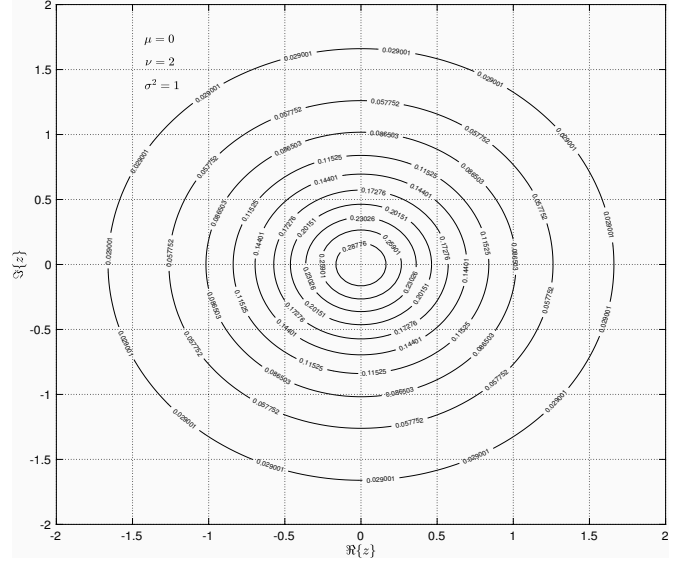
$$f_G(g) = \frac{\nu^\nu}{\Gamma(\nu)} g^{\nu-1} \exp(-\nu g), \quad (85)$$

defined over $g \in \mathbb{R}_+$. This consequence can also be reached from the ratio of $|X_2 - \mu_2|$ and $|Y_0|$ in conformity with (82). Eventually, with the aid of [3, Eq. (2.3-67)] and [1, Eqs. (2.20) and (2.21)], we notice that G is a non-negative distribution following Gamma (squared Nakagami- m) distribution. Therefore, $G \sim \mathcal{G}(\nu, 1)$, where the diversity figure is given by $\nu \triangleq \mathbb{E}[G]^2 / \text{Var}[G]$ [3, Eq. (2.3-69)] and the average power is by $\mathbb{E}[G] \triangleq 1$ [3, Eq. (2.3-68)]. Consequently, the definition of CCS McLeish distribution, given in (78), is rewritten as in (79), which proves Theorem 10. ■

With the aid of Theorem 10, the PDF of Z (i.e., the joint PDF $f_{\mathbf{Z}}(x, y)$ of \mathbf{Z}) is given in the following theorem.



(a) PDF illustration in complex space.



(b) PDF contour curves.

 Fig. 4: The PDF and contour of $\mathcal{CM}_\nu(0, \sigma^2)$ (i.e., the illustration of (86) for $\mu=0$).

Theorem 11. Under the condition of being CCS, the PDF of $Z \sim \mathcal{CM}_\nu(\mu, \sigma^2)$ is given by

$$f_Z(z) = \frac{2}{\pi} \frac{|z - \mu|^{\nu-1}}{\Gamma(\nu) \lambda^{\nu+1}} K_{\nu-1} \left(\frac{2|z - \mu|}{\lambda} \right), \quad (86)$$

defined over $z \in \mathbb{C}$, where the factor $\lambda = \sqrt{2\sigma^2/\nu}$.

Proof. Referring to Theorem 10, the PDF of $Z \sim \mathcal{CM}_\nu(\mu, \sigma^2)$ conditioned on G is therefore written as [3, Eq. (2.6-1)]

$$f_{Z|G}(z|g) = \frac{1}{\pi g \sigma^2} \exp \left(-\frac{1}{g} \left\langle \frac{z - \mu}{\sigma}, \frac{z - \mu}{\sigma} \right\rangle \right), \quad (87)$$

for $g \in \mathbb{R}_+$. In accordance, the PDF of Z can be expressed as $f_Z(z) = \int_0^\infty f_{Z|G}(z|g) f_G(g) dg$, where substituting (85) and (87), and subsequently employing [148, Eq. (3.471/9)] results in (86), which proves Theorem 11. ■

The PDF of $Z \sim \mathcal{CM}_\nu(\mu, \sigma^2)$ and its contour plot are well described in Fig. 4a and Fig. 4b, respectively. Further worth noting that the CS property of $Z \sim \mathcal{CM}_\nu(\mu, \sigma^2)$ is observed in Fig. 4b such that $\forall \theta \in [-\pi, \pi)$, $f_Z(z) = f_Z(z \exp(j\theta))$ for $\mu = 0$. Accordingly, for a given contour value $c \in \mathbb{R}_+$, the contours, presented in Fig. 4b, can be obtained by

$$(z|c) = \{z = \hat{\xi} \exp(j\theta) \mid \theta \in [-\pi, \pi), \text{ and} \\ \hat{\xi} = \arg \min_{\xi \in \mathbb{R}_+} \|f_Z^2(\xi) - c\|^2\}. \quad (88)$$

For consistency, let us now consider some special cases of Theorem 11. Substituting $\nu = 1$ into (86) yields the PDF of $\mathcal{CL}(\mu, \sigma^2)$ [170, Eq. (6)], that is

$$f_Z(z) = \frac{2}{\pi \lambda^2} K_0 \left(\frac{2}{\lambda} |z - \mu| \right). \quad (89)$$

Moreover, substituting $\nu \rightarrow \infty$ results in

$$f_Z(z) = \frac{1}{2\pi\sigma^2} \exp \left(-\frac{1}{2\sigma^2} |z - \mu|^2 \right), \quad (90)$$

which is the PDF of $\mathcal{CN}(\mu, \sigma^2)$ [3, Eq. (2.6-1)].

Theorem 12. Under the condition of being CCS, the CDF of $Z \sim \mathcal{CM}_\nu(\mu, \sigma^2)$ is given for the complex quadrants, that is

$$F_Z(z) = 1 - Q_\nu \left(\sqrt{2} \left\langle 1, \frac{z - \mu}{\sigma} \right\rangle \right) \\ - Q_\nu \left(\sqrt{2} \left\langle j, \frac{z - \mu}{\sigma} \right\rangle \right) \\ + \frac{1}{2} Q_\nu \left(\sqrt{2 \left\langle \frac{z - \mu}{\sigma}, \frac{z - \mu}{\sigma} \right\rangle \sin^2(\phi), \phi} \right) \\ + \frac{1}{2} Q_\nu \left(\sqrt{2 \left\langle \frac{z - \mu}{\sigma}, \frac{z - \mu}{\sigma} \right\rangle \cos^2(\phi), \frac{\pi}{2} - \phi} \right), \quad (91a)$$

for the upper right quadrant (i.e., $\Re\{z\} \geq 0$ and $\Im\{z\} \geq 0$);

$$F_Z(z) = Q_{\nu z} \left(\sqrt{2} \left\langle 1, \frac{\mu - z}{\sigma} \right\rangle \right) \\ - \frac{1}{2} Q_\nu \left(\sqrt{2 \left\langle \frac{z - \mu}{\sigma}, \frac{z - \mu}{\sigma} \right\rangle \sin^2(\phi), \phi} \right) \\ - \frac{1}{2} Q_\nu \left(\sqrt{2 \left\langle \frac{z - \mu}{\sigma}, \frac{z - \mu}{\sigma} \right\rangle \cos^2(\phi), \frac{\pi}{2} - \phi} \right), \quad (91b)$$

for the upper left quadrant (i.e., $\Re\{z\} < 0$ and $\Im\{z\} \geq 0$);

$$F_Z(z) = \frac{1}{2} Q_\nu \left(\sqrt{2 \left\langle \frac{z - \mu}{\sigma}, \frac{z - \mu}{\sigma} \right\rangle \sin^2(\phi), \phi} \right) \\ + \frac{1}{2} Q_\nu \left(\sqrt{2 \left\langle \frac{z - \mu}{\sigma}, \frac{z - \mu}{\sigma} \right\rangle \cos^2(\phi), \frac{\pi}{2} - \phi} \right), \quad (91c)$$

for the lower left quadrant (i.e., $\Re\{z\} < 0$ and $\Im\{z\} < 0$);

$$F_Z(z) = Q_{\nu z} \left(\sqrt{2} \left\langle j, \frac{\mu - z}{\sigma} \right\rangle \right) \\ - \frac{1}{2} Q_\nu \left(\sqrt{2 \left\langle \frac{z - \mu}{\sigma}, \frac{z - \mu}{\sigma} \right\rangle \sin^2(\phi), \phi} \right) \\ - \frac{1}{2} Q_\nu \left(\sqrt{2 \left\langle \frac{z - \mu}{\sigma}, \frac{z - \mu}{\sigma} \right\rangle \cos^2(\phi), \frac{\pi}{2} - \phi} \right), \quad (91d)$$

for the lower right quadrant (i.e., $\Re\{z\} \geq 0$ and $\Im\{z\} < 0$); where $\phi \in [0, \frac{\pi}{2})$ is given by $\phi \triangleq \arctan(|\Re\{z\}|, |\Im\{z\}|)$.

Proof. Note that the CDF of $Z_0 \sim \mathcal{CN}(0, \sigma^2)$ is defined by $F_{Z_0}(z_\ell|\sigma) \triangleq \Pr\{X_0 \leq \langle 1, z_\ell \rangle \cap Y_0 \leq \langle j, z_\ell \rangle | \sigma\}$ conditioned on σ . Utilizing [3, Eqs. (2.3-10) and (2.3-11)] and [1, Eqs. (4.3)] with $\langle 1, z \rangle = \Re\{z\}$ and $\langle j, z \rangle = \Im\{z\}$, $F_{Z_0}(z_\ell|\sigma)$ can be readily expressed for a certain $z = x + jy \in \mathbb{C}$ as follows

$$F_{Z_0}(z|\sigma) = 1 - Q(\sqrt{2}\langle 1, z/\sigma \rangle) - Q(\sqrt{2}\langle j, z/\sigma \rangle) + Q(\sqrt{2}\langle 1, z/\sigma \rangle) Q(\sqrt{2}\langle j, z/\sigma \rangle), \quad (92a)$$

for the upper right quadrant (i.e., $\Re\{z\} \geq 0$ and $\Im\{z\} \geq 0$);

$$F_{Z_0}(z|\sigma) = Q(-\sqrt{2}\langle 1, z/\sigma \rangle) - Q(-\sqrt{2}\langle 1, z/\sigma \rangle) Q(\sqrt{2}\langle j, z/\sigma \rangle), \quad (92b)$$

for the upper left quadrant (i.e., $\Re\{z\} < 0$ and $\Im\{z\} \geq 0$);

$$F_{Z_0}(z|\sigma) = Q(-\sqrt{2}\langle 1, z/\sigma \rangle) Q(-\sqrt{2}\langle j, z/\sigma \rangle), \quad (92c)$$

for the lower left quadrant (i.e., $\Re\{z\} < 0$ and $\Im\{z\} < 0$);

$$F_{Z_0}(z|\sigma) = Q(-\sqrt{2}\langle j, z/\sigma \rangle) - Q(\sqrt{2}\langle 1, z/\sigma \rangle) Q(-\sqrt{2}\langle j, z/\sigma \rangle), \quad (92d)$$

for the lower right quadrant (i.e., $\Re\{z\} \geq 0$ and $\Im\{z\} < 0$). Worth noticing that *the argument of all Gaussian Q-functions in (92) is positive*, so the well-known Craig's representation [1, Eq. (4.2)] and Simon-Divsalar's representation [1, Eq. (4.6)] can be easily utilized in all equations from (92a) to (92d). Then, referring (79), the CDF of $Z \sim \mathcal{CM}_\nu(\mu, \sigma^2)$ is explicitly written as $F_Z(z) \triangleq \int_0^\infty F_{Z_0}(z - \mu | \sqrt{g}\sigma) f_G(g) dg$, where substituting (85) yields

$$F_Z(z) = 1 - I_1(\sqrt{2}\langle 1, (z - \mu)/\sigma \rangle) - I_1(\sqrt{2}\langle j, (z - \mu)/\sigma \rangle) + I_2(\sqrt{2}\langle 1, (z - \mu)/\sigma \rangle, \langle j, (z - \mu)/\sigma \rangle), \quad (93a)$$

for the upper right quadrant (i.e., $\Re\{z\} \geq 0$ and $\Im\{z\} \geq 0$);

$$F_Z(z) = I_1(\sqrt{2}\langle 1, (\mu - z)/\sigma \rangle) - I_2(\sqrt{2}\langle 1, (\mu - z)/\sigma \rangle, \langle j, (z - \mu)/\sigma \rangle), \quad (93b)$$

for the upper left quadrant (i.e., $\Re\{z\} < 0$ and $\Im\{z\} \geq 0$);

$$F_Z(z) = I_2(\sqrt{2}\langle 1, (\mu - z)/\sigma \rangle, \langle j, (\mu - z)/\sigma \rangle), \quad (93c)$$

for the lower left quadrant (i.e., $\Re\{z\} < 0$ and $\Im\{z\} < 0$);

$$F_Z(z) = I_1(\sqrt{2}\langle j, (\mu - z)/\sigma \rangle) - I_2(\sqrt{2}\langle 1, (z - \mu)/\sigma \rangle, \langle j, (\mu - z)/\sigma \rangle), \quad (93d)$$

for the lower right quadrant (i.e., $\Re\{z\} \geq 0$ and $\Im\{z\} < 0$), where $I_1(x)$ and $I_2(x, y)$ are respectively defined as

$$I_1(x) = \int_0^\infty Q(\sqrt{x^2/g}) f_G(g) dg, \quad (94)$$

$$I_2(x, y) = \int_0^\infty Q(\sqrt{x^2/g}) Q(\sqrt{y^2/g}) f_G(g) dg, \quad (95)$$

for $x, y \in \mathbb{R}_+$. Eventually, substituting $Q(x) = \frac{1}{2} \operatorname{erfc}(x/\sqrt{2})$ [3, Eq. (2.3-18)] and [149, Eq. (06.27.26.0006.01)] into (94), and then using [151, Eqs. (2.8.4) and (2.9.1)], $I_1(x)$ results in

(46). In addition, substituting [171, Eq. (4.6) and (4.8)] into (95) and using [148, Eq. (3.471/9)], $I_2(x, y)$ is obtained as

$$I_2(x, y) = \frac{1}{2} Q_\nu(\sqrt{(x^2 + y^2) \sin(\phi)^2}, \phi) + \frac{1}{2} Q_\nu(\sqrt{(x^2 + y^2) \cos(\phi)^2}, \frac{\pi}{2} - \phi), \quad (96)$$

where $\phi = \arctan(x, y)$. Consequently, substituting $I_1(x)$ and $I_2(x, y)$ into (93) yields (91), which proves Theorem 12. ■

The CDF of $Z \sim \mathcal{CM}_\nu(\mu, \sigma^2)$ and its contour plot are well described in Fig. 5a and Fig. 5b, respectively. For a given contour value $c \in [0, 1)$, the contours, presented in Fig. 5b, can be obtained by

$$(z|c) = \{z = \hat{\xi} \exp(j\theta) \mid \theta \in [-\pi, \pi), \text{ and } \hat{\xi} = \arg \min_{\xi \in \mathbb{R}_+} \|F_Z^2(\xi) - c\|^2\}. \quad (97)$$

Theorem 13. *Under the condition of being CCS, the MGF of $Z \sim \mathcal{CM}_\nu(\mu, \sigma^2)$ is given by*

$$M_Z(s) = e^{-\langle s, \mu \rangle} \left(1 - \frac{\lambda^2}{8} \langle s, s \rangle\right)^{-\nu}, \quad (98)$$

where $s \triangleq s_X + js_Y \in \mathbb{C}$ within the existence region $s \in \mathbb{C}_0$, and the region \mathbb{C}_0 is given by $\mathbb{C}_0 \triangleq \{s \mid \langle s, s \rangle \leq 8/\lambda^2\}$.

Proof. The MGF of Z (i.e., the joint MGF $M_Z(s_X, s_Y)$ of \mathbf{Z}) is defined as $M_Z(s) \triangleq \mathbb{E}[\exp(-\langle s, Z \rangle)]$, where utilizing Theorem 10 yields

$$M_Z(s) = e^{\langle s, \mu \rangle} \int_0^\infty \mathbb{E}[\exp(-\langle s, \sqrt{g}Z_0 \rangle)] f_G(g) dg, \quad (99)$$

where $\mathbb{E}[\exp(-\langle s, \sqrt{g}Z_0 \rangle)]$ is the MGF of $\mathcal{CN}(0, g\sigma^2)$ given by $\exp(-g\frac{\sigma^2}{4} \langle s, s \rangle)$ [146], [157]–[159]. Then, substituting (85) into (99), we have

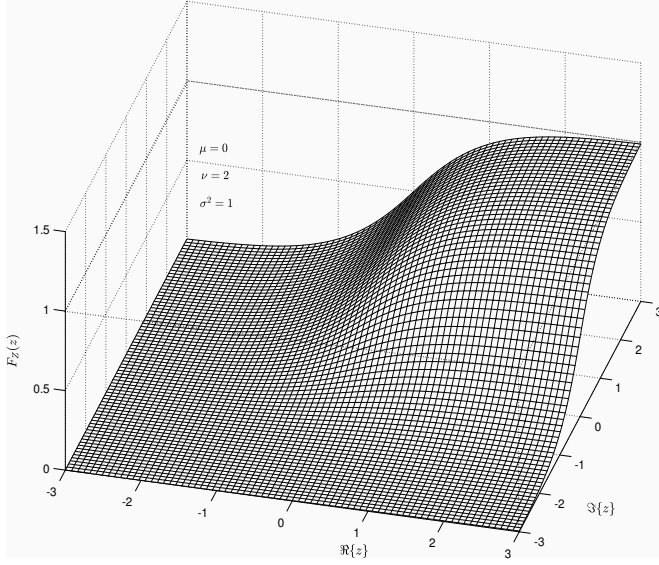
$$M_Z(s) = \frac{\nu^\nu e^{\langle s, \mu \rangle}}{\Gamma(\nu)} \int_0^\infty g^{\nu-1} e^{-g\nu(1 - \lambda^2 \langle s, s \rangle / 8)} dg. \quad (100)$$

Consequently, utilizing $\int_0^\infty x^{a-1} \exp(-bx) \triangleq b^{-a} \Gamma(a)$ for any $\Re\{a\}, \Re\{b\} > 0$ [148, Eq. (3.381/4)], and correspondingly in a certain existence region $1 - \lambda^2 \langle s, s \rangle / 8 > 0$, we simplify (100) into (98), which proves Theorem 13. ■

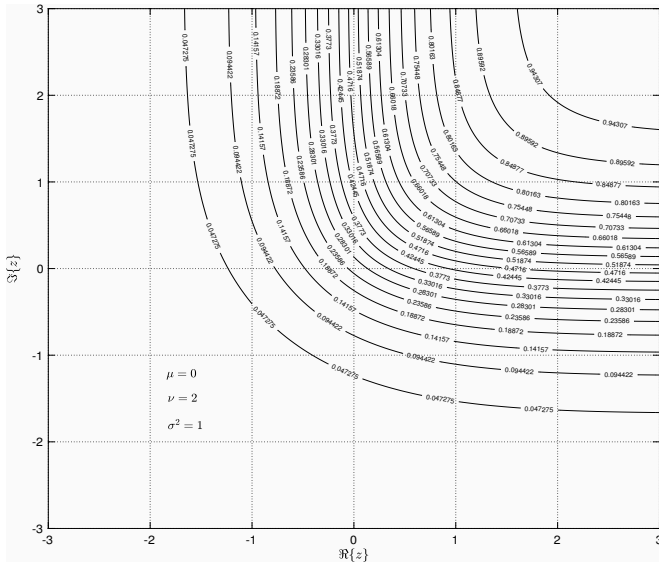
For consistency, setting $\nu \rightarrow 0$ simplifies (98) into the MGF of Dirac's distribution, that is $M_Z(s) = \exp(-\langle s, \mu \rangle)$. Further, setting $\nu = 1$ simplifies (98) into the MGF of $\mathcal{CL}(\mu, \sigma^2)$, that is $M_Z(s) = e^{-\langle s, \mu \rangle} (1 - \sigma^2 \langle s, s \rangle / 4)^{-1}$. In addition, setting the limit $\nu \rightarrow \infty$ on (98) and applying [148, Eq. (1.211/4)] results in $M_Z(s) = \exp(-\langle s, \mu \rangle - \frac{1}{4} \sigma^2 \langle s, s \rangle)$, which is the MGF of $\mathcal{CN}(\mu, \sigma^2)$ [146], [157]–[159] as expected.

For the purpose of achieving statistical characterization, the moment of $Z \sim \mathcal{CM}_\nu(\mu, \sigma^2)$ (i.e., the joint moment $\mathbb{E}[X_1^m X_2^n]$ of $\mathbf{Z} \triangleq [X_1, X_2]^T$ as referring to (78), where $m \in \mathbb{N}$ and $n \in \mathbb{N}$) are needed in a closed form, and for which the MGF is a very useful instrument [158, Eqs. (3.79) and (3.80)] as follows

$$\mathbb{E}[X_1^m X_2^n] = (-1)^{m+n} \frac{\partial^{m+n}}{\partial s_1^m \partial s_2^n} M_Z(s) \Big|_{s_1 \rightarrow 0, s_2 \rightarrow 0} \quad (101)$$



(a) CDF illustration in complex space.



(b) CDF contour curves.

 Fig. 5: The CDF and contour of $\mathcal{CM}_\nu(0, \sigma^2)$ (i.e., the illustration of (91) for $\mu=0$).

where $s = s_1 + js_2 \in \mathbb{C}$. Hence, replacing (98) into (101) and thereon applying two times the Leibniz's higher order derivative rule [148, Eq. (0.42)] yields (102) as shown below.

Theorem 14. *Under the condition of being CCS, the joint moment $\mathbb{E}[X_1^m X_2^n]$, $m, n \in \mathbb{N}$, of $Z \sim \mathcal{CM}_\nu(\mu, \sigma^2)$ is given as referring to (78) by*

$$\mathbb{E}[X_1^m X_2^n] = \mu_1^m \mu_2^n \sum_{k=0}^m \sum_{l=0}^n \binom{m}{k} \binom{n}{l} \Xi_{k,l} \frac{\lambda^{k+l}}{\mu_1^k \mu_2^l} \text{en}(k, l), \quad (102)$$

where $\text{en}(k, l) \triangleq \text{en}(k)\text{en}(l)$, and the weight $\Xi_{k,l}$ is defined as

$$\Xi_{k,l} = \sqrt{2^{k+l}} \left(\frac{1}{2}\right)_{k/2} \left(\frac{1}{2}\right)_{l/2} (\nu)_{(k+l)/2}. \quad (103)$$

where $(a)_n \triangleq a(a+1) \cdots (a+n-1)$ denotes Pochhammer's symbol (or shifted factorial) [147], [148].

Proof. Based on Theorem 10, the joint moment $\mathbb{E}[X_1^m X_2^n]$ can be readily rewritten as

$$\mathbb{E}[X_1^m X_2^n] = \mathbb{E}[(\sqrt{G}X_0 - \mu_1)^m (\sqrt{G}Y_0 - \mu_2)^n]. \quad (104)$$

Afterwards, applying binomial expansion on (104), we have

$$\mathbb{E}[X_1^m X_2^n] = \mu_1^m \mu_2^n \sum_{k=0}^m \sum_{l=0}^n \binom{m}{k} \binom{n}{l} \frac{1}{\mu_1^k \mu_2^l} \times \mathbb{E}[G^{\frac{k+l}{2}}] \mathbb{E}[X_0^k] \mathbb{E}[Y_0^l], \quad (105)$$

where substituting [3, Eq. (2.3-20)] and [1, Eq. (2.23)]

$$\mathbb{E}[X_0^n] = \mathbb{E}[Y_0^n] = \frac{\Gamma(1/2 + n)}{2\Gamma(1/2)} \sigma^2 \text{en}(n) \quad (106)$$

$$\mathbb{E}[G^n] = \frac{\Gamma(\nu + n)}{\Gamma(\nu) \nu^n}, \quad (107)$$

and then performing simple algebraic manipulations results in (102), which proves Theorem 14. \blacksquare

D. Complex and Elliptically-Symmetric McLeish Distribution

The bivariate Gaussian PDF has several beneficial and elegant properties and, for this reason, it is a conventionally used model in the literature. Regarding this fact while to have more than the previous subsection, we infer many such properties, so let us consider a more generalized case, i.e., that the mixture $Z \triangleq X_1 + jX_2$ follows a CES distribution whose inphase $X_1 \sim \mathcal{M}_{\nu_1}(\mu_1, \sigma_1^2)$ and quadrature $X_2 \sim \mathcal{M}_{\nu_2}(\mu_2, \sigma_2^2)$ are *c.i.d.* two distributions correlated by $\rho \in [-1, 1]$. It is denoted by $Z \sim \mathcal{EM}_\nu(\mu, \sigma^2, \rho)$, the mean is $\mu \triangleq \mu_1 + j\mu_2$, the normality is $\nu \triangleq \nu_1 = \nu_2$, the variance is $\sigma^2 \triangleq 2\sigma_1^2 = 2\sigma_2^2$, and the correlation is

$$\rho \triangleq \frac{\text{Cov}[X_1, X_2]}{\sqrt{\text{Var}[X_1]\text{Var}[X_2]}} = \frac{2}{\sigma^2} (\mathbb{E}[X_1 X_2] - \mu_{X_1} \mu_{X_2}). \quad (108)$$

Accordingly, we present the definition of the CES MacLeish distribution in the following theorem.

Theorem 15. *Under the condition of being CES, the definition of $Z \sim \mathcal{EM}_\nu(\mu, \sigma^2, \rho)$ can be decomposed as*

$$Z \triangleq \sqrt{G}Z_0 + \mu, \quad (109a)$$

$$= \sqrt{G}(X_0 + j(\rho X_0 + \sqrt{1-\rho^2}Y_0)) + \mu, \quad (109b)$$

where $Z_0 \sim \mathcal{EN}(0, \sigma^2, \rho)$, $X_0 \sim \mathcal{N}(0, \sigma_1^2)$ and $Y_0 \sim \mathcal{N}(0, \sigma_2^2)$. X_0 and Y_0 are i.i.d. random distributions (i.e., $2\sigma_1^2 = 2\sigma_2^2 = \sigma^2$). Further, $G \sim \text{Gamma}(\nu, 1)$.

Proof. Referring to Theorem 10, the correlation between the inphase and quadrature of $Z \sim \mathcal{EM}_\nu(\mu, \sigma^2, \rho)$ is certainly determined by that between the inphase and quadrature of $Z_0 \sim \mathcal{EN}(0, \sigma^2, \rho)$. For a certain correlation $\rho \in [-1, 1]$, the inphase and quadrature of $Z_0 \sim \mathcal{EN}(0, \sigma^2, \rho)$ are respectively written as

$$\Re\{Z_0\} = X_0 \quad (110)$$

$$\Im\{Z_0\} = \rho X_0 + \sqrt{1-\rho^2}Y_0, \quad (111)$$

such that $\text{Cov}[\Re\{Z_0\}, \Im\{Z_0\}] = \rho \sigma^2/2$ and $\text{Var}[\Re\{Z_0\}] = \text{Var}[\Im\{Z_0\}] = \sigma^2/2$. Accordingly, the correlation between the

inphase and quadrature of $Z \sim \mathcal{EM}_{\nu Z}(\mu_Z, \sigma_Z^2, \rho)$ is written in terms of that between $\Re\{Z_0\}$ and $\Im\{Z_0\}$, that is

$$\rho \triangleq \frac{\text{Cov}[X_1, X_2]}{\sqrt{\text{Var}[X_1]\text{Var}[X_2]}} = \frac{\text{Cov}[\Re\{Z_0\}, \Im\{Z_0\}]}{\sqrt{\text{Var}[\Re\{Z_0\}]\text{Var}[\Im\{Z_0\}]}}. \quad (112)$$

Accordingly, the proof is obvious. \blacksquare

With the aid of Theorem 15, the PDF of Z is given in the following theorem.

Theorem 16. *Under the condition of being CES, the PDF of $Z \sim \mathcal{EM}_{\nu}(\mu, \sigma^2, \rho)$ is given by*

$$f_Z(z) = \frac{2}{\pi\Gamma(\nu)} \frac{|z - \mu|_{\rho}^{\nu-1}}{\sqrt{1 - \rho^2} \lambda^{\nu+1}} K_{\nu-1} \left(\frac{2|z - \mu|_{\rho}}{\lambda} \right) \quad (113)$$

defined over $z \in \mathbb{C}$, where the deviation factor $\lambda = \sqrt{2\sigma^2/\nu}$.

Proof. With the aid of (113), the PDF of Z conditioned on G is readily written as [3, Eq.(2.3-78)]

$$f_{Z|G}(z|g) = \frac{1}{\pi g \sqrt{1 - \rho^2} \sigma^2} \exp\left(-\frac{|z - \mu|_{\rho}^2}{g\sigma^2}\right), \quad (114)$$

for $g \in \mathbb{R}_+$, where setting the correlation $\rho = 0$ yields into (87) as expected. Accordingly, the PDF of Z can be expressed as $f_Z(z) = \int_0^{\infty} f_{Z|G}(z|g) f_G(g) dg$. Then, the proof is obvious following the same steps in the proof of Theorem 11. \blacksquare

The PDF contour curves of $Z \sim \mathcal{CM}_{\nu}(\mu, \sigma^2)$ are clearly illustrated in Fig. 6 for $\rho = \pm 3/4$. In addition to them, let us consider the consistency of (113). Setting the correlation $\rho = 0$ yields (86) as expected. Furthermore, setting $\nu = 1$ reduces (113) to the PDF of CES Laplacian distribution, and equivalently so does $\nu \rightarrow \infty$ to the PDF of the bivariate correlated Gaussian distribution [3, Eq.(2.3-78)], whose inphase and quadrature are mutually correlated with $\rho \neq 0$. In contrast to the evidence that zero correlation implies independence between Gaussian distributions, the two uncorrelated McLeish distributions are not independent of each other unless $\nu \rightarrow \infty$. Eventually, having treated the correlation, it is useful to define the McLeish's bivariate Q-function with the aid of (113).

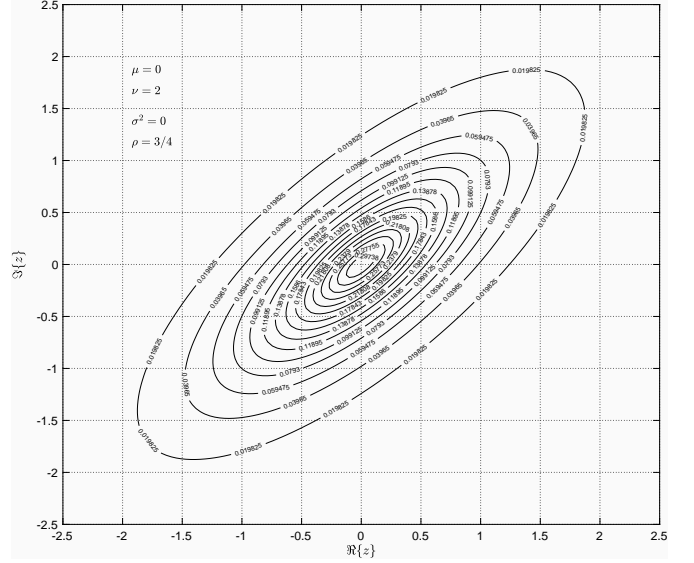
Definition 3 (McLeish's Bivariate Quantile). *The McLeish's bivariate Q-function is defined for $x \in \mathbb{R}$ and $y \in \mathbb{R}$ by*

$$Q_{\nu}(x, y, \rho) = \int_x^{\infty} \int_y^{\infty} \frac{2}{\pi\Gamma(\nu)} \frac{|z_{\ell}|_{\rho}^{\nu-1}}{\sqrt{1 - \rho^2} \lambda_0^{\nu+1}} \times K_{\nu-1} \left(\frac{2|z_{\ell}|_{\rho}}{\lambda_0} \right) dx_{\ell} dy_{\ell}, \quad (115)$$

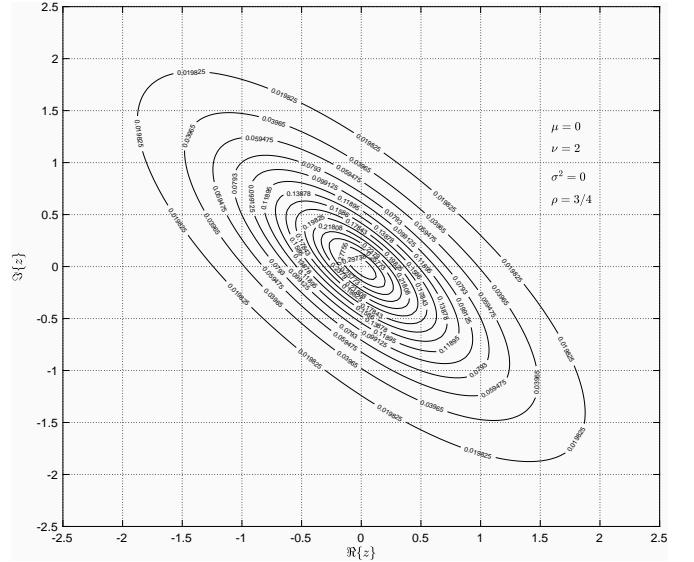
where $z_{\ell} = x_{\ell} + jy_{\ell} \in \mathbb{C}$.

Theorem 17. *Under the condition of being CES, the CDF of $Z \sim \mathcal{EM}_{\nu Z}(\mu, \sigma^2, \rho)$ is given by*

$$F_Z(z) = 1 - Q_{\nu} \left(\sqrt{2} \left\langle 1, \frac{z - \mu}{\sigma} \right\rangle \right) - Q_{\nu} \left(\sqrt{2} \left\langle j, \frac{z - \mu}{\sigma} \right\rangle \right) + Q_{\nu} \left(\sqrt{2} \left\langle 1, \frac{z - \mu}{\sigma} \right\rangle, \sqrt{2} \left\langle j, \frac{z - \mu}{\sigma} \right\rangle, \rho \right), \quad (116a)$$



(a) The contour curves for $\rho = 3/4$.



(b) The contour curves for $\rho = -3/4$.

Fig. 6: The PDF contour curves of $\mathcal{EM}_{\nu}(0, \sigma^2, \rho)$ (i.e., the illustration of (113) for $\mu = 0$).

for the upper right quadrant (i.e., $\Re\{z\} \geq 0$ and $\Im\{z\} \geq 0$);

$$F_Z(z) = Q_{\nu} \left(\sqrt{2} \left\langle 1, \frac{\mu - z}{\sigma} \right\rangle \right) - Q_{\nu} \left(\sqrt{2} \left\langle 1, \frac{\mu - z}{\sigma} \right\rangle, \sqrt{2} \left\langle j, \frac{z - \mu}{\sigma} \right\rangle, \rho \right), \quad (116b)$$

for the upper left quadrant (i.e., $\Re\{z\} < 0$ and $\Im\{z\} \geq 0$);

$$F_Z(z) = Q_{\nu} \left(\sqrt{2} \left\langle 1, \frac{\mu - z}{\sigma} \right\rangle, \sqrt{2} \left\langle j, \frac{\mu - z}{\sigma} \right\rangle, \rho \right), \quad (116c)$$

for the lower left quadrant (i.e., $\Re\{z\} < 0$ and $\Im\{z\} < 0$);

$$F_Z(z) = Q_{\nu} \left(\sqrt{2} \left\langle j, \frac{\mu - z}{\sigma} \right\rangle \right) - Q_{\nu} \left(\sqrt{2} \left\langle 1, \frac{z - \mu}{\sigma} \right\rangle, \sqrt{2} \left\langle j, \frac{\mu - z}{\sigma} \right\rangle, \rho \right), \quad (116d)$$

for the lower right quadrant (i.e., $\Re\{z\} \geq 0$ and $\Im\{z\} < 0$).

Proof. Note that the CDF of $Z_0 \sim \mathcal{EN}(0, \sigma_Z^2, \rho)$ is defined by $F_{Z_0}(z_\ell | \sigma_Z) \triangleq \Pr\{X_0 \leq \langle 1, z_\ell \rangle \cap Y_0 \leq \langle j, z_\ell \rangle | \sigma_Z\}$ conditioned on σ_Z and expressed for a certain $z = x + jy \in \mathbb{C}$ as

$$F_{Z_0}(z | \sigma_Z) = \int_{-\infty}^x \int_{-\infty}^y \frac{\exp(-\langle z_\ell, z_\ell \rangle_\rho / \sigma^2)}{\pi \sigma^2 \sqrt{1 - \rho^2}} dx_\ell dy_\ell, \quad (117)$$

where $z_\ell = x_\ell + jy_\ell \in \mathbb{C}$. Utilizing [3, Eqs. (2.3-10) and (2.3-11)] and [1, Eqs. (4.3)] with $\langle 1, z \rangle = \Re\{z\}$ and $\langle j, z \rangle = \Im\{z\}$, (117) simplifies for the quadrants of complex plane, that is

$$F_{Z_0}(z | \sigma) = 1 - Q(\sqrt{2}\langle 1, z/\sigma \rangle) - Q(\sqrt{2}\langle j, z/\sigma \rangle) + Q(\sqrt{2}\langle 1, z/\sigma \rangle, \sqrt{2}\langle j, z/\sigma \rangle, \rho), \quad (118a)$$

for the upper right quadrant (i.e., $\Re\{z\} \geq 0$ and $\Im\{z\} \geq 0$);

$$F_{Z_0}(z | \sigma) = Q(\sqrt{2}\langle j, z/\sigma \rangle) - Q(-\sqrt{2}\langle 1, z/\sigma \rangle, \sqrt{2}\langle j, z/\sigma \rangle, \rho), \quad (118b)$$

for the upper left quadrant (i.e., $\Re\{z\} < 0$ and $\Im\{z\} \geq 0$);

$$F_{Z_0}(z | \sigma) = Q(-\sqrt{2}\langle 1, z/\sigma \rangle, -\sqrt{2}\langle j, z/\sigma \rangle, \rho), \quad (118c)$$

for the lower left quadrant (i.e., $\Re\{z\} < 0$ and $\Im\{z\} < 0$);

$$F_{Z_0}(z | \sigma) = Q(\sqrt{2}\langle 1, z/\sigma \rangle) - Q(\sqrt{2}\langle 1, z/\sigma \rangle, -\sqrt{2}\langle j, z/\sigma \rangle, \rho), \quad (118d)$$

for the lower right quadrant (i.e., $\Re\{z\} \geq 0$ and $\Im\{z\} < 0$). Accordingly, referring to (109a), the CDF of $Z \sim \mathcal{CM}_\nu(\mu, \sigma^2, \rho)$ is explicitly written as $F_Z(z) \triangleq \int_0^\infty F_{Z_0}(z - \mu | \sqrt{g}\sigma) f_G(g) dg$. With the aid of Theorem 12, we rewrite (36) and (115) as

$$Q_\nu(x) = \int_0^\infty Q(\sqrt{2gx}) f_G(g) dg, \quad (119)$$

$$Q_\nu(x, y, \rho) = \int_0^\infty Q(\sqrt{2gx}, \sqrt{2gy}, \rho) f_G(g) dg, \quad (120)$$

the CDF $F_Z(z)$ is readily obtained as (116), which completes the proof of Theorem 17. ■

Theorem 18. *Under the condition of being CES, the MGF of $Z \sim \mathcal{EM}_\nu(\mu, \sigma^2, \rho)$ is given by*

$$M_Z(s) = e^{-(s, \mu)} \left(1 - \frac{\lambda^2}{8} (1 - \rho^2) \langle s, s \rangle_{-\rho}\right)^{-\nu}, \quad (121)$$

where $s \triangleq s_X + js_Y \in \mathbb{C}$ within the existence region $s \in \mathbb{C}_0$, and the region \mathbb{C}_0 is given by

$$\mathbb{C}_0 \triangleq \left\{s \mid \lambda^2 (1 - \rho^2) \langle s, s \rangle_{-\rho} \leq 8\right\}. \quad (122)$$

Proof. Note that, referring to Theorem 15, the MGF of $Z \sim \mathcal{EM}_\nu(\mu, \sigma^2, \rho)$ conditioned on G is written as

$$M_{Z|G}(s|g) = \exp\left(-\langle s, \mu \rangle + \frac{g}{4} \sigma^2 (1 - \rho^2) \langle s, s \rangle_{-\rho}\right). \quad (123)$$

Then, performing the almost same steps followed in the proof of Theorem 13, the MGF of $Z \sim \mathcal{EM}_\nu(\mu, \sigma^2, \rho)$ is obtained as (121), which completes the proof of Theorem 18. ■

E. Multivariate McLeish Distribution

In this subsection, we deal with random vectors instead of just individual random distributions, and we define multivariate McLeish distribution and derive its statistical characterization. For that purpose, we begin with a vector of independent McLeish distributions and work ourselves up to the general case where they are no longer mutually independent. Let us start with a vector that consists of *uncorrelated and identically distributed* random distributions of the same family, that is

$$\mathbf{S} \triangleq [S_1, S_2, \dots, S_L]^T, \quad (124)$$

where S_ℓ denotes a random distribution with zero mean and unit variance, i.e., $\mathbb{E}[S_\ell] = 0$ and $\mathbb{V}[S_\ell] = 1$, $1 \leq \ell \leq L$ such that any pair of S_k and S_ℓ , $k \neq \ell$ must be uncorrelated (i.e., $\mathbb{E}[S_k S_\ell] = 0$). Hence, the mean vector $\boldsymbol{\mu} \triangleq \mathbb{E}[\mathbf{S}]$ is given by

$$\boldsymbol{\mu} = [0, 0, \dots, 0]^T, \quad (125)$$

and the covariance matrix $\boldsymbol{\Sigma} \triangleq \mathbb{E}[\mathbf{S}\mathbf{S}^T]$ is given by

$$\boldsymbol{\Sigma} = \begin{bmatrix} 1 & 0 & \dots & 0 \\ 0 & 1 & \dots & 0 \\ \vdots & \vdots & \ddots & \vdots \\ 0 & 0 & \dots & 1 \end{bmatrix}. \quad (126)$$

By definition of standard multivariate distribution [172]–[176], \mathbf{S} follows a standard multivariate distribution with zero mean vector and unit covariance matrix iff $\forall \mathbf{a} \in \mathbb{R}^L$, $\mathbf{a}^T \mathbf{S}$ follows a random distribution of the same family with zero mean and $\mathbf{a}^T \mathbf{a}$ variance. Accordingly, in case of that all marginal distributions $S_\ell \sim \mathcal{M}_{\nu_\ell}(0, 1)$, $1 \leq \ell \leq L$, if \mathbf{S} follows a standard multivariate McLeish distribution with zero mean vector and unit covariance matrix, $\mathbf{a}^T \mathbf{S}$ should have to follow a McLeish distribution with zero mean and $\mathbf{a}^T \mathbf{a}$ variance, which surely imposes that there must be a condition among ν_ℓ , $1 \leq \ell \leq L$. By the uniqueness property of MGF [177], we know that the MGF of $\mathbf{a}^T \mathbf{S}$ has to be in the same form of the MGF of $S_\ell \sim \mathcal{M}_{\nu_\ell}(0, 1)$ for all $1 \leq \ell \leq L$. With the aid of Theorem 5, the MGF of $\mathbf{a}^T \mathbf{S}$, i.e., $M_{\mathbf{a}^T \mathbf{S}}(s) \triangleq \mathbb{E}[\exp(-s \mathbf{a}^T \mathbf{S})]$ can be written as the product of the MGFs of all marginal distributions $S_\ell \sim \mathcal{M}_{\nu_\ell}(0, 1)$ for all $1 \leq \ell \leq L$, that is $M_{\mathbf{a}^T \mathbf{S}}(s) = \prod_{\ell=1}^L (1 - \frac{1}{4} \lambda_\ell^2 s^2)^{-\nu_\ell}$ with $\lambda_\ell = \sqrt{2a_\ell^2 / \nu_\ell}$. When the all component deviation factors are exactly the same (i.e., $\lambda_\ell = \lambda_\Sigma$, $1 \leq \ell \leq L$), we can rewrite it in the form of (52), that is $M_{\mathbf{a}^T \mathbf{S}}(s) = (1 - \frac{1}{4} \lambda_\Sigma^2 s^2)^{-\nu_\Sigma}$, where $\nu_\Sigma = \sum_{\ell=1}^L \nu_\ell$ and $\sigma_\Sigma^2 = \mathbf{a}^T \mathbf{a}$, and therefore $\lambda_\Sigma = \sqrt{2\sigma_\Sigma^2 / \nu_\Sigma}$. Eventually, we reach $\nu_\Sigma = L\nu_\ell$, $1 \leq \ell \leq L$, where each equality can be satisfied when and only when $\nu_\ell = \nu_k = \nu$ for any $\ell \neq k$. Consequently, \mathbf{S} follows a standard multivariate McLeish distribution iff $S_\ell \sim \mathcal{M}_\nu(0, 1)$ for all $1 \leq \ell \leq L$. There hence, each marginal distribution is decomposed as $S_\ell \triangleq \sqrt{G_\ell} N_\ell$ with $G_\ell \sim \mathcal{G}(\nu, 1)$ and $N_\ell \sim \mathcal{N}(0, 1)$ for all $1 \leq \ell \leq L$. Owing to preserving the being CS, any given pair of $S_k \sim \mathcal{M}_\nu(0, 1)$ and $S_\ell \sim \mathcal{M}_\nu(0, 1)$, $k \neq \ell$, must be uncorrelated, and what is more accordingly, $\Phi_{k,\ell} = \arctan(S_k, S_\ell)$ has to be uniformly distributed over $[-\pi, \pi)$ and independent of both S_k and S_ℓ . Referring to the proof of Theorem 10, we notice that G_ℓ , $1 \leq \ell \leq L$, are the same distribution (i.e., the correlation between any pair

of $G_k \sim \mathcal{G}(\nu, 1)$ and $G_\ell \sim \mathcal{G}(\nu, 1)$, $k \neq \ell$ is surely 1 without loss of generality), and thus \mathbf{S} certainly follows a CS standard multivariate distribution decomposed as

$$\mathbf{S} \triangleq \sqrt{G} \mathbf{N}, \quad (127)$$

where $\mathbf{N} \sim \mathcal{N}^L(\mathbf{0}, \mathbf{I})$. Therewith, we conclude that since any non-empty subset of multivariate Gaussian distribution follows a multivariate Gaussian distribution [172]–[176], the random vector $\mathbf{W} \triangleq [S_{k_1}, S_{k_2}, \dots, S_{k_K}]^T$ constructed from \mathbf{S} for a subset $\{k_1, k_2, \dots, k_K\}$ of $\{1, 2, \dots, L\}$ with cardinal $K \leq L$ follows a standard multivariate CS McLeish distribution. Eventually, the PDF of standard multivariate CS McLeish distribution denoted by $\mathbf{S} \sim \mathcal{M}_\nu^L(\mathbf{0}, \mathbf{I})$ is given in the following theorem.

Theorem 19. *The PDF of $\mathbf{S} \sim \mathcal{M}_\nu^L(\mathbf{0}, \mathbf{I})$ is given by*

$$f_{\mathbf{S}}(\mathbf{x}) = \frac{2}{\sqrt{\pi^L} \Gamma(\nu) \lambda_0^{\nu+L/2}} K_{\nu-L/2} \left(\frac{2}{\lambda_0} \|\mathbf{x}\| \right), \quad (128)$$

for a certain $\mathbf{x} \triangleq [x_1, x_2, \dots, x_L]^T \in \mathbb{R}^L$.

Proof. Referring to (127), the PDF of \mathbf{S} conditioned on G , i.e., $f_{\mathbf{S}|G}(\mathbf{x}|g)$ can be readily written as [3, Eq. (2.3-74)]

$$f_{\mathbf{S}|G}(\mathbf{x}|g) = \frac{1}{(2\pi)^{L/2} g^{L/2}} \exp\left(-\frac{\|\mathbf{x}\|^2}{2g}\right), \quad (129)$$

for $g \in \mathbb{R}_+$. In accordance, the joint PDF $f_{\mathbf{S}}(\mathbf{x})$ can be readily expressed as $f_{\mathbf{S}}(\mathbf{x}) \triangleq \int_0^\infty f_{\mathbf{S}|G}(\mathbf{x}|g) f_G(g) dg$, that is

$$f_{\mathbf{S}}(\mathbf{x}) = \frac{1}{(2\pi)^{L/2}} \int_0^\infty \frac{1}{g^{L/2}} \exp\left(-\frac{\|\mathbf{x}\|^2}{2g}\right) f_G(g) dg, \quad (130)$$

where $f_G(g)$ denotes the PDF of $G \sim \mathcal{G}(\nu, 1)$ (i.e., given in (85)). Subsequently, using [148, Eq. (3.471/9)], (130) simplifies to (128), which proves Theorem 19. ■

Note that $\mathbf{S} \sim \mathcal{M}_\nu^L(\mathbf{0}, \mathbf{I})$ is termed as standard multivariate McLeish distribution which is a collection of identical standard McLeish distributions. As observed in Theorem 19, the PDF of $\mathbf{S} \sim \mathcal{M}_\nu^L(\mathbf{0}, \mathbf{I})$ is given by $f_{\mathbf{S}}(\mathbf{x})$, and it does only depend on the squared Euclidean distance $\|\mathbf{x}\|^2 \triangleq \mathbf{x}^T \mathbf{x}$ of \mathbf{x} from the origin. That is, there exists a circularly symmetry among all $S_\ell \sim \mathcal{M}_\nu(0, 1)$, $1 \leq \ell \leq L$. However, we cannot partition (128) into the product of the PDFs of marginal distributions even in spite of that they are uncorrelated. However, it simplifies to (25) for $L=1$ as expected. Furthermore, since an orthogonal transformation \mathbf{O} (i.e., $\mathbf{O}^T \mathbf{O} = \mathbf{O} \mathbf{O}^T = \mathbf{I}$) preserves the norm of any vector (i.e., $\|\mathbf{O}\mathbf{x}\| = \|\mathbf{x}\|$), we can immediately conclude $\mathbf{O}\mathbf{S} \sim \mathcal{M}_\nu^L(\mathbf{0}, \mathbf{I})$, which remarks that $\mathbf{S} \sim \mathcal{M}_\nu^L(\mathbf{0}, \mathbf{I})$ has the same distribution in any orthonormal basis. Geometrically, it is invariant to rotations and reflections and hence does not prefer any specific direction.

Definition 4 (McLeish's Multivariate Quantile and Complementary Quantile). *For a fixed $\mathbf{x} \in \mathbb{R}^L$ in higher dimensional space, the McLeish's multivariate Q-function is defined by*

$$Q_\nu^L(\mathbf{x}) = \int_{x_1}^\infty \int_{x_2}^\infty \dots \int_{x_L}^\infty \frac{2}{\sqrt{\pi^L} \Gamma(\nu) \lambda_0^{\nu+L/2}} \|\mathbf{u}\|^{\nu-L/2} \times K_{\nu-L/2} \left(\frac{2}{\lambda_0} \|\mathbf{u}\| \right) du_1 du_2 \dots du_L, \quad (131)$$

and the McLeish's multivariate complementary Q-function by

$$\widehat{Q}_\nu^L(\mathbf{x}) = \int_{-\infty}^{x_1} \int_{-\infty}^{x_2} \dots \int_{-\infty}^{x_L} \frac{2}{\sqrt{\pi^L} \Gamma(\nu) \lambda_0^{\nu+L/2}} \|\mathbf{u}\|^{\nu-L/2} \times K_{\nu-L/2} \left(\frac{2}{\lambda_0} \|\mathbf{u}\| \right) du_1 du_2 \dots du_L. \quad (132)$$

The CDF of $\mathbf{S} \sim \mathcal{M}_\nu^L(\mathbf{0}, \mathbf{I})$ is completely descriptive of the probability of that \mathbf{S} are less than or equal to \mathbf{x} , and defined by $F_{\mathbf{S}}(\mathbf{x}) \triangleq \Pr\{\mathbf{S} \leq \mathbf{x}\} = \Pr\{S_1 \leq x_1, S_2 \leq x_2, \dots, S_L \leq x_L\}$ and obtained in the following. It is worth noting the properties of the CDF $F_{\mathbf{S}}(\mathbf{x})$; $0 \leq F_{\mathbf{S}}(\mathbf{x}) \leq 1$, $F_{\mathbf{S}}(-\infty) = 0$, and $F_{\mathbf{S}}(\infty) = 1$. Furthermore, $F_{\mathbf{S}}(\mathbf{x})$ is a monotonically increasing function of \mathbf{x} , that is $F_{\mathbf{S}}(\mathbf{x}) \leq F_{\mathbf{S}}(\mathbf{x} + \Delta)$ for $\Delta \in \mathbb{R}_+$.

Theorem 20. *The CDF of $\mathbf{S} \sim \mathcal{M}_\nu^L(\mathbf{0}, \mathbf{I})$ is given by*

$$F_{\mathbf{S}}(\mathbf{x}) = \widehat{Q}_\nu^L(\mathbf{x}), \quad (133)$$

defined over $\mathbf{x} \in \mathbb{R}^L$.

Proof. The CDF of $\mathbf{S} \sim \mathcal{M}_\nu^L(\mathbf{0}, \mathbf{I})$ is readily given by $F_{\mathbf{S}}(\mathbf{x}) = \int_{-\infty}^{x_1} \int_{-\infty}^{x_2} \dots \int_{-\infty}^{x_L} f_{\mathbf{S}}(\mathbf{u}) du_1 du_2 \dots du_L$ defined over $\mathbf{x} \in \mathbb{R}^L$, where $f_{\mathbf{S}}(\mathbf{x})$ is given in (128). Therewith, exploiting (132), the proof is obvious. ■

Note that the C^2 DF of $\mathbf{S} \sim \mathcal{M}_\nu^L(\mathbf{0}, \mathbf{I})$ is also useful to derive especially when considering tail probabilities, and defined by $\widehat{F}_{\mathbf{S}}(\mathbf{x}) \triangleq \Pr\{\mathbf{S} > \mathbf{x}\} = \Pr\{S_1 > x_1, S_2 > x_2, \dots, S_L > x_L\}$ and obtained in the following. As opposite to the CDF, $\widehat{F}_{\mathbf{S}}(\mathbf{x})$ has the following properties: $0 \leq \widehat{F}_{\mathbf{S}}(\mathbf{x}) \leq 1$, $\widehat{F}_{\mathbf{S}}(-\infty) = 1$, and $\widehat{F}_{\mathbf{S}}(\infty) = 0$, and it is a monotonically decreasing function of \mathbf{x} , that is $\widehat{F}_{\mathbf{S}}(\mathbf{x}) \geq \widehat{F}_{\mathbf{S}}(\mathbf{x} + \Delta)$ for $\Delta \in \mathbb{R}_+$.

Theorem 21. *The C^2 DF of $\mathbf{S} \sim \mathcal{M}_\nu^L(\mathbf{0}, \mathbf{I})$ is given by*

$$\widehat{F}_{\mathbf{S}}(\mathbf{x}) = Q_\nu^L(\mathbf{x}), \quad (134)$$

defined over $\mathbf{x} \in \mathbb{R}^L$.

Proof. The proof is obvious following almost the same steps performed in the proof of Theorem 20. ■

Since any (non-empty) subset of multivariate McLeish distribution is a multivariate McLeish distribution, both the CDF and C^2 DF of any subset of multivariate McLeish distribution can be obtained by respectively using (133) and (133), where setting $x_\ell = 0$ for X_ℓ which is not in the subset of interest, i.e., the CDF of $S_1 \sim \mathcal{M}_\nu(0, 1)$ is $F_{S_1}(x) \triangleq F_{\mathbf{S}}([x, 0, \dots, 0]^T)$ and the corresponding C^2 DF is $\widehat{F}_{S_1}(x) \triangleq \widehat{F}_{\mathbf{S}}([x, 0, \dots, 0]^T)$, which are respectively as expected the special case of (37) and (51) with zero mean and unit variance. Besides, in the case of the bivariate distribution of any pair of S_k and S_ℓ , $k \neq \ell$, we readily obtain the bivariate CDF as follows $F_{S_k, S_\ell}(x_k, x_\ell) \triangleq F_{\mathbf{S}}([0, \dots, 0, x_k, 0, \dots, 0, x_\ell, 0, \dots, 0]^T)$ as expected. In the similar manner, the bivariate C^2 DF $\widehat{F}_{S_k, S_\ell}(x_k, x_\ell)$ can also be readily obtained using Theorem 21.

Theorem 22. *The MGF of $\mathbf{S} \sim \mathcal{M}_\nu^L(\mathbf{0}, \mathbf{I})$ is given by*

$$M_{\mathbf{S}}(\mathbf{s}) = \left(1 - \frac{\lambda_0^2}{4} \mathbf{s}^T \mathbf{s}\right)^{-\nu}, \quad (135)$$

for a certain $\mathbf{s} \in \mathbb{R}^L$ within the existence region $\mathbf{s} \in \mathbb{C}_0$, where the region \mathbb{C}_0 is given by

$$\mathbb{C}_0 \triangleq \left\{ \mathbf{s} \mid \lambda_0^2 \mathbf{s}^T \mathbf{s} \leq 4 \right\}. \quad (136)$$

Proof. The MGF of $\mathbf{S} \sim \mathcal{M}_\nu^L(\mathbf{0}, \mathbf{I})$ is described by $M_{\mathbf{S}}(\mathbf{s}) \triangleq \mathbb{E}[\exp(-\mathbf{s}^T \mathbf{S})] = \int_{-\infty}^{\infty} \cdots \int_{-\infty}^{\infty} \exp(-\mathbf{s}^T \mathbf{x}) f_{\mathbf{S}}(\mathbf{x}) dx_1 \dots dx_L$, where substituting (130) yields

$$M_{\mathbf{S}}(\mathbf{s}) = \int_0^{\infty} \frac{1}{g^{L/2}} I(g) f_G(g) dg, \quad (137)$$

where $f_G(g)$ denotes the PDF of $G \sim \mathcal{G}(\nu, 1)$ (i.e., given in (85)) and $I(g)$ is given by

$$I(g) = \int_{-\infty}^{\infty} \cdots \int_{-\infty}^{\infty} \frac{e^{-\frac{1}{2g}(\|\mathbf{x}\|^2 + g\mathbf{s}^T \mathbf{x})}}{(2\pi)^{L/2}} dx_1 \dots dx_L, \quad (138)$$

where achieving the equivalent of completing the square, i.e., substituting $\|\mathbf{x}\|^2 + 2g\mathbf{s}^T \mathbf{x} = \|\mathbf{x} + g\mathbf{s}\|^2 - g^2 \mathbf{s}^T \mathbf{s}$ readily results in $I(g) = \exp(\frac{g}{2} \mathbf{s}^T \mathbf{s})$. Accordingly, (137) simplifies with the aid of [148, Eq.(3.381/4)] to (135) with the convergence (136), which proves Theorem 22. ■

As similar to the CDF and C^2DF of the subset of multivariate McLeish distribution, the corresponding MGF is obtained utilizing (135). For instance, we can easily obtain the MGF of $S_1 \sim \mathcal{M}_\nu(0, 1)$ by means of $M_{S_1}(\mathbf{s}) \triangleq M_{\mathbf{S}}([s_1, 0, \dots, 0]^T) = (1 - \lambda_0^2 s_1^2/4)^{-\nu}$, which is consistent with (52) for zero mean and unit variance. Besides, in the case of the bivariate distribution of any given pair of S_k and S_ℓ , $k \neq \ell$, we readily obtain $M_{S_k, S_\ell}(s_k, s_\ell) \triangleq M_{\mathbf{S}}([0, \dots, 0, s_k, 0, \dots, 0, s_\ell, 0, \dots, 0]^T) = (1 - \lambda_0^2 (s_k^2 + s_\ell^2)/4)^{-\nu}$ as expected. It is lastly worth noting that these results and the ones given above are restricted to the case where all $S_\ell \sim \mathcal{M}_\nu(0, 1)$, $1 \leq \ell \leq L$, are identically distributed. A more general case is investigated in the following.

Let us have a vector of uncorrelated and non-identically distributed McLeish distributions, that is

$$\mathbf{X} \triangleq [X_1, X_2, \dots, X_L]^T, \quad (139)$$

where $X_\ell \sim \mathcal{M}_\nu(0, \sigma_\ell^2)$ for all $1 \leq \ell \leq L$, and any given pair of $X_k \sim \mathcal{M}_\nu(0, \sigma_k^2)$ and $X_\ell \sim \mathcal{M}_\nu(0, \sigma_\ell^2)$, $k \neq \ell$ are assumed uncorrelated (i.e., $\text{Cov}[X_k, X_\ell] = 0$). It is worth noticing that \mathbf{X} follows a multivariate McLeish distribution iff $\mathbf{a}^T \mathbf{X}$ for all $\mathbf{a} \in \mathbb{R}^L$ follows a McLeish distribution by the definition of multivariate distribution. Define $\boldsymbol{\sigma}^2 \triangleq [\sigma_1^2, \sigma_2^2, \dots, \sigma_L^2]^T$ consisting of variances of marginal distributions, and accordingly $\boldsymbol{\sigma} \triangleq [\sigma_1, \sigma_2, \dots, \sigma_L]^T$. Due to possessing $\text{Cov}[X_k, X_\ell] = 0$ for any $k \neq \ell$, \mathbf{X} can be decomposed as

$$\mathbf{X} \triangleq \text{diag}(\boldsymbol{\sigma}) \mathbf{S}. \quad (140)$$

Since $\boldsymbol{\sigma}^T \mathbf{S} \sim \mathcal{M}_\nu(0, \boldsymbol{\sigma}^T \boldsymbol{\sigma})$, the random vector \mathbf{X} certainly follows a multivariate elliptically symmetric (ES) McLeish distribution denoted by $\mathbf{X} \sim \mathcal{M}_\nu^L(\mathbf{0}, \text{diag}(\boldsymbol{\sigma}^2))$ with the PDF given in the following.

Theorem 23. *The PDF of $\mathbf{X} \sim \mathcal{M}_\nu^L(\mathbf{0}, \text{diag}(\boldsymbol{\sigma}^2))$ is given by*

$$f_{\mathbf{X}}(\mathbf{x}) = \frac{2}{\pi^{L/2}} \frac{\|\boldsymbol{\Lambda}^{-1} \mathbf{x}\|^{\nu-L/2}}{\Gamma(\nu) \det(\boldsymbol{\Lambda})} K_{\nu-L/2} \left(2 \|\boldsymbol{\Lambda}^{-1} \mathbf{x}\| \right) \quad (141)$$

for a certain $\mathbf{x} \triangleq [x_1, x_2, \dots, x_L]^T \in \mathbb{R}^L$, where $\boldsymbol{\Lambda} \triangleq \text{diag}(\boldsymbol{\lambda})$, and $\boldsymbol{\lambda} \triangleq \lambda_0 \boldsymbol{\sigma}$ denotes the component deviation vector.

Proof. Note that, referring to (140), we express $\mathbf{S} \sim \mathcal{M}_\nu^L(\mathbf{0}, \mathbf{I})$ with the aid of a linear transform, that is $\mathbf{S} = \text{diag}(\boldsymbol{\sigma})^{-1} \mathbf{X}$, and therefrom we notice the Jacobian $J_{\mathbf{X}|\mathbf{S}} = \det(\boldsymbol{\sigma})^{-1}$. Hence, we can write the PDF of \mathbf{X} as

$$f_{\mathbf{X}}(\mathbf{x}) = f_{\mathbf{S}}(\text{diag}(\boldsymbol{\sigma})^{-1} \mathbf{x}) J_{\mathbf{X}|\mathbf{S}}. \quad (142)$$

Further, defining the component deviation factor matrix as

$$\boldsymbol{\Lambda} \triangleq \lambda_0 \text{diag}(\boldsymbol{\sigma}) = \begin{bmatrix} \lambda_1 & 0 & \dots & 0 \\ 0 & \lambda_2 & \dots & 0 \\ \vdots & \vdots & \ddots & \vdots \\ 0 & 0 & \dots & \lambda_L \end{bmatrix}. \quad (143)$$

where $\lambda_\ell = \sqrt{2\sigma_\ell^2/\nu}$, $1 \leq \ell \leq L$, we directly acknowledge that $\text{diag}(\boldsymbol{\sigma})^{-1} = \lambda_0 \boldsymbol{\Lambda}^{-1}$ and $\det(\text{diag}(\boldsymbol{\sigma}))^{-1} = \lambda_0^L \det(\boldsymbol{\Lambda})^{-1}$. Finally, with these results, substituting (128) into (142) results in (141), which proves Theorem 23. ■

For consistency, accuracy, and clarity, setting $\text{diag}(\boldsymbol{\sigma}^2) \triangleq \boldsymbol{\sigma}^2 \mathbf{I}$ (i.e., making each component have equal power), we can readily reduce (141) to the PDF of $\mathbf{X} \sim \mathcal{M}_\nu^L(\mathbf{0}, \boldsymbol{\sigma}^2 \mathbf{I})$ given by

$$f_{\mathbf{X}}(\mathbf{x}) = \frac{2}{\pi^{L/2}} \frac{\|\mathbf{x}\|^{\nu-L/2}}{\Gamma(\nu) \lambda^{\nu+L/2}} K_{\nu-L/2} \left(\frac{2}{\lambda} \|\mathbf{x}\| \right) \quad (144)$$

where $\lambda \triangleq \sqrt{2\sigma^2/\nu}$ is the component deviation defined before.

Theorem 24. *The CDF of $\mathbf{X} \sim \mathcal{M}_\nu^L(\mathbf{0}, \text{diag}(\boldsymbol{\sigma}^2))$ is given by*

$$F_{\mathbf{X}}(\mathbf{x}) = \widehat{Q}_\nu^L(\lambda_0 \boldsymbol{\Lambda}^{-1} \mathbf{x}), \quad (145)$$

defined over $\mathbf{x} \in \mathbb{R}^L$.

Proof. Using (140) and $\text{diag}(\boldsymbol{\sigma})^{-1} = \lambda_0 \boldsymbol{\Lambda}^{-1}$, we have $\mathbf{S} \triangleq \lambda_0 \boldsymbol{\Lambda}^{-1} \mathbf{X}$. The proof is then obvious using Theorem 20. ■

Theorem 25. *The C^2DF of $\mathbf{X} \sim \mathcal{M}_\nu^L(\mathbf{0}, \text{diag}(\boldsymbol{\sigma}^2))$ is given by*

$$F_{\mathbf{X}}(\mathbf{x}) = Q_\nu^L(\lambda_0 \boldsymbol{\Lambda}^{-1} \mathbf{x}), \quad (146)$$

defined over $\mathbf{x} \in \mathbb{R}^L$.

Proof. The proof is obvious following almost the same steps performed in the proof of Theorem 24. ■

Theorem 26. *The MGF of $\mathbf{X} \sim \mathcal{M}_\nu^L(\mathbf{0}, \text{diag}(\boldsymbol{\sigma}^2))$ is given by*

$$M_{\mathbf{S}}(\mathbf{s}) = \left(1 - \frac{1}{4} \mathbf{s}^T \boldsymbol{\Lambda}^2 \mathbf{s} \right)^{-\nu}, \quad (147)$$

for a certain $\mathbf{s} \in \mathbb{R}^L$ within the existence region $\mathbf{s} \in \mathbb{C}_0$, where the region \mathbb{C}_0 is given by

$$\mathbb{C}_0 \triangleq \left\{ \mathbf{s} \mid \mathbf{s}^T \boldsymbol{\Lambda}^2 \mathbf{s} \leq 4 \right\}. \quad (148)$$

Proof. Note that, with the aid of (140), we can readily rewrite $M_{\mathbf{X}}(\mathbf{s}) \triangleq \mathbb{E}[\exp(-\mathbf{s}^T \mathbf{X})]$ as $M_{\mathbf{X}}(\mathbf{s}) = M_{\mathbf{S}}(\text{diag}(\boldsymbol{\sigma}) \mathbf{s})$. Then, using Theorem 22, $M_{\mathbf{X}}(\mathbf{s})$ is expressed as

$$M_{\mathbf{X}}(\mathbf{s}) = \left(1 - \frac{\lambda_0^2}{4} \mathbf{s}^T \text{diag}(\boldsymbol{\sigma})^2 \mathbf{s} \right)^{-\nu}, \quad (149)$$

within the region $\mathbb{C}_0 \triangleq \left\{ \mathbf{s} \mid \lambda_0^2 \mathbf{s}^T \text{diag}(\boldsymbol{\sigma})^2 \mathbf{s} \leq 4 \right\}$, where substituting (143) yields (147) within the region (148), which completes the proof of Theorem 26. ■

Due to the main importance of special cases for clarity and consistency, let us consider a special case in which $\sigma_\ell = \sigma$ for all $1 \leq \ell \leq L$. Appropriately, we can readily simplify (141) to (128), and accordingly, (145) to (133), (146) to (134), (147) to (135), as respectively expected. In addition, both the results and conclusions presented above are restricted only to the case, where McLeish distributions are assumed to be uncorrelated. Deducing statistical structures benefiting from these results, we investigate in the following the most general case in which McLeish distributions are assumed to be correlated and non-identically distributed.

Let us consider a vector of correlated and non-identically distributed (*c.n.i.d.*) McLeish distributions with $\boldsymbol{\mu}$ mean vector and $\boldsymbol{\Sigma}$ covariance matrix, that is

$$\mathbf{X} \triangleq [X_1, X_2, \dots, X_L], \quad (150)$$

where $X_\ell \sim \mathcal{M}_{\nu_\ell}(\mu_\ell, \sigma_\ell^2)$, $1 \leq \ell \leq L$. Accordingly, $\boldsymbol{\mu}$ is defined by $\boldsymbol{\mu} \triangleq \mathbb{E}[\mathbf{X}]$, that is

$$\boldsymbol{\mu} = [\mu_1, \mu_2, \dots, \mu_L]^T, \quad (151)$$

where $\mu_\ell \triangleq \mathbb{E}[X_\ell]$, $1 \leq \ell \leq L$. $\boldsymbol{\Sigma}$ is defined by $\boldsymbol{\Sigma} \triangleq \mathbb{E}[\mathbf{X}\mathbf{X}^T] - \boldsymbol{\mu}\boldsymbol{\mu}^T$, that is

$$\boldsymbol{\Sigma} = \begin{bmatrix} \sigma_{11} & \sigma_{12} & \dots & \sigma_{1L} \\ \sigma_{21} & \sigma_{22} & \dots & \sigma_{2L} \\ \vdots & \vdots & \ddots & \vdots \\ \sigma_{L1} & \sigma_{L2} & \dots & \sigma_{LL} \end{bmatrix}, \quad (152)$$

where $\sigma_{k\ell} \triangleq \text{Cov}[X_k, X_\ell] = \mathbb{E}[X_k X_\ell] - \mu_k \mu_\ell$ for $1 \leq k, \ell \leq L$. Note that the covariance matrix $\boldsymbol{\Sigma}$ is by construction a symmetric matrix, i.e., $\boldsymbol{\Sigma} = \boldsymbol{\Sigma}^T$. It is also a positive definite matrix, i.e., $\mathbf{x}^T \boldsymbol{\Sigma} \mathbf{x} \geq 0$ for all $\mathbf{x} \in \mathbb{R}^L$, which immediately implies that $\text{rank}(\boldsymbol{\Sigma}) = L$ and $\det(\boldsymbol{\Sigma}) \geq 0$, and therefrom $\min_{\mathbf{x}} \mathbf{x}^T \boldsymbol{\Sigma} \mathbf{x} = \text{Tr}(\boldsymbol{\Sigma})$. In terms of the entries $\sigma_{k\ell}$ of $\boldsymbol{\Sigma} \triangleq [\sigma_{k\ell}]_{L \times L}$, the preceding imposes the following necessary conditions:

- $\sigma_{k\ell} = \sigma_{\ell k}$, $1 \leq k, \ell \leq L$ (symmetry),
- $\sigma_{\ell\ell} > 0$ for all $1 \leq \ell \leq L$ since $\sigma_{\ell\ell} \triangleq \sigma_\ell^2$ which is the variance of X_ℓ (i.e., $\text{Var}[X_\ell] = \sigma_\ell^2$),
- $\sigma_{k\ell} \leq \sigma_{kk} \sigma_{\ell\ell}$ for all $1 \leq k, \ell \leq L$ due to Cauchy-Schwarz' inequality [178, Sec. 2.3].

Since $\boldsymbol{\Sigma}$ is a positive definite matrix, there is a certain triangular decomposition, which is known as Cholesky decomposition [179, Chap. 10], [180, Sec. 2.2], in reduced form of $\boldsymbol{\Sigma} = \mathbf{L}^T \mathbf{L}$ with a uniquely defined non-singular lower triangular matrix $\mathbf{L} \triangleq [L_{k\ell}]_{L \times L}$ such that $L_{\ell\ell} > 0$ for $1 \leq \ell \leq L$. Consequently, we are certain that \mathbf{L}^{-1} exists, and accordingly we indicate in the following the existence of multivariate McLeish distribution. By definition of multivariate distribution [172]–[176], \mathbf{X} follows a multivariate McLeish distribution iff

$$\mathbf{Y} \triangleq \mathbf{L}^{-1}(\mathbf{X} - \boldsymbol{\mu}) = [Y_1, Y_2, \dots, Y_L]^T, \quad (153)$$

jointly follows a multivariate McLeish distribution with zero mean vector and unit covariance matrix. As explained before Theorem 19, if $\mathbf{a}^T \mathbf{Y}$ for all vectors $\mathbf{a} \in \mathbb{R}_+$ follows a McLeish distribution, then we can declare that \mathbf{Y} follows a multivariate McLeish distribution. Therefore, $\nu_\ell = \nu$ for all $1 \leq \ell \leq L$ since circularity imposes that $\arctan(Y_k, Y_\ell)$, $k \neq \ell$ has to follow a uniform distribution over $[-\pi, \pi)$. By the virtue of both (127)

and (153), we find out $\mathbf{Y} \sim \mathcal{M}_\nu^L(\mathbf{0}, \mathbf{I})$, and therefore, we can decompose \mathbf{X} as

$$\mathbf{X} \triangleq \sqrt{G} \mathbf{N} + \boldsymbol{\mu}, \quad (154)$$

where $G \sim \mathcal{G}(\nu, 1)$, and $\mathbf{N} \sim \mathcal{N}^L(\mathbf{0}, \boldsymbol{\Sigma})$. In consequence, \mathbf{X} follows a multivariate ES McLeish distribution due to the both facts: (i) the types of all marginal distributions are the same, (ii) for any pair of $X_k \sim \mathcal{M}_\nu(\mu_k, \sigma_k^2)$ and $X_\ell \sim \mathcal{M}_\nu(\mu_\ell, \sigma_\ell^2)$, $k \neq \ell$, $\arctan((X_k - \mu_k)/\sigma_k, (X_\ell - \mu_\ell)/\sigma_\ell)$ follows uniform distribution over $[-\pi, \pi)$. Since it is uniquely determined by its mean vector, covariance matrix and normality, it is denoted by $\mathbf{X} \sim \mathcal{M}_\nu^L(\boldsymbol{\mu}, \boldsymbol{\Sigma})$, whose decomposition and PDF are obtained in the following.

Theorem 27. *If $\mathbf{X} \sim \mathcal{M}_\nu^L(\boldsymbol{\mu}, \boldsymbol{\Sigma})$, then it is decomposed as*

$$\mathbf{X} \triangleq \boldsymbol{\Sigma}^{1/2} \mathbf{S} + \boldsymbol{\mu}, \quad (155)$$

where $\mathbf{S} \sim \mathcal{M}_\nu^L(\mathbf{0}, \mathbf{I})$.

Proof. Note that, using [3, Eq. (??)], we can decompose $\mathbf{N} \sim \mathcal{N}^L(\mathbf{0}, \boldsymbol{\Sigma})$ as $\mathbf{N} \triangleq \boldsymbol{\Sigma}^{1/2} \mathbf{U}$, where $\mathbf{U} \sim \mathcal{N}^L(\mathbf{0}, \mathbf{I})$. Furthermore, with the aid of (127), we can also decompose $\mathbf{S} \sim \mathcal{M}_\nu^L(\mathbf{0}, \mathbf{I})$ as $\mathbf{S} \triangleq G \mathbf{U}$, where $G \sim \mathcal{G}(\nu, 1)$. Then, substituting these results into (154) yields (155), which proves Theorem 27. ■

Theorem 28. *The PDF of $\mathbf{X} \sim \mathcal{M}_\nu^L(\boldsymbol{\mu}, \boldsymbol{\Sigma})$ is given by*

$$f_{\mathbf{X}}(\mathbf{x}) = \frac{2}{\sqrt{\pi^L} \Gamma(\nu)} \frac{\|\mathbf{x} - \boldsymbol{\mu}\|_{\boldsymbol{\Sigma}}^{\nu-L/2}}{\sqrt{\det(\boldsymbol{\Sigma})} \lambda_0^{\nu+L/2}} \times K_{\nu-L/2} \left(\frac{2}{\lambda_0} \|\mathbf{x} - \boldsymbol{\mu}\|_{\boldsymbol{\Sigma}} \right), \quad (156)$$

defined over $\mathbf{x} \in \mathbb{R}^L$, where $\|\mathbf{x} - \boldsymbol{\mu}\|_{\boldsymbol{\Sigma}} \triangleq (\mathbf{x} - \boldsymbol{\mu})^T \boldsymbol{\Sigma}^{-1} (\mathbf{x} - \boldsymbol{\mu})$.

Proof. With the aid of Theorem 27, we readily recognize that $\mathbf{X} \sim \mathcal{M}_\nu^L(\boldsymbol{\mu}, \boldsymbol{\Sigma})$ is a linear transform of $\mathbf{S} \sim \mathcal{M}_\nu^L(\mathbf{0}, \mathbf{I})$. Hence, we can write $\mathbf{S} = \boldsymbol{\Sigma}^{-1/2}(\mathbf{X} - \boldsymbol{\mu})$ and therefrom immediately obtain its Jacobian $J_{\mathbf{X}|\mathbf{S}} = \det(\boldsymbol{\Sigma})^{-1/2}$ in order to express the PDF of \mathbf{X} in terms of the PDF of \mathbf{S} , that is

$$f_{\mathbf{X}}(\mathbf{x}) = f_{\mathbf{S}}(\boldsymbol{\Sigma}^{-1/2}(\mathbf{X} - \boldsymbol{\mu})) J_{\mathbf{X}|\mathbf{S}}. \quad (157)$$

where $f_{\mathbf{S}}(\mathbf{x})$ has been already given in (128). Finally, substituting (128) into (157) and utilizing the symmetry of $\boldsymbol{\Sigma}$ (i.e., $\boldsymbol{\Sigma} = \boldsymbol{\Sigma}^T$) with the results given above, we obtain (156), which completes the proof of Theorem 28. ■

Note that we can compute the CDF of $\mathbf{X} \sim \mathcal{M}_\nu^L(\boldsymbol{\mu}, \boldsymbol{\Sigma})$ as $F_{\mathbf{X}}(\mathbf{x}) \triangleq \Pr\{X_1 \leq x_1, X_2 \leq x_2, \dots, X_L \leq x_L\}$, and similarly, its C²DF as $\widehat{F}_{\mathbf{X}}(\mathbf{x}) \triangleq \Pr\{X_1 > x_1, X_2 > x_2, \dots, X_L > x_L\}$, and obtain them in the following.

Theorem 29. *The CDF of $\mathbf{X} \sim \mathcal{M}_\nu^L(\boldsymbol{\mu}, \boldsymbol{\Sigma})$ is given by*

$$F_{\mathbf{X}}(\mathbf{x}) = \widehat{Q}_\nu^L(\boldsymbol{\Sigma}^{-1/2}(\mathbf{X} - \boldsymbol{\mu})), \quad (158)$$

defined over $\mathbf{x} \in \mathbb{R}^L$.

²An alternative proof of Theorem 28 can be found as follows. According to (155), the PDF of \mathbf{X} conditioned on G , i.e., the conditional PDF $f_{\mathbf{X}|G}(\mathbf{x}|g)$ can be readily written as [3, Eq. (2.3-74)]

$$f_{\mathbf{X}|G}(\mathbf{x}|g) = \frac{1}{\sqrt{(2\pi)^L g^L \det(\boldsymbol{\Sigma})}} \exp\left(-\frac{\|\mathbf{x} - \boldsymbol{\mu}\|_{\boldsymbol{\Sigma}}^2}{2g}\right), \quad (\text{F-2.1})$$

for $g \in \mathbb{R}_+$. Then, performing the almost same steps followed in the proof of Theorem 19, the PDF $f_{\mathbf{X}}(\mathbf{x})$ is expressed as (156), which proves Theorem 28.

Proof. With the aid of Theorem 27, we have $\mathbf{S} = \boldsymbol{\Sigma}^{-1/2}(\mathbf{X} - \boldsymbol{\mu})$. Then, using (132), the proof is obvious. ■

Theorem 30. *The C^2DF of $\mathbf{X} \sim \mathcal{M}_\nu^L(\boldsymbol{\mu}, \boldsymbol{\Sigma})$ is given by*

$$\widehat{F}_{\mathbf{X}}(\mathbf{x}) = Q_\nu^L(\boldsymbol{\Sigma}^{-1/2}(\mathbf{X} - \boldsymbol{\mu})), \quad (159)$$

defined over $\mathbf{x} \in \mathbb{R}^L$.

Proof. The proof is obvious using Theorem 29. ■

As expected based on the mentioned above, the marginal CDF of $X_\ell \sim (\mu_\ell, \sigma_\ell^2)$ is given by $F_{X_\ell}(x_\ell) = F_{\mathbf{X}}(\infty, \dots, \infty, x_\ell, \infty, \dots, \infty)$. In the same manner, the bivariate CDF of X_k and X_ℓ , $k < \ell$, is derived as $F_{X_k, X_\ell}(x_k, x_\ell) = F_{\mathbf{X}}(\infty, \dots, \infty, x_k, \infty, \dots, \infty, x_\ell, \infty, \dots, \infty)$, which can be readily generalized for the case more than two marginal distributions. The same manner is also valid for the C^2DF .

We further note that the MGF of $\mathbf{X} \sim \mathcal{M}_\nu^L(\boldsymbol{\mu}, \boldsymbol{\Sigma})$, defined by $M_{\mathbf{X}}(\mathbf{s}) \triangleq \mathbb{E}[\exp(-\mathbf{s}^T \mathbf{X})]$, is obtained in the following.

Theorem 31. *The MGF of $\mathbf{X} \sim \mathcal{M}_\nu^L(\boldsymbol{\mu}, \boldsymbol{\Sigma})$ is given by*

$$M_{\mathbf{X}}(\mathbf{s}) = \exp(-\mathbf{s}^T \boldsymbol{\mu}) \left(1 - \frac{\lambda_0^2}{4} \mathbf{s}^T \boldsymbol{\Sigma} \mathbf{s}\right)^{-\nu}, \quad (160)$$

for a certain $\mathbf{s} \in \mathbb{R}^L$ within the existence region $\mathbf{s} \in \mathbb{C}_0$, where the region \mathbb{C}_0 is given by

$$\mathbb{C}_0 \triangleq \left\{ \mathbf{s} \mid \lambda_0^2 \mathbf{s}^T \boldsymbol{\Sigma} \mathbf{s} \leq 4 \right\}. \quad (161)$$

Proof. Using (155) with $M_{\mathbf{X}}(\mathbf{s}) \triangleq \mathbb{E}[\exp(-\mathbf{s}^T \mathbf{X})]$, we have

$$M_{\mathbf{X}}(\mathbf{s}) = \mathbb{E}[\exp(-\mathbf{s}^T (\boldsymbol{\Sigma}^{1/2} \mathbf{S} + \boldsymbol{\mu}))], \quad (162a)$$

$$= \exp(-\mathbf{s}^T \boldsymbol{\mu}) \mathbb{E}[\exp(-\mathbf{s}^T \boldsymbol{\Sigma}^{1/2} \mathbf{S})], \quad (162b)$$

$$= \exp(-\mathbf{s}^T \boldsymbol{\mu}) M_{\mathbf{S}}(\boldsymbol{\Sigma}^{1/2} \mathbf{s}), \quad (162c)$$

Eventually, substituting (135) into (162c) yields (160) with the existence region (161), which proves Theorem 31. ■

Given a non-singular covariance matrix $\boldsymbol{\Sigma}$, the correlation matrix \mathbf{P} can be expressed as

$$\mathbf{P} \triangleq \begin{bmatrix} 1 & \rho_{12} & \dots & \rho_{1L} \\ \rho_{21} & 1 & \dots & \rho_{2L} \\ \vdots & \vdots & \ddots & \vdots \\ \rho_{L1} & \rho_{L2} & \dots & 1 \end{bmatrix}, \quad (163a)$$

$$= \text{diag}(\boldsymbol{\sigma})^{-1} \boldsymbol{\Sigma} \text{diag}(\boldsymbol{\sigma})^{-1}, \quad (163b)$$

where for $1 \leq k, \ell \leq L$, $\rho_{k\ell} \in [-1, 1]$ denotes the correlation between X_k and X_ℓ , and it is defined by

$$\rho_{k\ell} \triangleq \frac{\text{Cov}[X_k, X_\ell]}{\sqrt{\text{Var}[X_k] \text{Var}[X_\ell]}} = \frac{\mathbb{E}[X_k X_\ell] - \mu_k \mu_\ell}{\sigma_k \sigma_\ell}. \quad (164)$$

³An alternative proof of Theorem 31 can be done using $\mathbf{X} = G \boldsymbol{\Sigma}^{1/2} \mathbf{N} + \boldsymbol{\mu}$ derived from (127) and (155). Thus, the MGF of \mathbf{X} conditioned on G is

$$M_{\mathbf{X}|G}(\mathbf{s}|g) = \exp\left(-\mathbf{s}^T \boldsymbol{\mu} + \frac{g}{2} \mathbf{s}^T \boldsymbol{\Sigma} \mathbf{s}\right), \quad (\text{F-3.1})$$

for $g \in \mathbb{R}_+$. In accordance, $M_{\mathbf{S}}(\mathbf{s}) \triangleq \int_0^\infty M_{\mathbf{S}|G}(\mathbf{s}|g) f_G(g) dg$ is written as

$$M_{\mathbf{S}}(\mathbf{s}) = \exp(-\mathbf{s}^T \boldsymbol{\mu}) \int_0^\infty \exp\left(\frac{g}{2} \mathbf{s}^T \boldsymbol{\Sigma} \mathbf{s}\right) f_G(g) dg, \quad (\text{F-3.2})$$

where $f_G(g)$ denotes the PDF of $G \sim \mathcal{G}(\nu, 1)$ (i.e., given in (85)). So, using [148, Eq. (3.381/4)], (F-3.2) simplifies to (160), which proves Theorem 31.

After using (163b), the inverse of $\boldsymbol{\Sigma}$ is readily rewritten as

$$\boldsymbol{\Sigma}^{-1} = \text{diag}(\boldsymbol{\sigma})^{-1} \mathbf{P}^{-1} \text{diag}(\boldsymbol{\sigma})^{-1}, \quad (165a)$$

$$= \lambda_0^2 \boldsymbol{\Lambda}^{-1} \mathbf{P}^{-1} \boldsymbol{\Lambda}^{-1} \quad (165b)$$

where $\boldsymbol{\Lambda} \triangleq \lambda_0 \text{diag}(\boldsymbol{\sigma})$. In case of $\boldsymbol{\Lambda} = \lambda \mathbf{I}$ with $\lambda = \sigma \lambda_0$, we have $\boldsymbol{\Sigma} = \sigma^2 \mathbf{P}$, and thus (156) simplifies to

$$f_{\mathbf{X}}(\mathbf{x}) = \frac{2}{\sqrt{\pi^L} \Gamma(\nu)} \frac{\|\mathbf{x} - \boldsymbol{\mu}\|_{\mathbf{P}}^{\nu-L/2}}{\sqrt{\det(\mathbf{P})} \lambda^{\nu+L/2}} \times K_{\nu-L/2}\left(\frac{2}{\lambda} \|\mathbf{x} - \boldsymbol{\mu}\|_{\mathbf{P}}\right). \quad (166)$$

Accordingly, we can readily simplify (158) to

$$F_{\mathbf{X}}(\mathbf{x}) = \widehat{Q}_\nu^L(\lambda_0 \mathbf{P}^{-1/2} \boldsymbol{\Lambda}^{-1/2}(\mathbf{X} - \boldsymbol{\mu})), \quad (167)$$

and (159) to

$$\widehat{F}_{\mathbf{X}}(\mathbf{x}) = Q_\nu^L(\lambda_0 \mathbf{P}^{-1/2} \boldsymbol{\Lambda}^{-1/2}(\mathbf{X} - \boldsymbol{\mu})), \quad (168)$$

and (160) to

$$M_{\mathbf{X}}(\mathbf{s}) = \exp(-\mathbf{s}^T \boldsymbol{\mu}) \left(1 - \frac{1}{4} \mathbf{s}^T \boldsymbol{\Lambda} \mathbf{P} \boldsymbol{\Lambda} \mathbf{s}\right)^{-\nu}, \quad (169)$$

In addition, in case of no correlation among marginal McLeish distributions (i.e., when $\mathbf{P} = \mathbf{I}$), we have the covariance matrix $\boldsymbol{\Sigma} = \boldsymbol{\Lambda}^2 / \lambda_0^2$. Accordingly, for zero mean $\boldsymbol{\mu} = \mathbf{0}$, we simplify (166) to (141), (167) to (145), (168) to (146), and (169) to (147), as respectively expected.

There are also, however, two notable properties of multivariate ES McLeish distributions to be explicitly considered: (i) any non-degenerate affine transform of $\mathbf{X} \sim \mathcal{M}_\nu^L(\boldsymbol{\mu}, \boldsymbol{\Sigma})$ is also a multivariate ES McLeish distribution, (ii) its conditional and marginal distributions are jointly multivariate ES McLeish distribution. The first property is given in the following.

Theorem 32. *If $\mathbf{X} \sim \mathcal{M}_\nu^L(\boldsymbol{\mu}, \boldsymbol{\Sigma})$ and if $\mathbf{Y} = \mathbf{B}\mathbf{X} + \mathbf{b}$, where $\text{rank}(\mathbf{B}) \leq L$, then $\mathbf{Y} \sim \mathcal{M}_\nu^L(\mathbf{B}\boldsymbol{\mu} + \mathbf{b}, \mathbf{B}\boldsymbol{\Sigma}\mathbf{B}^T)$.*

Proof. Using Theorem 27, we have $\mathbf{Y} = \mathbf{B}(\boldsymbol{\Sigma}^{1/2} \mathbf{S} + \boldsymbol{\mu}) + \mathbf{b}$, which can be rearranged as $\mathbf{Y} = \mathbf{B}\boldsymbol{\Sigma}^{1/2} \mathbf{S} + (\mathbf{B}\boldsymbol{\mu} + \mathbf{b})$ with $\mathbf{B}\boldsymbol{\mu} + \mathbf{b}$ mean vector and $\mathbf{B}\boldsymbol{\Sigma}\mathbf{B}^T$ covariance matrix. ■

As for the second property, the conditional distribution of $\mathbf{X} \sim \mathcal{M}_\nu^L(\boldsymbol{\mu}, \boldsymbol{\Sigma})$ is given in the following.

Theorem 33. *Let $\mathbf{X} \sim \mathcal{M}_\nu^L(\boldsymbol{\mu}, \boldsymbol{\Sigma})$ be $\mathbf{X} \triangleq [\mathbf{X}_1^T, \mathbf{X}_2^T]^T$ with $\mathbf{X}_1 \sim \mathcal{M}_{\nu_1}^{L_1}(\boldsymbol{\mu}_1, \boldsymbol{\Sigma}_{11})$ and $\mathbf{X}_2 \sim \mathcal{M}_{\nu_2}^{L_2}(\boldsymbol{\mu}_2, \boldsymbol{\Sigma}_{22})$, where $L = L_1 + L_2$, and $\boldsymbol{\mu}$ and $\boldsymbol{\Sigma}$ are respectively by*

$$\boldsymbol{\mu} = \begin{bmatrix} \boldsymbol{\mu}_1 \\ \boldsymbol{\mu}_2 \end{bmatrix}, \text{ and } \boldsymbol{\Sigma} = \begin{bmatrix} \boldsymbol{\Sigma}_{11} & \boldsymbol{\Sigma}_{12} \\ \boldsymbol{\Sigma}_{21} & \boldsymbol{\Sigma}_{22} \end{bmatrix}. \quad (170)$$

The conditional distribution of \mathbf{X}_1 given $\mathbf{X}_2 = \mathbf{x}_2$ is given by $\mathbf{X}_1 | \mathbf{X}_2 \sim \mathcal{M}_{\nu_1}^{L_1}(\boldsymbol{\mu}_1 + \boldsymbol{\Sigma}_{12} \boldsymbol{\Sigma}_{22}^{-1}(\mathbf{x}_2 - \boldsymbol{\mu}_2), \boldsymbol{\Sigma}_{11} - \boldsymbol{\Sigma}_{12} \boldsymbol{\Sigma}_{22}^{-1} \boldsymbol{\Sigma}_{21})$.

Proof. As substituting (127) in Theorem 27, we can decompose $\mathbf{X} \sim \mathcal{M}_\nu^L(\boldsymbol{\mu}, \boldsymbol{\Sigma})$ as follows

$$\mathbf{X} \triangleq \sqrt{G} \mathbf{N} = \sqrt{G} \begin{bmatrix} \mathbf{N}_1 \\ \mathbf{N}_2 \end{bmatrix} + \begin{bmatrix} \boldsymbol{\mu}_1 \\ \boldsymbol{\mu}_2 \end{bmatrix}, \quad (171)$$

with definitions of $\mathbf{X}_1 \triangleq \sqrt{G} \mathbf{N}_1 + \boldsymbol{\mu}_1$ and $\mathbf{X}_2 \triangleq \sqrt{G} \mathbf{N}_2 + \boldsymbol{\mu}_2$, where $G \sim \mathcal{G}(\nu, 1)$, $\mathbf{N}_1 \sim \mathcal{N}^{L_1}(\mathbf{0}, \boldsymbol{\Sigma}_{11})$ and $\mathbf{N}_2 \sim \mathcal{N}^{L_2}(\mathbf{0}, \boldsymbol{\Sigma}_{22})$. The conditional distribution of \mathbf{X}_1 given both $G = g$ and

$\mathbf{X}_2 = \mathbf{x}_2$ is therefore defined by the ratio between two multivariate Gaussian densities, that is $f_{\mathbf{X}_1|\mathbf{X}_2,G}(\mathbf{x}_1|\mathbf{x}_2,g) \triangleq f_{\mathbf{X}_1|G}(\mathbf{x}_1|g)/f_{\mathbf{X}_2|G}(\mathbf{x}_2|g)$ given by

$$f_{\mathbf{X}_1|\mathbf{X}_2,G}(\mathbf{x}_1|\mathbf{x}_2,g) = \frac{\sqrt{\det(\boldsymbol{\Sigma}_{22})}}{\sqrt{(2\pi g)^{L_1} \det(\boldsymbol{\Sigma})}} \times \exp\left(-\frac{1}{2g}(\|\mathbf{x} - \boldsymbol{\mu}\|_{\boldsymbol{\Sigma}}^2 - \|\mathbf{x}_2 - \boldsymbol{\mu}_2\|_{\boldsymbol{\Sigma}_{22}}^2)\right) \quad (172)$$

for $\mathbf{x} \triangleq [\mathbf{x}_1^T, \mathbf{x}_2^T]^T \in \mathbb{R}^L$, where $\|\mathbf{x} - \boldsymbol{\mu}\|_{\boldsymbol{\Sigma}}^2$ can be given by

$$\|\mathbf{x} - \boldsymbol{\mu}\|_{\boldsymbol{\Sigma}}^2 = \|\mathbf{x}_2 - \boldsymbol{\mu}_2\|_{\boldsymbol{\Sigma}_{22}}^2 + \|\mathbf{x}_1 - \boldsymbol{\mu}_1 - \boldsymbol{\Sigma}_{12}\boldsymbol{\Sigma}_{22}^{-1}\mathbf{x}_2\|_{\boldsymbol{\Sigma}_{11} - \boldsymbol{\Sigma}_{12}\boldsymbol{\Sigma}_{22}^{-1}\boldsymbol{\Sigma}_{21}}^2, \quad (173)$$

After substituting (173) in (172), the PDF of \mathbf{X}_1 given \mathbf{X}_2 is written as $f_{\mathbf{X}_1|\mathbf{X}_2}(\mathbf{x}_1|\mathbf{x}_2) = \int_0^\infty f_{\mathbf{X}_1|\mathbf{X}_2,G}(\mathbf{x}_1|\mathbf{x}_2,g)f_G(g)dg$. Accordingly, and pursuant to utilizing Theorem 28 with [148, Eq. (3.381/4)], the PDF of $\mathbf{X}_1|\mathbf{X}_2$ is obtained in the form of (156) with mean vector $\boldsymbol{\mu}_1 + \boldsymbol{\Sigma}_{12}\boldsymbol{\Sigma}_{22}^{-1}(\mathbf{x}_2 - \boldsymbol{\mu}_2)$ and covariance matrix $\boldsymbol{\Sigma}_{11} - \boldsymbol{\Sigma}_{12}\boldsymbol{\Sigma}_{22}^{-1}\boldsymbol{\Sigma}_{21}$. Then, the proof is obvious. ■

Note that, when $\boldsymbol{\Sigma}_{12} = \boldsymbol{\Sigma}_{21} = \mathbf{0}$, (173) reduces to

$$\|\mathbf{x} - \boldsymbol{\mu}\|_{\boldsymbol{\Sigma}}^2 = \|\mathbf{x}_1 - \boldsymbol{\mu}_1\|_{\boldsymbol{\Sigma}_{11}}^2 + \|\mathbf{x}_2 - \boldsymbol{\mu}_2\|_{\boldsymbol{\Sigma}_{22}}^2, \quad (174)$$

which implies that \mathbf{X}_1 and \mathbf{X}_2 are mutually uncorrelated, and thus $\mathbf{X}_1|\mathbf{X}_2 \sim \mathcal{M}_\nu^{L_1}(\boldsymbol{\mu}_1, \boldsymbol{\Sigma}_{11})$ and $\mathbf{X}_2|\mathbf{X}_1 \sim \mathcal{M}_\nu^{L_2}(\boldsymbol{\mu}_2, \boldsymbol{\Sigma}_{22})$.

F. Multivariate Complex McLeish Distribution

Let us have $\mathbf{S} \sim \mathcal{M}_\nu^{2L}(\mathbf{0}, \mathbf{I})$ be represented by

$$\mathbf{S} \triangleq \begin{bmatrix} \mathbf{S}_1 \\ \mathbf{S}_2 \end{bmatrix}, \quad (175)$$

where both $\mathbf{S}_1 \sim \mathcal{M}_\nu^{L}(\mathbf{0}, \mathbf{I})$ and $\mathbf{S}_2 \sim \mathcal{M}_\nu^{L}(\mathbf{0}, \mathbf{I})$ are two such uncorrelated standard multivariate McLeish distributions that $\mathbb{E}[\mathbf{S}_1\mathbf{S}_2^T] = \mathbf{0}$ and $\mathbb{E}[\mathbf{S}_2\mathbf{S}_1^T] = \mathbf{0}$. Form this point of view, we can define a multivariate complex McLeish distribution as

$$\mathbf{W} \triangleq \mathbf{S}_1 + j\mathbf{S}_2, \quad (176)$$

which is more considered as a vector of uncorrelated and identically distributed standard CCS McLeish distributions, i.e., $\mathbf{W} \triangleq [W_1, W_2, \dots, W_L]^T$, where $W_\ell \sim \mathcal{CM}(0, 1)$, $1 \leq \ell \leq L$ such that the quadrature and inphase components of any given pair of $W_k \sim \mathcal{CM}(0, 1)$ and $W_\ell \sim \mathcal{CM}(0, 1)$, $k \neq \ell$ are CS by default. Therefore, using (127), we can decompose \mathbf{W} as

$$\mathbf{W} \triangleq \sqrt{G}(\mathbf{N}_1 + j\mathbf{N}_2), \quad (177)$$

where $\mathbf{N}_1 \sim \mathcal{N}^L(\mathbf{0}, \mathbf{I})$ and $\mathbf{N}_2 \sim \mathcal{N}^L(\mathbf{0}, \mathbf{I})$ are such two standard multivariate Gaussian distributions that $\mathbb{E}[\mathbf{N}_1\mathbf{N}_2^T] = \mathbf{0}$ and $\mathbb{E}[\mathbf{N}_2\mathbf{N}_1^T] = \mathbf{0}$. Further, $G \sim \mathcal{G}(\nu, 1)$. By the definition of multivariate distribution [172]–[176], \mathbf{W} has a multivariate complex distribution iff $\forall \mathbf{a} \in \mathbb{C}^L$, $\mathbf{a}^T \mathbf{W}$ follows a complex random distribution of the same family. Accordingly, our intention is to come up to the PDF of \mathbf{W} , denoted by $f_{\mathbf{W}}(\mathbf{z})$, to check its distribution family. Taking into account the definition of multivariate distribution, and pursuant to what presented in Section III-E above, we conclude that the PDF of \mathbf{W} is exactly the same as the PDF of $\mathbf{S} \sim \mathcal{M}_\nu^{2L}(\mathbf{0}, \mathbf{I})$, i.e., $f_{\mathbf{W}}(\mathbf{z}) = f_{\mathbf{S}}(\mathbf{z})$. The multivariate distribution \mathbf{W} is therefore explicitly termed

as standard multivariate CCS McLeish distribution and properly denoted by $\mathbf{W} \sim \mathcal{CM}_\nu^L(\mathbf{0}, \mathbf{I})$, whose PDF is given in the following.

Theorem 34. *The PDF of $\mathbf{W} \sim \mathcal{CM}_\nu^L(\mathbf{0}, \mathbf{I})$ is given by*

$$f_{\mathbf{W}}(\mathbf{z}) = \frac{2}{\pi^L} \frac{\|\mathbf{z}\|^{\nu-L}}{\Gamma(\nu)\lambda_0^{\nu+L}} K_{\nu-L}\left(\frac{2}{\lambda_0}\|\mathbf{z}\|\right), \quad (178)$$

for a certain $\mathbf{z} \triangleq [z_1, z_2, \dots, z_L]^T \in \mathbb{C}^L$, where $\|\mathbf{z}\| \triangleq \mathbf{z}^H \mathbf{z}$.

Proof. Referring to the distributional equality between (175) and (176), well explained above, we acknowledge that both $\mathbf{S} \sim \mathcal{M}_\nu^{2L}(\mathbf{0}, \mathbf{I})$ and $\mathbf{W} \sim \mathcal{CM}_\nu^L(\mathbf{0}, \mathbf{I})$ have the same PDF, i.e.

$$f_{\mathbf{S}}(\mathbf{x}) = f_{\mathbf{W}}(\mathbf{z}_I + j\mathbf{z}_Q), \quad (179)$$

where $\mathbf{z}_I \in \mathbb{R}^L$ and $\mathbf{z}_Q \in \mathbb{R}^L$ such that $\mathbf{z} = \mathbf{z}_I + j\mathbf{z}_Q$ and

$$\mathbf{x} = \begin{bmatrix} \mathbf{z}_I \\ \mathbf{z}_Q \end{bmatrix}. \quad (180)$$

Then, using Theorem 19, we easily deduce the PDF of \mathbf{W} as in (178), which completes the proof of Theorem 34. ■

As observed in Theorem 34, the PDF $f_{\mathbf{W}}(\mathbf{z})$ is a function of squared Euclidean norm $\|\mathbf{z}\|^2 \triangleq \mathbf{z}^H \mathbf{z}$ in complex space. Since a unitary transformation \mathbf{U} (i.e., $\mathbf{U}\mathbf{U}^H = \mathbf{U}^H \mathbf{U} = \mathbf{I}$) preserves the Euclidean norm of all complex vectors (i.e., $\|\mathbf{U}\mathbf{z}\| = \|\mathbf{z}\|$), we immediately obtain the covariance matrix of $\mathbf{U}\mathbf{W}$ as

$$\mathbb{E}[\mathbf{U}\mathbf{W}(\mathbf{U}\mathbf{W})^H] = \mathbf{U}\mathbb{E}[\mathbf{W}\mathbf{W}^H]\mathbf{U}^H = 2\mathbf{I}, \quad (181)$$

and its pseudo-covariance matrix as

$$\mathbb{E}[\mathbf{U}\mathbf{W}(\mathbf{U}\mathbf{W})^T] = \mathbf{U}\mathbb{E}[\mathbf{W}\mathbf{W}^T]\mathbf{U}^T = \mathbf{0}. \quad (182)$$

These same conclusions are also being drawn for an orthogonal transformations. Further, we notice that

$$\text{Tr}(\mathbb{E}[\mathbf{W}\mathbf{W}^H]) = \text{Tr}(\mathbb{E}[\mathbf{S}\mathbf{S}^T]), \quad (183a)$$

$$= 2\text{Tr}(\mathbb{E}[\mathbf{S}_j\mathbf{S}_j^T]), \quad j \in \{1, 2\}, \quad (183b)$$

$$= 2L, \quad (183c)$$

Both (181) and (182) together impose that $f_{\mathbf{U}\mathbf{W}}(\mathbf{z}) = f_{\mathbf{W}}(\mathbf{z})$, and therefore $\mathbf{U}\mathbf{W} \sim \mathcal{CM}_\nu^L(\mathbf{0}, \mathbf{I})$. In addition, for clarity and consistency, we readily rewrite $f_{\mathbf{W}}(\mathbf{z})$ in terms of Meijer's G function using [150, Eq. (8.4.23/1)], that is

$$f_{\mathbf{W}}(\mathbf{z}) = \frac{1}{\pi^L \lambda_0^{2L} \Gamma(\nu)} G_{0,2}^{2,0} \left[\frac{\|\mathbf{z}\|^2}{\lambda_0^2} \middle| \begin{matrix} - \\ 0, \nu - L \end{matrix} \right]. \quad (184)$$

With the aid of whose Mellin-Barnes contour integration [150, Eq. (8.2.1/1)], we rewrite

$$f_{\mathbf{W}}(\mathbf{z}) = \frac{1}{2\pi j} \int_{c-j\infty}^{c+j\infty} \frac{\Gamma(s)\Gamma(\nu-L+s)}{\pi^L \lambda_0^{2L} \Gamma(\nu)} \|\mathbf{z}\|^{-2s} ds \quad (185)$$

within the existence region $s \in \Omega_0$, where $\Omega_0 = \{s | \Re\{s\} > \max(0, L - \nu)\}$. As observing $\mathbf{z} = \mathbf{x} + j\mathbf{y}$ and employing both (185) and [148, Eq. (3.241/4)] together, we have both $\int_{\mathbb{R}^L} f_{\mathbf{W}}(\mathbf{x} + j\mathbf{y}) d\mathbf{x}$ and $\int_{\mathbb{R}^L} f_{\mathbf{W}}(\mathbf{x} + j\mathbf{y}) d\mathbf{y}$ reduced to (128) as intuitively expected. In addition, when $\nu = 1$, (178) is then reduced to the PDF of standard multivariate CCS Laplacian distribution, that is

$$f_{\mathbf{W}}(\mathbf{z}) = \frac{1}{2^{(L-1)/2} \pi^L} \|\mathbf{z}\|^{1-L} K_{1-L}(\sqrt{2}\|\mathbf{z}\|), \quad (186)$$

which simplifies more to [122, Eq. (5.1.2)] for $L = 1$. The other special case, which is obtained when $\nu \rightarrow \infty$, is

$$f_{\mathbf{W}}(\mathbf{z}) = \frac{1}{(2\pi)^L} \exp\left(-\frac{1}{2}\|\mathbf{z}\|^2\right), \quad (187)$$

which is the PDF of standard multivariate Gaussian distribution [3, Eq. (2.6-29)] as expected.

Definition 5 (McLeish's Multivariate Complex Quantile and Complementary Complex Quantile). *For a fixed $\mathbf{z} \in \mathbb{C}^L$ in higher dimensional complex space, the McLeish's multivariate complex Q -function is defined by*

$$Q_{\nu}^L(\mathbf{z}) = Q_{\nu}^{2L}([\Re\{\mathbf{z}\}^T, \Im\{\mathbf{z}\}^T]^T), \quad (188)$$

and whose complementary complex Q -function is defined by

$$\widehat{Q}_{\nu}^L(\mathbf{z}) = Q_{\nu}^{2L}([\Re\{\mathbf{z}\}^T, \Im\{\mathbf{z}\}^T]^T), \quad (189)$$

where $Q_{\nu}^{2L}(\mathbf{x})$ and $\widehat{Q}_{\nu}^{2L}(\mathbf{x})$, defined for real vectors $\mathbf{x} \in \mathbb{R}^{2L}$, are given in (131) and (132), respectively.

As we mentioned above, referring to both (175) and (176) together, we have $f_{\mathbf{W}}(\mathbf{z}) = f_{\mathbf{S}}(\mathbf{z})$. Therefore, we can readily obtain the CDF and C²DF of $\mathbf{W} \sim \mathcal{CM}_{\nu}^L(\mathbf{0}, \mathbf{I})$, especially by using Theorem 20 and Theorem 21, respectively. Accordingly, the CDF of $\mathbf{W} \sim \mathcal{CM}_{\nu}^L(\mathbf{0}, \mathbf{I})$ is properly defined in complex space by $F_{\mathbf{W}}(\mathbf{z}) \triangleq \Pr\{\mathbf{W} \leq \mathbf{z}\} = \Pr\{W_1 \leq z_1, W_2 \leq z_2, \dots, W_L \leq z_L\}$ and obtained in the following.

Theorem 35. *The CDF of $\mathbf{W} \sim \mathcal{CM}_{\nu}^L(\mathbf{0}, \mathbf{I})$ is given by*

$$F_{\mathbf{W}}(\mathbf{z}) = \widehat{Q}_{\nu}^L(\mathbf{z}), \quad (190)$$

defined over $\mathbf{z} \in \mathbb{C}^L$, where $\widehat{Q}_{\nu}^L(\mathbf{z})$ is given in (189).

Proof. From the distributional equality between (175) and (176), the proof is obvious using (189). ■

The C²DF of $\mathbf{W} \sim \mathcal{CM}_{\nu}^L(\mathbf{0}, \mathbf{I})$ is defined by $\widehat{F}_{\mathbf{W}}(\mathbf{z}) \triangleq \Pr\{\mathbf{W} > \mathbf{z}\} = \Pr\{W_1 > z_1, W_2 > z_2, \dots, W_L > z_L\}$ and obtained in the following.

Theorem 36. *The C²DF of $\mathbf{W} \sim \mathcal{CM}_{\nu}^L(\mathbf{0}, \mathbf{I})$ is given by*

$$\widehat{F}_{\mathbf{W}}(\mathbf{z}) = Q_{\nu}^L(\mathbf{z}), \quad (191)$$

defined over $\mathbf{z} \in \mathbb{C}^L$, where $Q_{\nu}^L(\mathbf{z})$ is given in (188).

Proof. The proof is obvious using (188). ■

In L -dimensional complex space $\mathbf{s} \in \mathbb{C}^L$, we can define the MGF by $M_{\mathbf{W}}(\mathbf{s}) \triangleq \mathbb{E}[\exp(-\langle \mathbf{s}, \mathbf{W} \rangle)]$ that uniquely determines the distribution of $\mathbf{W} \sim \mathcal{CM}_{\nu}^L(\mathbf{0}, \mathbf{I})$ and is obtained in the following.

Theorem 37. *The MGF of $\mathbf{W} \sim \mathcal{CM}_{\nu}^L(\mathbf{0}, \mathbf{I})$ is given by*

$$M_{\mathbf{W}}(\mathbf{s}) = \left(1 - \frac{\lambda_0^2}{4} \mathbf{s}^H \mathbf{s}\right)^{-\nu}, \quad (192)$$

for a certain $\mathbf{s} \in \mathbb{C}^L$ within the existence region $\mathbf{s} \in \mathbb{C}_0$, where the region \mathbb{C}_0 is given by

$$\mathbb{C}_0 \triangleq \left\{ \mathbf{s} \mid \lambda_0^2 \mathbf{s}^H \mathbf{s} \leq 4 \right\}. \quad (193)$$

Proof. Following the same logic presented in the proof of Theorem 34, and noticing that MGF uniquely determines the

distributions, we can conclude that the distributional equality between (175) and (176) also makes both $\mathbf{S} \sim \mathcal{M}_{\nu}^{2L}(\mathbf{0}, \mathbf{I})$ and $\mathbf{W} \sim \mathcal{CM}_{\nu}^L(\mathbf{0}, \mathbf{I})$ have the same MGF, i.e.

$$\mathcal{M}_{\mathbf{S}}(\hat{\mathbf{s}}) = \mathcal{M}_{\mathbf{W}}(\mathbf{s}_I + j\mathbf{s}_Q), \quad (194)$$

where $\mathbf{x} \in \mathbb{R}^L$ and $\mathbf{y}_Q \in \mathbb{R}^L$ such that $\mathbf{s} \in \mathbb{R}^{2L}$, that is

$$\hat{\mathbf{s}} = \begin{bmatrix} \mathbf{s}_I \\ \mathbf{s}_Q \end{bmatrix}. \quad (195)$$

Then, using Theorem 22, we easily deduce the MGF of \mathbf{W} as in (192), which completes the proof of Theorem 37. ■

Let us have a vector of uncorrelated and non-identically distributed (*u.n.i.d.*) CCS McLeish distributions, that is

$$\mathbf{Z} \triangleq [Z_1, Z_2, \dots, Z_L]^T, \quad (196)$$

where $Z_{\ell} \triangleq X_{\ell} + jY_{\ell}$ such that $X_{\ell} \sim \mathcal{M}_{\nu}(0, \sigma_{\ell}^2)$ and $Y_{\ell} \sim \mathcal{M}_{\nu}(0, \sigma_{\ell}^2)$ (i.e., $Z_{\ell} \sim \mathcal{CM}_{\nu}(0, \sigma_{\ell}^2)$), $1 \leq \ell \leq L$. Furthermore, we assume $\text{Cov}[X_k, X_{\ell}] = 0$ and $\text{Cov}[Y_k, Y_{\ell}] = 0$ for all $k \neq \ell$, and more $\text{Cov}[X_k, Y_{\ell}] = 0$ for all $1 \leq k, \ell \leq L$. In accordance with the definition of multivariate distribution, \mathbf{Z} follows a multivariate CES McLeish distribution because $\mathbf{a}^T \mathbf{Z}$ for all $\mathbf{a} \in \mathbb{C}^L$ follows a McLeish distribution. It is then worth noticing that $\text{Var}[X_{\ell}] = \text{Var}[Y_{\ell}] = \sigma_{\ell}^2$ and $\text{Var}[Z_{\ell}] = \text{Var}[X_{\ell}] + \text{Var}[Y_{\ell}] = 2\sigma_{\ell}^2$. Herewith, as similar to what defined before, let us define $\sigma^2 \triangleq [\sigma_1^2, \sigma_2^2, \dots, \sigma_L^2]^T$, and therefrom $\sigma \triangleq [\sigma_1, \sigma_2, \dots, \sigma_L]^T$. Thus, we can decompose \mathbf{W} as a non-degenerate affine transform, that is

$$\mathbf{Z} \triangleq \text{diag}(\sigma) \mathbf{W}. \quad (197)$$

Owing to processing $\sigma^T \mathbf{W} \sim \mathcal{M}_{\nu}(0, \sigma^T \sigma)$, we conclude that \mathbf{Z} certainly follows a multivariate CES McLeish distribution denoted by $\mathbf{Z} \sim \mathcal{CM}_{\nu}^L(\mathbf{0}, \text{diag}(\sigma^2))$ with the distributional functions such as PDF, CDF, C²DF and MGF, each of which is given in the following.

Theorem 38. *The PDF of $\mathbf{Z} \sim \mathcal{CM}_{\nu}^L(\mathbf{0}, \text{diag}(\sigma^2))$ is given by*

$$f_{\mathbf{Z}}(\mathbf{z}) = \frac{2}{\pi^L} \frac{\|\Lambda^{-1} \mathbf{z}\|^{\nu-L}}{\Gamma(\nu) \det(\Lambda)} K_{\nu-L} \left(2 \|\Lambda^{-1} \mathbf{z}\| \right) \quad (198)$$

for a certain $\mathbf{z} \triangleq [z_1, z_2, \dots, z_L]^T \in \mathbb{C}^L$, where $\Lambda \triangleq \text{diag}(\lambda)$ and $\lambda \triangleq \lambda_0 \sigma$ denotes the component deviation vector.

Proof. Note that, using (197), we can write $\mathbf{W} = \text{diag}(\sigma)^{-1} \mathbf{Z}$ and therefrom obtain its Jacobian $J_{\mathbf{W}|\mathbf{Z}} = \det(\text{diag}(\sigma)^{-1})$. We can write the PDF of \mathbf{X} as

$$f_{\mathbf{Z}}(\mathbf{z}) = f_{\mathbf{W}}(\text{diag}(\sigma)^{-1} \mathbf{Z}) J_{\mathbf{W}|\mathbf{Z}}, \quad (199a)$$

$$= f_{\mathbf{W}}(\text{diag}(\sigma)^{-1} \mathbf{Z}) \det(\text{diag}(\sigma)^{-1}), \quad (199b)$$

where substituting (178) and utilizing both $\det(\text{diag}(\sigma)^{-1}) = \det(\text{diag}(\sigma))^{-1}$ and $\det(\text{diag}(\sigma)^2) = \det(\text{diag}(\sigma))^2$ yields (198), which completes the proof of Theorem 34. ■

Note that, for consistency and clarity, setting $\text{diag}(\sigma^2) \triangleq \sigma^2 \mathbf{I}$ (i.e., making each component have equal power) reduces (198) to the PDF of $\mathbf{Z} \sim \mathcal{CM}_{\nu}^L(\mathbf{0}, \sigma^2 \mathbf{I})$ given by

$$f_{\mathbf{Z}}(\mathbf{z}) = \frac{2}{\pi^L} \frac{\|\mathbf{z}\|^{\nu-L}}{\Gamma(\nu) \lambda^{\nu+L}} K_{\nu-L} \left(\frac{2}{\lambda} \|\mathbf{z}\| \right) \quad (200)$$

where $\lambda \triangleq \sqrt{2\sigma^2/\nu}$ as defined before.

Theorem 39. *The CDF of $\mathbf{Z} \sim \mathcal{CM}_\nu^L(\mathbf{0}, \text{diag}(\boldsymbol{\sigma}^2))$ is given by*

$$F_{\mathbf{Z}}(\mathbf{z}) = \widehat{Q}_\nu^L(\lambda_0 \boldsymbol{\Lambda}^{-1} \mathbf{z}), \quad (201)$$

defined over $\mathbf{z} \in \mathbb{C}^L$.

Proof. With the aid of the distributional relation between $\mathbf{Z} \sim \mathcal{CM}_\nu^L(\mathbf{0}, \text{diag}(\boldsymbol{\sigma}^2))$ and $\mathbf{W} \sim \mathcal{CM}_\nu^L(\mathbf{0}, \mathbf{I})$, presented in (197), we have $\mathbf{W} \triangleq \text{diag}(\boldsymbol{\sigma})^{-1} \mathbf{Z}$ and therefrom write

$$F_{\mathbf{Z}}(\mathbf{z}) = F_{\mathbf{W}}(\mathbf{w}), \quad (202a)$$

$$= F_{\mathbf{W}}(\text{diag}(\boldsymbol{\sigma})^{-1} \mathbf{z}), \quad (202b)$$

Finally, substituting the CDF $F_{\mathbf{W}}(\mathbf{z})$, which is given in (190), into (202b) and therein using $\text{diag}(\boldsymbol{\sigma})^{-1} = \lambda_0 \boldsymbol{\Lambda}^{-1}$, we readily obtain (201), which proves Theorem 39. ■

Theorem 40. *The C^2DF of $\mathbf{Z} \sim \mathcal{CM}_\nu^L(\mathbf{0}, \text{diag}(\boldsymbol{\sigma}^2))$ is given by*

$$\widehat{F}_{\mathbf{X}}(\mathbf{z}) = Q_\nu^L(\lambda_0 \boldsymbol{\Lambda}^{-1} \mathbf{z}), \quad (203)$$

defined over $\mathbf{z} \in \mathbb{C}^L$.

Proof. The proof is obvious using (191) and Theorem 36 and then performing almost same steps followed in the proof of Theorem 39. ■

Theorem 41. *The MGF of $\mathbf{Z} \sim \mathcal{CM}_\nu^L(\mathbf{0}, \text{diag}(\boldsymbol{\sigma}^2))$ is given by*

$$M_{\mathbf{Z}}(\mathbf{s}) = \left(1 - \frac{1}{4} \mathbf{s}^H \boldsymbol{\Lambda}^2 \mathbf{s}\right)^{-\nu}, \quad (204)$$

for a certain $\mathbf{s} \in \mathbb{C}^L$ within the existence region $\mathbf{s} \in \mathbb{C}_0$, where the region \mathbb{C}_0 is given by

$$\mathbb{C}_0 \triangleq \left\{ \mathbf{s} \mid \mathbf{s}^H \boldsymbol{\Lambda}^2 \mathbf{s} \leq 4 \right\}. \quad (205)$$

Proof. We can write the MGF of $\mathbf{Z} \sim \mathcal{CM}_\nu^L(\mathbf{0}, \text{diag}(\boldsymbol{\sigma}^2))$ as $M_{\mathbf{Z}}(\mathbf{s}) \triangleq \mathbb{E}[\exp(-\langle \mathbf{s}, \mathbf{Z} \rangle)]$, where putting (197) gives

$$M_{\mathbf{Z}}(\mathbf{s}) = \mathbb{E}[\exp(-\langle \mathbf{s}, \text{diag}(\boldsymbol{\sigma}) \mathbf{W} \rangle)], \quad (206)$$

$$= \mathbb{E}[\exp(-\langle \text{diag}(\boldsymbol{\sigma}) \mathbf{s}, \mathbf{W} \rangle)], \quad (207)$$

and therefrom we conclude that $M_{\mathbf{Z}}(\mathbf{s}) = M_{\mathbf{W}}(\text{diag}(\boldsymbol{\sigma}) \mathbf{s})$, where $M_{\mathbf{W}}(\mathbf{s})$ denotes the MGF of \mathbf{W} and is given in (192). Finally, substituting $\text{diag}(\boldsymbol{\sigma}) \mathbf{s} = \boldsymbol{\Lambda} \mathbf{s} / \lambda_0$ into (192) results in (204), which completes the proof of Theorem 41. ■

In what follows, the most general case in which we assume that complex McLeish distributions are mutually correlated and non-identically distributed is investigated using the results obtained previously. Hence, referring to (176), let us have a random vector of complex McLeish distributions given as

$$\mathbf{Z} \triangleq \mathbf{X}_1 + j \mathbf{X}_2, \quad (208)$$

where $\mathbf{X}_1 \sim \mathcal{M}_{\nu_1}^L(\boldsymbol{\mu}_1, \boldsymbol{\Sigma}_{11})$ and $\mathbf{X}_2 \sim \mathcal{M}_{\nu_2}^L(\boldsymbol{\mu}_2, \boldsymbol{\Sigma}_{22})$. Moreover, we assume that both \mathbf{X}_1 and \mathbf{X}_2 are without loss of generality correlated with each other, i.e.,

$$\boldsymbol{\Sigma}_{12} \triangleq \mathbb{E}[(\mathbf{X}_1 - \boldsymbol{\mu}_1)(\mathbf{X}_2 - \boldsymbol{\mu}_2)^T] \neq \mathbf{0}, \quad (209)$$

$$\boldsymbol{\Sigma}_{21} \triangleq \mathbb{E}[(\mathbf{X}_2 - \boldsymbol{\mu}_2)(\mathbf{X}_1 - \boldsymbol{\mu}_1)^T] \neq \mathbf{0}. \quad (210)$$

As noticing the mean vector of \mathbf{Z} is readily obtained as $\boldsymbol{\mu} \triangleq \mathbb{E}[\mathbf{Z}] = \boldsymbol{\mu}_1 + \boldsymbol{\mu}_2$, then we properly write its pseudo-covariance matrix as follows

$$\mathbb{E}[(\mathbf{Z} - \boldsymbol{\mu})(\mathbf{Z} - \boldsymbol{\mu})^T] = \boldsymbol{\Sigma}_{11} - \boldsymbol{\Sigma}_{22} + j(\boldsymbol{\Sigma}_{12} + \boldsymbol{\Sigma}_{21}), \quad (211)$$

and its covariance matrix as follows

$$\mathbb{E}[(\mathbf{Z} - \boldsymbol{\mu})(\mathbf{Z} - \boldsymbol{\mu})^H] = \boldsymbol{\Sigma}_{11} + \boldsymbol{\Sigma}_{22} + j(\boldsymbol{\Sigma}_{12} - \boldsymbol{\Sigma}_{21}), \quad (212)$$

We acknowledge that circular symmetry for McLeish random vectors is more detailed than circular symmetry for individual McLeish distributions. For preserving the circularly symmetry around the mean [167], i.e., in order to have the components of \mathbf{X}_1 become circular to those of \mathbf{X}_2 , we should provide that, as well explained in [167], $\mathbb{E}[(\mathbf{Z} - \boldsymbol{\mu})(\mathbf{Z} - \boldsymbol{\mu})^T]$ has to be a null matrix [167]. For that purpose, we strictly impose from (211) that $\boldsymbol{\Sigma}_{11} = \boldsymbol{\Sigma}_{22} = \mathbf{R}$ and $\boldsymbol{\Sigma}_{12} = -\boldsymbol{\Sigma}_{21} = \mathbf{J}$. Accordingly, we have

$$\mathbb{E}[(\mathbf{Z} - \boldsymbol{\mu})(\mathbf{Z} - \boldsymbol{\mu})^T] = \mathbf{0}, \quad (213)$$

$$\mathbb{E}[(\mathbf{Z} - \boldsymbol{\mu})(\mathbf{Z} - \boldsymbol{\mu})^H] = 2(\mathbf{R} + j\mathbf{J}) = 2\boldsymbol{\Sigma}, \quad (214)$$

where $\boldsymbol{\Sigma} = \mathbf{R} + j\mathbf{J}$ such that $\boldsymbol{\Sigma}$ is a complex symmetric matrix (i.e., $\boldsymbol{\Sigma}^H = \boldsymbol{\Sigma}$). Furthermore, we acknowledge that $\Im\{\boldsymbol{\Sigma}\} = \mathbf{0}$ when $\boldsymbol{\Sigma}_{12} = \boldsymbol{\Sigma}_{21} = \mathbf{0}$. By the definition of multivariate distribution [172]–[176], \mathbf{Z} is a multivariate complex distribution iff $\mathbf{a}^T \mathbf{Z}$ for all $\mathbf{a} \in \mathbb{C}^L$ follows a complex random distribution of the same family. Taking into account this definition, and pursuant to what presented in Section III-E above, we note that \mathbf{Z} follows a multivariate complex distribution only when $\nu_1 = \nu_2 = \nu$ with $\boldsymbol{\Sigma}_{11} = \boldsymbol{\Sigma}_{22}$ and $\boldsymbol{\Sigma}_{12} = -\boldsymbol{\Sigma}_{21}$. Since being an Hermitian positive definite matrix, $\boldsymbol{\Sigma}$ is decomposed using Cholesky decomposition as

$$\boldsymbol{\Sigma} \triangleq \mathbf{D} \mathbf{D}^H. \quad (215)$$

When there is no correlation between quadrature and inphase components of \mathbf{Z} (i.e., when $\boldsymbol{\Sigma}_{12} = \boldsymbol{\Sigma}_{21} = \mathbf{0}$), we have $\mathbf{J} = \mathbf{0}$, and therefrom $\mathbf{D} = \boldsymbol{\Sigma}^{-1/2}$. We conclude that

$$\mathbf{X}_1 \triangleq \sqrt{G} \mathbf{D} \mathbf{N}_1 \text{ and } \mathbf{X}_2 \triangleq \sqrt{G} \mathbf{D} \mathbf{N}_2, \quad (216)$$

where $\mathbf{N}_1 \sim \mathcal{N}^L(0, \mathbf{I})$, $\mathbf{N}_2 \sim \mathcal{N}^L(0, \mathbf{I})$ and $G \sim \mathcal{G}(\nu, 1)$. As a consequence, referring to Theorem 27, we decompose \mathbf{Z} as

$$\mathbf{Z} \triangleq \mathbf{D} \mathbf{W} + \boldsymbol{\mu}, \quad (217)$$

where $\mathbf{W} \sim \mathcal{CM}_\nu^L(\mathbf{0}, \mathbf{I})$, and which follows a multivariate CES McLeish distribution, properly denoted by $\mathbf{Z} \sim \mathcal{CM}_\nu^L(\boldsymbol{\mu}, \boldsymbol{\Sigma})$, whose PDF is given in the following.

Theorem 42. *The PDF of $\mathbf{Z} \sim \mathcal{CM}_\nu^L(\boldsymbol{\mu}, \boldsymbol{\Sigma})$ is given by*

$$f_{\mathbf{Z}}(\mathbf{z}) = \frac{2}{\pi^L \Gamma(\nu)} \frac{\|\mathbf{z} - \boldsymbol{\mu}\|_{\boldsymbol{\Sigma}}^{\nu-L}}{\det(\boldsymbol{\Sigma}) \lambda_0^{\nu+L}} K_{\nu-L} \left(\frac{2}{\lambda_0} \|\mathbf{z} - \boldsymbol{\mu}\|_{\boldsymbol{\Sigma}} \right), \quad (218)$$

defined over $\mathbf{z} \in \mathbb{C}^L$, where $\|\mathbf{z} - \boldsymbol{\mu}\|_{\boldsymbol{\Sigma}} \triangleq (\mathbf{z} - \boldsymbol{\mu})^H \boldsymbol{\Sigma}^{-1} (\mathbf{z} - \boldsymbol{\mu})$.

Proof. Note that $\mathbf{Z} \sim \mathcal{CM}_\nu^L(\boldsymbol{\mu}, \boldsymbol{\Sigma})$ is, as observed in (217), described by a linear affine transformation of $\mathbf{W} \sim \mathcal{CM}_\nu^L(\mathbf{0}, \mathbf{I})$. Appropriately, using $\boldsymbol{\Sigma} = \mathbf{D} \mathbf{D}^H$, we have

$$\mathbf{W} = \mathbf{D}^{-1} (\mathbf{Z} - \boldsymbol{\mu}) \quad (219)$$

and therefrom find the Jacobian $J_{\mathbf{Z}|\mathbf{W}} = \det(\mathbf{D})$ and $J_{\mathbf{W}|\mathbf{Z}} = \det(\mathbf{D})^{-1}$. Then, using $\det(\boldsymbol{\Sigma}) = \det(\mathbf{D})^2$, we have the PDF of \mathbf{Z} using (178), i.e.,

$$f_{\mathbf{Z}}(\mathbf{z}) = f_{\mathbf{W}}(\mathbf{D}^{-1} (\mathbf{Z} - \boldsymbol{\mu})) J_{\mathbf{W}|\mathbf{Z}}. \quad (220)$$

Finally, utilizing $\Sigma = \Sigma^H$ with these results, substituting (218) into (220) results in (156), which proves Theorem 42. ■

For consistency and clarity, note that the complex covariance matrix Σ can also be rewritten as $\Sigma = \lambda_0^{-2} \Lambda \mathbf{P} \Lambda$, where $\Lambda \triangleq \lambda_0 \text{diag}(\boldsymbol{\sigma}) = \text{diag}(\lambda_1, \lambda_2, \dots, \lambda_L)$ is previously defined. Moreover, $\mathbf{P} \in \mathbb{C}^{L \times L}$ denotes the complex correlation matrix. When the variance of all the components are the same (i.e., when $\sigma_\ell^2 = \sigma^2$, and thus $\lambda_\ell = \lambda = \sqrt{2\sigma^2/\nu}$, $1 \leq \ell \leq L$), we have $\Sigma = \lambda^2 \mathbf{P}$ and $\det(\Sigma) = \lambda^{2L} \det(\mathbf{P})$, and correspondingly simplify (218) to

$$f_{\mathbf{Z}}(\mathbf{z}) = \frac{2}{\pi^L \Gamma(\nu)} \frac{\|\mathbf{z} - \boldsymbol{\mu}\|_{\mathbf{P}}^{\nu-L}}{\det(\mathbf{P}) \lambda^{\nu+L}} K_{\nu-L} \left(\frac{2}{\lambda} \|\mathbf{z} - \boldsymbol{\mu}\|_{\mathbf{P}} \right). \quad (221)$$

In addition, in case of no correlation and zero mean (i.e., when $\mathbf{P} = \mathbf{I}$ and $\boldsymbol{\mu} = \mathbf{0}$), we also simplify (218) to (198) as expected.

Theorem 43. *The CDF of $\mathbf{Z} \sim \mathcal{CM}_\nu^L(\boldsymbol{\mu}, \Sigma)$ is given by*

$$F_{\mathbf{Z}}(\mathbf{z}) = \widehat{Q}_\nu^L(\mathbf{D}(\mathbf{Z} - \boldsymbol{\mu})), \quad (222)$$

defined over $\mathbf{z} \in \mathbb{C}^L$, where \mathbf{D} is given in (215).

Proof. Following almost the same steps presented in the proof of Theorem 39, the proof is quite obvious. Specifically, from (217), we have $F_{\mathbf{Z}}(\mathbf{z}) = F_{\mathbf{W}}(\mathbf{w})$ with $\mathbf{W} = \mathbf{D}(\mathbf{Z} - \boldsymbol{\mu})$, where substituting the CDF $F_{\mathbf{W}}(\mathbf{z})$, given in (190), we readily obtain (222), which proves Theorem 43. ■

Theorem 44. *The C^2 DF of $\mathbf{Z} \sim \mathcal{CM}_\nu^L(\boldsymbol{\mu}, \Sigma)$ is given by*

$$\widehat{F}_{\mathbf{X}}(\mathbf{z}) = Q_\nu^L(\mathbf{D}(\mathbf{Z} - \boldsymbol{\mu})), \quad (223)$$

defined over $\mathbf{z} \in \mathbb{C}^L$, where \mathbf{D} is given in (215).

Proof. The proof is obvious using (217) and Theorem 36 and then performing nearly same steps taken after within the proof of Theorem 43. ■

Theorem 45. *The MGF of $\mathbf{Z} \sim \mathcal{CM}_\nu^L(\boldsymbol{\mu}, \Sigma)$ is given by*

$$M_{\mathbf{Z}}(\mathbf{s}) = \exp(-\mathbf{s}^H \boldsymbol{\mu}) \left(1 - \frac{1}{4} \mathbf{s}^H \Sigma \mathbf{s} \right)^{-\nu}, \quad (224)$$

for a certain $\mathbf{s} \in \mathbb{C}^L$ within the existence region $\mathbf{s} \in \mathbb{C}_0$, where the region \mathbb{C}_0 is given by

$$\mathbb{C}_0 \triangleq \left\{ \mathbf{s} \mid \mathbf{s}^H \Sigma \mathbf{s} \leq 4 \right\}. \quad (225)$$

Proof. With the aid of (217), we can write the MGF of $\mathbf{Z} \sim \mathcal{CM}_\nu^L(\boldsymbol{\mu}, \Sigma)$ in terms of the MGF of $\mathbf{W} \sim \mathcal{CM}_\nu^L(\mathbf{0}, \mathbf{I})$, i.e.

$$M_{\mathbf{Z}}(\mathbf{s}) = \mathbb{E}[\exp(-\langle \mathbf{s}, \mathbf{Z} \rangle)], \quad (226a)$$

$$= \mathbb{E}[\exp(-\langle \mathbf{s}, \mathbf{D}\mathbf{W} + \boldsymbol{\mu} \rangle)], \quad (226b)$$

$$= \exp(-\langle \mathbf{s}, \boldsymbol{\mu} \rangle) \mathbb{E}[\exp(-\langle \mathbf{s}, \mathbf{D}\mathbf{W} \rangle)], \quad (226c)$$

$$= \exp(-\langle \mathbf{s}, \boldsymbol{\mu} \rangle) \mathbb{E}[\exp(-\langle \mathbf{D}\mathbf{s}, \mathbf{W} \rangle)], \quad (226d)$$

$$= \exp(-\langle \mathbf{s}, \boldsymbol{\mu} \rangle) M_{\mathbf{W}}(\mathbf{D}\mathbf{s}), \quad (226e)$$

where $M_{\mathbf{W}}(\mathbf{s})$ denotes the MGF of \mathbf{W} and is given in (192), and where both substituting (192) and using $\langle \mathbf{s}, \mathbf{x} \rangle \triangleq \mathbf{s}^H \mathbf{x}$ yields (204), which completes the proof of Theorem 41. ■

Eventually, we will exploit the closed-form results obtained in the preceding as a statistical and mathematical framework to introduce in the following sections some preliminary and

fundamental results not only about how to properly exercise McLeish distribution to model the additive non-Gaussian white noise in wireless communications, but also about how to use the statistical characterization of McLeish distribution to obtain closed-form BER/SER expressions of modulation schemes and develop an analytical approach for the averaged BER/SER performance of diversity reception in slowly time-varying flat fading environments.

IV. ADDITIVE WHITE MCLEISH NOISE CHANNELS

In wireless digital communications, various types of modulation techniques are utilized to map the digital information sequence into signal waveforms in order to transmit them through a communication channel. Within a symbol transmission time $t \in (0, T_S]$, this communication channel is without of loss of generality described by the mathematical relation

$$R(t) = h(t) S(t) + Z(t), \quad t \in (0, T_S] \quad (227)$$

where T_S denotes the symbol transmission time, $s(t)$ denotes the transmitted symbol, and with respect to the information, it is chosen from the set of all possible modulation symbols $\{s_1(t), s_2(t), \dots, s_M(t)\}$ such that $\sum_m \Pr\{s_m(t)\} = 1$, where $M \in \mathbb{N}$ is the modulation level. $h(t)$ denotes the fading process originating from the random nature of diffraction, refraction, and reflection within the channel, and due to coherence in time, it is assumed to be approximately constant for a number of symbol intervals. $Z(t)$ denotes a sample waveform of a zero-mean additive McLeish noise process, and $R(t)$ denotes the received waveform. The receiver makes observations on the received signal $R(t)$ and then makes an optimal decision based on the detection of which symbol m , $1 \leq m \leq M$, was transmitted. As well explained in [1]–[3], not only can an L -orthonormal basis be used to represent each modulation symbol by a L -dimensional vector, but it can also used to represent a zero-mean additive noise process as a vector of additive CES noise distributions. With the aid of this observation, for the n th symbol received over additive noise channels, we can readily give a well-known mathematical base-band model, which is in vector form, while we assume that many symbols are sequentially transmitted, that is [1]–[4]

$$\mathbf{R}[n] \triangleq H[n] \exp(j\Theta[n]) \mathbf{S}[n] + \mathbf{Z}[n], \quad (228)$$

where all vectors are without loss of generality L -dimensional complex vectors. Specifically, $\mathbf{S}[n]$ denotes the vector form of the n th transmitted symbol, and thus during each symbol transmission, it is randomly chosen from the set of all possible vectors $\{\mathbf{S}_1, \mathbf{S}_2, \dots, \mathbf{S}_M\}$. $H[n]$ denotes the fading envelope following a non-negative random distribution whereas $\Theta[n]$ denotes the fading phase following a random distribution over $[-\pi, \pi]$. Further, both $H[n]$ and $\Theta[n]$ are assumed constant during symbol duration due to the existence of channel coherence in time [1]–[3]. $\mathbf{Z}[n]$ denotes the additive noise, and it is always present in all communication channels and it is the major cause of impairment in many communication systems. Further, modeling $\mathbf{Z}[n]$ by a Gaussian distribution is well supported and widely evidenced from both theoretical and practical viewpoints. However, we show in what follows

that the random power nature of the additive noise indicates that $\mathbf{Z}[n]$ follows non-Gaussian distribution. It is thus prudent to pick a non-Gaussian noise model, which will let us to find out the performance and bottlenecks of non-Gaussian communication channels. Accordingly, for the first time in the literature, we introduce McLeish distribution as an additive noise model that approaches to Gaussian distribution in the worst case scenarios. We call the additive McLeish noise channel to the communication channel that is subjected to the additive noise modeled by McLeish distribution.

A. Random Fluctuations of Noise Variance

In wireless digital communications, we assume that the total variance of the additive noise vector $\mathbf{Z}[n] \sim \mathcal{CM}_v^L(\boldsymbol{\mu}, \boldsymbol{\Sigma})$ is constant for short-term conditions, and actually observe that it is a stationary random process in long-term conditions. We further estimate both the mean and the total variance of $\mathbf{Z}[n]$, respectively, as

$$\boldsymbol{\mu}_\tau[n] = \frac{1}{\lfloor \frac{\tau}{\tau_0} \rfloor} \sum_{k=n-\lfloor \frac{\tau}{\tau_0} \rfloor}^n \mathbf{Z}[k], \quad (229)$$

$$\sigma_\tau^2[n] = \frac{1}{\lfloor \frac{\tau}{\tau_0} \rfloor} \sum_{k=n-\lfloor \frac{\tau}{\tau_0} \rfloor}^n (\mathbf{Z}[k] - \boldsymbol{\mu}_\tau[n])^H (\mathbf{Z}[k] - \boldsymbol{\mu}_\tau[n]), \quad (230)$$

where $\tau \in \mathbb{R}_+$ denotes the coherence window that characterizes the dispersive nature of the total variance, τ_0 denotes the sample duration, and $\lfloor x \rfloor$ yields the maximum integer less than or equal to x . It is important for theoreticians and practitioners to be aware that the total variance contains fluctuations over time (i.e., the total variance is not constant over time), and be able to precisely quantify the amount of fluctuations associated with the total variance. Accordingly, we can write the exact total variance of $\mathbf{Z}[n]$ as

$$\sigma^2 = \lim_{\tau \rightarrow \infty} \sigma_\tau^2[n]. \quad (231)$$

As matter of fact that the stability of the total variance depends on the chosen window τ , we can perform the Allan's variance [181]–[183], which is a time domain measure representing root mean square (RMS) random drift within the total variance as a function of averaged time, on $\sigma_\tau^2[n]$ to express the stability the total variance with respect to $\tau \in \mathbb{R}_+$ and write

$$\mathbb{A}[\mathbf{Z}[n]; \tau] \triangleq \frac{1}{2} \mathbb{E}[(\sigma_\tau^2[n] - \sigma_\tau^2[n - \tau])^2], \quad (232)$$

where $\mathbb{E}[\cdot]$ denotes the expectation operator, and $\mathbb{A}[y[n]; \tau]$ is termed as Allan's operator applied on the sequence of $y[n]$. By means of (230) and (231), we introduce

$$\Delta\sigma_\tau^2[n] = \sigma_\tau^2[n] - \sigma^2, \quad (233)$$

which is the variance fluctuation (i.e., the random drift within the total variance over samples) such that $\mathbb{E}[\Delta\sigma_\tau^2[n]] = 0$ for $\tau \in \mathbb{R}_+$. From (231) and (233), we observe $\lim_{\tau \rightarrow \infty} \Delta\sigma_\tau^2[n] = 0$. Substituting $\sigma_\tau^2[n] = \Delta\sigma_\tau^2[n] + \sigma^2$ into (232), we can rewrite $\mathbb{A}[\mathbf{Z}[n]; \tau]$ in terms of the statistics of $\Delta\sigma_\tau^2[n]$ as follows

$$\mathbb{A}[\mathbf{Z}[n]; \tau] = \frac{1}{2} \left(\mathbb{E}[(\Delta\sigma_\tau^2[n])^2] + \mathbb{E}[(\Delta\sigma_\tau^2[n - \tau])^2] - 2\mathbb{E}[\Delta\sigma_\tau^2[n]\Delta\sigma_\tau^2[n - \tau]] \right). \quad (234)$$

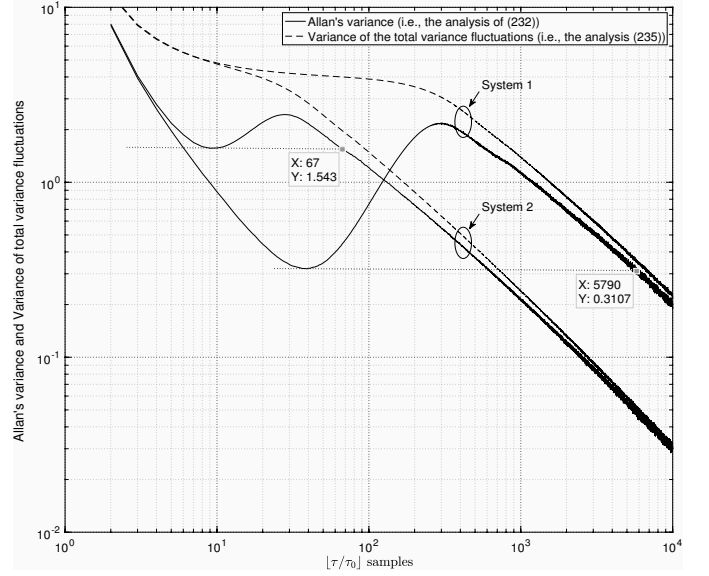


Fig. 7: The Allan's variance $\mathbb{A}[\mathbf{Z}[n]; \tau]$ and the variance of the total variance fluctuations $\text{Var}[\sigma_\tau^2[n]]$ with respect to τ , where $\sigma_\tau^2[n]$ follows a WSS random process.

After recognizing the variance and covariance terms associated with the variance fluctuation, i.e., using

$$\text{Var}[\sigma_\tau^2[n]] = \mathbb{E}[(\Delta\sigma_\tau^2[n])^2], \quad (235)$$

$$\text{Cov}[\sigma_\tau^2[n], \sigma_\tau^2[n - \tau]] = \mathbb{E}[\Delta\sigma_\tau^2[n]\Delta\sigma_\tau^2[n - \tau]], \quad (236)$$

we eventually rewrite (234) as

$$\mathbb{A}[\mathbf{Z}[n]; \tau] = \frac{1}{2} \left(\text{Var}[\sigma_\tau^2[n]] + \text{Var}[\sigma_\tau^2[n - \tau]] - 2\text{Cov}[\sigma_\tau^2[n], \sigma_\tau^2[n - \tau]] \right). \quad (237)$$

Note that, without loss of generality, we can consider $\sigma_\tau^2[n]$ as a wide sense stationary (WSS) random process with respect to $n \in \mathbb{N}$, especially since $\mathbf{Z}[n]$ is a sample vector of WSS random processes. Consequently, from the WSS feature of $\sigma_\tau^2[n]$ with respect to n , we write

$$0 < \mathbb{A}[\mathbf{Z}[n]; \tau] < 2 \text{Var}[\sigma_\tau^2[n]] \quad (238)$$

for all $\tau \in \mathbb{N}$, and further we write

$$\lim_{\tau \rightarrow \infty} \mathbb{A}[\mathbf{Z}[n]; \tau] \leq \lim_{\tau \rightarrow \infty} \text{Var}[\sigma_\tau^2[n]]. \quad (239)$$

With together aid of (238) and (239), we notice that the Allan's variance $\mathbb{A}[\mathbf{Z}[n]; \tau]$ is not a monotonically decreasing function with respect to τ , which suggest some τ -values for which the variance of the variance fluctuations, which is denoted by $\text{Var}[\sigma_\tau^2[n]]$, is at desired level. Accordingly, $\text{Var}[\sigma_\tau^2[n]]$ with respect to $\lfloor \tau/\tau_0 \rfloor$ is depicted in Fig. 7 for the additive noise data that belongs to different two systems, where the variances of these additive noise are not constant and follow a WSS non-negative random process. As such, the variance for system 1 is much more auto-correlated than that for system 2. Herein, we readily observe that, as τ increases, the variance of the total variance fluctuation decreases as expected. This fact does not reveal a minimum τ value that will keep the total variance fluctuation as small as possible.

On the other hand, as shown in Fig. 7, the fact that the Allan's variance is not a monotonic function of τ can help to determine this minimum τ value, namely $\tau \approx 5790\tau_0$ for system 1 and $\tau \approx 67\tau_0$ for system 2.

Theorem 46 (Autocorrelation of Noise Variance). *The correlation between $\sigma_\tau^2[n]$ and $\sigma_\tau^2[n - \tau]$ is given by*

$$\text{Cov}[\sigma_\tau^2[n], \sigma_\tau^2[n - \tau]] = \text{Var}[\sigma_\tau^2[n]] - \mathbb{A}[\mathbf{Z}[n]; \tau] \quad (240)$$

for any window $\tau \in \mathbb{N}$.

Proof. From the WSS view of $\sigma_\tau^2[n]$, we have $\text{Var}[\sigma_\tau^2[n]] = \text{Var}[\sigma_\tau^2[n - t]]$ for all $t \in \mathbb{N}$, and then simplify (237) to

$$\mathbb{A}[\mathbf{Z}[n]; \tau] = \text{Var}[\sigma_\tau^2[n]] - \text{Cov}[\sigma_\tau^2[n], \sigma_\tau^2[n - \tau]]. \quad (241)$$

which completes the proof of Theorem 46. \blacksquare

Note that the correlation between two consecutive estimated variances for a certain τ is given by Theorem 46, from which we observe that, when τ becomes as large as possible, this correlation $\text{Cov}[\sigma_\tau^2[n], \sigma_\tau^2[n - \tau]]$ closes to zero, and therefrom with (239), the total variance fluctuation becomes minimized. In the context of correlation, the auto-correlation coefficient between two consecutive estimated variances is obtained in the following.

Theorem 47 (Autocorrelation Coefficient of Noise Variance). *The correlation coefficient between $\sigma_\tau^2[n]$ and $\sigma_\tau^2[n - \tau]$ is given by*

$$\mathbb{R}[\sigma_\tau^2[n]; \tau] \triangleq 1 - \frac{\mathbb{A}[\mathbf{Z}[n]; \tau]}{\text{Var}[\sigma_\tau^2[n]]}, \quad (242)$$

for any window $\tau \in \mathbb{R}_+$ such that

$$-1 < \mathbb{R}[\sigma_\tau^2[n]; \tau] < 1. \quad (243)$$

Proof. The correlation coefficient between $\sigma_\tau^2[n]$ and $\sigma_\tau^2[n - \tau]$ is readily written as

$$\mathbb{R}[\sigma_\tau^2[n]; \tau] \triangleq \frac{\text{Cov}[\sigma_\tau^2[n], \sigma_\tau^2[n - \tau]]}{\sqrt{\text{Var}[\sigma_\tau^2[n]]\text{Var}[\sigma_\tau^2[n - \tau]]}}. \quad (244)$$

Noticing $\text{Var}[\sigma_\tau^2[n]] = \text{Var}[\sigma_\tau^2[n - \tau]]$ from the WSS feature and subsequently substituting (240) into (240), we readily obtain (242). Further, from (238) and (242), we readily observe the existence of (243), which proves Theorem 47. \blacksquare

Note that, according to Theorem 47, $\mathbb{R}[\sigma_\tau^2[n]; \tau] \in [-1, 1]$ is such a measurement that it describes the degree to which $\sigma_\tau^2[n]$ and $\sigma_\tau^2[n - \tau]$ are correlated with each other. For a specific coherence window $0 \leq \tau \leq \tau_\ell$, if the consecutively-estimated two variances $\sigma_\tau^2[n]$ and $\sigma_\tau^2[n - \tau]$ are highly correlated, then we have $\mathbb{R}[\sigma_\tau^2[n]; \tau] \approx 1$ and thus $\mathbb{A}[\mathbf{Z}[n]; \tau] \ll \text{Var}[\sigma_\tau^2[n]]$, which means that the estimation $\sigma_\tau^2[n]$ has the minimum error, i.e., $\sigma_\tau^2[n]$ is approximately constant. Accordingly, we can exploit Theorem 47 to estimate the coherence window τ of the random fluctuations in the nature of variance.

Theorem 48 (Coherence of Noise Variance). *The length of the coherence window $[0, \tau_C]$ of the additive noise variance can be estimated as*

$$\tau_C = \arg \min_{\tau \in \mathbb{R}_+} \left(\frac{\mathbb{A}[\mathbf{Z}[n]; \tau]}{\text{Var}[\sigma_\tau^2[n]]} + R - 1 \right)^2, \quad (245)$$

where $R \in [0, 1]$ denotes a certain correlation level, typically chosen as 0.95, 0.68, or 0.5. \square

Proof. Note that $|\mathbb{R}[\sigma_\tau^2[n]; \tau]|$ decreases monotonically with respect to $\tau \in \mathbb{R}_+$, i.e., $|\mathbb{R}[\sigma_\tau^2[n]; \tau]| \leq |\mathbb{R}[\sigma_\tau^2[n]; 0]|$. Hence, we can determine the width τ_C of the coherence window as that of $|\mathbb{R}[\sigma_\tau^2[n]; \tau]|$ where it drops to a certain level R . Having an objective to minimize the Euclidean distance between R and $|\mathbb{R}[\sigma_\tau^2[n]; \tau]|$, we can formulate this problem as

$$\tau_C \triangleq \arg \min_{\tau \in \mathbb{N}} \left(R - |\mathbb{R}[\sigma_\tau^2[n]; \tau]| \right)^2. \quad (246)$$

where substituting (242) and using $1 - |x| \leq |1 - x|$ results in (245), which proves Theorem 48. \blacksquare

Based upon the concepts and procedures for noise-variance fluctuations described above, let us now briefly consider different types of variance fluctuations/uncertainties, each of which is commonly observed in wireless communications. Let $T_C \in \mathbb{R}_+$ be the coherence time of the fading conditions in the wireless channel, and T_S be the symbol duration. In literature, it is widely assumed that $T_C \gg T_S$ in flat fading environments. In order to get the idea how to elucidate which values of τ_C cause variance fluctuations, we need to compare both τ_C and T_C with each other with regard to T_S .

(Constant variance). In the literature of wireless communications [1]–[3, and references therein], τ_C is often assumed to be pretty much large enough as compared both to T_C and T_S such that $\tau_C/T_C \gg T_S$. In such a case, we observe that $\sigma^2[n]$ does actually have no fluctuations, namely, that it is constant (i.e., $\sigma_\tau^2[n] \triangleq 2N_0$ for all $n \in \mathbb{N}$ and $\tau \in \mathbb{R}_+$, where $2N_0$ denotes the power spectral density of $\mathbf{Z}[n]$) since

$$\lim_{\tau_C \rightarrow \infty} \mathbb{A}[\mathbf{Z}[n]; \tau] = 0^+, \quad (247)$$

In other words, the variance fluctuations vanish when $\tau_C \rightarrow \infty$ (i.e., $\lim_{\tau_C \rightarrow \infty} \sigma_\tau^2[n] = \sigma^2[n] = 2N_0$ as expected). Accordingly, we suitably use multivariate CES Gaussian distribution to model the additive noise $\mathbf{Z}[n]$. \square

(Slow variance-uncertainty). If τ_C is either comparable to or greater than T_C with respect to T_S , i.e. when $\tau_C/T_C \geq T_S$, then as a matter of fact, we can observe that the instantaneous variance $\sigma^2[n]$ is approximately constant during the symbols transmitted in the coherence time T_C of fading conditions but fluctuates arbitrarily over all transmitted symbols. For example, either in high-speed transmission in ultra-high frequencies, or in wireless powered diversity receivers, $\mathbf{Z}[n]$ follows a multivariate CES Gaussian distribution whose total variance $\sigma^2[n]$ fluctuates randomly in long-term conditions, as being confirmed in our experiments. This phenomenon is called *noise uncertainty* [184]. That is to say, $\sigma^2[n]$ follows a non-negative distribution, which modulates complex Gaussian distribution, and thus causes impulsive effects on the performance of the transmission system. Accordingly, we show that $\mathbf{Z}[n]$ is accurately modeled in terms of Hall's noise model [185], [186] as follows

$$\mathbf{Z}[n] = \sigma[n] \mathbf{N}[n], \quad (248)$$

where $\mathbf{N}[n]$ is a multivariate CES Gaussian distribution with zero mean vector and $\mathbf{\Sigma}$ covariance matrix, and independent

of $\sigma[n]$. According to (248), $\mathbf{Z}[n]$ follows a multivariate CES Gaussian distribution given the total variance $\sigma[n]$. Therefore, (248) is found to be a spherically invariant random process (SIRP) [187], which has been widely adopted in wireless communications [1, and references therein]. It is worth mentioning that, as well explained in the following sections, $\sigma^2[n]$ can be perfectly estimated in the coherence time T_C as a channel-side information (CSI) to maximize the SNR in the case of diversity reception over generalized fading environments. \square

(*Fast variance-uncertainty*). When τ_C is much smaller than T_C such that $\tau_C/T_C \ll T_S$, the estimation of $\sigma^2[n]$ within the coherence time T_C is a more difficult task, and mostly not possible. In such a case, the noise model presented in (248) still applies, but optimum detection and optimum combining schemes have to be reconsidered to minimize the performance degradation originated from the variance uncertainty. \square

Eventually, from the statements given above, we conclude that, in both slow and fast uncertainty of the variance, the product of $\sigma[n]$ and $G[n]$ yields some impulsive fluctuations as a result from the fact that the random distribution of $\sigma[n]$ modulates the inphase and quadrature components of $\mathbf{N}[n]$ since they belong to the same channel. In the following, we show that the variance fluctuations exists in real life scenarios, and the additive noise, whose model is introduced in (248), follows McLeish distribution.

For the sake of brevity, clarity and readability, the symbol indexing $[n]$ is deliberately omitted in the following.

B. Existence of McLeish noise distribution

The existence of McLeish noise in communication systems is observed in many forms and in various ways.

1) *Johnson noise and the Nyquist formula*: If the additive noise is primarily originated from electronic materials at the receiver, it is then called thermal noise. The electrical conduction is governed by how freely mobile electrons can move throughout the electronic material while their movements are hindered and impeded by scattering with other electrons, as well as with impurities or thermal excitations (phonons) [188]. At this point, the thermal noise is explained as a phenomenon associated with the discreteness and random motion of the electrons, and always exists in varying degrees in all electrical parts of systems. Regarding the model of thermal agitation [189], [190, Sec. 8.10], which goes back to the classical theory introduced by Drude in 1900 [191], let us consider a steady electrical current composed of many electrons, each passing through a resistor which is illustrated in Fig. 8 as a cylinder of finite conductive material of length L and cross-sectional area A (i.e., its volume is $V \triangleq AL$). The velocity of an electron in the x -direction (i.e. the velocity along the direction of the steady electric field impressed upon the resistor by the battery) is given by $v_x \triangleq v_d + v_t$, where v_d is the drift velocity due to electric field and v_t is the x -velocity due to the *thermal agitation* of the electrons. Further, since the electric field inside the resistor is, without loss of generality, assumed to be constant, the field-based velocity v_d has no random nature. However, as a result of $v_d \gg v_t$, the thermal-based velocity

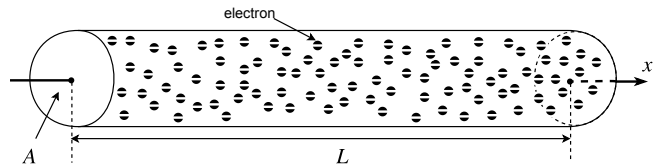


Fig. 8: Finite conductive material.

v_t has random nature in the x -direction, following Gaussian PDF given by

$$f_{v_t}(v) = \sqrt{\frac{m_0}{2\pi KT}} \exp\left(-m_0 \frac{v^2}{2KT}\right), \quad v \in \mathbb{R}, \quad (249)$$

with mean $\mathbb{E}[v_t] = 0$ and variance $\mathbb{E}[v_t^2] = \frac{KT}{2m_0}$, where the constant $m_0 \approx 9.10938356 \times 10^{-31}$ kg is the mass of an electron, and K and T are respectively the Boltzmann constant and the absolute temperature. If temperature is measured in Kelvins, and energy is measured in Joules, then the Boltzmann constant is *approximately* given by $K \approx 1.38064852 \times 10^{-23}$ J/K. Accordingly, average thermal kinetic energy of an electron can be written for one dimension as

$$E_t = \mathbb{E}\left[\frac{1}{2}m_0v_t^2\right] = \frac{1}{2}KT \quad (250)$$

in accordance within the literature [188]–[199]. Further, free electrons will move randomly due to thermal energy, so they experience many collisions. Let C be the number of collisions in 1 second and τ be the time between any two sequential collisions of an electron. In accordance with the statistical theory of collisions, we notice that C has a random relaxation nature that follows Poisson process [198], [199] with the probability mass function (PMF) given by

$$f_C(n) \triangleq \Pr\{n \text{ collisions}\} = \frac{1}{n!} \left(\frac{1}{\Delta\tau}\right)^n \exp\left(-\frac{1}{\Delta\tau}\right), \quad (251)$$

where $\Delta\tau$ is the mean relaxation time between collisions (i.e. $\Delta\tau = \mathbb{E}[\tau]$) and decreases as with temperature T , i.e., $\Delta\tau \propto 1/\sqrt{T}$. In average sense, each electron should experience $1/\Delta\tau$ collisions per 1 second. In the best electron excitation, τ follows an exponential distribution, that is

$$f_\tau(t) \triangleq \frac{1}{\Delta\tau} \exp\left(-\frac{t}{\Delta\tau}\right), \quad (252)$$

for $t \in \mathbb{R}_+$. It is worth emphasizing either $\Pr\{\tau < \Delta\tau\} > 1 - \Pr\{\tau < \Delta\tau\}$ under the best electron excitation conditions or $\Pr\{\tau < \Delta\tau\} \leq 1 - \Pr\{\tau < \Delta\tau\}$ otherwise. In other words, τ is the most probably less than $\Delta\tau$ under the best electron excitation conditions. Let us denote the electron excitation condition by $\nu \in \mathbb{R}_+$. We notice that ν increases while the electron excitation conditions get worse, which results the fact that each electron displacement occurs after more than one collisions under the worst electron excitation conditions. Therefore, under the best electron excitation conditions, we have $\Pr\{\tau < \Delta\tau\} \leq 1 - \Pr\{\tau < \Delta\tau\}$ and therefrom notice that τ is the most probably larger than or equal to $\Delta\tau$. In pursuance of the electron excitation conditions, in which the variation in time between any two sequential collisions of an electron arises from fluctuations in the momentum of electrons

created by collisions, we conveniently deduce that τ follows a Gamma distribution, that is

$$f_\tau(t) \triangleq \frac{1}{\Gamma(\nu)} \left(\frac{\nu}{\Delta\tau}\right)^\nu t^{\nu-1} \exp\left(-\frac{\nu}{\Delta\tau}t\right), \quad (253)$$

which readily simplifies to (252) for the best electron excitation conditions $\nu=1$ as expected. But, for the worst electron excitation conditions, we have $\nu \rightarrow \infty$, and correspondingly we notice that (253) approximates to the Dirac's distribution, that is $f_\tau(t) \triangleq \delta(t - \Delta\tau)$. This fact means that the randomness of τ disappears (i.e., constantly $\tau = \Delta\tau$), and implies in other words that the thermal displacement of each electron along the x -direction for a period of 1 second will precisely occur as a result of its certain $1/\Delta\tau$ number of collisions.

Note that the number of free electrons causing thermal noise depends on the finite conductivity of the resistor. Accordingly, let ρ denote the density of free electrons, then the total number of free electrons in the finite conductive material, depicted in Fig. 8, is given by $\eta_f \triangleq \rho AL$, and then the total number of possible displacement steps taken by all the free electrons in 1 seconds should be $\eta \approx \eta_f/\tau = \rho AL/\tau$. In accordance with the velocity of an electron explained above, let $v_t[n]$ be the n th thermal displacement of an electron along the x -direction for the period of 1 second. The distribution of $v_t[n]$ is given in (249). Accordingly, in terms of fractional sum, we can write the total charge movement due to thermal energy, i.e., the additive noise current passing through the resistor of length L , that is

$$I = \sum_{n=0}^{\eta} e_0 \tau \frac{v_t[n]}{L} = \sum_{n=0}^{\eta} Q[n], \quad (254)$$

where $e_0 \approx 1.60217662 \times 10^{-19}$ C denotes the charge on each electron. Under the assumption that τ is instantaneously known, $Q[n]$, $0 \leq n \leq \eta$, has Gaussian distribution. Therefore, the additive noise current I conditioned on τ , which is denoted by $I|\tau$, will follow Gaussian distribution with mean and variance, respectively obtained with the aid of the Euler-like identities of fractional sums [200]–[202] as follows

$$\mu_{I|\tau} \triangleq \mathbb{E}[I|\tau] = 0, \quad (255)$$

$$\sigma_{I|\tau}^2 \triangleq \mathbb{E}[I^2|\tau] = \tau \rho e_0^2 \frac{AKT}{2m_0L}. \quad (256)$$

Accordingly, the PDF of I given τ , i.e., $f_{I|\tau}(x)$ is written as

$$f_{I|\tau}(x) = \sqrt{\frac{m_0L}{\pi\tau\rho e_0^2 AKT}} \exp\left(-\frac{m_0L}{\tau\rho e_0^2 AKT}x^2\right). \quad (257)$$

In pursuance, the PDF of I is readily expressed as $f_I(x) = \int_0^\infty f_{I|\tau}(x|\tau)f_\tau(t)dt$, where substituting (257) and (253), and subsequently employing [148, Eq. (3.471/9)] results in

$$f_I(x) = \frac{2}{\sqrt{\pi}} \frac{|x|^{\nu-\frac{1}{2}}}{\Gamma(\nu) \lambda^{\nu+\frac{1}{2}}} K_{\nu-\frac{1}{2}}\left(\frac{2|x|}{\lambda}\right), \quad (258)$$

which is surprisingly the PDF of McLeish distribution with zero mean and σ^2 variance. Hence, we have $I \sim \mathcal{M}_\nu(0, \sigma^2)$, where the admittance per collision is given by $\lambda \triangleq \sqrt{2\sigma^2/\nu}$.

We obtain the variance $\sigma^2 \triangleq \mathbb{E}[I^2]$ by $\sigma^2 \triangleq \int_0^\infty \sigma_{I|\tau}^2 f_\tau(t) dt$, where substituting (256) and (253) results in

$$\sigma^2 = \Delta\tau \rho e_0^2 \frac{AKT}{2m_0L}. \quad (259)$$

According to the Nyquist's theorem [190], [195], [203], the power spectral density of the additive noise current is given by $S_I(f) = 2KT/R$ for all $f \in \mathbb{R}$, where R denotes the thermal resistance of the finite conductive material, to which the additive thermal noise is associated. With the aid of $S_I(0) = \sigma^2$, we obtain the resistance as

$$R = \frac{2KT}{S_I(0)} = \frac{4m_0L}{\Delta\tau \rho e_0^2 A}. \quad (260)$$

Let us consider some crucial special cases. For the best electron excitation conditions (i.e., $\nu=1$), we can simplify (258) to the PDF of Laplacian distribution with zero mean and σ^2 variance, that is $f_I(x) = \frac{1}{\sqrt{2\sigma^2}} \exp(-\sqrt{2/\sigma^2}|x|)$. On the other hand, for the worst electron excitation conditions (i.e., $\nu \rightarrow \infty$), we can simplify (258) to $f_I(x) = \frac{1}{\sqrt{2\pi\sigma^2}} \exp(-x^2/2\sigma^2)$, which the PDF of Gaussian distribution with zero mean and σ^2 variance as expected. We notice that these facts are compliant for the fact that the additive noise following Gaussian distribution the worst-case noise distribution for communication channels [84]–[86]. Furthermore, we observe both from (259) and (260) that the variance of the additive noise proportional to both the temperature T and the length L but inversely to the cross-sectional area A as expected.

In addition to all stated above, we acknowledge one extra point in which McLeish distribution also occurs in resistance circuits. Let us assume that there exist N resistors connected in parallel, then we will observe the total additive noise current as the sum of these numerous low-power impulsive noise sources $I_\Sigma = \sum_{n=1}^N I_n$, where I_n , $1 \leq n \leq N$, denotes the additive noise originated from the n th resistor, and therein we have $I_n \sim \mathcal{L}_\nu(0, \sigma^2)$ under the best electron excitation conditions. Consequently, the total additive noise I follows a McLeish distribution, i.e., $I_\Sigma \sim \mathcal{M}_\nu(0, N\sigma^2)$. As the number of resistors increases, the number of additive Laplacian components increases, which yields the convergence of the additive noise to a Gaussian distribution according to the CLT. Consequently, we remark that McLeish distribution is found to be a noise model capturing different impulsive noise environment.

2) *Multiple access/ser interference*: In wireless communications, both MAI and MUI resembles impulse noise more than Gaussian noise was rigorously investigated and soundly concluded in [35], [47]–[52], and the impulsive effects of the interference caused by each one of the other multiple users is often reasonably be modeled by Laplacian process. It is reported in [48] that MAI follows Laplacian distribution in direct sequence (DS) code division multiple access (CDMA) systems. Not only the theoretical background necessary to understand why MAI and MUI have Laplace distribution but also the further details are presented in the following. The total interference a user experiences in a MAI/MUI communication system can be written as

$$I = \sum_{n=1}^N I_n, \quad (261)$$

due to a small number of interfering users at close range, where the configuration of the interference originating from the n th interferer can be written as

$$I_n = \sum_{k=1}^{\infty} \alpha_k e^{j\theta_k} I_{nk}, \quad (262)$$

where $\{I_{nk}\}_{k=1}^{\infty}$ denotes the set of interference components originating from the signaling of the n th interfering user, where I_{nk} is the interference originating from the k th signaling configuration the n th interfering user employs, and modeled as $I_{nk} \sim \mathcal{CN}(0, \sigma_{nk}^2)$. In accordance, let us assume that the interference components are without loss of generality ordered with respect to their variances, i.e.,

$$\sigma_{n1} \geq \sigma_{n2} \geq \sigma_{n3} \geq \dots \geq \sigma_{nk} \geq \dots \geq 0. \quad (263)$$

As a result of $\lim_{k \rightarrow \infty} \sigma_{nk}^2 = 0$ using the strong law of large numbers, we have $\sum_{k=1}^{\infty} \sigma_{nk}^2 < \infty$. Moreover, in (262), α_k , $1 \leq k \leq \infty$ is the indicator for the k th possible signaling configuration, and modeled as Bernoulli distribution taking values 1 and 0 with probabilities p and $1 - p$, respectively, such that $0 < p < 1$. The phase θ_k is the component phase with respect to user, and it is uniformly distributed over $[-\pi, \pi)$. We can easily show that each interference component I_n , which is given by (262), is decomposed as

$$I_n \triangleq \sigma \sqrt{E}(X_0 + jY_0), \quad (264)$$

where $X_0 \sim \mathcal{N}(0, 1)$, $Y_0 \sim \mathcal{N}(0, 1)$ and $E \sim \mathcal{G}(1, 1)$. Upon using Theorem 10 with CS property and making use of (89), we note that I_n follows a Laplace distribution that has zero mean, i.e., $\mathbb{E}[I_n] = 0$, and has a variance given by

$$\sigma^2 = p \sum_{k=1}^{\infty} \sigma_{nk}^2 < \infty. \quad (265)$$

Since $I_n \sim \mathcal{CL}(0, \sigma^2)$, $1 \leq n \leq N$, the total interference, given in (261), follows a CCS McLeish distribution with zero mean and $\nu\sigma^2$ variance (i.e., $I \sim \mathcal{CM}_{\nu}(0, \nu\sigma^2)$). Consequently, we have remarked that CCS McLeish distribution is found to be a better model for the total MAI/MUI interference.

3) *Versatility*: The additive noise in most communication systems is supposed to be modeled as Gaussian distribution [1]–[4, and references therein]. These systems are also subjected to impulsive noise effects. Many statistical distributions have been proposed in the literature to model impulsive noise effects. As such, the so-called non-Gaussian distributions such as Laplacian, symmetric α -stable ($S\alpha S$), and generalized Gaussian distributions have attracted the interest of the research community due to their ability to capture different impulsive noise effects [50], [55], [96]–[114]. The lack of characterizing the impulsive noise effects from non-Gaussianity to Gaussianity is one of the essential weaknesses of these distributions mentioned above. On the other hand, note that the statistical description of McLeish distribution is typically defined according to the two observations, one of which is that the additive noise is caused by the summation of numerous impulsive noise sources of low power, each of which is found to be properly characterized by a Laplacian distribution. The other observation is that, according

to the CLT, the additive noise certainly converges to follow Gaussian distribution as the limit case of that the number of impulsive noise sources. As a result, the McLeish distribution demonstrates a superior fit to the different impulsive noise characteristics from non-Gaussian to Gaussian distributions with respect to its normality parameter $\nu \in \mathbb{R}_+$. As such, let W be a additive noise distribution we would like to fit the PDF of McLeish distribution by using MOM estimation technique. Then, we can estimate the mean by $\hat{\mu} \triangleq \mathbb{E}[W]$, and further the variance and the normality respectively by

$$\hat{\sigma}^2 \triangleq \text{Var}[W], \text{ and } \hat{\nu} \triangleq \frac{3}{\text{Kurt}[W] - 3}, \quad (266)$$

where $\text{Var}[\cdot]$ and $\text{Kurt}[\cdot]$ denote the well-known variance and Kurtosis operators, respectively. Consequently, we have remarked that the McLeish distribution is a very useful additive noise model that can be used in wireless communication performance analysis and research due to its versatility, experimental validity and analytical tractability.

V. SIGNALLING OVER AWMN CHANNELS

In what follows, for signaling over impulsive additive noise channels, we will introduce complex correlated AWMN vector channels and therein benefit from the vectorization that removes the redundancy in signal waveforms and that provides a compact presentation for them. Let us proceed to establish a mathematical model, which is in vector form using (227), for the baseband signaling over complex correlated AWMN vector channels, that is [1]–[4]

$$\mathbf{R} \triangleq H e^{j\Theta} \mathbf{F} \mathbf{S} + \mathbf{Z}, \quad (267)$$

where all vectors are without loss of generality L -dimensional complex vectors. Specifically, $\mathbf{R} \triangleq [R_1, R_2, \dots, R_L]^T$ denotes the received signal vector. When we start explaining from the right of (267), the random vector \mathbf{Z} is the additive noise modeled as multivariate CES McLeish distribution with ν normality, zero mean vector and Σ covariance matrix, and it is denoted by $\mathbf{Z} \sim \mathcal{CM}_{\nu}^L(\mathbf{0}, \Sigma)$. With the aid of Theorem 42, we readily write the PDF of \mathbf{Z} as

$$f_{\mathbf{Z}}(\mathbf{z}) = \frac{2}{\pi^L \Gamma(\nu)} \frac{\|\mathbf{z}\|_{\Sigma}^{\nu-L}}{\det(\Sigma) \lambda_0^{\nu+L}} K_{\nu-L} \left(\frac{2}{\lambda_0} \|\mathbf{z}\|_{\Sigma} \right), \quad (268)$$

where $\lambda_0 \triangleq \sqrt{2/\nu}$ denotes the standard component deviation. *It is worth noticing that \mathbf{Z} has a CES distribution (i.e., it is a colored (non-white) additive complex noise), which is the most essential issue at the receiver to be solved in making a decision of which symbol vector was transmitted based on the observation of \mathbf{R} . Moreover, for a fixed modulation level $M \in \mathbb{N}$, the random vector \mathbf{S} denotes the modulation symbol vector randomly chosen from the set of possible fixed modulation symbols $\{\mathbf{s}_1, \mathbf{s}_2, \dots, \mathbf{s}_M\}$ according to a priori probabilities $\{p_1, p_2, \dots, p_M\}$, where $p_m \triangleq \Pr\{\mathbf{S} = \mathbf{s}_m\}$, $1 \leq m \leq M$ with the fact that $\sum_m p_m = 1$. As such, upon while considering the overall transmission, we write the PMF of \mathbf{S} in continuous form [141, Eq. (4-15)], that is*

$$f_{\mathbf{S}}(\mathbf{s}) = \sum_{m=1}^M p_m \delta(\|\mathbf{s} - \mathbf{s}_m\|). \quad (269)$$

Further, in (267), $\mathbf{F} \in \mathbb{C}^{L \times L}$ is a precoding matrix filter that precodes each modulation symbol before transmission in order to compensate the performance degradation originating from the correlation between channels. In addition, in (267), H denotes the fading envelope following a non-negative random distribution whereas Θ denotes the fading phase uniformly distributed over $[-\pi, \pi]$. As well explained in Section IV above, both H and Θ are assumed constant during the period of each modulation symbol because of the transmission coherence time arising out of fading conditions [1]–[3], but each has a random nature while considering the overall transmission. Therefore, in coherent receiver, both H and Θ is required to be without loss of generality perfectly estimated at the receiver during the period of each modulation symbol vector. However, there is no need to estimate H and Θ in non-coherent receiver. Additionally, the covariance matrix Σ of $\mathbf{Z} \sim \mathcal{CM}_\nu^L(\mathbf{0}, \Sigma)$ is assumed perfectly estimated during that period. Eventually, thanks to the ES property of $\mathbf{Z} \sim \mathcal{CM}_\nu^L(\mathbf{0}, \Sigma)$ (i.e., with the aid of $f_{\mathbf{Z}}(\mathbf{z}) = f_{\mathbf{Z}}(e^{j\Theta}\mathbf{z})$ when $\mathbb{E}[\mathbf{Z}] = \mathbf{0}$), the received vector \mathbf{R} depends statistically on \mathbf{S} with the conditional PDF $f_{\mathbf{R}|\mathbf{S}}(\mathbf{r}|\mathbf{s})$, which we derive from (267) with the aid of Theorem 43 as

$$f_{\mathbf{R}|\mathbf{S}}(\mathbf{r}|\mathbf{s}) = \frac{2}{\pi^L \Gamma(\nu)} \frac{\|\mathbf{r} - He^{j\Theta}\mathbf{F}\mathbf{s}\|_{\Sigma}^{\nu-L}}{\det(\Sigma) \lambda_0^{\nu+L}} \times K_{\nu-L} \left(\frac{2}{\lambda_0} \|\mathbf{r} - He^{j\Theta}\mathbf{F}\mathbf{s}\|_{\Sigma} \right). \quad (270)$$

Having the joint PDF of \mathbf{R} and \mathbf{S} , i.e., $f_{\mathbf{R},\mathbf{S}}(\mathbf{r}, \mathbf{s}) \triangleq f_{\mathbf{R}|\mathbf{S}}(\mathbf{r}|\mathbf{s}) f_{\mathbf{S}}(\mathbf{s})$ by means of (269) and (270), we obtain the PDF of the received vector \mathbf{R} as

$$f_{\mathbf{R}}(\mathbf{r}) \triangleq \int f_{\mathbf{R},\mathbf{S}}(\mathbf{r}, \mathbf{s}) d\mathbf{s}, \quad (271a)$$

$$= \sum_{m=1}^M f_{\mathbf{R}|\mathbf{S}}(\mathbf{r}|\mathbf{s}_m) \Pr\{\mathbf{S} = \mathbf{s}_m\}, \quad (271b)$$

$$= \sum_{m=1}^M p_m \frac{2}{\pi^L \Gamma(\nu)} \frac{\|\mathbf{r} - He^{j\Theta}\mathbf{F}\mathbf{s}_m\|_{\Sigma}^{\nu-L}}{\det(\Sigma) \lambda_0^{\nu+L}} \times K_{\nu-L} \left(\frac{2}{\lambda_0} \|\mathbf{r} - He^{j\Theta}\mathbf{F}\mathbf{s}_m\|_{\Sigma} \right). \quad (271c)$$

After transmission of each modulation symbol, if the transmitted symbol m and the optimally detected symbol \hat{m} are not the same, then we say that a transmission error has occurred with the probability given by

$$\Pr\{e|m\} = \Pr\{\hat{m} \neq m\}, \quad (272)$$

whose averaging with respect to all possible modulation symbols results in the SER of the transmission, that is

$$\Pr\{e\} = \sum_{m=1}^M \Pr\{e|m\} \Pr\{\mathbf{S} = \mathbf{s}_m\}, \quad (273)$$

which will be derived for coherent/non-coherent signaling using digital modulation schemes over CES AWMN channels.

A. Coherent Signalling

As referring to the mathematical model given by (267), we assume that the receiver has a perfect knowledge of the phase,

or in some cases, that of both the amplitude and the phase in coherent signaling. As such, during the transmission of each modulation symbol while being conditioned on H and Θ , if the transmitted symbol m and the optimally detected symbol \hat{m} are not the same, then we say that an instantaneous symbol error has occurred with the probability given by

$$\Pr\{e|H, \Theta\} = \Pr\{\hat{m} \neq m|H, \Theta\}. \quad (274)$$

whose averaging with respect to H and Θ while considering all symbols results in the averaged SER of the transmission. The receiver observes \mathbf{R} , and based on this observation, decides which modulation symbol was transmitted, essentially by an optimal detection rule that minimizes the error probability or equivalently maximizes correct decision. The optimal detection rule, which is also occasionally called MAP rule [1]–[3], produces the index of the most probable transmitted symbol that maximizes $f_{\mathbf{R},\mathbf{S}}(\mathbf{r}, \mathbf{s})$. In more details, in order to acquire the index of the most probable transmitted symbol, we write the MAP decision rule accordingly as follows

$$\hat{m} \triangleq \arg \max_{1 \leq m \leq M} f_{\mathbf{R},\mathbf{S}}(\mathbf{R}, \mathbf{s}_m), \quad (275a)$$

$$= \arg \max_{1 \leq m \leq M} f_{\mathbf{S}|\mathbf{R}}(\mathbf{s}_m|\mathbf{R}) f_{\mathbf{R}}(\mathbf{r}), \quad (275b)$$

$$= \arg \max_{1 \leq m \leq M} f_{\mathbf{S}|\mathbf{R}}(\mathbf{s}_m|\mathbf{R}), \quad (275c)$$

which decides in favor of the modulation symbol that maximizes the conditional PDF $f_{\mathbf{S}|\mathbf{R}}(\mathbf{s}_m|\mathbf{r})$. Further, we simplify the MAP rule more to

$$\hat{m} \triangleq \arg \max_{1 \leq m \leq M} f_{\mathbf{R}|\mathbf{S}}(\mathbf{R}|\mathbf{s}_m) \Pr\{\mathbf{S} = \mathbf{s}_m\}, \quad (276)$$

where we often call $f_{\mathbf{R}|\mathbf{S}}(\mathbf{R}|\mathbf{s}_m)$ the likelihood of the symbol \mathbf{s}_m given the received vector \mathbf{R} . Hence also, we often remark that the MAP rule, given above, clearly illustrates how each decision given the received vector \mathbf{R} maps into one of the M possible transmitted modulation symbols. Corresponding to the M possible decisions, we partition the sample space of \mathbf{R} into M regions, and therefrom define the decision region for the symbol \hat{m} as

$$\mathbb{D}_{\hat{m}}^{\text{MAP}} = \left\{ \mathbf{r} \in \mathbb{C}^L \mid f_{\mathbf{R}|\mathbf{S}}(\mathbf{r}|\mathbf{s}_{\hat{m}}) \Pr\{\mathbf{S} = \mathbf{s}_{\hat{m}}\} \geq f_{\mathbf{R}|\mathbf{S}}(\mathbf{r}|\mathbf{s}_m) \Pr\{\mathbf{S} = \mathbf{s}_m\}, \forall m \neq \hat{m} \right\}, \quad (277)$$

which imposes that the decision regions are non-overlapping (i.e., $\mathbb{D}_m \cap \mathbb{D}_n = \emptyset$ for all $m \neq n$). In addition, (277) stipulates that each decision region can be described in terms of at most $M-1$ inequalities. In general, these M decision regions need not be connected with each other. When the receiver observes that the received vector \mathbf{R} has fallen into the region \mathbb{D}_m (i.e., when $\mathbf{R} \in \mathbb{D}_m$), it decides that the transmitted symbol is the modulation symbol m . Eventually, substituting (270) into (276) yields the MAP decision rule as follows

$$\hat{m} \triangleq \arg \max_{1 \leq m \leq M} \frac{2p_m}{\pi^L \Gamma(\nu)} \frac{\|\mathbf{R} - He^{j\Theta}\mathbf{F}\mathbf{s}_m\|_{\Sigma}^{\nu-L}}{\det(\Sigma) \lambda_0^{\nu+L}} \times K_{\nu-L} \left(\frac{2}{\lambda_0} \|\mathbf{R} - He^{j\Theta}\mathbf{F}\mathbf{s}_m\|_{\Sigma} \right), \quad (278)$$

which can be even simplified more using the CES property around mean, as shown in the following.

Theorem 49. For the complex vector channel introduced in (267), the coherent MAP detection rule is given by

$$\hat{m} \triangleq \arg \max_{1 \leq m \leq M} \left(2 \log(p_m) - \|\mathbf{R} - He^{j\Theta} \mathbf{F} \mathbf{s}_m\|_{\Sigma}^2 \right), \quad (279)$$

under the condition that $H \in \mathbb{R}_+$ and $\Theta \in [-\pi, \pi)$ are assumed perfectly estimated during each modulation symbol.

Proof. Note that the received vector \mathbf{R} given the transmitted symbol $\mathbf{S} = \mathbf{s}_m$ follows a multivariate CES McLeish distribution, i.e., $\mathbf{R} \sim \mathcal{CM}_{\nu}^L(He^{j\Theta} \mathbf{s}_m, \Sigma)$. According to both (216) and (217), the received vector \mathbf{R} given the transmitted symbol \mathbf{S} can be decomposed as

$$(\mathbf{R}|\mathbf{S}) \triangleq He^{j\Theta} \mathbf{F} \mathbf{S} + \sqrt{G} \mathbf{D} (N_1 + jN_2), \quad (280)$$

where \mathbf{D} is the Cholesky decomposition of Σ such that $\Sigma = \mathbf{D} \mathbf{D}^H$, and where $N_1 \sim \mathcal{N}^L(0, \mathbf{I})$, $N_2 \sim \mathcal{N}^L(0, \mathbf{I})$ and $G \sim \mathcal{G}(\nu, 1)$. Accordingly, the PDF of \mathbf{R} conditioned on both \mathbf{S} and G , i.e., $f_{\mathbf{R}|\mathbf{S}, G}(\mathbf{r}|\mathbf{s}, g)$ can be written as

$$f_{\mathbf{R}|\mathbf{S}, G}(\mathbf{r}|\mathbf{s}, g) = \frac{\exp\left(-\frac{1}{2g} \|\mathbf{r} - He^{j\Theta} \mathbf{F} \mathbf{s}\|_{\Sigma}^2\right)}{(2\pi)^L g^L \det(\Sigma)}, \quad (281)$$

for $g \in \mathbb{R}_+$. Then, the conditional PDF $f_{\mathbf{R}|\mathbf{S}}(\mathbf{R}|\mathbf{s})$ is obtained by $f_{\mathbf{R}|\mathbf{S}}(\mathbf{R}|\mathbf{s}) = \int_0^{\infty} f_{\mathbf{R}|\mathbf{S}, G}(\mathbf{R}|\mathbf{s}, g) f_G(g) dg$, where $f_G(g)$ is the PDF of $G \sim \mathcal{G}(\nu, 1)$, and given in (85). Upon substituting $f_{\mathbf{R}|\mathbf{S}}(\mathbf{R}|\mathbf{s}_m)$ into (276), we rewrite the MAP rule as

$$\hat{m} \stackrel{(a)}{=} \arg \max_{1 \leq m \leq M} p_m \int_0^{\infty} f_{\mathbf{R}|\mathbf{S}, G}(\mathbf{R}|\mathbf{s}_m, g) f_G(g) dg, \quad (282a)$$

$$\stackrel{(b)}{=} \arg \max_{1 \leq m \leq M} p_m f_{\mathbf{R}|\mathbf{S}, G}(\mathbf{R}|\mathbf{s}_m, \mathbb{E}[G]), \quad (282b)$$

where we have used the following steps in simplifying the expression. In step (a), we observe that (281) is being averaged by the PDF $f_G(g)$, and notice that $f_G(g) \geq 0$ for all $g \in \mathbb{R}_+$, which simplifies (282a) to (282b) with $\mathbb{E}[G] = 1$. Then, in step (b), we substitute (281) into (282b) and drop all the positive constant terms. Accordingly, we obtain

$$\hat{m} = \arg \max_{1 \leq m \leq M} p_m \exp\left(-\frac{1}{2} \|\mathbf{R} - He^{j\Theta} \mathbf{F} \mathbf{s}_m\|_{\Sigma}^2\right). \quad (283)$$

We acknowledge that, since the $\log(\cdot)$ function is a monotonically increasing function, we simplify this maximization by applying the $\log(\cdot)$ function to (283). Eventually, multiplying the resultant by 2, we obtain (279), which proves Theorem 49. ■

In some signaling conditions, some parameters within (279) may be discarded without loss of performance. Appropriately, the MAP rule can be even reduced more to a simple form. In case of that the modulation symbol vectors are equiprobable (i.e., when $\Pr\{\mathbf{S} = \mathbf{s}_m\} = \Pr\{\mathbf{S} = \mathbf{s}_n\}$, $1 \leq m, n \leq M$), we ignore the term $\Pr\{\mathbf{S} = \mathbf{s}_m\}$ in (276), and thereby further simplify the MAP decision rule to

$$\hat{m} \triangleq \arg \max_{1 \leq m \leq M} f_{\mathbf{R}|\mathbf{S}}(\mathbf{R}|\mathbf{s}_m), \quad (284)$$

which we call the ML decision rule. Appropriately, we simply define the decision region for the symbol \hat{m} as follows

$$\mathbb{D}_{\hat{m}}^{\text{ML}} = \left\{ \mathbf{r} \in \mathbb{C}^L \mid f_{\mathbf{R}|\mathbf{S}}(\mathbf{r}|\mathbf{s}_{\hat{m}}) \geq f_{\mathbf{R}|\mathbf{S}}(\mathbf{r}|\mathbf{s}_m), \hat{m} \neq m \right\}. \quad (285)$$

Further, in (284), We calculate the likelihood of the modulation symbol m , i.e., $f_{\mathbf{R}|\mathbf{S}}(\mathbf{R}|\mathbf{s}_m)$ by using the conditional PDF given in (270), and we simplify it more in the following.

Theorem 50. For the complex vector channel introduced in (267), the coherent ML detection rule is given by

$$\hat{m} \triangleq \arg \min_{1 \leq m \leq M} \|\mathbf{R} - He^{j\Theta} \mathbf{F} \mathbf{s}_m\|_{\Sigma}^2, \quad (286)$$

under the condition that $H \in \mathbb{R}_+$ and $\Theta \in [-\pi, \pi)$ are assumed perfectly estimated during each modulation symbol.

Proof. The ML decision rule states that each modulation symbol has the same probability of transmission. In accordance, in (279), we make $p_m = 1/M$ for all $1 \leq m \leq M$ and therein ignore the term $2 \log(p_m)$ same for all modulation symbols. Finally, changing the maximization to the minimization, we readily deduce (286), which proves Theorem 49. ■

Note that, as an interpretation of (286), we explicate that the receiver observes the received vector \mathbf{R} and searches among all modulation symbols $\{\mathbf{s}_m\}_{m=1}^M$ using a detection rule to find the one that is closest to the received vector \mathbf{R} using Mahalanobis distance. When the modulation symbols are equiprobable, the optimal detector uses the ML decision rule, and therefore we occasionally call it the minimum-distance (or nearest-neighbor) detector. In this case, we corroborate the finding that the boundaries of between the decision region of \mathbf{s}_m and that of \mathbf{s}_n are the set of hyper-plane points that are equidistant from these two modulation symbols.

In case of that the modulation symbols are equiprobable and have equal power (i.e., when $\Pr\{\mathbf{S} = \mathbf{s}_m\} = \Pr\{\mathbf{S} = \mathbf{s}_n\}$ and $\|\mathbf{s}_m\|^2 = \|\mathbf{s}_n\|^2$ for all $1 \leq m, n \leq M$), we revise the optimal detection rule either from the MAP rule or the ML rule and accordingly we put it in much simpler form, that is

$$\hat{m} \triangleq \arg \max_{1 \leq m \leq M} \Re\{e^{-j\Theta} \mathbf{s}_m^H \mathbf{R}\}, \quad (287)$$

whose decision region $\mathbb{D}_{\hat{m}}$ is given by

$$\mathbb{D}_{\hat{m}}^{\text{ML}} = \left\{ \mathbf{r} \in \mathbb{C}^L \mid \Re\{e^{-j\Theta} \mathbf{s}_{\hat{m}}^H \mathbf{r}\} \geq \Re\{e^{-j\Theta} \mathbf{s}_m^H \mathbf{r}\}, \forall m \neq \hat{m} \right\}, \quad (288)$$

where $\Re\{e^{-j\Theta} \mathbf{s}_m^H \mathbf{r}\}$, $1 \leq m \leq M$ can be readily rewritten as

$$\Re\{e^{-j\Theta} \mathbf{s}_m^H \mathbf{r}\} = \frac{1}{2} (e^{-j\Theta} \mathbf{s}_m^H \mathbf{r} + e^{j\Theta} \mathbf{r}^H \mathbf{s}_m). \quad (289)$$

It is worth mentioning that when we compare both ML and MAP decision rules given above, we differ only the inclusion of a priori probabilities $\Pr\{\mathbf{S} = \mathbf{s}_m\}$, $1 \leq m \leq M$ in the MAP rule, otherwise we observe that they are conceptually identical. This means that we perceive the MAP rule when we weight the ML rule with a priori probabilities. In addition, in both Theorem 49 and Theorem 50, the term $\|\mathbf{R} - He^{j\Theta} \mathbf{F} \mathbf{s}_m\|_{\Sigma}^2$ is the square of the Mahalanobis distance between the received vector \mathbf{R} and its mean $He^{j\Theta} \mathbf{F} \mathbf{s}_m$. We decompose it as

$$\|\mathbf{R} - He^{j\Theta} \mathbf{F} \mathbf{s}_m\|_{\Sigma}^2 = \|e^{j\Theta} (e^{-j\Theta} \mathbf{R} - H \mathbf{F} \mathbf{s}_m)\|_{\Sigma}^2, \quad (290a)$$

$$\stackrel{(a)}{=} \|e^{-j\Theta} \mathbf{R} - H \mathbf{F} \mathbf{s}_m\|_{\Sigma}^2, \quad (290b)$$

$$\stackrel{(b)}{=} \|\mathbf{R} - H \mathbf{F} \mathbf{s}_m\|_{\Sigma}^2, \quad (290c)$$

Thanks to the ES property of $\mathbf{Z} \sim \mathcal{CM}_\nu^L(\mathbf{0}, \Sigma)$, i.e., with the aid of the fact that $f_{\mathbf{Z}}(\mathbf{z}) = f_{\mathbf{Z}}(e^{j\Theta}\mathbf{z})$, we progress (290) from step (a) to step (b). Being aware of that \mathbf{Z} and $e^{j\Theta}\mathbf{Z}$ follow the same distribution, we have

$$e^{-j\Theta}\mathbf{R} = e^{-j\Theta}(He^{j\Theta}\mathbf{F}\mathbf{S} + \mathbf{Z}), \quad (291a)$$

$$= H\mathbf{F}\mathbf{S} + e^{j\Theta}\mathbf{Z}, \quad (291b)$$

$$\equiv H\mathbf{F}\mathbf{S} + \mathbf{Z}, \quad (291c)$$

from which we notice that, without any performance degradation, the receiver completely compensates the fading phase Θ by co-phasing the received vector \mathbf{R} with $\exp(-j\Theta)$ before the optimal detection (i.e., MAP/ML decision rules). The other crucial point we notice is the decorrelation of the channels to further simplify the receiver. For this purpose, we decompose

$$\begin{aligned} \|\mathbf{R} - He^{j\Theta}\mathbf{F}\mathbf{s}_m\|_{\Sigma}^2 &= H^2\mathbf{s}_m^H\mathbf{F}^H\Sigma^{-1}\mathbf{F}\mathbf{s}_m \\ &\quad - 2H\Re\{e^{-j\Theta}\mathbf{s}_m^H\mathbf{F}^H\Sigma^{-1}\mathbf{F}\mathbf{R}\} + \mathbf{R}^H\Sigma^{-1}\mathbf{R}, \end{aligned} \quad (292)$$

where, in order to avoid the performance degradation resulting from non-zero cross correlation between channels, we need to carefully choose the precoding matrix filter \mathbf{F} in such a way that eliminates the term $\mathbf{F}^H\Sigma^{-1}\mathbf{F}$ while maximizing the power of the received signal. The covariance matrix and total power of $\mathbf{Z} \sim \mathcal{M}_\nu^L(\mathbf{0}, \Sigma)$ are given by

$$\mathbb{E}[\mathbf{Z}\mathbf{Z}^H] = 2\Sigma, \quad (293)$$

$$\mathbb{E}[\mathbf{Z}^H\mathbf{Z}] = 2\text{Tr}(\Sigma), \quad (294)$$

respectively, where we remark that Σ is a square and conjugate symmetric matrix and hence lets us use Cholesky's decomposition [179, Chap. 10], [180, Sec. 2.2] to map Σ into the product of $\Sigma = \mathbf{D}\mathbf{D}^H$, where \mathbf{D} is the lower triangular matrix and \mathbf{D}^H is the transposed, complex conjugate, and therefore of upper triangular form. We find that

$$\mathbf{F} = \sqrt{\frac{2L}{\text{Tr}(\Sigma)}}\mathbf{D} = \sqrt{\frac{2}{N_0}}\mathbf{D}, \quad (295)$$

where N_0 is the averaged total variance per noise component in the complex vector channel. Accordingly, we express Σ as

$$\Sigma = \frac{N_0}{2}\mathbf{F}\mathbf{F}^H. \quad (296)$$

Substituting (296) into (292), we obtain

$$\begin{aligned} \|\mathbf{R} - He^{j\Theta}\mathbf{F}\mathbf{s}_m\|_{\Sigma}^2 &= 2\frac{H^2}{N_0}\|\mathbf{s}_m\|^2 \\ &\quad - 4\frac{H}{N_0}\Re\{e^{-j\Theta}\mathbf{s}_m^H\mathbf{R}\} + \|\mathbf{R}\|_{\Sigma}^2. \end{aligned} \quad (297)$$

Accordingly, choosing \mathbf{F} as (295) equalizes the received vector \mathbf{R} from the channel, introduced in (267), to yield the equalized version before it is fed to the optimal detector, that is

$$\mathbf{F}^{-1}\mathbf{R} = \mathbf{F}^{-1}(He^{j\Theta}\mathbf{F}\mathbf{S} + \mathbf{Z}), \quad (298a)$$

$$= He^{j\Theta}\mathbf{S} + \mathbf{F}^{-1}\mathbf{Z}, \quad (298b)$$

$$= He^{j\Theta}\mathbf{S} + \mathbf{Z}_c, \quad (298c)$$

where $\mathbf{Z} \sim \mathcal{CM}_\nu^L(\mathbf{0}, \Sigma)$ whose PDF is already given by (268), and $\mathbf{Z}_c \sim \mathcal{CM}_\nu^L(\mathbf{0}, \frac{N_0}{2}\mathbf{I})$ follows the PDF obtained with the aid of both Theorem 38 and the special case (200), that is

$$f_{\mathbf{Z}_c}(\mathbf{z}) = \frac{2}{\pi^L} \frac{\|\mathbf{z}\|^{\nu-L}}{\Gamma(\nu)\Lambda_0^{\nu+L}} K_{\nu-L}\left(\frac{2}{\Lambda_0}\|\mathbf{z}\|\right) \quad (299)$$

where Λ_0 is the component deviation (i.e., the variance per each Laplacian component) and obtained by

$$\Lambda_0 \triangleq \sqrt{\frac{2}{\nu} \frac{\text{Tr}(\mathbf{F}^H\Sigma^{-1}\mathbf{F})}{\text{Tr}(\mathbf{D}^H\Sigma^{-1}\mathbf{D})}} = \sqrt{\frac{N_0}{\nu}}. \quad (300)$$

Properly, both from the phase compensation presented in (291) and the equalization steps presented in (298), we conclude that, thanks to the coherence time of the vector channel, the received vector can be equalized by the precoding matrix filter \mathbf{F} and also can be maximized by phase compensation before the optimal detection as follows

$$\mathbf{R}_c \triangleq e^{-j\Theta}\mathbf{F}^{-1}\mathbf{R}, \quad (301a)$$

$$= e^{-j\Theta}\mathbf{F}^{-1}(He^{j\Theta}\mathbf{F}\mathbf{S} + \mathbf{Z}), \quad (301b)$$

$$\equiv H\mathbf{S} + \mathbf{F}^{-1}\mathbf{Z}, \quad (301c)$$

$$= H\mathbf{S} + \mathbf{Z}_c, \quad (301d)$$

which simplifies the complex correlated AWMN vector channel, introduced above in (267), to the simple one, which we call the uncorrelated complex AWMN vector channels, whose mathematical model is typically given by

$$\mathbf{R}_c \triangleq H\mathbf{S} + \mathbf{Z}_c. \quad (302)$$

where during each modulation symbol, \mathbf{R}_c depends statistically on \mathbf{S} . With the aid of (299), we obtain the conditional PDF $f_{\mathbf{R}_c|\mathbf{S}}(\mathbf{r}|\mathbf{s})$ as

$$f_{\mathbf{R}_c|\mathbf{S}}(\mathbf{r}|\mathbf{s}) = \frac{2}{\pi^L} \frac{\|\mathbf{r} - H\mathbf{s}\|^{\nu-L}}{\Gamma(\nu)\Lambda_0^{\nu+L}} K_{\nu-L}\left(\frac{2}{\Lambda_0}\|\mathbf{r} - H\mathbf{s}\|\right). \quad (303)$$

Accordingly, thanks to the CS property of multivariate CCS McLeish distribution (for more details, see Section III-F), we just state that the BER/SER performance of the vector channel in (302) is completely the same as that of one in (267) when we choose the precoding matrix filter \mathbf{F} as $\Sigma = N_0/2\mathbf{F}\mathbf{F}^H$.

Theorem 51. *The MAP rule for complex uncorrelated AWMN vector channels, defined in (302), is given by*

$$\hat{m} \triangleq \arg \max_{1 \leq m \leq M} \left(N_0 \log(p_m) - \|\mathbf{R}_c - H\mathbf{s}_m\|^2 \right), \quad (304a)$$

$$= \arg \max_{1 \leq m \leq M} \left(N_0 \log(p_m) + 2H\Re\{\mathbf{s}_m^H\mathbf{R}_c\} - H^2\|\mathbf{s}_m\|^2 \right). \quad (304b)$$

with the decision region $\mathbb{D}_{\hat{m}}^{\text{MAP}}$ given by

$$\begin{aligned} \mathbb{D}_{\hat{m}}^{\text{MAP}} &= \left\{ \mathbf{r} \in \mathbb{C}^L \mid N_0 \log(p_{\hat{m}}) + 2H\Re\{\mathbf{s}_{\hat{m}}^H\mathbf{r}\} - H^2\|\mathbf{s}_{\hat{m}}\|^2 \geq \right. \\ &\quad \left. N_0 \log(p_m) + 2H\Re\{\mathbf{s}_m^H\mathbf{r}\} - H^2\|\mathbf{s}_m\|^2, \forall m \neq \hat{m} \right\}, \end{aligned} \quad (305)$$

Proof. The proof is obvious putting $\Sigma = \frac{N_0}{2}\mathbf{I}$ in Theorem 49 and selecting $\mathbf{F} = e^{-j\Theta}\mathbf{I}$ as per the phase compensation. With

the aid of the MAP decision rule (276), we accordingly write the decision region of the modulation symbol \hat{m} as follows

$$\mathbb{D}_{\hat{m}}^{\text{MAP}} = \left\{ \mathbf{r} \in \mathbb{C}^L \mid N_0 \log(p_{\hat{m}}) - \|\mathbf{r} - H\mathbf{s}_{\hat{m}}\|^2 \geq N_0 \log(p_m) - \|\mathbf{r} - H\mathbf{s}_m\|^2, \forall m \neq \hat{m} \right\}, \quad (306)$$

where putting $\|\mathbf{r} - H\mathbf{s}_m\|^2 = \|\mathbf{r}\|^2 - 2H\Re\{\mathbf{s}_m^H \mathbf{r}\} + H^2\|\mathbf{s}_m\|^2$, and therein ignoring the term $\|\mathbf{r}\|^2$ similar to all the modulation symbols, we immediately derive (305), which completes the proof of Theorem 51. ■

In case of that the modulation symbols are transmitted with equal a priori probabilities (i.e., $p_m = 1/M$ for all $1 \leq m \leq M$), the MAP rule decision given in Theorem 51 is readily reduced to the ML decision rule given in the following.

Theorem 52. *The ML rule for complex uncorrelated AWMN vector channels, defined in (302), is given by*

$$\hat{m} \triangleq \arg \min_{1 \leq m \leq M} \|\mathbf{R}_c - H\mathbf{s}_m\|^2, \quad (307a)$$

$$= \arg \min_{1 \leq m \leq M} \left(H^2\|\mathbf{s}_m\|^2 - 2H\Re\{\mathbf{s}_m^H \mathbf{R}_c\} \right), \quad (307b)$$

with the decision region $\mathbb{D}_{\hat{m}}^{\text{ML}}$ given by

$$\mathbb{D}_{\hat{m}}^{\text{ML}} = \left\{ \mathbf{r} \in \mathbb{C}^L \mid H^2\|\mathbf{s}_{\hat{m}}\|^2 - 2H\Re\{\mathbf{s}_{\hat{m}}^H \mathbf{r}\} \leq H^2\|\mathbf{s}_m\|^2 - 2H\Re\{\mathbf{s}_m^H \mathbf{r}\}, \forall m \neq \hat{m} \right\}. \quad (308)$$

Proof. The proof is obvious setting $p_m = 1/M$, $1 \leq m \leq M$ in Theorem 51 and ignoring $N_0 \log(p_m) = -N_0 \log(M)$. ■

Note that, when the modulation symbols have equal power, we identify that the term $\|\mathbf{s}_m\|^2$ in (307b) is constant for all $1 \leq m \leq M$ and therefore can be ignored. In accordance, the optimal detection rule either from the MAP rule or the ML rule for complex uncorrelated AWMN vector channels, defined in (302), reduces to

$$\hat{m} \triangleq \arg \max_{1 \leq m \leq M} \Re\{\mathbf{s}_m^H \mathbf{R}_c\}, \quad (309)$$

whose decision region $\mathbb{D}_{\hat{m}}^{\text{ML}}$ is given by

$$\mathbb{D}_{\hat{m}}^{\text{ML}} = \left\{ \mathbf{r} \in \mathbb{C}^L \mid \Re\{\mathbf{s}_{\hat{m}}^H \mathbf{r}\} \geq \Re\{\mathbf{s}_m^H \mathbf{r}\}, \forall m \neq \hat{m} \right\}. \quad (310)$$

Additionally, we notice that the other important point in the nature of complex vector channels, which is well-known in the literature [1]–[4], is the rotational invariance property. As being typically observed either in Theorem 51 or Theorem 52 in accordance with the channel model given by (302), the ML decision rule partitions the sample space of the received vector \mathbf{R} depending on the modulation constellation. However, the rotation of the modulation constellation does not change the probability of making a decision error, primarily because of two facts, one of which corresponds to that the ML decision error depends only on distances between modulation symbols. The other fact is that the additive complex noise $\mathbf{Z}_c \sim \mathcal{CM}_{\nu}^L(\mathbf{0}, \frac{N_0}{2}\mathbf{I})$ is CS in all directions in signaling space.

1) *Symbol Error Probability:* In order to determine and assess the SER of a detection scheme, let us assume that the modulation symbol m (i.e. \mathbf{s}_m) is randomly selected from a modulation constellation and then transmitted through the complex vector channel, introduced above in (302). Appropriately, we write the received vector \mathbf{R} as

$$\mathbf{R}_c = H\mathbf{s}_m + \mathbf{Z}_c \quad (311)$$

where $\mathbf{Z}_c \sim \mathcal{M}_{\nu}^L(\mathbf{0}, \frac{N_0}{2}\mathbf{I})$. A decision error occurs only when the received vector \mathbf{R}_c does not fall into the decision region $\mathbb{D}_m^{\text{MAP}}$ of the modulation symbol m (i.e., $\mathbf{R}_c \notin \mathbb{D}_m^{\text{MAP}}$ causes an error). Making allowance for all decision regions $\{\mathbb{D}_m^{\text{MAP}}, 1 \leq m \leq M\}$ of the modulation constellation $\{\mathbf{s}_m, 1 \leq m \leq M\}$, the probability of that a receiver makes an error in detection of the modulation symbol m is readily written as

$$\Pr\{e \mid H, \mathbf{s}_m\} = \Pr\{\mathbf{R}_c \notin \mathbb{D}_m^{\text{MAP}} \mid \mathbf{s}_m\}, \quad (312a)$$

$$= \sum_{\substack{n=1 \\ n \neq m}}^M \Pr\{\mathbf{R}_c \in \mathbb{D}_n^{\text{MAP}} \mid \mathbf{s}_m\}, \quad (312b)$$

$$= \sum_{\substack{n=1 \\ n \neq m}}^M \int_{\mathbb{D}_n^{\text{MAP}}} f_{\mathbf{R}_c|\mathbf{s}}(\mathbf{r}|\mathbf{s}_m) d\mathbf{r}, \quad (312c)$$

where the conditional PDF $f_{\mathbf{R}|\mathbf{s}}(\mathbf{r}|\mathbf{s})$ is given in (303). The conditional SER of the receiver is therefore given by

$$\Pr\{e \mid H\} = \sum_{m=1}^M \Pr\{\mathbf{s}_m\} \Pr\{e \mid H, \mathbf{s}_m\}, \quad (313a)$$

$$= \sum_{m=1}^M p_m \Pr\{e \mid H, \mathbf{s}_m\}, \quad (313b)$$

where the probability of the modulation symbol m we select to transmit is typically denoted by $p_m \triangleq \Pr\{\mathbf{s}_m\}$, and where inserting (312c) yields

$$\Pr\{e \mid H\} = \sum_{m=1}^M p_m \sum_{\substack{\hat{m}=1 \\ \hat{m} \neq m}}^M \int_{\mathbb{D}_{\hat{m}}^{\text{MAP}}} f_{\mathbf{R}_c|\mathbf{s}}(\mathbf{r}|\mathbf{s}_m) d\mathbf{r}. \quad (314)$$

Accordingly, considering the whole transmission, we express the averaged SER of the signaling as

$$\Pr\{e\} = \int_0^{\infty} \Pr\{e \mid h\} f_H(h) dh, \quad (315)$$

where $f_H(h)$ is the PDF of the channel fading the signaling is subjected to. In this context, we mention that, in many cases, having exact information about a priori probabilities of the modulation symbols is difficult and actually impossible. We thus assume $p_m = 1/M$ for all $1 \leq m \leq M$ and then use the ML decision rule at the receiver. Accordingly, we simplify (314) more to

$$\Pr\{e \mid H\} = \frac{1}{M} \sum_{m=1}^M \sum_{\substack{\hat{m}=1 \\ \hat{m} \neq m}}^M \int_{\mathbb{D}_{\hat{m}}^{\text{ML}}} f_{\mathbf{R}_c|\mathbf{s}}(\mathbf{r}|\mathbf{s}_m) d\mathbf{r}. \quad (316)$$

Note that for very few modulation constellations, all decision regions $\{\mathbb{D}_m^{\text{ML}}, 1 \leq m \leq M\}$ are regular enough to be defined

mathematically such that we can compute the integrals in (316) in closed forms. But, in cases where these integrals cannot be expressed in a closed form, it is useful to have a union upper bound for the SER and hence for averaged SER since being quite tight particularly at high signal-to-noise ratio (SNR). From (316), we obtain the union upper bound for the averaged SER over additive complex AWMN channels as

$$\Pr\{e | H\} \leq \frac{1}{M} \sum_{m=1}^M \sum_{\substack{\hat{m}=1 \\ \hat{m} \neq m}}^M \Pr\{s_{\hat{m}} \text{ detected} | s_m \text{ sent}\}, \quad (317)$$

where $\Pr\{s_{\hat{m}} \text{ detected} | s_m \text{ sent}\}$, $m \neq \hat{m}$ is the probability of the error as a result of detection of $s_{\hat{m}}$ given the modulation symbol s_m transmitted. Note that the boundary between \mathbb{D}_m and $\mathbb{D}_{\hat{m}}$ is perpendicular bisector of the line connecting s_m and $s_{\hat{m}}$, $m \neq \hat{m}$. Accordingly, since s_m is transmitted, a decision error occurs considering only s_m and $s_{\hat{m}}$, $m \neq \hat{m}$ when the projection of $\mathbf{R}_c - Hs_m$ on $Hs_{\hat{m}} - Hs_m$ becomes larger than $Hd_{m\hat{m}}/2$, where $d_{m\hat{m}}$ is the Euclidean distance between s_m and $s_{\hat{m}}$, and defined by

$$d_{m\hat{m}}^2 \triangleq \|s_m - s_{\hat{m}}\|^2. \quad (318)$$

As acknowledging $\mathbf{Z}_c \triangleq \mathbf{R}_c - Hs_m$ and $\mathbf{Z}_c \sim \mathcal{CM}_\nu^L(\mathbf{0}, \frac{N_0}{2}\mathbf{I})$, the probability of making an error when considering only s_m and $s_{\hat{m}}$, $m \neq \hat{m}$ is given by

$$\begin{aligned} & \Pr\{s_{\hat{m}} \text{ detected} | s_m \text{ sent}\} \\ &= \Pr\left\{ \Re\left\{ \frac{\mathbf{Z}_c^H (Hs_{\hat{m}} - Hs_m)}{Hd_{m\hat{m}}} \right\} > \frac{Hd_{m\hat{m}}}{2} \right\}, \quad (319a) \end{aligned}$$

$$= \Pr\left\{ \Re\left\{ \mathbf{Z}_c^H (s_{\hat{m}} - s_m) \right\} > \frac{Hd_{m\hat{m}}^2}{2} \right\}, \quad (319b)$$

$$= \Pr\left\{ N > \frac{Hd_{m\hat{m}}^2}{2} \right\}, \quad (319c)$$

where $N \sim \mathcal{M}_\nu(0, \frac{N_0}{2}d_{m\hat{m}}^2)$ as a result from the CS property of $\mathbf{Z}_c \sim \mathcal{CM}_\nu^L(\mathbf{0}, \frac{N_0}{2}\mathbf{I})$.

Theorem 53. *The union upper bound of the conditional SER of the modulation constellation $\{s_m, 1 \leq m \leq M\}$ is given by*

$$\Pr\{e | H\} \leq \frac{1}{M} \sum_{m=1}^M \sum_{\substack{\hat{m}=1 \\ \hat{m} \neq m}}^M Q_\nu\left(\frac{H\|s_m - s_{\hat{m}}\|}{\sqrt{2N_0}}\right), \quad (320)$$

where $Q_\nu(\cdot)$ is the McLeish's Q-function defined in (36).

Proof. From (319c), with the aid of Theorem 4, we have

$$\Pr\left\{ N > \frac{Hd_{m\hat{m}}^2}{2} \right\} = Q_\nu\left(\frac{Hd_{m\hat{m}}}{\sqrt{2N_0}}\right). \quad (321)$$

Eventually, substituting both (319) and (321) into (317) yields

$$\Pr\{e | H\} \leq \frac{1}{M} \sum_{m=1}^M \sum_{\substack{\hat{m}=1 \\ \hat{m} \neq m}}^M Q_\nu\left(\frac{Hd_{m\hat{m}}}{\sqrt{2N_0}}\right), \quad (322)$$

where inserting (318) results in (320), which completes the proof of Theorem 53. \blacksquare

It is worth mentioning that Theorem 53 proposes the general union bound expression for the conditional SER of modulation constellation over uncorrelated complex AWMN vector channels. Let us consider the accuracy and completeness of Theorem 53, setting $\nu \rightarrow \infty$ in (320) yields [3, Eq. (4.2-72)]

$$\Pr\{e | H\} \leq \frac{1}{M} \sum_{m=1}^M \sum_{\substack{\hat{m}=1 \\ \hat{m} \neq m}}^M Q\left(\frac{H\|s_m - s_{\hat{m}}\|}{\sqrt{2N_0}}\right), \quad (323)$$

which is as expected the union upper bound of the conditional SER for signaling over complex additive white Gaussian noise (AWGN) channels. Further, for $\nu = 1$, (320) simplifies to the union upper bound for complex additive white Laplacian noise (AWLN) channels, that is

$$\Pr\{e | H\} \leq \frac{1}{M} \sum_{m=1}^M \sum_{\substack{\hat{m}=1 \\ \hat{m} \neq m}}^M LQ\left(\frac{H\|s_m - s_{\hat{m}}\|}{\sqrt{2N_0}}\right), \quad (324)$$

where $LQ(\cdot)$ is the Laplacian Q-function defined by (41). In addition, if we know the distance structure of the modulation constellation, we can further simplify (320) by exploiting the fact that the decision error is mostly contributed by the closest modulation symbols. The distance between the two closest modulation symbols is given by

$$d_{min} \triangleq \min_{m \neq \hat{m}} \|s_m - s_{\hat{m}}\| \quad (325)$$

Accordingly, we have

$$Q_\nu\left(\frac{Hd_{m\hat{m}}}{\sqrt{2N_0}}\right) \leq Q_\nu\left(\frac{Hd_{min}}{\sqrt{2N_0}}\right), \quad (326)$$

for all $\hat{m} \neq m$. Therefore, substituting this result in (322) yields

$$\Pr\{e | H\} \leq (M-1) Q_\nu\left(\frac{Hd_{min}}{\sqrt{2N_0}}\right). \quad (327)$$

In the following, we consider the well-known modulation constellations such as binary phase shift keying (BPSK), binary frequency shift keying (BFSK), M-ASK, M-PSK, and M-QAM, each of which is mainly characterized by their low bandwidth requirements. Appropriately, we will obtain the conditional SER of the coherent optimal detector for these modulation constellations.

a) Conditional BER of Binary Keying Modulation: When binary signaling is used, let us denote the modulation constellation by $\{s_+, s_-\}$ such that the transmitter transmits s_+ and s_- with priori probabilities p and $1-p$, respectively, and with powers $E_+ \triangleq \|s_+\|^2$ and $E_- \triangleq \|s_-\|^2$, respectively. Referring to the mathematical model given by (302), the received vector \mathbf{R}_c is readily written as

$$\mathbf{R}_c = Hs_\pm + \mathbf{Z}_c \quad (328)$$

where $\mathbf{Z}_c \sim \mathcal{M}_\nu^L(\mathbf{0}, \frac{N_0}{2}\mathbf{I})$, and therein $\mathbf{R}_c \sim \mathcal{M}_\nu^L(Hs_\pm, \frac{N_0}{2}\mathbf{I})$ since both the fading envelope H and the modulation symbols s_\pm are invariably known during one symbol duration. It is worth re-emphasizing that the received vector \mathbf{R}_c depends on the transmitted binary symbol \mathbf{S} through the conditional PDF $f_{\mathbf{R}_c|\mathbf{S}}(\mathbf{r}|\mathbf{s})$, which is obtained in (303). Accordingly, utilizing Theorem 51, we establish the MAP decision rule in the following theorem.

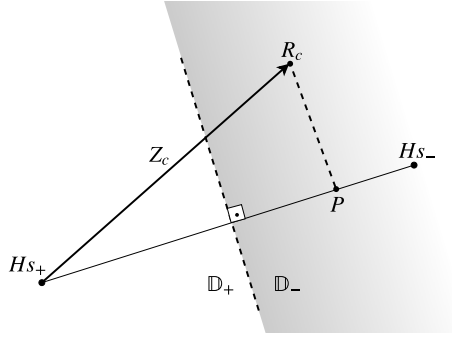


Fig. 9: Received vector representation using binary keying symbols s_{\pm} with the decision regions \mathbb{D}_{\pm} .

Theorem 54. *In the case where coherent binary signaling is used, the MAP decision rule, given in Theorem 52, reduces to*

$$\text{Decide } s_{\pm} \text{ iff } \|\mathbf{R}_c - Hs_{\pm}\|^2 + \eta_{\pm} \leq \|\mathbf{R}_c - Hs_{\mp}\|^2 \quad (329)$$

with the decision regions $\mathbb{D}_+^{\text{MAP}}$ and $\mathbb{D}_-^{\text{MAP}}$, given by

$$\mathbb{D}_{\pm}^{\text{MAP}} = \left\{ \mathbf{r} \in \mathbb{C}^L \mid \|\mathbf{r} - Hs_{\pm}\|^2 + R_{\pm} \leq \|\mathbf{r} - Hs_{\mp}\|^2 \right\}, \quad (330)$$

where the threshold value, originated from the priori probabilities of modulation symbols, is given by

$$\eta_{\pm} = N_0 \log \left(\frac{1 \mp 1 \pm 2p}{1 \pm 1 \mp 2p} \right). \quad (331)$$

Proof. The proof is obvious utilizing Theorem 51 with the CS property of multivariate CCS McLeish distribution (for more details, see Section III-F). ■

In accordance with Theorem 54, the decision regions $\mathbb{D}_+^{\text{MAP}}$ and $\mathbb{D}_-^{\text{MAP}}$ are separated by a boundary hyperline perpendicular to the hyperline connecting Hs_+ and Hs_- . The decision regions and this boundary line are together illustrated in Fig. 9. Let us assume that s_+ is transmitted, then an error occurs when the received vector \mathbf{R}_c falls into \mathbb{D}_- instead of \mathbb{D}_+ , which means that the projection of $(\mathbf{R}_c - Hs_+)$ on $(Hs_+ - Hs_-)$ is larger than the distance of Hs_+ from the boundary hyperline.

Theorem 55. *For the MAP decision rule given by Theorem 54, the conditional BER of binary signaling is given by*

$$\begin{aligned} \Pr\{e | H\} &= p Q_{\nu} \left(\frac{H^2 \|s_+ - s_-\|^2 - \eta_+}{H \|s_+ - s_-\| \sqrt{2N_0}} \right) + \\ & (1-p) Q_{\nu} \left(\frac{H^2 \|s_+ - s_-\|^2 - \eta_-}{H \|s_+ - s_-\| \sqrt{2N_0}} \right). \end{aligned} \quad (332)$$

Proof. From (329), we can write the decision correct decision when assuming that s_{\pm} is transmitted as follows

$$\begin{aligned} \|\mathbf{R}_c\|^2 + H^2 \|s_{\pm}\|^2 - 2H \Re\{s_{\pm}^H \mathbf{R}_c\} + \eta_{\pm} &\leq \\ \|\mathbf{R}_c\|^2 + H^2 \|s_{\mp}\|^2 - 2H \Re\{s_{\mp}^H \mathbf{R}_c\}, \end{aligned} \quad (333)$$

where inserting (328) yields

$$D \leq H^2 \|s_{\pm} - s_{\mp}\|^2 - \eta_{\pm}, \quad (334)$$

where the decision variable D is given by

$$D = -2H \Re\{(s_{\pm} - s_{\mp})^H \mathbf{Z}_c\}, \quad (335)$$

where $(s_{\mp} - s_{\pm})^H \mathbf{Z}_c$ follows a CCS McLeish distribution with zero mean and $N_0 \|s_{\pm} - s_{\mp}\|^2 / 2$ variance per dimension. Therefore, $D \sim \mathcal{M}_{\nu}(0, 2H^2 N_0 \|s_{\pm} - s_{\mp}\|^2)$, and accordingly, a decision error occurs when $D > H^2 \|s_{\pm} - s_{\mp}\|^2 - \eta_{\pm}$. Thus, with the aid of Theorem 4, when s_{\pm} is transmitted, we write the probability of decision error as

$$\Pr\{e | H, s_{\pm}\} = Q_{\nu} \left(\frac{H^2 \|s_{\pm} - s_{\mp}\|^2 - \eta_{\pm}}{H \|s_{\pm} - s_{\mp}\| \sqrt{2N_0}} \right), \quad (336)$$

From (313b), we write $\Pr\{e | H\} = \Pr\{e | H, s_+\} \Pr\{s_+\} + \Pr\{e | H, s_-\} \Pr\{s_-\}$, where replacing (336) yields (332), which completes the proof of Theorem 55. ■

In the special case where the binary modulation symbols are equiprobable (i.e., when $\Pr\{s_{\pm}\} = 1/2$), we have the threshold value $\eta_{\pm} = 0$ and then reduce the MAP rule to the ML rule given below.

Theorem 56. *In the case where coherent binary signaling is used, the ML decision rule, given in Theorem 52, reduces to*

$$\text{Decide } s_{\pm} \text{ iff } \|\mathbf{R}_c - Hs_{\pm}\| \leq \|\mathbf{R}_c - Hs_{\mp}\|. \quad (337)$$

with the decision regions \mathbb{D}_+^{ML} and \mathbb{D}_-^{ML} , given by

$$\mathbb{D}_{\pm}^{\text{ML}} = \left\{ \mathbf{r} \in \mathbb{C}^L \mid \|\mathbf{R}_c - Hs_{\pm}\| \leq \|\mathbf{R}_c - Hs_{\mp}\| \right\}. \quad (338)$$

Proof. The proof is obvious using Theorem 54 by assuming that the symbols are equiprobable, i.e., $\Pr\{s_{\pm}\} = 1/2$. ■

As it can be easily observed from Theorem 54, the decision regions \mathbb{D}_+^{ML} and \mathbb{D}_-^{ML} are separated by a perpendicular bisector to the hyperline connecting Hs_+ and Hs_- . As a result of the fact that the decision error probabilities when the modulation symbol s_+ or s_- is transmitted are equal, we have a symmetry with respect to the perpendicular bisector (i.e., the minimum distance of s_+ and that of s_- from the perpendicular bisector are certainly equal).

Theorem 57. *For the ML decision rule, given by Theorem 56, the conditional BER of binary signaling is given by*

$$\Pr\{e | H\} = Q_{\nu} \left(\frac{H \|s_+ - s_-\|}{\sqrt{2N_0}} \right). \quad (339)$$

Proof. The proof is obvious setting $p = \frac{1}{2}$ in Theorem 55. ■

Let us consider the special cases of Theorem 57 for certain binary modulation constellations. When the binary modulation symbols s_+ and s_- are equiprobable (i.e., $\Pr\{s_{\pm}\} = 1/2$) and have equal power (i.e., $\|s_+\|^2 = \|s_-\|^2$), we can rewrite the distance between s_+ and s_- as

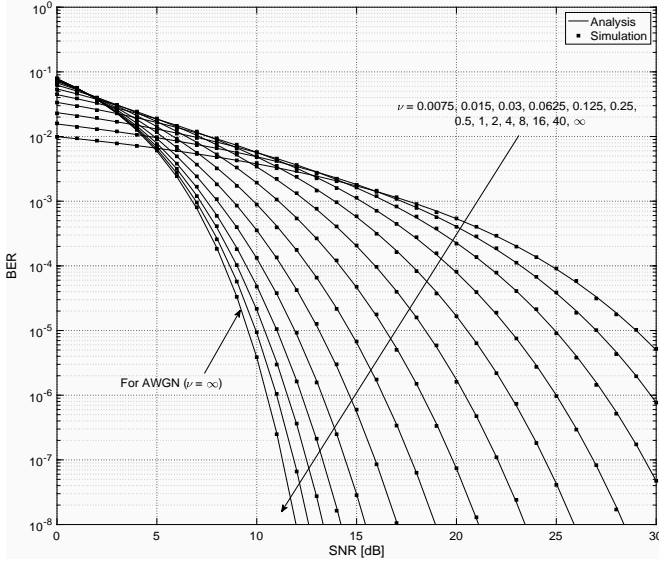
$$\|s_+ - s_-\| \triangleq \sqrt{2E_S(1-\rho)}, \quad (340)$$

where $E_S \triangleq \mathbb{E}[S^H S]$ denotes the transmitted average power and can be written in more details as follows

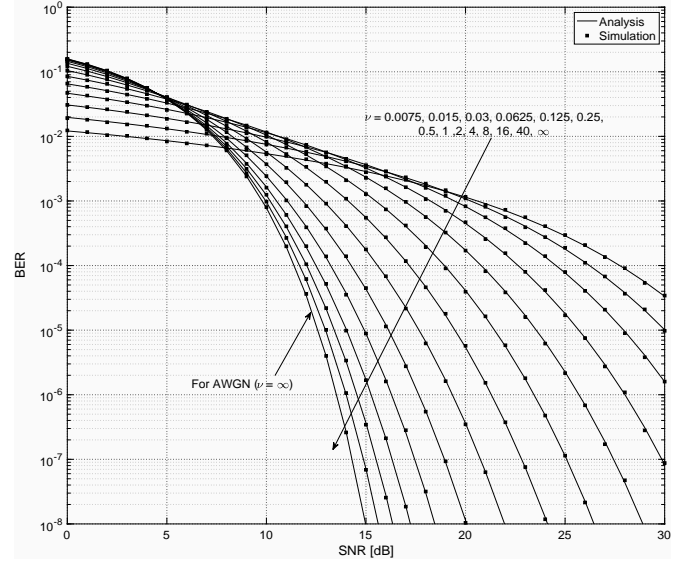
$$E_S = \Pr\{s_+\} \|s_+\|^2 + \Pr\{s_-\} \|s_-\|^2, \quad (341a)$$

$$= \frac{1}{2} \|s_+\|^2 + \frac{1}{2} \|s_-\|^2, \quad (341b)$$

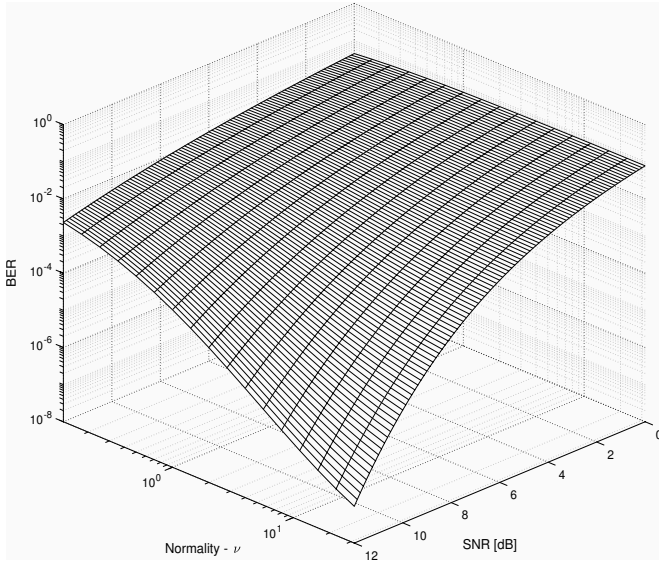
$$= E_+ \text{ (or } E_-), \quad (341c)$$



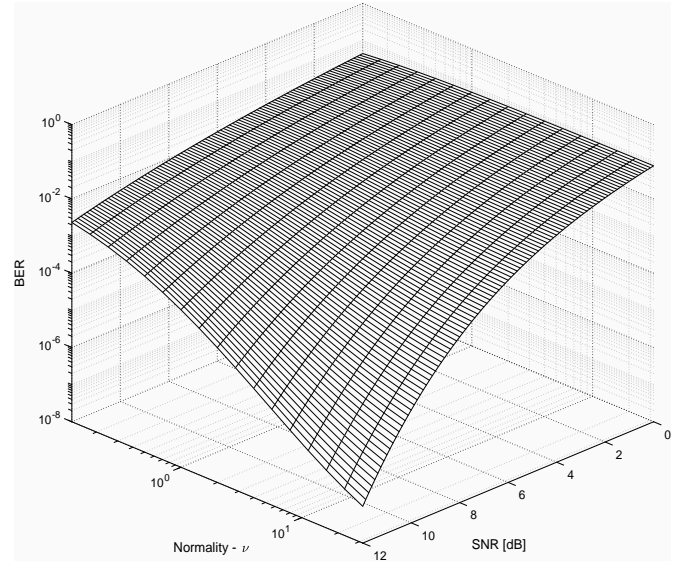
(a) With respect to SNR.



(a) With respect to SNR.



(b) With respect to SNR and normality.



(b) With respect to SNR and normality.

Fig. 10: The BER of BPSK signaling over AWMN channels.

Fig. 11: The BER of BFSK signaling over AWMN channels.

Further, in (340), ρ denotes the cross-correlation coefficient between the modulation symbols \mathbf{s}_+ and \mathbf{s}_- , defined by

$$\rho \triangleq \frac{\Re\{\mathbf{s}_+^H \mathbf{s}_-\}}{\|\mathbf{s}_+\| \|\mathbf{s}_-\|}, \quad (342a)$$

$$= \frac{1}{E_S} \left(\Re\{\mathbf{s}_+^T\} \Re\{\mathbf{s}_-\} + \Im\{\mathbf{s}_+^T\} \Im\{\mathbf{s}_-\} \right). \quad (342b)$$

It is consequently valuable to notice that, since $-1 \leq \rho \leq 1$, (340) is maximally increased when $\rho = -1$, i.e., when the binary modulation symbols are antipodal (i.e., when $\mathbf{s}_\pm = \mp \mathbf{s}_\mp$). Consequently, substituting (340) into (339) results in

$$\Pr\{e | H\} = Q_\nu \left(\sqrt{(1 - \rho)\gamma} \right), \quad (343)$$

where γ is the instantaneous SNR during transmission of one

modulation symbol and defined by

$$\gamma = \frac{\mathbb{E}[\langle HS, \mathbf{R}_c \rangle]^2}{\text{Var}[\langle HS, \mathbf{R}_c \rangle]}, \quad (344a)$$

$$= \frac{\mathbb{E}[\langle HS, \mathbf{R}_c \rangle]^2}{\mathbb{E}[\langle HS, \mathbf{R}_c \rangle^2] - \mathbb{E}[\langle HS, \mathbf{R}_c \rangle]^2}, \quad (344b)$$

$$= H^2 \frac{E_S}{N_0}, \quad (344c)$$

with the aid of the optimal decision rules given above.

Theorem 58. The conditional BER $\Pr\{e | H\}$ of BPSK signaling over CCS AWMN channels is given by

$$\Pr\{e | H\} = Q_\nu(\sqrt{2\gamma}), \quad (345)$$

where γ is the instantaneous SNR defined above.

Proof. Note that the BPSK symbols are defined by $\{s_+, s_-\}$ such that $s_- = -s_+$, which means that s_+ and s_- have equal power. In case of that they are equiprobable, we have $\|s_\pm\|^2 = E_S$. Therefore, with the aid of (342a), $\rho = -1$, and then (343) simplifies to (345), which proves Theorem 58. ■

Theorem 59. *The contional BER $\Pr\{e | H\}$ of BFSK signaling over CCS AWMN channels is given by*

$$\Pr\{e | H\} = Q_\nu(\sqrt{\gamma}), \quad (346)$$

where γ is the instantaneous SNR defined above.

Proof. Note that the BFSK symbols are defined by $\{s_+, s_-\}$ such that $s_\pm^H s_\mp = 0$. In case where s_+ and s_- are equiprobable and have equal power, we obtain the correlation $\rho = 0$ with the aid of (342a), and accordingly, we reduce (343) into (346), which proves Theorem 59. ■

As mentioned before, the impulsive nature of McLeish noise distribution is simply expressed by its normality $\nu \in \mathbb{R}_+$. As such, when $\nu \rightarrow \infty$, the impulsive nature vanishes and McLeish noise distribution approaches to Gaussian noise distribution. For that purpose, we demonstrated the effect of non-Gaussian noise on communication performance by plotting in Fig. 10 and Fig. 11 the conditional BER of BPSK and BFSK modulations, respectively, with respect to different normalities $\nu \in \{0.0075, 0.015, 0.03, 0.0625, 0.125, 0.25, 0.5, 1, 2, 4, 8, 16, 40, \infty\}$. We evidently observe that the impulsive nature of McLeish noise distribution deteriorates the performance of binary modulations in high-SNR regime while negligibly improves it in low-SNR regime.

The other binary keying signaling is the on-off keying (OOK) modulation, in case of which the binary information is transmitted by the presence or absence of a modulation symbol. Accordingly, the modulation symbols $s_+ \neq \mathbf{0}$ and $s_- = \mathbf{0}$ are employed to transmit 1 and 0 binary information, respectively, with equal a priori probabilities $\Pr\{s_+\} = \Pr\{s_-\} = 1/2$. At this point, note that the OOK constellation can be achieved by shifting the BPSK/BFSK constellation up to $s_- = 0$. Accordingly, $E_+ = \|s_+\|^2 \neq 0$ and $E_- = \|s_-\|^2 = 0$, such that the average power of the OOK modulation is written as $E_S = \Pr\{s_+\} \|s_+\|^2 + \Pr\{s_-\} \|s_-\|^2 = \frac{1}{2} \|s_+\|^2$. With that result, we can rewrite the distance between s_+ and s_- for the OOK modulation as

$$\|s_+ - s_-\| = \|s_+\| = \sqrt{2E_S}, \quad (347)$$

Theorem 60. *The contional BER $\Pr\{e | H\}$ of OOK signaling over CCS AWMN channels is given by*

$$\Pr\{e | H\} = Q_\nu(\sqrt{\gamma}), \quad (348)$$

where γ is the instantaneous SNR defined in (344).

Proof. The proof is obvious inserting (347) into Theorem 57 and using (344c). ■

At the moment, the conditional BER performance of binary signaling over AWMN channels has been investigated to derive closed-form BER expressions. We consider in the following the conditional SER of M-ary signaling over CCS AWMN vector channels.

b) Conditional SER of M-ASK Modulation: Let us denote the M-ASK constellation by $\mathcal{S} = \{s_1, s_2, \dots, s_M\}$ such that its constellation center is zero (i.e., $s_1 + s_2 + \dots + s_M = \mathbf{0}$) and that $s_m^H s_{\hat{m}} = s_{\hat{m}}^H s_m$ for all $m \neq \hat{m}$. Accordingly, the correlation between s_m and $s_{\hat{m}}$ for all $m \neq \hat{m}$ is given by

$$\rho_{m\hat{m}} = \frac{\Re\{s_m^H s_{\hat{m}}\}}{\|s_m\| \|s_{\hat{m}}\|} = \pm 1, \quad (349)$$

which consequence that, without loss of generality, the modulation symbols are ordered by $\|s_{\hat{m}} - s_1\| < \|s_m - s_1\|$, $m < \hat{m}$ on a hyperline. Therefore, the modulation symbol m can be written as

$$s_m = a_m s, \quad 1 \leq m \leq M, \quad (350)$$

where s denotes an arbitrary unit vector, i.e., $\|s\| = 1$, and thus a_m , $1 \leq m \leq M$ are such real amplitudes that they support $s_1 + s_2 + \dots + s_M = \mathbf{0}$, which imposes that

$$a_1 + a_2 + \dots + a_M = 0. \quad (351)$$

From the condition that the modulation symbols are ordered, we have $a_1 < a_2 < \dots < a_M$. For each s_m except for the two outside ones s_1 and s_M , the distance of s_m from $s_{m\pm 1}$ is the constant we readily express

$$\|s_m - s_{m\pm 1}\| = (a_m - a_{m\pm 1})^2 = \Delta \text{ (constant)}. \quad (352)$$

Accordingly, we formulate the modulation symbols as

$$s_m = (m - m_0)\Delta s, \quad 1 \leq m \leq M. \quad (353)$$

which imposes that $a_m = (m - m_0)\Delta$, $1 \leq m \leq M$, where Δ is the minimum distance between modulation symbols, and the offset m_0 is found to be $m_0 = (M + 1)/2$ due to $a_1 + a_2 + \dots + a_M = 0$. Then, the power of s_m , which is written as $E_m = \|s_m\|^2$, can be obtained in terms of Δ as

$$E_m = (m - m_0)^2 \Delta^2 \quad (354)$$

Correspondingly, since the modulation symbols are equiprobable, we write the average power of the M-ASK modulation as $E_S = (\sum_{m=1}^M E_m)/M$, and therein substituting (354), we have

$$E_S = \frac{1}{12} (M^2 - 1) \Delta^2, \quad (355)$$

from which the value of Δ can be determined as

$$\Delta = \sqrt{\frac{12E_S}{M^2 - 1}}. \quad (356)$$

The distance between s_m and s_n , $m \neq n$ is written as

$$\|s_m - s_n\| = \sqrt{\frac{12|m - n|E_S}{M^2 - 1}}. \quad (357)$$

Let us find the conditional SER for the M-ASK modulation. Assuming s_m is transmitted, we can write the received vector \mathbf{R}_c using the mathematical model given by (302) as follows

$$\mathbf{R}_c = H a_m s + \mathbf{Z}_c \quad (358)$$

where $\mathbf{Z}_c \sim \mathcal{M}_\nu^L(\mathbf{0}, \frac{N_0}{2} \mathbf{I})$, and hence $\mathbf{R}_c \sim \mathcal{M}_\nu^L(H a_m s, \frac{N_0}{2} \mathbf{I})$. Since all modulation symbols are assumed equiprobable, a symbol error occurs for each s_m except for the two s_1 and s_M when the the projection of $\mathbf{R}_c - H s_m$ on $H s_{m\pm 1} - H s_m$, i.e.,

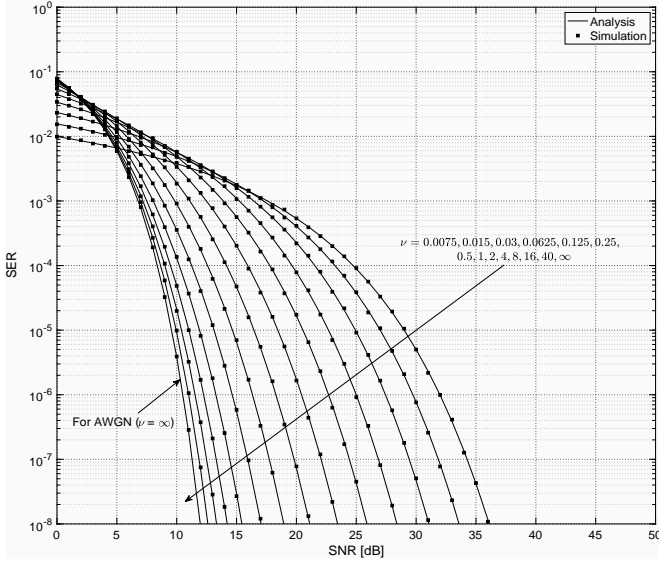
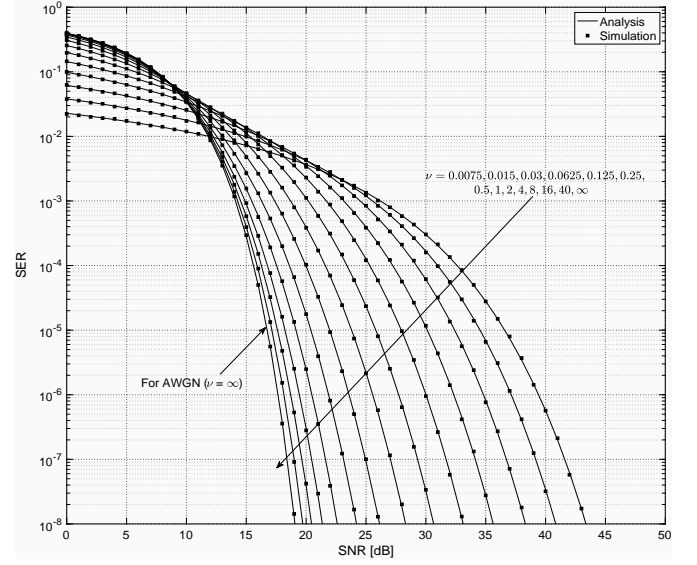
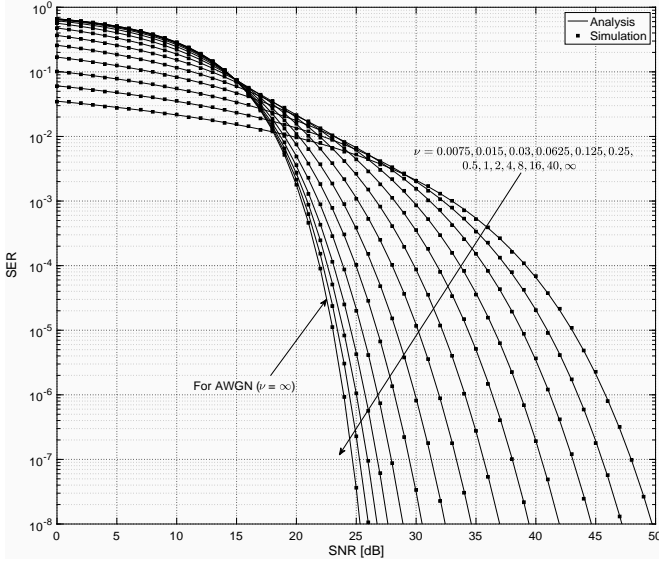
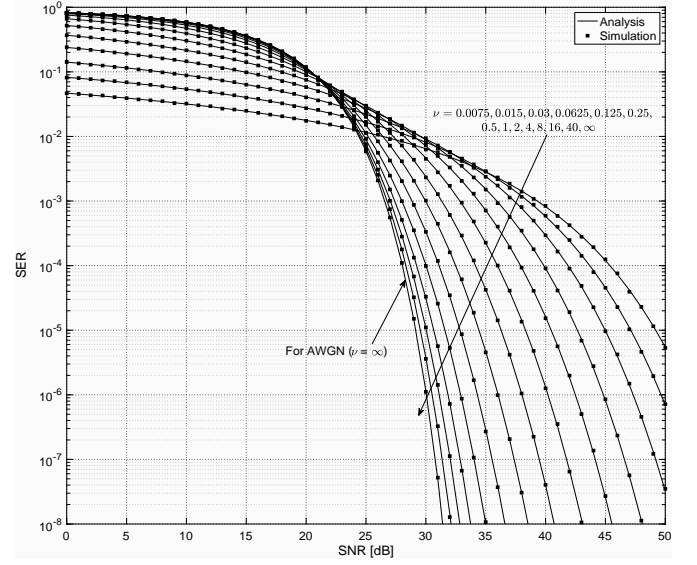

 (a) Modulation level $M = 2$.

 (b) Modulation level $M = 4$.

 (c) Modulation level $M = 8$.

 (d) Modulation level $M = 16$.

Fig. 12: The SER of M-ASK signaling over AWMN channels.

$\Re\{(Hs_{m\pm 1} - Hs_m)^H(\mathbf{R}_c - Hs_m)\}$ is greater than the distance of Hs_m from the perpendicular bisector of the hyperline that connects Hs_m and $Hs_{m\pm 1}$, and the probability of this error is written with the aid of Theorem 57 as follows

$$\Pr\{e | H, s_m\} \triangleq Q_\nu \left(\frac{H\|s_m - s_{m+1}\|}{\sqrt{2N_0}} \right) + Q_\nu \left(\frac{H\|s_m - s_{m-1}\|}{\sqrt{2N_0}} \right), \quad (359a)$$

$$= 2Q_\nu \left(\frac{H\Delta}{\sqrt{2N_0}} \right), \quad (359b)$$

where substituting (356) results in

$$\Pr\{e | H, s_m\} = 2Q_\nu \left(\sqrt{\frac{6\gamma}{M^2 - 1}} \right), \quad (360)$$

where $\gamma \triangleq H^2 E_S / N_0$ denotes the SNR during transmission of one modulation symbol. Additionally, we also need to obtain $\Pr\{e | H, s_1\}$ and $\Pr\{e | H, s_M\}$. For the modulation symbol s_1 , we obtain

$$\Pr\{e | H, s_1\} \triangleq Q_\nu \left(\frac{H\|s_1 - s_2\|}{\sqrt{2N_0}} \right), \quad (361a)$$

$$= Q_\nu \left(\sqrt{\frac{6\gamma}{M^2 - 1}} \right). \quad (361b)$$

Similarly, for the modulation symbol s_M , we obtain

$$\Pr\{e | H, s_M\} \triangleq Q_\nu \left(\frac{H\|s_M - s_{M-1}\|}{\sqrt{2N_0}} \right), \quad (362a)$$

$$= Q_\nu \left(\sqrt{\frac{6\gamma}{M^2 - 1}} \right). \quad (362b)$$

Theorem 61. For the ML decision rule, the conditional SER of the M-ASK signaling is given by

$$\Pr\{e | H\} = 2\left(1 - \frac{1}{M}\right)Q_\nu\left(\sqrt{\frac{6\gamma}{M^2 - 1}}\right), \quad (363)$$

where γ is the instantaneous SNR defined in (344).

Proof. When the modulation symbols are equiprobable, we write the conditional SER of the M-ASK signaling as

$$\Pr\{e | H\} = \frac{1}{M} \sum_{m=1}^M \Pr\{e | H, \mathbf{s}_m\}, \quad (364)$$

where substituting (360), (361b) and (362b) results in (363), which completes the proof of Theorem 61. ■

Let us check the special cases. First, when the normality factor $\nu = 1$, we reduce (363) to the conditional SER of the M-ASK signaling in CCS AWLN channels, that is

$$\Pr\{e | H\} = 2\left(1 - \frac{1}{M}\right)LQ\left(\sqrt{\frac{6\gamma}{M^2 - 1}}\right), \quad (365)$$

Secondly, when the normality factor $\nu \rightarrow \infty$, we also reduce (363) with the aid of (39) to [3, Eq. (4.3-5)], [1, Eq. (8.3)]

$$\Pr\{e | H\} = 2\left(1 - \frac{1}{M}\right)Q\left(\sqrt{\frac{6\gamma}{M^2 - 1}}\right), \quad (366)$$

which is the conditional SER of the M-ASK signaling in CCS AWGN channels as expected.

Properly with the aid of Theorem 61, we disclose in Fig. 12 the conditional SER of M-ASK signaling with respect to the different normalities in AWGN channels. In addition to our previous observations of that the impulsive nature of the additive noise distribution deteriorates the performance in high-SNR regime while negligibly improves in low-SNR regime, we observe that the system performance gets more vulnerable to the impulsive nature of the additive noise distribution as the modulation level M increases.

c) *Conditional SER of M-QAM Modulation:* Considering the M-QAM constellation as the extension of the two M-ASK constellations to the complex amplitude keying, we denote its modulations symbols by $\{\mathbf{s}_1, \mathbf{s}_2, \dots, \mathbf{s}_M\}$, where we express each modulation symbol as

$$\mathbf{s}_m = (a_m + j b_m)\mathbf{s}, \quad 1 \leq m \leq M, \quad (367)$$

where \mathbf{s} denotes an arbitrary unit vector, i.e., $\|\mathbf{s}\|=1$. Further, the inphase keying $a_m \in \mathbb{R}$ and the quadrature keying $b_m \in \mathbb{R}$ are chosen such that we can redefine the M-QAM modulation by the Cartesian product of two M-ASK constellations whose modulation levels are M_I and M_Q , where the modulation level M of the M-QAM modulation is factorized to M_I and M_Q , i.e., $M = M_I M_Q$. We write the symbols of the inphase M-ASK constellation as

$$\mathbf{s}_m^I = \alpha_m \mathbf{s}, \quad 1 \leq m \leq M_I, \quad (368)$$

where $\alpha_m \in \mathbb{R}$. Its average power is $E_I = (\sum_m \alpha_m^2)/M_I$ since its modulation symbols are assumed equiprobable. We write the symbols of the quadrature M-ASK constellation as

$$\mathbf{s}_n^Q = \beta_n \mathbf{s}, \quad 1 \leq n \leq M_Q, \quad (369)$$

where $\beta_n \in \mathbb{R}$. The average power is $E_Q = (\sum_n \beta_n^2)/M_Q$ since the modulation symbols are assumed equiprobable. In terms of α_m and β_n , we can write $a_m \in \mathbb{R}$ and $b_m \in \mathbb{R}$ as

$$a_m = \alpha_{[m/M_Q]+1}, \text{ and } b_m = \beta_{m-[m/M_Q]M_Q}, \quad (370)$$

for all $1 \leq m \leq M$. Accordingly and appropriately, we obtain the average power of the M-QAM constellation as

$$E_S = \frac{1}{M} \sum_{m=1}^M \|\mathbf{s}_m\|^2, \quad (371a)$$

$$= \frac{1}{M} \sum_{m=1}^M (a_m^2 + b_m^2), \quad (371b)$$

where substituting (370) yields

$$E_S = \frac{1}{M_I} \sum_{m=1}^{M_I} \alpha_m^2 + \frac{1}{M_Q} \sum_{n=1}^{M_Q} \beta_n^2, \quad (372a)$$

$$= E_I + E_Q. \quad (372b)$$

such that $E_I = (1 - \kappa)E_S$ and $E_Q = \kappa E_S$, where κ denotes the inphase-to-quadrature ratio (IQR) given by

$$\kappa = \frac{(M_Q^2 - 1)\Delta_Q^2}{(M_Q^2 - 1)\Delta_Q^2 + (M_I^2 - 1)\Delta_I^2}. \quad (373)$$

where Δ_I and Δ_Q are the minimum distance of the inphase and quadrature M-ASK constellations, respectively. In addition, when $M_I = M_Q$ and $\Delta_I = \Delta_Q$, the M-QAM signaling is termed as a square M-QAM signaling, and otherwise, a rectangular M-QAM signaling. Further, with the aid of the definition of the instantaneous SNR given by (344), we can rewrite the instantaneous SNR as $\gamma = H^2 E_S / N_0 = \gamma_I + \gamma_Q$, where we have $\gamma_I = H^2 E_I / N_0$ and $\gamma_Q = H^2 E_Q / N_0$ such that $\gamma_I = (1 - \kappa)\gamma$ and $\gamma_I = \kappa\gamma$.

Let us find the conditional SER for the rectangular M-QAM modulation based on the resultants given above. Assuming \mathbf{s}_m is transmitted, we can readily write the received vector \mathbf{R}_c using the mathematical model given by (302) as follows

$$\mathbf{R}_c = H(a_m + j b_m)\mathbf{s} + \mathbf{Z}_c \quad (374)$$

where $\mathbf{Z}_c \sim \mathcal{CM}_\nu^L(\mathbf{0}, \frac{N_0}{2}\mathbf{I})$, and then the received vector is $\mathbf{R}_c \sim \mathcal{CM}_\nu^L(H(a_m + j b_m)\mathbf{s}, \frac{N_0}{2}\mathbf{I})$. Further, we have

$$\mathbf{Z}_c = \mathbf{I}_c + j\mathbf{Q}_c \quad (375)$$

where $\mathbf{I}_c \sim \mathcal{M}_\nu^L(\mathbf{0}, \frac{N_0}{2}\mathbf{I})$ and $\mathbf{Q}_c \sim \mathcal{M}_\nu^L(\mathbf{0}, \frac{N_0}{2}\mathbf{I})$. It is further extremely important and necessary to note that \mathbf{I}_c and \mathbf{Q}_c are mutually uncorrelated but not independent since both are belong to the same CCS AWMN channel. The projection of the received vector \mathbf{R}_c on the space of modulation symbols, i.e., $P_c \triangleq \mathbf{s}^H \mathbf{R}_c$ is given by

$$P_c = H(a_m + j b_m)\mathbf{s} + Z_c \quad (376)$$

$$\begin{aligned} \Pr\{e | H\} &= 2(1 - 1/M_I)Q_\nu\left(\sqrt{\beta_I^2\gamma}\right) + 2(1 - 1/M_Q)Q_\nu\left(\sqrt{\beta_Q^2\gamma}\right) \\ &\quad - 2(1 - 1/M_I)(1 - 1/M_Q)Q_\nu\left(\sqrt{\beta_I^2\gamma}, \frac{\pi}{2} - \phi\right) - 2(1 - 1/M_I)(1 - 1/M_Q)Q_\nu\left(\sqrt{\beta_Q^2\gamma}, \phi\right), \end{aligned} \quad (378)$$

where we decompose $Z_c \sim \mathcal{CM}_\nu(\mathbf{0}, N_0/2)$ as

$$Z_c = I_c + jQ_c \quad (377)$$

where the inphase $I_c \sim \mathcal{M}_\nu(\mathbf{0}, N_0/2)$ and the quadrature $Q_c \sim \mathcal{M}_\nu(\mathbf{0}, N_0/2)$ are mutually uncorrelated but not independent due to the reason mentioned above. Appropriately, with the aid of (363), the probability of an erroneous detection for this M-QAM constellation is given in the following theorem.

Theorem 62. *For the ML decision rule, the conditional SER of the rectangular M-QAM signaling is given by (378) at the top of this page, in which γ is the instantaneous SNR defined in (344), κ is the IQR defined in (373). Further, β_I and β_Q are respectively the minimum inphase and quadrature distances normalized by noise power and are respectively defined by*

$$\beta_I \triangleq \sqrt{\frac{6(1-\kappa)}{M_I^2-1}}, \text{ and } \beta_Q \triangleq \sqrt{\frac{6\kappa}{M_Q^2-1}}. \quad (379)$$

The phase $\phi \triangleq \arctan(\beta_I/\beta_Q)$ is given by

$$\phi = \arctan\left(\sqrt{\frac{\kappa(M_I^2-1)}{(1-\kappa)(M_Q^2-1)}}\right). \quad (380)$$

Proof. With the aid of Theorem 10, let us further decompose the additive complex noise Z_c as

$$Z_c = \sqrt{G}(X_c + jY_c) \quad (381)$$

where $G \sim \mathcal{G}(\nu, 1)$, $X_c \sim \mathcal{N}(\mathbf{0}, N_0/2)$, and $Y_c \sim \mathcal{N}(\mathbf{0}, N_0/2)$ such that we define the inphase $I_c \triangleq \sqrt{G}X_c$ and the quadrature $Q_c \triangleq \sqrt{G}Y_c$. Hence, we notice that both $I_c|G$ and $Q_c|G$ (i.e., both I_c and Q_c conditioned on G) are mutually independent Gaussian distributions with zero mean and $GN_0/2$ variance. Appropriately, exploiting (366) and using the coefficients (379), we can write the conditional SER of the inphase M_I -ASK as $\Pr\{e_I | H, G\} = 2(1 - 1/M_I)Q(\beta_I\sqrt{\gamma/G})$. Similarly, we can write the conditional SER of the quadrature M_Q -ASK as $\Pr\{e_Q | H, G\} = 2(1 - 1/M_Q)Q(\beta_Q\sqrt{\gamma/G})$. The mutual independence between $I_c|G$ and $Q_c|G$ yields the conclusion that the probability of the correct symbol decision is the product of the conditional probabilities $\Pr\{c_I | H, G\} = 1 - \Pr\{e_I | H, G\}$ and $\Pr\{c_Q | H, G\} = 1 - \Pr\{e_Q | H, G\}$, which are respectively correct decision probabilities for constituent M_I -ASK and M_Q -ASK constellations when conditioned on G , we can thus write the probability of an erroneous detection as

$$\Pr\{e | H, G\} = 1 - \Pr\{c | H, G\}, \quad (382a)$$

$$= 1 - \Pr\{c_I | H, G\} \Pr\{c_Q | H, G\}, \quad (382b)$$

$$= 1 - (1 - \Pr\{e_I | H, G\}) \times (1 - \Pr\{e_Q | H, G\}), \quad (382c)$$

where substituting $\Pr\{e_I | H, G\}$ and $\Pr\{e_Q | H, G\}$ yields

$$\begin{aligned} \Pr\{e | H, G\} &= 2(1 - 1/M_I)Q(\beta_I\sqrt{\gamma/G}) \\ &\quad + 2(1 - 1/M_Q)Q(\beta_Q\sqrt{\gamma/G}) \\ &\quad - 4(1 - 1/M_I)(1 - 1/M_Q) \\ &\quad \times Q(\beta_I\sqrt{\gamma/G})Q(\beta_Q\sqrt{\gamma/G}). \end{aligned} \quad (383)$$

Then, the conditional SER of the rectangular M-QAM constellation is written as $\Pr\{e | H\} = \int_0^\infty \Pr\{e | H, g\} f_G(g) dg$, where substituting (85) yields

$$\begin{aligned} \Pr\{e | H\} &= 2(1 - 1/M_I)I_1(\beta_I\sqrt{\gamma}) \\ &\quad + 2(1 - 1/M_Q)I_1(\beta_Q\sqrt{\gamma}) \\ &\quad - 4(1 - 1/M_I)(1 - 1/M_Q)I_2(\beta_I\sqrt{\gamma}, \beta_Q\sqrt{\gamma}), \end{aligned} \quad (384)$$

where $I_1(x)$ and $I_2(x, y)$ are given by

$$I_1(x) = \int_0^\infty Q(\sqrt{x^2/g}) f_G(g) dg, \quad (385)$$

$$I_2(x, y) = \int_0^\infty Q(\sqrt{x^2/g}) Q(\sqrt{y^2/g}) f_G(g) dg, \quad (386)$$

where $x, y \in \mathbb{R}_+$. Inserting $Q(x) = \frac{1}{2}\text{erfc}(x/\sqrt{2})$ [3, Eq. (2.3-18)] and [149, Eq. (06.27.26.0006.01)] into (385), and accordingly using [151, Eqs. (2.8.4) and (2.9.1)], $I_1(x)$ results in (46). Therefore, we have $I_1(x) = Q_\nu(x)$. In addition, inserting [171, Eq. (4.6) and (4.8)] into (386) and using [148, Eq. (3.471/9)] and then exploiting Definition 2, we obtain $I_2(x, y)$ as $I_2(x, y) = \frac{1}{2}Q_\nu(x, \pi/2 - \phi) + \frac{1}{2}Q_\nu(y, \phi)$. Finally, substituting $I_1(x)$ and $I_2(x, y)$ into (384) results in (378), which completes the proof of Theorem 62. ■

Theorem 63. *For the ML decision rule, the conditional SER of the square M-QAM signaling is given by*

$$\begin{aligned} \Pr\{e | H\} &= 4\left(1 - \frac{1}{\sqrt{M}}\right)Q_\nu\left(\sqrt{\frac{3\gamma}{M-1}}\right) \\ &\quad - 4\left(1 - \frac{1}{\sqrt{M}}\right)^2 Q_\nu\left(\sqrt{\frac{3\gamma}{M-1}}, \frac{\pi}{4}\right), \end{aligned} \quad (387)$$

where γ is the SNR defined in (344).

Proof. Note that when we have $M_I = M_Q = \sqrt{M}$, we perceive that the M-QAM constellation becomes a two-dimensional square constellation, where each of the inphase and quadrature components can be therefore considered as \sqrt{M} -amplitude shift keying (ASK) constellation. Accordingly, with the aid of (356), we find out that the inphase and quadrature minimum distances, i.e., Δ_I and Δ_Q are equal, that is

$$\Delta_I = \Delta_Q = \sqrt{\frac{6E_s}{M-1}}, \quad (388)$$

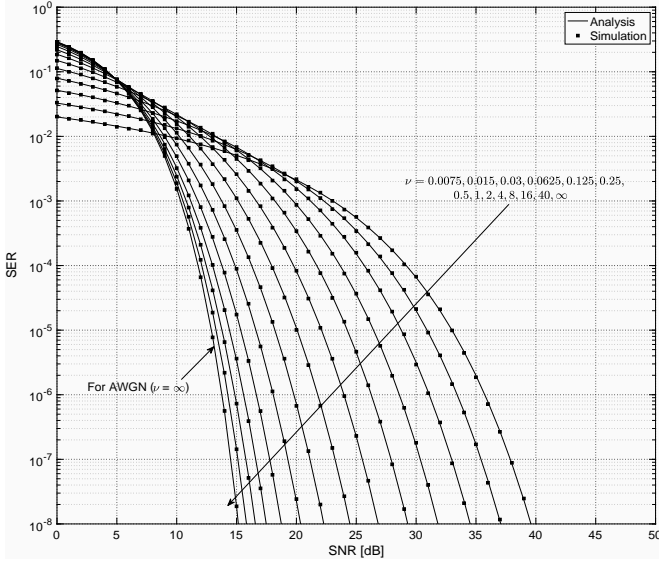
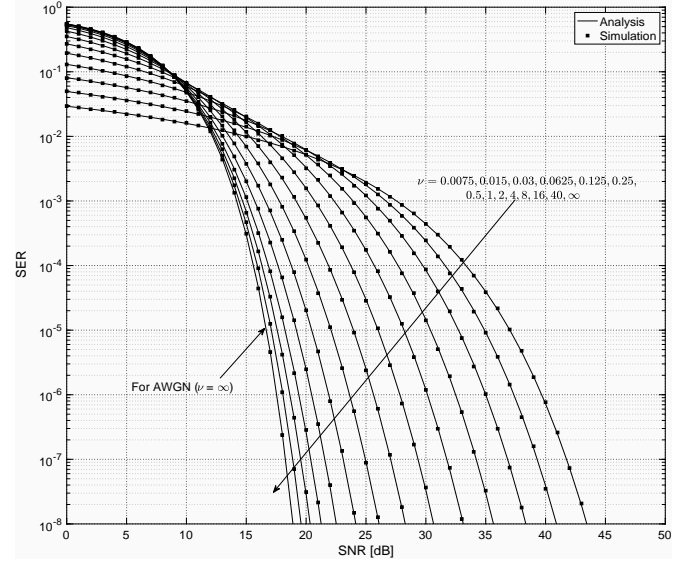
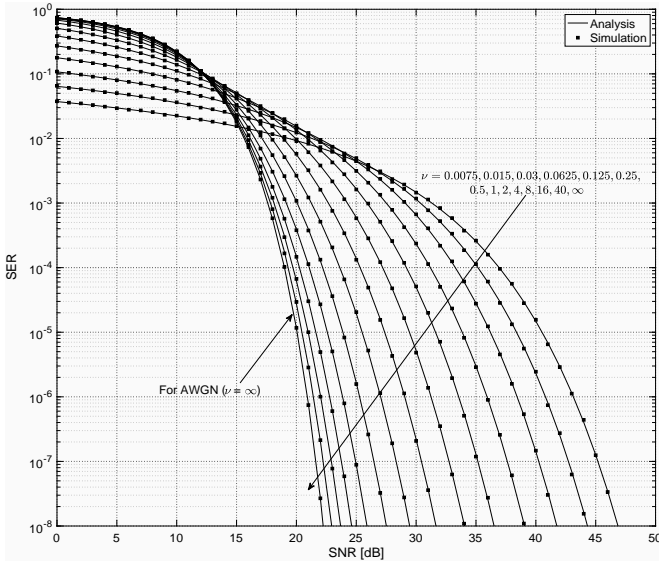
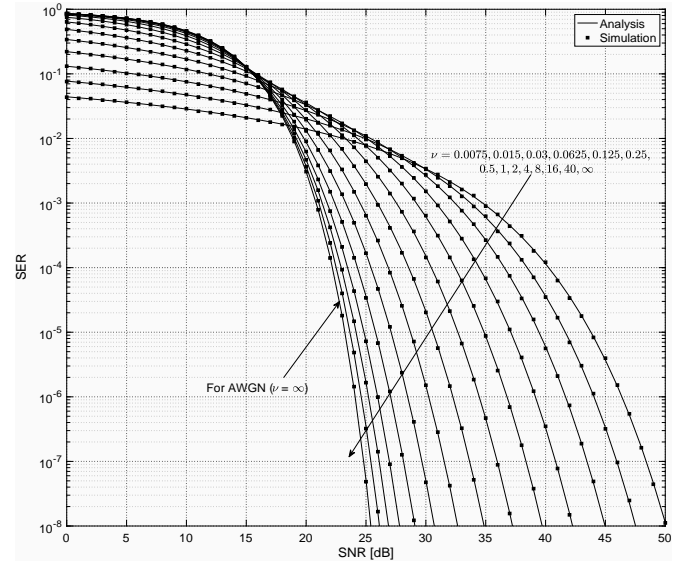

 (a) Modulation level $M = 4$.

 (b) Modulation level $M = 8$.

 (c) Modulation level $M = 16$.

 (d) Modulation level $M = 32$.

Fig. 13: The SER of M-QAM signaling over AWMN channels.

which yields $\kappa = 1/2$ as observed from (373), and further $\beta_I = \beta_Q = \sqrt{3/(M-1)}$ from (379). Eventually, substituting these results into (378) yields (387), which proves Theorem 63. ■

Let us check some special cases for completeness. For 4-QAM, (387) reduces to

$$\Pr\{e|H\} = 2Q_\nu(\sqrt{\gamma}) - Q_\nu(\sqrt{\gamma}, \pi/4), \quad (389)$$

where referring (50) with the total integration angle, i.e., $\pi/2 + \pi/2 - \pi/4 = \pi - \pi/4$, we can reduce (389) more to

$$\Pr\{e|H\} = Q_\nu(\sqrt{\gamma}, 3\pi/4), \quad (390)$$

In addition, note that we have

$$\lim_{\nu \rightarrow \infty} Q_\nu\left(x, \frac{\pi}{4}\right) = Q(x)^2. \quad (391)$$

Thus, when the normality factor $\nu \rightarrow \infty$, (387) reduces to [3, Eq. (4.3-30)], [1, Eq. (8.10)] as expected.

For analytical accuracy and numerical correctness, we show in Fig. 13 the SER of M-QAM signaling over AWMN channels by using Theorem 63 for analytical accuracy and performing simulations for numerical correctness. We also therein observe that, for $\nu \rightarrow 0$, the system performance deteriorates in high-SNR regime. When we compare the performance of M-QAM to that of M-ASK (i.e., namely Fig. 13b to Fig. 12c for $M=8$), we notice that M-QAM gives better performance.

d) Conditional SER of M-PSK Modulation: Considering the M-PSK constellation as the rotational extension of the BPSK constellation to the phase shift keying, let us denote its modulation symbols by $\{s_1, s_2, \dots, s_M\}$, where $s_m = \alpha e^{j\theta_m} s$ such that s denotes an arbitrary unit vector (i.e., $\|s\| = 1$), the amplitude $\alpha \in \mathbb{R}_+$ determines the power per modulation symbol such that we can readily express the power of s_m as $E_m \triangleq \|s_m\|^2 = \alpha^2$. Further, the phase rotations θ_m , $1 \leq m \leq M$

encode information within the M-PSK modulation symbols and are uniformly chosen for a modulation level M , that is

$$\theta_m = 2\pi(m-1)/M, \quad 1 \leq m \leq M. \quad (392)$$

Accordingly, we can rewrite the M-PSK modulation symbols as $\mathbf{s}_m = \alpha \exp(j2\pi(m-1)/M)\mathbf{s}$, $1 \leq m \leq M$ and therein making use of $E_m = \alpha^2$, $1 \leq m \leq M$, we obtain the average power E_S as follows

$$E_S \triangleq \sum_{m=1}^M \Pr\{\mathbf{s}_m\} E_m = \alpha^2. \quad (393)$$

Therefore, we have $\alpha = \sqrt{E_S}$. Let us now find the conditional SER for the M-PSK modulation. Assuming \mathbf{s}_m is transmitted, we can write the received vector \mathbf{R}_c using the mathematical model given by (302) as follows

$$\mathbf{R}_c = \alpha H e^{j\theta_m} \mathbf{s} + \mathbf{Z}_c \quad (394)$$

where $\mathbf{Z}_c \sim \mathcal{CM}_\nu^L(\mathbf{0}, \frac{N_0}{2}\mathbf{I})$ and $\mathbf{R}_c \sim \mathcal{CM}_\nu^L(\alpha H e^{j\theta_m} \mathbf{s}, \frac{N_0}{2}\mathbf{I})$. Since the information is carried by means of phase shift keying in form of $2\pi/M$ multiplies (i.e., the angle difference between the adjacent symbols is $2\pi/M$), a decision error occurs when the additive noise \mathbf{Z}_c causes an enough rotational shift more than π/M in clockwise or counterclockwise direction in \mathbf{R}_c . We give the projection of \mathbf{R}_c on \mathbf{s}_m as

$$P_c \triangleq \mathbf{s}_m^H \mathbf{R}_c = \alpha H + Z_c \quad (395)$$

where $Z_c \sim \mathcal{CM}_\nu(0, N_0/2)$ follows the PDF that we write with the aid of Theorem 11 as

$$f_{Z_c}(z) = \frac{2}{\pi} \frac{|z|^{\nu-1}}{\Gamma(\nu) \Lambda_0^{\nu+1}} K_{\nu-1} \left(\frac{2|z|}{\Lambda_0} \right), \quad (396)$$

defined over $z \in \mathbb{C}$ with the normality factor $\Lambda_0 = \sqrt{N_0/\nu}$. Therefore, $P_c \sim \mathcal{CM}_\nu(\alpha H, N_0/2)$ is decomposed as

$$P_c = I_c + jQ_c, \quad (397)$$

where $I_c \sim \mathcal{M}_\nu(\alpha H, N_0/2)$ and $Q_c \sim \mathcal{M}_\nu(0, N_0/2)$. Hence, the amplitude fluctuation caused by the additive complex noise \mathbf{Z}_c is apparently written as $A_c \triangleq \sqrt{I_c^2 + Q_c^2}$. The rotational shift, which is another effect caused by the additive complex noise \mathbf{Z}_c , is written as $\Theta_c \triangleq \arctan(Q_c/I_c)$, which follows such a random distribution that a decision error occurs when $|\Theta_c| > \pi/M$ (i.e., a correct decision occurs when $|\Theta_c| < \pi/M$). In other words, the error probability when \mathbf{s}_m was transmitted is readily written as

$$\Pr\{e | H, \mathbf{s}_m\} = \Pr\{|\Theta_c| > \pi/M\}, \quad (398a)$$

$$= 1 - \Pr\{-\pi/M < \Theta_c < \pi/M\}. \quad (398b)$$

Since assuming that all modulation symbols are equiprobable, we perceive that, due to the rotational symmetry of the M-PSK constellation, $\Pr\{e | H, \mathbf{s}_m\} = \Pr\{e | H, \mathbf{s}_{\hat{m}}\}$ for all $m \neq \hat{m}$. The conditional SER of the M-PSK is therefore equal to the probability of making a decision error when \mathbf{s}_m is transmitted, and accordingly we write

$$\Pr\{e | H\} = \sum_{m=1}^M \Pr\{e | H, \mathbf{s}_m\} \Pr\{\mathbf{s}_m\}, \quad (399a)$$

$$= \Pr\{e | H, \mathbf{s}_m\}, \quad (399b)$$

$$= 1 - \Pr\{-\pi/M < \Theta_c < \pi/M\}. \quad (399c)$$

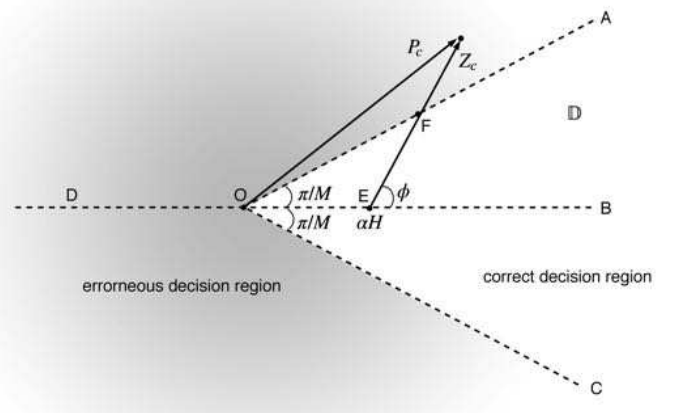


Fig. 14: Received vector representation of the M-PSK signaling whose projection model is given by (395) with the decision region $\mathbb{D} = \{z \in \mathbb{C} \mid -\pi/M < \arg(z) < \pi/M\}$.

Referring to (397), and therefrom having both the amplitude $A_c = \sqrt{I_c^2 + Q_c^2}$ and the phase $\Theta_c = \arctan(Q_c/I_c)$, we can deduce the inphase and quadrature of the projection P_c as $I_c = A_c \cos(\Theta_c)$ and $Q_c = A_c \sin(\Theta_c)$, from which we derive the joint PDF of A_c and Θ_c by utilizing (396), that is

$$f_{A_c, \Theta_c}(a, \theta) = \frac{2 \Omega(a, \theta)^{\nu-1}}{\pi \Gamma(\nu) \Lambda_0^{\nu+1}} K_{\nu-1} \left(\frac{2}{\Lambda_0} \Omega(a, \theta) \right), \quad (400)$$

where $\Omega(a, \theta)$ is given by

$$\Omega(a, \theta) = \sqrt{a^2 - 2a\sqrt{H^2 E_S} \cos(\theta) + H^2 E_S}. \quad (401)$$

Accordingly, when we integrate (400) over $a \in \mathbb{R}_+$, we obtain the marginal PDF of Θ_c , that is $f_{\Theta_c}(\theta) \triangleq \int_0^\infty f_{A_c, \Theta_c}(a, \theta) da$, where substituting (400) yields

$$f_{\Theta_c}(\theta) = \int_0^\infty \frac{2 \Omega(a, \theta)^{\nu-1}}{\pi \Gamma(\nu) \Lambda_0^{\nu+1}} K_{\nu-1} \left(\frac{2}{\Lambda_0} \Omega(a, \theta) \right) da. \quad (402)$$

which does not simplify to a simple closed form and thus must be evaluated numerically. Nevertheless, making use of $f_{\Theta_c}(\theta)$, we calculate the probability $\Pr\{\theta_0 < \Theta_c < \theta_1\} = \int_{\theta_0}^{\theta_1} f_{\Theta_c}(\theta) d\theta$ and thereby derive the conditional SER of M-PSK constellation in the following.

Theorem 64. For the ML decision rule, the conditional SER of the rectangular M-PSK signaling is given by

$$\Pr\{e | H\} = 1 - \int_{-\pi/M}^{\pi/M} f_{\Theta_c}(\theta) d\theta. \quad (403)$$

Proof. The proof is obvious using (398b) with the marginal PDF of Θ_c given in (402) above. ■

A closed-form expression to (403) does not exist for $M > 4$, and therefore the exact value of $\Pr\{e | H\}$ must be calculated numerically and of course can be accurately approximated using Chebyshev-Gauss quadrature formula [147, Eq. (25.4.39)]. The other approach, which is similar to the one followed in [153], to find the conditional SER of M-PSK constellation is to integrate the PDF of $Z_c \sim \mathcal{CM}_\nu(0, N_0/2)$ over the region of $\mathbb{D} = \{z \in \mathbb{C} \mid -\pi/M < \arg(z) < \pi/M\}$ and as presented in the following.

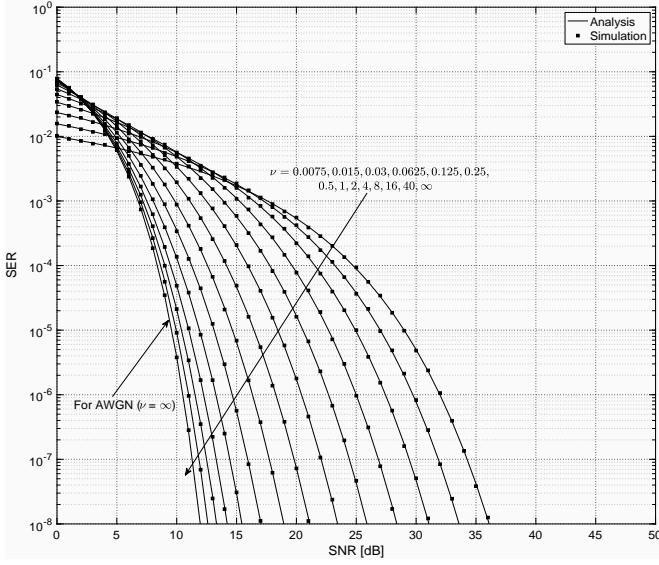
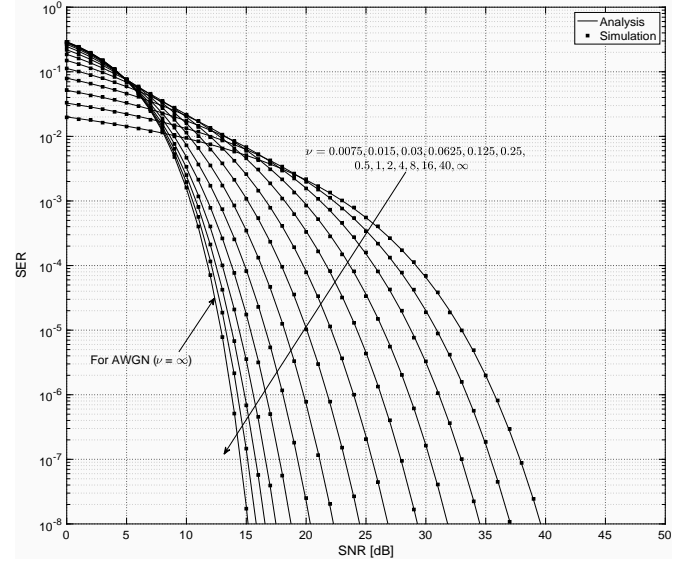
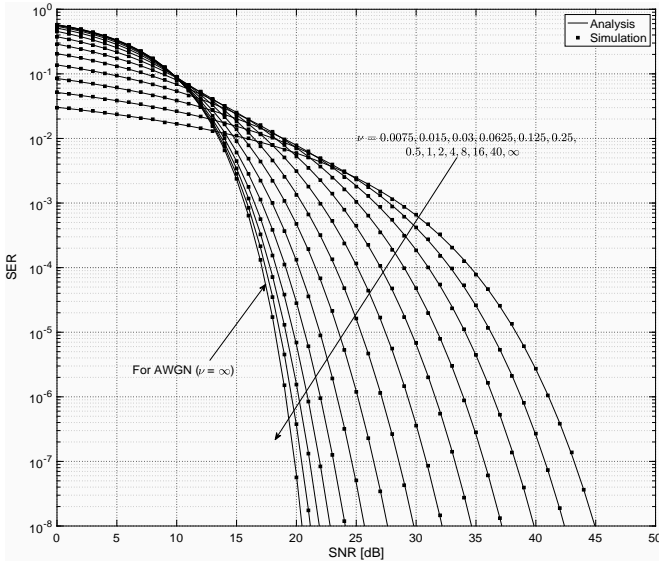
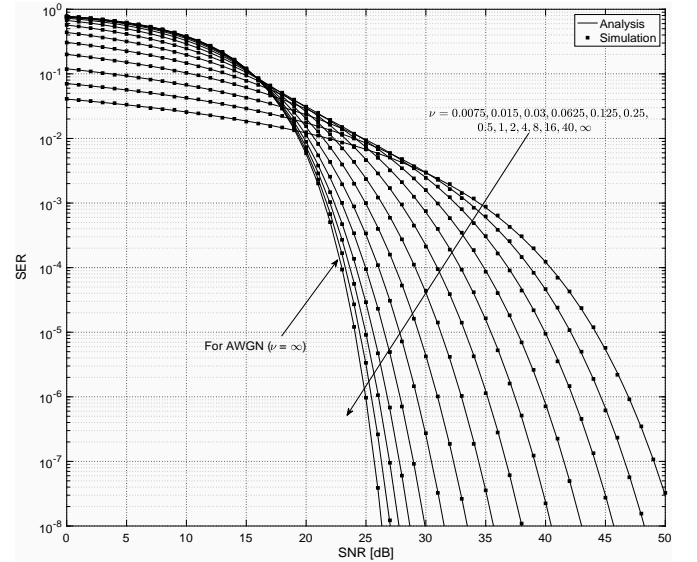

 (a) Modulation level $M = 2$.

 (b) Modulation level $M = 4$.

 (c) Modulation level $M = 8$.

 (d) Modulation level $M = 16$.

Fig. 15: The SER of M-PSK modulation over AWMN channels.

Theorem 65. For the ML decision rule, the conditional SER of the M-PSK signaling is given by

$$\Pr\{e | H\} = Q_\nu\left(\sqrt{2\gamma} \sin\left(\frac{\pi}{M}\right), \pi - \frac{\pi}{M}\right), \quad (404)$$

where γ is the instantaneous SNR defined in (344).

Proof. Referring to (395), we have $Z_c \sim \mathcal{CM}_\nu(0, N_0/2)$ with the decomposition $Z_c = X_c + jY_c$ in Cartesian form, where $X_c \sim \mathcal{M}_\nu(0, N_0/2)$ and $Y_c \sim \mathcal{M}_\nu(0, N_0/2)$. Further, we also have the decomposition $Z_c = A_c \exp(j\Phi_c)$ in polar form, where we express $A_c = \sqrt{X_c^2 + Y_c^2}$ and $\Phi_c = \arctan(Y_c/X_c)$. Using (396), we obtain the joint PDF of A_c and Φ_c as

$$f_{A_c, \Phi_c}(a, \phi) = f_{Z_c}(z) J_{Z_c|A_c, \Phi_c}, \quad (405a)$$

$$= f_{Z_c}(a \exp(j\phi)) J_{Z_c|A_c, \Phi_c}, \quad (405b)$$

where $f_{Z_c}(z)$ is given in (396). Further, $J_{Z_c|A_c, \Phi_c}$ denotes the Jacobian of $z = a \exp(j\phi)$ and is derived as $J_{Z_c|A_c, \Phi_c} = a$, whose replacement in (405) yields

$$f_{A_c, \Phi_c}(a, \phi) = \frac{2}{\pi} \frac{a^\nu}{\Gamma(\nu) \Lambda_0^{\nu+1}} K_{\nu-1}\left(\frac{2a}{\Lambda_0}\right), \quad (406)$$

which is defined over $a \in \mathbb{R}_+$ and $\theta \in [-\pi, \pi)$. We notice that, as depicted in Fig. 14, a decision error occurs if Z_c falls into the erroneous decision region. Then, we write the conditional SER of M-PSK constellation as

$$\Pr\{e | H\} = 2 \int_{\pi/M}^{\pi} \int_{|\text{EF}|}^{\infty} f_{A_c, \Phi_c}(a, \phi) d\phi da, \quad (407)$$

where $|\text{EF}|$ is the distance between the modulation symbol (i.e., point E) and the boundary point (i.e., point F). The length

$|\text{EF}|$ is written from $H\alpha \sin(\pi/M) = |\text{EF}| \sin(\phi - \pi/M)$ as

$$|\text{EF}| = 2\gamma \left(\frac{\Lambda_0}{\lambda_0} \right)^2 \frac{\sin(\pi/M)}{\sin(\phi - \pi/M)}, \quad (408)$$

where the parameters $\Lambda_0 \triangleq \sqrt{N_0/\nu} = \sqrt{N_0/2}\lambda_0$, $\lambda_0 \triangleq \sqrt{2/\nu}$ and $\gamma \triangleq H^2 E_S/N_0$ are defined previously. Consequently, substituting (408) into (407), and sequentially using [150, Eqs. (8.2.2/8), (2.24.2/3) and (8.4.23/1)], we readily obtain

$$\Pr\{e | H\} = \frac{2^{1-\nu}}{\pi\Gamma(\nu)} \int_{\pi/M}^{\pi} \left(\frac{2\sqrt{2\gamma} \sin(\pi/M)}{\lambda_0 \sin(\phi - \pi/M)} \right)^\nu \times K_\nu \left(\frac{2\sqrt{2\gamma} \sin(\pi/M)}{\lambda_0 \sin(\phi - \pi/M)} \right) d\phi, \quad (409)$$

where applying the change of variable $\theta = \phi - \pi/M$ and using Definition 2 yields (404), which proves Theorem 65. ■

Let us now consider some special cases for the closed-form conditional SER of the M-PSK signaling. The BPSK constellation is the most reliable modulation as a special case of the M-PSK constellation. Accordingly, setting $M = 2$ in (404) and utilizing the property $Q_\nu(x) = Q_\nu(x, \pi/2)$, we obtain the conditional SER of BPSK constellation as follows

$$\Pr\{e | H\} = Q_\nu(\sqrt{2\gamma}, \pi/2), \quad (410a)$$

$$= Q_\nu(\sqrt{2\gamma}), \quad (410b)$$

which is perfect agreement with (345). Further, setting $M = 4$ in (404), we obtain the conditional SER of quadrature phase shift keying (QPSK) (i.e., 4-QAM) constellation, that is

$$\Pr\{e | H\} = Q_\nu(\sqrt{2\gamma} \sin(\pi/M), \pi - \pi/M) \Big|_{M=4}, \quad (411a)$$

$$= Q_\nu(\sqrt{\gamma}, 3\pi/4), \quad (411b)$$

which is in agreement with (390) as expected.

For the analysis of impulsive noise effects on the performance, we demonstrate in Fig. 15 how the conditional SER of M-PSK signaling over complex AWMN channels varies with respect to the SNR, the normality ν and the modulation level M , and notice that numerical and simulation-based results are in perfect agreement. Further, we have observed previously obtained results. As such, the impulsive nature of the additive noise increases (i.e., the normality ν decreases), the performance deteriorates in high-SNR regime while negligibly improves in low-SNR regime.

B. Non-Coherent Signalling

In the previous subsection, we have investigated the coherent signaling in which the receiver has perfect knowledge about the received carrier phase. Detection techniques based on the absence of any knowledge about the received carrier phase are referred to as non-coherent detection techniques [1]–[3]. In the following, we consider the MAP and ML detection rules for non-coherent signaling in which the receiver does not have any information about both the transmitted modulation symbols and the carrier phase, and we obtain the SER performance of non-coherent signaling. With the aid of the mathematical model, which is given in (267), we can re-express the received vector as $\mathbf{R} \triangleq H e^{j\Theta} \mathbf{F} \mathbf{S} + \mathbf{Z}$, where

the variables are well-explained immediately after (267). In needing to re-explain these variables, H denotes the fading envelope following a non-negative random distribution, Θ denotes the fading phase uniformly distributed over $[0, 2\pi]$. Further, both H and Θ are assumed constant due to channel coherence [1]–[3]. Further, \mathbf{S} denotes the modulation symbol vector randomly chosen from the fixed set of modulation symbols $\{\mathbf{s}_1, \mathbf{s}_2, \dots, \mathbf{s}_M\}$ according to the probabilities given by

$$p_m = \Pr\{\mathbf{S} = \mathbf{s}_m\}, \text{ for all } 1 \leq m \leq M, \quad (412)$$

such that $\sum_{m=1}^M p_m = 1$. For non-coherent DPSK signaling [2], [3], the modulation symbols $\mathbf{s}_1, \mathbf{s}_2, \dots, \mathbf{s}_M$ are not required to be orthogonal with each other, i.e.,

$$\mathbf{s}_m^H \mathbf{s}_n \neq 0, \text{ for } m \neq n \quad (413a)$$

$$\mathbf{s}_m^H \mathbf{s}_m = E_m, \quad (413b)$$

where E_m is the energy of the modulation symbol m . Without loss of generality, we assume that the energy of the modulation symbols are ordered, i.e., $E_1 \leq E_2 \leq \dots \leq E_M$. During each modulation symbol, the received vector \mathbf{R} depends statistically on \mathbf{S} and Θ with the conditional PDF $f_{\mathbf{R}|\mathbf{S},\Theta}(\mathbf{r}|\mathbf{s},\theta)$, that is

$$f_{\mathbf{R}|\mathbf{S},\Theta}(\mathbf{r}|\mathbf{s},\theta) = \frac{2}{\pi^L} \frac{\|\mathbf{r} - H e^{j\Theta} \mathbf{F} \mathbf{s}\|_{\Sigma}^{\nu-L}}{\Gamma(\nu) \det(\Sigma) \lambda_0^{\nu+L}} \times K_{\nu-L} \left(\frac{2}{\lambda_0} \|\mathbf{r} - H e^{j\Theta} \mathbf{F} \mathbf{s}\|_{\Sigma} \right). \quad (414)$$

The PDF of the received vector \mathbf{R} conditioned on the modulation symbols \mathbf{S} , i.e., $f_{\mathbf{R}|\mathbf{S}}(\mathbf{r}|\mathbf{s})$ is written as $f_{\mathbf{R}|\mathbf{S}}(\mathbf{r}|\mathbf{s}) \triangleq \int_0^{2\pi} f_{\mathbf{R}|\mathbf{S},\Theta}(\mathbf{r}|\mathbf{s},\theta) f_{\Theta}(\theta) d\theta$, and thus the joint PDF of \mathbf{R} and \mathbf{S} is written as $f_{\mathbf{R},\mathbf{S}}(\mathbf{r}, \mathbf{s}) \triangleq f_{\mathbf{R}|\mathbf{S}}(\mathbf{r}|\mathbf{s}) f_{\mathbf{S}}(\mathbf{s})$, where $f_{\mathbf{S}}(\mathbf{s})$ is given by (269). In the receiver, the optimal detector without knowledge of the fading phase Θ observes the received vector \mathbf{R} and produces the index of the most probable transmitted modulation symbol that maximizes $f_{\mathbf{R},\mathbf{S}}(\mathbf{r}, \mathbf{s})$, that is

$$\hat{m} \triangleq \arg \max_{1 \leq m \leq M} f_{\mathbf{R},\mathbf{S}}(\mathbf{R}, \mathbf{s}_m), \quad (415a)$$

$$= \arg \max_{1 \leq m \leq M} f_{\mathbf{R}|\mathbf{S}}(\mathbf{R}|\mathbf{s}_m) \Pr\{\mathbf{S} = \mathbf{s}_m\}, \quad (415b)$$

$$= \arg \max_{1 \leq m \leq M} \frac{p_m}{2\pi} \int_0^{2\pi} \frac{2}{\pi^L} \frac{\|\mathbf{r} - H e^{j\Theta} \mathbf{F} \mathbf{s}_m\|_{\Sigma}^{\nu-L}}{\Gamma(\nu) \det(\Sigma) \lambda_0^{\nu+L}} \times K_{\nu-L} \left(\frac{2}{\lambda_0} \|\mathbf{r} - H e^{j\Theta} \mathbf{F} \mathbf{s}_m\|_{\Sigma} \right) d\theta, \quad (415c)$$

which means that if the transmitted symbol m and the optimally detected symbol \hat{m} are not the same, a decision error occurs with the probability $\Pr\{e\} = \Pr\{\hat{m} \neq m\}$. We can even simplify (415c) more as shown in the following.

Theorem 66. *For the complex vector channel introduced in (267), the non-coherent MAP detection rule is given by*

$$\hat{m} \triangleq \arg \max_{1 \leq m \leq M} p_m \exp \left(\frac{1}{2} H^2 \mathbf{s}_m^H \mathbf{F}^H \Sigma^{-1} \mathbf{F} \mathbf{s}_m \right) \times I_0 \left(H \left| \mathbf{s}_m^H \mathbf{F}^H \Sigma^{-1} \mathbf{F} \mathbf{R} \right| \right), \quad (416)$$

where $I_0(\cdot)$ is the modified Bessel function of the first kind of zero order [148, Eq. (8.406/3)], [149, Eq. (03.02.02.0001.01)].

Proof. In the mathematical channel model given by (267), the vector \mathbf{R} received during the transmission of the modulation symbol \mathbf{s}_m will have a multivariate CES McLeish distribution, i.e., $\mathbf{R} \sim \mathcal{CM}_\nu^L(He^{j\Theta}\mathbf{s}_m, \Sigma)$. Exploiting both (216) and (217), we decompose the vector \mathbf{R} given the symbol \mathbf{S} as

$$(\mathbf{R}|\mathbf{S}) \triangleq He^{j\Theta}\mathbf{F}\mathbf{s}_m + \sqrt{G}\mathbf{D}(\mathbf{N}_1 + j\mathbf{N}_2), \quad (417)$$

where $\Sigma = \mathbf{D}\mathbf{D}^H$, $\mathbf{N}_1 \sim \mathcal{N}^L(0, \mathbf{I})$, $\mathbf{N}_2 \sim \mathcal{N}^L(0, \mathbf{I})$ and $G \sim \mathcal{G}(\nu, 1)$. Further, \mathbf{N}_1 and \mathbf{N}_2 are mutually independent. Accordingly, the PDF of \mathbf{R} conditioned on both \mathbf{S} and G , i.e., $f_{\mathbf{R}|\mathbf{S}, G}(\mathbf{r}|\mathbf{s}, g)$ can be written as

$$f_{\mathbf{R}|\mathbf{S}, G}(\mathbf{r}|\mathbf{s}, g) = \frac{1}{2\pi} \int_0^{2\pi} \frac{\exp(-\frac{1}{2g}\|\mathbf{r} - He^{j\theta}\mathbf{F}\mathbf{s}\|_\Sigma^2)}{(2\pi)^L g^L \det(\Sigma)} d\theta,$$

with the aid of which the conditional PDF $f_{\mathbf{R}|\mathbf{S}}(\mathbf{R}|\mathbf{s})$ is obtained by $f_{\mathbf{R}|\mathbf{S}}(\mathbf{R}|\mathbf{s}) = \int_0^\infty f_{\mathbf{R}|\mathbf{S}, G}(\mathbf{R}|\mathbf{s}, g) f_G(g) dg$, where $f_G(g)$ is the PDF of $G \sim \mathcal{G}(\nu, 1)$, and given in (85). Upon substituting $f_{\mathbf{R}|\mathbf{S}}(\mathbf{R}|\mathbf{s}_m)$ into (276), the rule is rewritten as

$$\hat{m} \stackrel{(a)}{=} \arg \max_{1 \leq m \leq M} p_m \int_0^\infty f_{\mathbf{R}|\mathbf{S}, G}(\mathbf{R}|\mathbf{s}_m, g) f_G(g) dg, \quad (418a)$$

$$\stackrel{(b)}{=} \arg \max_{1 \leq m \leq M} p_m f_{\mathbf{R}|\mathbf{S}, G}(\mathbf{R}|\mathbf{s}_m, \mathbb{E}[G]), \quad (418b)$$

where the following steps are used. In step (a), we observe that (281) is being averaged by the PDF $f_G(g)$, and notice that $f_G(g) \geq 0$ for all $g \in \mathbb{R}_+$, which simplifies (282a) to (282b) with $\mathbb{E}[G] = 1$. In step (b), we insert (281) into (282b) and drop all the positive constant terms. Then, we obtain

$$\hat{m} = \arg \max_{1 \leq m \leq M} \frac{p_m}{2\pi} \int_0^{2\pi} \exp\left(-\frac{1}{2}\|\mathbf{R} - He^{j\theta}\mathbf{F}\mathbf{s}_m\|_\Sigma^2\right) d\theta, \quad (419)$$

where $\|\mathbf{R} - He^{j\theta}\mathbf{F}\mathbf{s}_m\|_\Sigma^2$ can be decomposed as

$$\begin{aligned} \|\mathbf{R} - He^{j\theta}\mathbf{F}\mathbf{s}_m\|_\Sigma^2 &= H^2 \mathbf{s}_m^H \mathbf{F}^H \Sigma^{-1} \mathbf{F} \mathbf{s}_m \\ &\quad - 2H \Re\{e^{-j\theta} \mathbf{s}_m^H \mathbf{F}^H \Sigma^{-1} \mathbf{F} \mathbf{R}\} + \mathbf{R}^H \Sigma^{-1} \mathbf{R}. \end{aligned} \quad (420)$$

Substituting (420) into (419) and ignoring the term $\mathbf{R}^H \Sigma^{-1} \mathbf{R}$ since not depending on the modulation index m yields

$$\begin{aligned} \hat{m} &= \arg \max_{1 \leq m \leq M} \frac{p_m}{2\pi} \exp\left(\frac{1}{2} H^2 \mathbf{s}_m^H \mathbf{F}^H \Sigma^{-1} \mathbf{F} \mathbf{s}_m\right) \\ &\quad \times \int_0^{2\pi} \exp\left(H |\mathbf{s}_m^H \mathbf{F}^H \Sigma^{-1} \mathbf{F} \mathbf{R}| \cos(\phi - \theta)\right) d\theta, \end{aligned} \quad (421)$$

where ϕ denotes the phase of $\mathbf{s}_m^H \mathbf{F}^H \Sigma^{-1} \mathbf{F} \mathbf{R}$. Notice that the integration in (421) is certainly a periodic function of ϕ with period 2π , and thus ϕ has no effect on the result. Utilizing the equality $I_0(x) = \frac{1}{2\pi} \int_0^{2\pi} \exp(x \cos(\theta)) d\theta$ [148, Eq. (8.431/3)], [149, Eq. (03.02.07.0001.01)], we readily obtain (416), which proves Theorem 66. ■

Note that the decision rule given in (416) cannot be made simpler. However, in the case of equiprobable modulation symbols, the non-coherent ML rule is given in the following.

Theorem 67. For the complex vector channel introduced in (267), the non-coherent ML detection rule is given by

$$\begin{aligned} \hat{m} &\triangleq \arg \max_{1 \leq m \leq M} \exp\left(\frac{1}{2} H^2 \mathbf{s}_m^H \mathbf{F}^H \Sigma^{-1} \mathbf{F} \mathbf{s}_m\right) \\ &\quad \times I_0\left(H |\mathbf{s}_m^H \mathbf{F}^H \Sigma^{-1} \mathbf{F} \mathbf{R}|\right). \end{aligned} \quad (422)$$

Proof. The proof is obvious using Theorem 66. ■

In order to avoid non-zero cross correlation between channels, we should choose the precoding matrix filter \mathbf{F} to maximize the power of the received signal. Then, referring to the mathematical model given by (267), the precoding matrix filter \mathbf{F} meets $\Sigma = \frac{N_0}{2} \mathbf{F} \mathbf{F}^H$, and the received vector equalized by \mathbf{F} before being fed to the optimal detection is given by

$$\mathbf{R}_{nc} \triangleq \mathbf{F}^{-1} \mathbf{R}, \quad (423a)$$

$$= \mathbf{F}^{-1} (He^{j\Theta} \mathbf{F} \mathbf{S} + \mathbf{Z}), \quad (423b)$$

$$\equiv He^{j\Theta} \mathbf{S} + \mathbf{F}^{-1} \mathbf{Z}, \quad (423c)$$

$$= He^{j\Theta} \mathbf{S} + \mathbf{Z}_{nc}, \quad (423d)$$

where $\mathbf{Z} \sim \mathcal{CM}_\nu^L(\mathbf{0}, \Sigma)$ whose PDF is already given by (268), and $\mathbf{Z}_{nc} \sim \mathcal{CM}_\nu^L(\mathbf{0}, \frac{N_0}{2} \mathbf{I})$ follows the PDF obtained with the aid of both Theorem 38 and the special case (200), that is

$$f_{\mathbf{Z}_c}(\mathbf{z}) = \frac{2}{\pi^L} \frac{\|\mathbf{z}\|^{\nu-L}}{\Gamma(\nu) \Lambda_0^{\nu+L}} K_{\nu-L}\left(\frac{2}{\Lambda_0} \|\mathbf{z}\|\right) \quad (424)$$

with the component deviation factor $\Lambda_0 = \sqrt{N_0/\nu}$ (i.e., N_0/ν variance per each CCS Laplacian noise component). Further, the equalization, which is presented above in (423), simplifies the complex correlated AWMN vector channel the uncorrelated complex AWMN vector channels, whose mathematical model is typically given by

$$\mathbf{R}_{nc} \triangleq He^{j\Theta} \mathbf{S} + \mathbf{Z}_{nc}. \quad (425)$$

where the knowledge of Θ is as mentioned above not available at the receiver. The power of the modulation symbol m , which is denoted by E_m , is given by $E_m \triangleq \|\mathbf{s}_m\|^2 = \mathbf{s}_m^H \mathbf{s}_m$ for all $1 \leq m \leq M$, and thus we write the average power of \mathbf{S} as

$$E_S = \sum_{m=1}^M \Pr\{\mathbf{S} = \mathbf{s}_m\} E_m = \sum_{m=1}^M p_m E_m. \quad (426)$$

Therefore, considering the all modulation symbols, the total SNR is written as

$$\gamma \triangleq \frac{H^2 E_S}{N_0} = \sum_{m=1}^M p_m \gamma_m, \quad (427)$$

where γ_m is the instantaneous SNR for the transmission of the modulation symbol m and written as $\gamma_m = H^2 E_m / N_0$. In addition, note that, during each modulation symbol, the received vector \mathbf{R}_c statistically depends on both \mathbf{S} and Θ with the conditional PDF $f_{\mathbf{R}_{nc}|\mathbf{S}, \Theta}(\mathbf{r}|\mathbf{s}, \theta)$, that is

$$\begin{aligned} f_{\mathbf{R}_{nc}|\mathbf{S}, \Theta}(\mathbf{r}|\mathbf{s}, \theta) &= \frac{2}{\pi^L} \frac{\|\mathbf{r} - He^{j\theta} \mathbf{s}\|_\Sigma^{\nu-L}}{\Gamma(\nu) \Lambda_0^{\nu+L}} \\ &\quad \times K_{\nu-L}\left(\frac{2}{\Lambda_0} \|\mathbf{r} - He^{j\theta} \mathbf{s}\|\right). \end{aligned} \quad (428)$$

Accordingly and correspondingly, the non-coherent MAP decision rule is obtained for the uncorrelated complex AWMN vector channels in the following.

Theorem 68. *For complex uncorrelated AWMN vector channels, defined in (425), the non-coherent MAP rule is given by*

$$\hat{m} \triangleq \arg \max_{1 \leq m \leq M} p_m \exp(\gamma_m) I_0 \left(2 \frac{H}{N_0} |s_m^H \mathbf{R}_{nc}| \right), \quad (429a)$$

$$\stackrel{(a)}{=} \arg \max_{1 \leq m \leq M} p_m \gamma_m I_0 \left(2 \frac{H}{N_0} |s_m^H \mathbf{R}_{nc}| \right), \quad (429b)$$

$$\stackrel{(b)}{=} \arg \max_{1 \leq m \leq M} 2 p_m \gamma_m \frac{H}{N_0} |s_m^H \mathbf{R}_{nc}|, \quad (429c)$$

$$= \arg \max_{1 \leq m \leq M} p_m \gamma_m |s_m^H \mathbf{R}_{nc}|, \quad (429d)$$

$$= \arg \max_{1 \leq m \leq M} p_m \gamma_m R_m, \quad (429e)$$

where the decision variable $R_m \triangleq |s_m^H \mathbf{R}_{nc}|$, $1 \leq m \leq M$.

Proof. It is obvious to obtain (429a) by using Theorem 66 and then selecting both $\Sigma = \frac{N_0}{2} \mathbf{I}$ and $\mathbf{F} = \mathbf{I}$. Subsequently, the following steps are performed. In step (a) of (429), The fact that $\exp(x)$ is monotonically increasing simplifies (429a) to (429b). In step (b), we notice that $I_0(x)$ is also a monotonically increasing function for all $x \in \mathbb{R}_+$. Therefore, we can reduce (429b) to (429c). Eventually, ignoring the constant terms 2, H and N_0 , and subsequently denoting $R_m \triangleq |s_m^H \mathbf{R}_{nc}|$, we can readily produce (429e), which completes the proof of Theorem 68. ■

From Theorem 68 above, we conclude that a non-coherent optimal detection correlates \mathbf{R}_{nc} with all modulation symbols $\{s_1, s_2, \dots, s_M\}$ and chooses the one that yields the maximum envelope. However, the probabilities of the modulation symbols must be available. Otherwise, the MAP detection reduces to the ML detection given in the following theorem.

Theorem 69. *For complex uncorrelated AWMN vector channels, defined in (425), the non-coherent ML rule is given by*

$$\hat{m} \triangleq \arg \max_{1 \leq m \leq M} \exp(\gamma_m) I_0 \left(2 \frac{H}{N_0} |s_m^H \mathbf{R}_{nc}| \right), \quad (430a)$$

$$= \arg \max_{1 \leq m \leq M} \gamma_m I_0 \left(2 \frac{H}{N_0} |s_m^H \mathbf{R}_{nc}| \right), \quad (430b)$$

$$= \arg \max_{1 \leq m \leq M} \gamma_m |s_m^H \mathbf{R}_{nc}|, \quad (430c)$$

$$= \arg \max_{1 \leq m \leq M} \gamma_m R_m, \quad (430d)$$

Proof. The proof is obvious using Theorem 67 and following the same steps in the proof of Theorem 68. ■

Note that, the non-coherent MAP and ML decision rules, given in (429) and (430), respectively, cannot be made much much simpler. However, in case of that the modulation sym-

bols are equiprobable and have equal-energy, we can ignore the scales p_m and γ_m , and the ML detection rule becomes

$$\hat{m} = \arg \max_{1 \leq m \leq M} |s_m^H \mathbf{R}_{nc}|, \quad (431a)$$

$$= \arg \max_{1 \leq m \leq M} R_m. \quad (431b)$$

a) *Conditional SER of Non-coherent Orthogonal Signalling:* Note that, in order to improve the performance of non-coherent receivers [2], [3] (i.e., to increase the separability of the modulation symbols while using non-coherent detection rules), we assume that the modulation symbols s_1, s_2, \dots, s_M are orthogonal with each other, i.e.,

$$s_m^H s_n = \begin{cases} 0 & \text{if } m \neq n, \\ E_m & \text{otherwise.} \end{cases} \quad (432)$$

As we observe in both (429e) and (430d), a non-coherent MAP/ML detection computes and compares the scaled versions of $R_m \triangleq |s_m^H \mathbf{R}_{nc}|$ for all $1 \leq m \leq M$, and subsequently chooses the modulation symbol that produces the maximum envelope. With the aid of Theorem 38, we know that R_m follows a CCS McLeish distribution, and thus its inphase and quadrature components follow McLeish distribution. In more details, if the transmitted symbol is not the modulation symbol m (i.e., $\mathbf{S} \neq s_m$), we notice

$$\Re\{s_m^H \mathbf{R}_{nc}\} \sim \mathcal{M}_\nu(0, E_m N_0/2), \quad (433a)$$

$$\Im\{s_m^H \mathbf{R}_{nc}\} \sim \mathcal{M}_\nu(0, E_m N_0/2). \quad (433b)$$

Moreover, if the transmitted symbol is the modulation symbol m (i.e., $\mathbf{S} = s_m$), we notice

$$\Re\{s_m^H \mathbf{R}_{nc}\} \sim \mathcal{M}_\nu(H E_m \cos(\Theta), E_m N_0/2), \quad (434a)$$

$$\Im\{s_m^H \mathbf{R}_{nc}\} \sim \mathcal{M}_\nu(H E_m \sin(\Theta), E_m N_0/2). \quad (434b)$$

It is accordingly worth mentioning that, in both (433) and (434), the components $\Re\{s_m^H \mathbf{R}_{nc}\}$ and $\Im\{s_m^H \mathbf{R}_{nc}\}$ are uncorrelated but statistically not independent.

Theorem 70. *In case of $\mathbf{S} \neq s_m$, the envelope $R_m \triangleq |s_m^H \mathbf{R}_{nc}|$ conditioned on the impulsive noise effects G follows Rayleigh distribution with the PDF given by*

$$f_{R_m|G}(r|g) = \frac{2r}{g E_m N_0} \exp\left(-\frac{r^2}{g E_m N_0}\right), \quad (435)$$

defined over $r \in \mathbb{R}^+$. Further, the envelope $R_m \triangleq |s_m^H \mathbf{R}_{nc}|$ has a non-negative random distribution, which is modeled by K -distribution, whose PDF is given by

$$f_{R_m}(r) = \frac{4r^\nu}{\Gamma(\nu) \Lambda_m^{\nu+1}} K_{\nu-1}\left(\frac{2r}{\Lambda_m}\right), \quad (436)$$

defined over $r \in \mathbb{R}^+$, where the component deviation factor is given by $\Lambda_m \triangleq \sqrt{E_m} \Lambda_0 = \sqrt{E_m N_0/\nu}$ (i.e., $\Lambda_0 = \sqrt{N_0/\nu}$).

Proof. Denoting by $I_m \triangleq \Re\{s_m^H \mathbf{R}_{nc}\}$ and $Q_m \triangleq \Im\{s_m^H \mathbf{R}_{nc}\}$, we notice that I_m and Q_m are uncorrelated but statistically not independent. Further, with the aid of Theorem 10, we have $I_m = \sqrt{G} X_m$ and $Q_m = \sqrt{G} Y_m$. Thus, we can write

$$R_m = \sqrt{G} \sqrt{X_m^2 + Y_m^2} = \sqrt{G} V_m, \quad (437)$$

with the distributions $G \sim \mathcal{G}(\nu, 1)$, $X_m \sim \mathcal{N}(0, E_m N_0/2)$ and $Y_m \sim \mathcal{N}(0, E_m N_0/2)$. Using [3, Eq. (2.3-42)], the component $V_m \triangleq \sqrt{X_m^2 + Y_m^2}$ follows a Rayleigh distribution whose PDF is given by [3, Eq. (2.3-43)]. Thus, the PDF of R_m conditioned on G is written as (435), which completes the first step of the proof. Accordingly, we obtain the PDF of R_m as

$$f_{R_m}(r) = \int_0^\infty f_{R_m|G}(r|g) f_G(g) dg, \quad (438a)$$

$$= \int_0^\infty \frac{2r}{g E_m N_0} \exp\left(-\frac{r^2}{g E_m N_0}\right) f_G(g) dg, \quad (438b)$$

where the PDF of $G \sim \mathcal{G}(\nu, 1)$ is given in (85). Finally, using [148, Eq. (3.478/4)] in (438b) yields (436), which completes the proof of Theorem 70. ■

Theorem 71. *In case of $\mathbf{S} = \mathbf{s}_m$, the envelope $R_m \triangleq |\mathbf{s}_m^H \mathbf{R}_{nc}|$ conditioned on the impulsive noise effects G follows Ricean distribution with the PDF given by*

$$f_{R_m|G}(r|g) = \frac{2r}{g E_m N_0} I_0\left(\frac{2\kappa_m r}{g E_m N_0}\right) \exp\left(-\frac{r^2 + \kappa_m^2}{g E_m N_0}\right), \quad (439)$$

where the Ricean parameter $\kappa_m = H E_m$. Further, the envelope $R_m \triangleq |\mathbf{s}_m^H \mathbf{R}_{nc}|$ has a non-negative distribution whose PDF is

$$f_{R_m}(r) = \frac{r}{\pi} \int_0^{2\pi} \frac{q_m(r, \theta)^{\nu-1}}{\Gamma(\nu) \Lambda^{\nu+1}} K_{\nu-1}\left(\frac{2}{\Lambda} q_m(r, \theta)\right) d\theta, \quad (440)$$

defined over $r \in \mathbb{R}^+$, where the deviation factor is given by $\Lambda \triangleq \sqrt{E_m \Lambda_0}$, and $q_m(r, \theta)$ is defined as

$$q_m(r, \theta) = \sqrt{r^2 + 2r\kappa_m \cos(\theta) + \kappa_m^2}. \quad (441)$$

Proof. In case of $\mathbf{S} = \mathbf{s}_m$, the envelope $R_m \triangleq |\mathbf{s}_m^H \mathbf{R}_{nc}|$ is also decomposed as (437) by following the same steps in the proof of Theorem 70. Referring to both (434a) and (434b), we notice that $G \sim \mathcal{G}(\nu, 1)$, and $X_m \sim \mathcal{N}(H E_m \cos(\Theta), E_m N_0/2)$ with $Y_m \sim \mathcal{N}(H E_m \sin(\Theta), E_m N_0/2)$. Further, utilizing [3, Eq. (2.3-55)], we notice that V_m follows the Ricean distribution with the PDF given by [3, Eq. (2.3-56)]. Therefore, the PDF of R_m conditioned on G is written as (439) in which we obtain $\kappa^2 = \mathbb{E}[I_m|G]^2 + \mathbb{E}[Q_m|G]^2 = H^2 E_m^2$ in accordance with Theorem 10. Herewith, by means of using [148, Eq. (3.339)], we can write

$$f_{R_m|G}(r|g) = \frac{2r}{g\pi E_m N_0} \int_0^\pi \exp\left(-\frac{q_m^2(r, \theta)}{g E_m N_0}\right) d\theta, \quad (442)$$

where $q_m(r, \theta)$ is defined above in (441). The PDF of R_m can be obtained by $f_{R_m}(r) = \int_0^\infty f_{R_m|G}(r|g) f_G(g) dg$, that is

$$f_{R_m}(r) = \frac{2r}{g\pi E_m N_0} \int_0^\pi \int_0^\infty \exp\left(-\frac{q_m^2(r, \theta)}{g E_m N_0}\right) \times f_G(g) dg d\theta, \quad (443)$$

where $f_G(g)$ is given in (85). Finally, using [148, Eq. (3.478/4)], we can readily rewrite the PDF of R_m as in (440), which completes the proof of Theorem 71. ■

Let us now consider the conditional SER of non-coherent MAP detection for orthogonal modulations. We can write The probability of erroneous decision as

$$\Pr\{e|H\} = 1 - \Pr\{c|H\}, \quad (444)$$

where $\Pr\{c|H\}$ is the the probability of correct decision, and can be readily rewritten as

$$\Pr\{c|H\} = \sum_{m=1}^M \Pr\{c|H, \mathbf{s}_m\} \Pr\{\mathbf{S} = \mathbf{s}_m\}, \quad (445)$$

where $\Pr\{c|H, \mathbf{s}_m\}$ denotes the probability of correct decision. Referring to Theorem 68, when the modulation symbol m is transmitted, a correct decision is made iff $p_n \gamma_n R_n < p_m \gamma_m R_m$ for all $1 \leq n \leq M$ and $m \neq n$. Therefore, the probability of correct decision can be readily written as

$$\Pr\{c|H, \mathbf{s}_m\} = \Pr\left\{\bigcap_{n \neq m} p_n \gamma_n R_n < p_m \gamma_m R_m \mid H, \mathbf{s}_m\right\},$$

where the envelopes R_1, R_2, \dots, R_M are certainly uncorrelated as a result of that modulation symbols are orthogonal (i.e., $\mathbf{s}_m^T \mathbf{s}_n = 0$ for all $m \neq n$). They will however be entirely independent when conditioned on impulsive noise effects (i.e., conditioned on G). Then, we rewrite $\Pr\{c|H, \mathbf{s}_m\}$ as

$$\Pr\{c|H, \mathbf{s}_m\} = \int_0^\infty \Pr\{c|H, \mathbf{s}_m, g\} f_G(g) dg, \quad (446)$$

where $\Pr\{c|H, \mathbf{s}_m, g\}$ is given by

$$\Pr\{c|H, \mathbf{s}_m, g\} = \prod_{n \neq m} \Pr\left\{R_n < \frac{p_m E_m}{p_n E_n} R_m\right\}, \quad (447)$$

where R_m follows a Ricean distribution whose PDF is given by (439). For $1 \leq n \neq m \leq M$, R_n has Rayleigh distribution whose PDF is given by (435). From this point on, we rewrite

$$\Pr\{c|H, \mathbf{s}_m, g\} = \mathbb{E}\left[\prod_{n \neq m} F_{R_n}\left(\frac{p_m E_m}{p_n E_n} R_m\right)\right], \quad (448)$$

where $F_{R_n}(r)$ is the CDFs of V_n for all $1 \leq n \neq m \leq M$. Appropriately, with the aid of the equations from (444) to (448), the conditional SER of non-coherent orthogonal signaling is given in the following.

Theorem 72. *For the MAP decision rule given by Theorem 68, the conditional SER of non-coherent orthogonal signaling is given by*

$$\Pr\{e|H\} = \frac{1}{\Gamma(\nu)} \sum_{k=1}^{2^M-1} \sum_{m=1}^M \frac{(-1)^{1+\sum_{n=1}^M k_n} p_m}{1 + \Phi_{k,m}} \times G_{0,2}^{2,0} \left[\frac{\nu \Phi_{k,m} \gamma_m}{1 + \Phi_{k,m}} \mid \overline{\quad}, 0, \nu \right] \delta_{k_m,0}, \quad (449a)$$

$$= \frac{1}{\Gamma(\nu)} \sum_{k=1}^{2^M-1} \sum_{m=1}^M \frac{(-1)^{1+\sum_{n=1}^M k_n} p_m}{(1 + \Phi_{k,m}) \Lambda_0^\nu} \times \left(\frac{2\Phi_{k,m} \gamma_m}{1 + \Phi_{k,m}}\right)^{\frac{\nu}{2}} \times K_\nu \left(\frac{2}{\Lambda_0} \sqrt{\frac{2\Phi_{k,m} \gamma_m}{1 + \Phi_{k,m}}}\right) \delta_{k_m,0}, \quad (449b)$$

where the indexing k_n is defined by $k_n \triangleq \lfloor 2k/2^n \rfloor - 2 \lfloor k/2^n \rfloor$. Further, $\Phi_{k,m}$ is defined by

$$\Phi_{k,m} = \sum_{n=1}^M \left(\frac{p_m}{p_n}\right)^2 \left(\frac{\gamma_m}{\gamma_n}\right)^3 k_n, \quad (450)$$

Further, for all $1 \leq m \leq M$, p_m is the probability of the modulation symbol m , and γ_m is the instantaneous SNR for the transmission of the modulation symbol m .

Proof. Note that, with the aid of [141, Eq. (4.24)], (447) can be shown to be (448), in which the expectation is achieved with respect to the distribution V_m , and where F_{V_n} is the CDF of the distribution V_n and easily found as [3, Eq. (2.3-50)],

$$F_{R_n}(r) = 1 - \exp\left(-\frac{r^2}{gE_n N_0}\right), \quad r \in \mathbb{R}^+. \quad (451)$$

For non-zero distinct x_1, x_2, \dots, x_N , we can show that

$$\prod_{n \neq m}^N (1 + x_n) = 1 + \sum_{k=1}^{2^N-1} \prod_{n=1}^N x_n^{k_n} \delta_{k_m,0}, \quad (452)$$

where $k_n = \lfloor 2k/2^n \rfloor - 2\lfloor k/2^n \rfloor$, and therein $\lfloor x \rfloor$ denotes the floor function that returns the greatest integer less than or equal to x . Further, Kronecker's delta function is denoted by $\delta_{x,y}$ that returns 1 iff $x=y$ and 0 otherwise. Accordingly, substituting (451) into (448) and using the novel series expansion given in (452), we can rewrite (448) as follows

$$\Pr\{c | H, \mathbf{s}_m, g\} = 1 + \sum_{k=1}^{2^M-1} (-1)^{\sum_{n=1}^M k_n} \times \mathbb{E}\left[\exp\left(-\frac{\Phi_{k,m}}{gE_0 N_0} R_m^2\right)\right] \delta_{k_m,0}, \quad (453)$$

where $\Phi_{k,m}$ is defined in (450). As mentioned before, R_m follows a Ricean distribution whose PDF is given by

$$f_{R_m}(r) = \frac{2\nu}{gE_m N_0} I_0\left(\frac{2\kappa_m r}{gE_m N_0}\right) \exp\left(-\frac{r^2 + \kappa_m^2}{gE_m N_0}\right), \quad (454)$$

where κ_m is defined as $\kappa_m = HE_m$. Note that $\mathbb{E}[\exp(-sR_m^2)]$, where $s = \Phi_{k,m}/(gE_0 N_0)$, is specifically required in (453). Thanks to $\int_0^\infty x \exp(-x^2/a) I_0(bx) dx = a \exp(ab^2)/2$ [148, Eq. (2.15.20/8)], we derive

$$\mathbb{E}[\exp(-sR_m^2)] = \frac{\exp\left(-\frac{s\kappa_m^2}{1+sgE_m N_0}\right)}{1+sgE_m N_0}. \quad (455)$$

Eventually, inserting both (453) and (455) into (446) yields

$$\Pr\{c | H, \mathbf{s}_m\} = 1 + \frac{1}{\Gamma(\nu)} \sum_{k=1}^{2^M-1} \frac{(-1)^{\sum_{n=1}^M k_n}}{1 + \Phi_{k,m}} \times M_{1/G}\left(\frac{\Phi_{k,m} \gamma_m}{1 + \Phi_{k,m}}\right) \delta_{k_m,0}. \quad (456)$$

where $M_{1/G}(s)$, $s \in \mathbb{R}^+$ is the reciprocal MGF and defined as $M_{1/G}(s) = \int_0^\infty \exp(-s/g) f_G(g) dg$, in which substituting (85) and using [150, Eqs. (8.4.3/1) and (8.4.3/2)] within [151, Eq. (2.8.4)] yields

$$M_{1/G}(s) = \frac{1}{\Gamma(\nu)} G_{0,2}^{2,0} \left[s\nu \left| \begin{matrix} - \\ 0, \nu \end{matrix} \right. \right]. \quad (457)$$

Finally, substituting (457) and (456) into (445) and accordingly performing simple algebraic manipulations utilizing (444), we readily obtain (449a), in which using [150, Eqs. (8.2.2/15) and (8.4.23/1)] results in (449b), which proves Theorem 72. ■

Theorem 73. For the ML decision rule given by Theorem 69, the conditional SER of non-coherent orthogonal signaling is given by

$$\Pr\{e | H\} = \frac{1}{M\Gamma(\nu)} \sum_{k=1}^{2^M-1} \sum_{m=1}^M \frac{(-1)^{1+\sum_{n=1}^M k_n}}{1 + \Phi_{k,m}} \times G_{0,2}^{2,0} \left[\frac{\nu \Phi_{k,m} \gamma_m}{1 + \Phi_{k,m}} \left| \begin{matrix} - \\ 0, \nu \end{matrix} \right. \right] \delta_{k_m,0}, \quad (458a)$$

$$= \frac{1}{M\Gamma(\nu)} \sum_{k=1}^{2^M-1} \sum_{m=1}^M \frac{(-1)^{1+\sum_{n=1}^M k_n}}{(1 + \Phi_{k,m}) \Lambda_0^\nu} \times \left(\frac{2\Phi_{k,m} \gamma_m}{1 + \Phi_{k,m}} \right)^{\nu/2} \times K_\nu \left(\frac{2}{\Lambda_0} \sqrt{\frac{2\Phi_{k,m} \gamma_m}{1 + \Phi_{k,m}}} \right) \delta_{k_m,0}, \quad (458b)$$

where $\Phi_{k,m} = \sum_{n=1}^M (\gamma_m/\gamma_n)^3 k_n$.

Proof. The proof is obvious setting $p_m = 1/M$ for $1 \leq m \leq M$ in Theorem 72. ■

Theorem 74. When the modulation symbols are equiprobable and have equal-energy, and referring to (431), the conditional SER of non-coherent orthogonal signaling is given by

$$\Pr\{e | H\} = \frac{1}{\Gamma(\nu)} \sum_{k=1}^{M-1} \frac{(-1)^{1+k}}{1+k} \binom{M-1}{k} \times G_{0,2}^{2,0} \left[\frac{\nu k \gamma}{1+k} \left| \begin{matrix} - \\ 0, \nu \end{matrix} \right. \right], \quad (459a)$$

$$= \frac{2}{\Gamma(\nu)} \sum_{k=1}^{M-1} \frac{(-1)^{1+k}}{(1+k) \Lambda_0^\nu} \binom{M-1}{k} \times \left(\frac{2k\gamma}{1+k} \right)^{\frac{\nu}{2}} K_\nu \left(\frac{2}{\Lambda_0} \sqrt{\frac{2k\gamma}{1+k}} \right), \quad (459b)$$

where $\gamma = H^2 E_S/N_0$ denotes the instantaneous SNR.

Proof. In case of that the modulation symbols \mathbf{s}_m , $1 \leq m \leq M$ are equiprobable and have equal energy (i.e., when $E_m = E_S$ and $\Pr\{\mathbf{S} = \mathbf{s}_m\} = 1/M$ for all $1 \leq m \leq M$), (447) can be shown to be

$$\Pr\{c | H, \mathbf{s}_m, g\} = \mathbb{E}[F_{R_n}(R_m)^{M-1}], \quad (460)$$

where substituting (451) and then utilizing binomial expansion [147, Eq. (3.1.1)] results in

$$\Pr\{c | H, \mathbf{s}_m, g\} = 1 + \sum_{k=1}^{M-1} (-1)^k \binom{M-1}{k} \times \mathbb{E}\left[\exp\left(-\frac{kR_m^2}{gE_S N_0}\right)\right], \quad (461)$$

where the expectation is achieved with respect to the distribution R_m and can be readily derived by setting $s = k/g/E_S/N_0$ in (455). From this point, we derive the closed-form expression of $\Pr\{e|H, \mathbf{s}_m\}$, from which we have $\Pr\{e|H, \mathbf{s}_m\} = \int_0^\infty \Pr\{e|H, \mathbf{s}_m, g\} f_G(g) dg$. Then, the proof is obvious performing almost the same steps in the proof of Theorem 72. ■

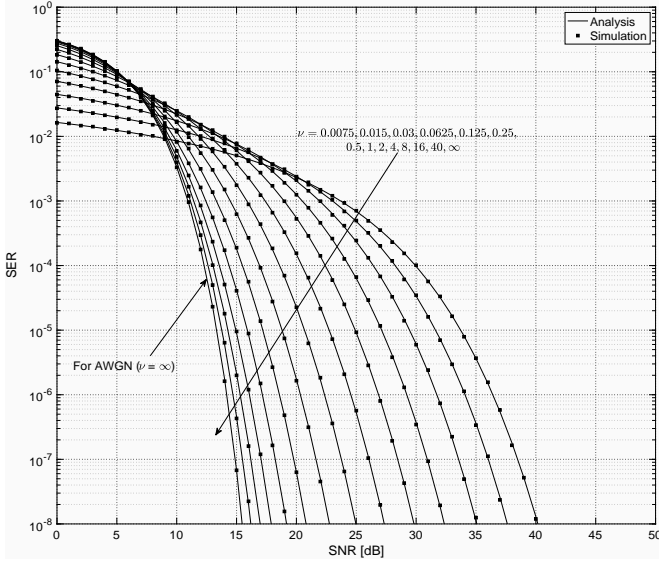
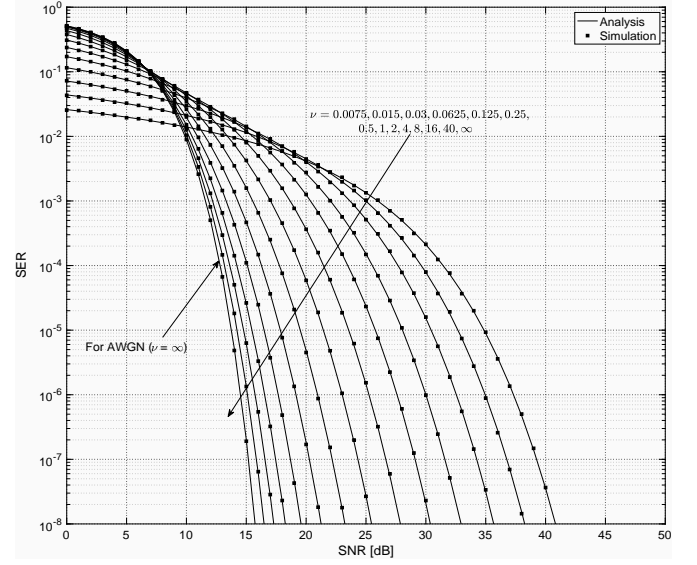
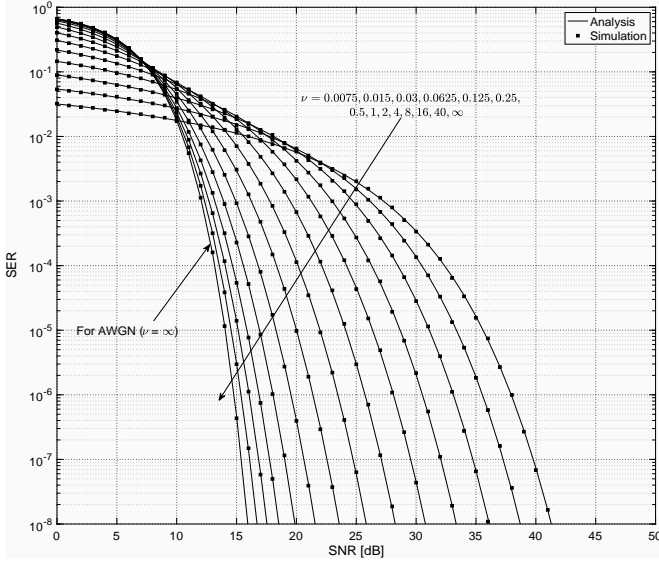
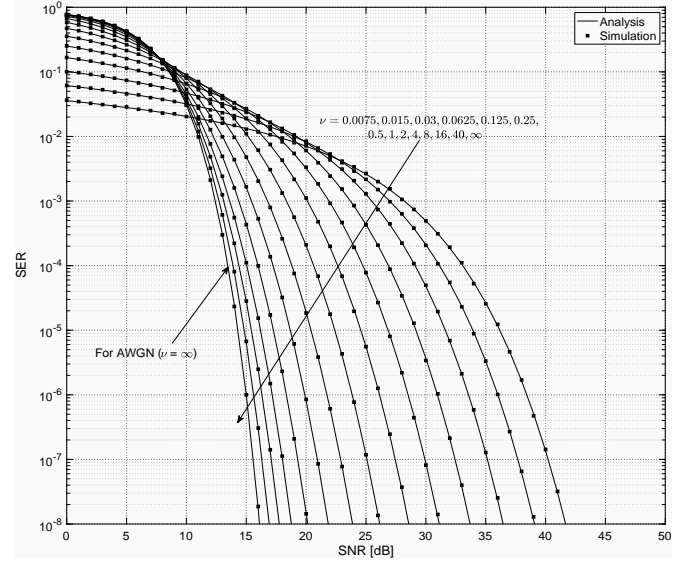

 (a) Modulation level $M = 2$.

 (b) Modulation level $M = 4$.

 (c) Modulation level $M = 8$.

 (d) Modulation level $M = 16$.

Fig. 16: The SER of non-coherent orthogonal signaling over AWMN channels.

Theorem 75. *The conditional BER of orthogonal signaling, including BFSK, with non-coherent ML detection, where the binary modulation symbols are equiprobable and have equal-energy, is given by*

$$\Pr\{e | H\} = \frac{1}{\Gamma(\nu)} G_{0,2}^{2,0} \left[\frac{\nu k \gamma}{1+k} \middle| \begin{matrix} - \\ 0, \nu \end{matrix} \right], \quad (462)$$

$$= \frac{1}{\Gamma(\nu)} \left(\frac{\gamma}{\Lambda_0^2} \right)^{\frac{\nu}{2}} K_{\nu} \left(2 \sqrt{\frac{\gamma}{\Lambda_0^2}} \right). \quad (463)$$

Proof. The proof is obvious setting $M=2$ in Theorem 72. ■

Let us now consider the special cases in order to check the numerical validity of the results presented above. It is worth noticing that, when the normality gets close to zero (i.e., while $\nu \rightarrow 0^+$), the complex AWMN channel turns into the noiseless channel and accordingly the conditional SER approaches to

zero (i.e., $\Pr\{e | H\} \rightarrow 0^+$) as expected. Further, in case of $\nu=1$, we simplify (459) to

$$\Pr\{e | H\} = \sum_{k=1}^{M-1} \frac{(-1)^{1+k}}{1+k} \binom{M-1}{k} \times G_{0,2}^{2,0} \left[\frac{k\gamma}{1+k} \middle| \begin{matrix} - \\ 0, 1 \end{matrix} \right], \quad (464a)$$

$$= 2 \sum_{k=1}^{M-1} \frac{(-1)^{1+k}}{1+k} \binom{M-1}{k} \times \sqrt{\frac{k\gamma}{1+k}} K_1 \left(2 \sqrt{\frac{k\gamma}{1+k}} \right), \quad (464b)$$

which is the conditional SER of non-coherent signaling over complex AWLN channels. Setting $M=2$ in (464) results in the error probability for binary orthogonal signaling, including

binary orthogonal FSK, with non-coherent detection in complex AWLN channels, that is

$$\Pr\{e | H\} = \sqrt{\gamma/2} K_1(\sqrt{2\gamma}). \quad (465)$$

When the normality factor ν gets larger (i.e., $\nu \rightarrow \infty$), the additive white noise turns into AWGN noise, and accordingly utilizing [150, Eqs. (8.2.2/12) and (8.4.3/1)] within

$$\lim_{\nu \rightarrow \infty} \frac{1}{\Gamma(\nu)} G_{0,2}^{2,0} \left[\frac{\nu k \gamma}{1+k} \middle| \begin{matrix} - \\ 0, \nu \end{matrix} \right] = \exp\left(-\frac{k\gamma}{1+k}\right), \quad (466)$$

the symbol error probability (459) readily simplifies more to

$$\Pr\{e | H\} = \sum_{k=1}^{M-1} \frac{(-1)^{1+k}}{1+k} \binom{M-1}{k} \exp\left(-\frac{k\gamma}{1+k}\right), \quad (467)$$

which is, as expected, in perfect agreement with the symbol error probability of non-coherent ML detection of equal-power orthogonal symbols [1, Eq. (8.67)], [3, Eq. (4.5-43)]. For binary orthogonal signaling, including binary orthogonal FSK with non-coherent detection over complex AWGN channels, (467) reduces to [3, Eq. (4.5-45)], [1, Eq. (8.69)], that is

$$\Pr\{e | H\} = \frac{1}{2} \exp\left(-\frac{\gamma}{2}\right). \quad (468)$$

For numerical accuracy and convenience, in Fig. 16, which is given at the top of the previous page, we give the conditional SER of non-coherent orthogonal signaling over complex AWMN channels.

b) Conditional SER of Non-coherent Differential PSK:

The other type of non-coherent signaling is the DPSK (i.e., the differentially encoded PSK) in which the information is encoded within the phase transition between two consecutive symbols and its demodulation/detection does not require the estimation of the carrier phase. In accordance with the channel model given by (267), the two consecutive received signal vectors can be readily written as

$$\mathbf{R}_1 = H e^{j\Theta} \mathbf{F} \mathbf{S}_1 + \mathbf{Z}_1, \quad (469)$$

$$\mathbf{R}_2 = H e^{j\Theta} \mathbf{F} \mathbf{S}_2 + \mathbf{Z}_2, \quad (470)$$

where $\mathbf{Z}_1 \sim \mathcal{CM}_\nu^L(\mathbf{0}, \Sigma)$ and $\mathbf{Z}_2 \sim \mathcal{CM}_\nu^L(\mathbf{0}, \Sigma)$ are uncorrelated but not independent, and \mathbf{S}_1 and \mathbf{S}_2 are two consecutive symbols. Accordingly, the vector representation of the lowpass equivalent of the received signal over a period of two symbol intervals is formally written as

$$\underbrace{\begin{bmatrix} \mathbf{R}_1 \\ \mathbf{R}_2 \end{bmatrix}}_{\mathbf{R}_s} = H e^{j\Theta} \underbrace{\begin{bmatrix} \mathbf{F} & \mathbf{0} \\ \mathbf{0} & \mathbf{F} \end{bmatrix}}_{\mathbf{F}_s} \underbrace{\begin{bmatrix} \mathbf{S}_1 \\ \mathbf{S}_2 \end{bmatrix}}_{\mathbf{S}} + \underbrace{\begin{bmatrix} \mathbf{Z}_1 \\ \mathbf{Z}_2 \end{bmatrix}}_{\mathbf{Z}_s}, \quad (471)$$

where $\mathbf{Z}_s \sim \mathcal{CM}_\nu^{2L}(\mathbf{0}, \Sigma_s)$ with the covariance matrix

$$\Sigma_s = \begin{bmatrix} \Sigma & \mathbf{0} \\ \mathbf{0} & \Sigma \end{bmatrix}. \quad (472)$$

Moreover, \mathbf{S} denotes the modulation symbol vector randomly chosen from the set of possible fixed modulation symbols $\{\mathbf{s}_1, \mathbf{s}_2, \dots, \mathbf{s}_M\}$. As such, the m th message over a period of two modulation symbols can be written as

$$\mathbf{s}_m = \begin{bmatrix} \mathbf{s} \exp(j\phi_\Sigma) \\ \mathbf{s} \exp(j(\phi_m + \phi_\Sigma)) \end{bmatrix}, \quad 1 \leq m \leq M \quad (473)$$

where \mathbf{s} is such a signal that the power of the m th message, i.e., $E_m \triangleq \mathbf{s}_m^H \mathbf{s}_m$ is derived as $E_m = 2\mathbf{s}^H \mathbf{s}$. Accordingly, the average power of signaling E_S is given by

$$E_S \triangleq \sum_{m=1}^M E_m \Pr\{\mathbf{S} = \mathbf{s}_m\} = 2\mathbf{s}^H \mathbf{s}. \quad (474)$$

Further, in (473), ϕ_Σ is the random phase due to non-coherent detection, and $\phi_m = 2\pi(m-1)/M$ is the phase transition that encodes the information into the m th message. Since the information is entirely encoded in the phase transition between two consecutive symbols, the detection has to be carried over a period of two consecutive symbols. Referring to the *slow variance uncertainty*, well explained in Section IV-A, the variance fluctuation during two consecutive symbols is therefore assumed approximately constant. With respect to (471), the non-coherent MAP receiver is given in the following theorem.

Theorem 76. *For the complex vector channel given in (471), the non-coherent MAP detection rule of DPSK is given by*

$$\hat{m} \triangleq \arg \max_{1 \leq m \leq M} p_m I_0 \left(H \left| \mathbf{s}^H \mathbf{F}^H \Sigma^{-1} \mathbf{F} \mathbf{R}_1 + \exp(-j\phi_m) \mathbf{s}^H \mathbf{F}^H \Sigma^{-1} \mathbf{F} \mathbf{R}_2 \right| \right). \quad (475)$$

Proof. Note that the MAP detection of DPSK uses (416) for optimal detection. Accordingly, we have

$$\hat{m} \triangleq \arg \max_{1 \leq m \leq M} p_m \exp\left(\frac{1}{2} H^2 \mathbf{s}_m^H \mathbf{F}_s^H \Sigma_s^{-1} \mathbf{F}_s \mathbf{s}_m\right) \times I_0 \left(H \left| \mathbf{s}_m^H \mathbf{F}_s^H \Sigma_s^{-1} \mathbf{F}_s \mathbf{R}_s \right| \right), \quad (476)$$

which can be rewritten in terms of \mathbf{R}_1 , \mathbf{R}_2 , \mathbf{F} , and Σ , that is

$$\hat{m} \triangleq \arg \max_{1 \leq m \leq M} p_m \exp\left(H^2 \mathbf{s}^H \mathbf{F}^H \Sigma^{-1} \mathbf{F} \mathbf{s}\right) \times I_0 \left(H \left| \exp(-j\phi_\Sigma) \mathbf{s}^H \mathbf{F}^H \Sigma^{-1} \mathbf{F} \mathbf{R}_1 + \exp(-j(\phi_\Sigma + \phi_m)) \mathbf{s}^H \mathbf{F}^H \Sigma^{-1} \mathbf{F} \mathbf{R}_2 \right| \right), \quad (477)$$

where $\exp(-j\phi_\Sigma)$ can be ignored due to $|e^{-j\phi_\Sigma} x| = |x|$. In addition, since the term $\exp(H^2 \mathbf{s}^H \mathbf{F}^H \Sigma^{-1} \mathbf{F} \mathbf{s})$ in (477) is independent of index m , we can readily ignore it, which results in (475) and completes the proof of Theorem 76. ■

Theorem 77. *For the complex vector channel given in (471), the non-coherent ML detection rule of DPSK is given by*

$$\hat{m} \triangleq \arg \max_{1 \leq m \leq M} I_0 \left(H \left| \mathbf{s}^H \mathbf{F}^H \Sigma^{-1} \mathbf{F} \mathbf{R}_1 + \exp(-j\phi_m) \mathbf{s}^H \mathbf{F}^H \Sigma^{-1} \mathbf{F} \mathbf{R}_2 \right| \right). \quad (478)$$

Proof. The proof is obvious using Theorem 76. ■

In order to avoid non-zero cross correlation between channels, we can equalize the channel by the precoding filter matrix \mathbf{F}_s whose diagonal matrix $\mathbf{F} \in \mathbb{C}^{2L \times 2L}$ supports $\Sigma = \frac{N_0}{2} \mathbf{F} \mathbf{F}^H$ for optimal reception, and then we can obtain

$$\mathbf{R}_{nc} \triangleq \mathbf{F}_s^{-1} \mathbf{R}_s, \quad (479a)$$

$$= \mathbf{F}_s^{-1} (H e^{j\Theta} \mathbf{F}_s \mathbf{S} + \mathbf{Z}_s), \quad (479b)$$

$$\equiv H e^{j\Theta} \mathbf{S} + \mathbf{F}_s^{-1} \mathbf{Z}_s, \quad (479c)$$

$$= H e^{j\Theta} \mathbf{S} + \mathbf{Z}_{nc}. \quad (479d)$$

where $\mathbf{R}_{nc} \triangleq [\mathbf{R}_{1,nc}^T \mathbf{R}_{2,nc}^T]^T$ denotes the the received random vector in which $\mathbf{R}_{1,nc} \triangleq \mathbf{F}^{-1} \mathbf{R}_1$ and $\mathbf{R}_{2,nc} \triangleq \mathbf{F}^{-1} \mathbf{R}_2$ are two random vectors non-coherently recovered over a period of two modulation symbols. Furthermore, $\mathbf{Z}_{nc} \sim \mathcal{CM}_\nu^{2L}(\mathbf{0}, \frac{N_0}{2} \mathbf{I})$ such that $\mathbf{Z}_{nc} \triangleq [\mathbf{Z}_{1,nc}^T \mathbf{Z}_{2,nc}^T]^T$ with $\mathbf{Z}_{1,nc} \sim \mathcal{CM}_\nu^L(\mathbf{0}, \frac{N_0}{2} \mathbf{I})$ and $\mathbf{Z}_{2,nc} \sim \mathcal{CM}_\nu^L(\mathbf{0}, \frac{N_0}{2} \mathbf{I})$. Consequently, the non-coherent MAP receiver is given in the following theorem.

Theorem 78. *For complex uncorrelated AWMN vector channels, defined in (479), the non-coherent MAP rule is given by*

$$\hat{m} \triangleq \arg \max_{1 \leq m \leq M} p_m \cos(\Phi - \phi_m), \quad (480)$$

where the decision variable Φ is defined as the phase difference of the received signal in two adjacent intervals, that is

$$\Phi \triangleq \arg(\mathbf{s}^H \mathbf{R}_{2,nc}) - \arg(\mathbf{s}^H \mathbf{R}_{1,nc}), \quad (481)$$

where $\arg(z)$ gives the argument of the complex number z [149, Eq. (12.02.02.0001.01)].

Proof. Using Theorem 77 and then selecting both $\Sigma = \frac{N_0}{2} \mathbf{I}$ and $\mathbf{F} = \mathbf{I}$, we have

$$\hat{m} \triangleq \arg \max_{1 \leq m \leq M} p_m I_0 \left(\frac{2H}{N_0} \left| \mathbf{s}^H \mathbf{R}_{1,nc} + e^{-j\phi_m} \mathbf{s}^H \mathbf{R}_{2,nc} \right| \right). \quad (482)$$

Noticing that $I_0(x)$ is a monotonic increasing function for all $x \in \mathbb{R}_+$, we have $\arg \max_x I_0(f(x)) = \arg \max_x f^2(x)$, for any monotonic increasing function $f: \mathbb{R} \rightarrow \mathbb{R}$. In consequence, ignoring $2H/N_0$, we can reduce (482), that is

$$\hat{m} = \arg \max_{1 \leq m \leq M} p_m \left| \mathbf{s}^H \mathbf{R}_{1,nc} + \exp(-j\phi_m) \mathbf{s}^H \mathbf{R}_{2,nc} \right|^2. \quad (483)$$

Using $|x + y|^2 = |x|^2 + |y|^2 + 2\Re\{x^*y\}$ and noticing that both $|\mathbf{s}^H \mathbf{R}_{1,nc}|^2$ and $|\mathbf{s}^H \mathbf{R}_{2,nc}|^2$ are independent of index m , we can simplify (483) into

$$\begin{aligned} \hat{m} &= \arg \max_{1 \leq m \leq M} p_m \Re \left\{ C_1^* C_2 \exp(-j\phi_m) \right\}. \quad (484a) \\ &= \arg \max_{1 \leq m \leq M} p_m \Re \left\{ |C_1| \exp(-j \arg(C_1)) \times \right. \\ &\quad \left. |C_2| \exp(j \arg(C_2)) \exp(-j\phi_m) \right\}, \quad (484b) \end{aligned}$$

where $C_1 \triangleq \mathbf{s}^H \mathbf{R}_{1,nc}$ and $C_2 \triangleq \mathbf{s}^H \mathbf{R}_{2,nc}$ are two complex envelopes recovered from two consecutive symbols, respectively, such that $C_1 \sim \mathcal{CM}_\nu(H e^{j\phi_\Sigma}, E_S N_0/4)$ and $C_2 \sim \mathcal{CM}_\nu(H e^{j(\phi_\Sigma + \phi_m)}, E_S N_0/4)$. Further, $\arg(z)$ is the argument of the complex number z , such that $z = |z| e^{j \arg(z)}$ [149, Eq. (12.02.16.0029.01)]. In addition, worth noting that $|C_1|$ and $|C_2|$ are independent of index m . Accordingly, (484b) is reformulated as

$$\hat{m} = \arg \max_{1 \leq m \leq M} p_m \Re \left\{ e^{j(\arg(C_2) - \arg(C_1) - \phi_m)} \right\}, \quad (485a)$$

$$= \arg \max_{1 \leq m \leq M} p_m \Re \left\{ e^{j(\Phi - \phi_m)} \right\}, \quad (485b)$$

where Φ denotes the phase difference of the received signal in two adjacent intervals, simply defined as $\Phi \triangleq \arg(C_2 C_1^*) = \arg(C_2) - \arg(C_1)$ and given by (481). Using Euler's formula [147, Eq. (4.3.2)], (484b) readily simplifies to (475), which completes the proof of Theorem 78. ■

Theorem 79. *For complex uncorrelated AWMN vector channels, defined in (479), the non-coherent ML rule is given by*

$$\hat{m} \triangleq \arg \max_{1 \leq m \leq M} \cos(\Phi - \phi_m). \quad (486)$$

Proof. The proof is obvious using Theorem 78. ■

As observed in both Theorem 78 and Theorem 77, the receiver computes this phase difference Φ by using (481) and compares it with all $\phi_m = 2\pi(m-1)/M$, $1 \leq m \leq M$ and selects the m for which ϕ_m maximizes $\cos(\Phi - \phi_m)$, thus resulting in minimum distance between Φ and ϕ_m . In the following, we obtain the exact error probability of M-ary differential phase shift keying (M-DPSK) signaling with non-coherent detection over complex AWMN noise channels.

Theorem 80. *The conditional SER of the M-DPSK signaling with non-coherent ML detection is given by*

$$\Pr\{e | H\} = \frac{2}{\pi \Gamma(\nu) \lambda_0^\nu} \int_0^{\pi - \frac{\pi}{M}} \left(\frac{2\gamma \sin^2(\frac{\pi}{M})}{1 + \cos(\frac{\pi}{M}) \cos(\theta)} \right)^{\frac{\nu}{2}} \times K_\nu \left(\frac{2}{\lambda_0} \sqrt{\frac{2\gamma \sin^2(\frac{\pi}{M})}{1 + \cos(\frac{\pi}{M}) \cos(\theta)}} \right) d\theta, \quad (487)$$

where $\gamma \triangleq H^2 E_S / N_0$ is the instantaneous SNR.

Proof. Note that, according to (481), the decision variable Φ is simply defined as the phase difference between $C_1 \triangleq \mathbf{s}^H \mathbf{R}_{1,nc}$ and $C_2 \triangleq \mathbf{s}^H \mathbf{R}_{2,nc}$, where $C_1 \sim \mathcal{CM}_\nu(H e^{j\phi_\Sigma}, E_S N_0/4)$ and $C_2 \sim \mathcal{CM}_\nu(H e^{j(\phi_\Sigma + \phi_m)}, E_S N_0/4)$ are such two uncorrelated but not independent complex McLeish distributions that, using Theorem 10, their decomposition can be written as

$$C_1 = \frac{1}{2} H E_S e^{j\phi_\Sigma} + G(X_1 + jY_1) \quad (488)$$

$$C_2 = \frac{1}{2} H E_S e^{j(\phi_\Sigma + \phi_m)} + G(X_2 + jY_2), \quad (489)$$

where $X_1 \sim \mathcal{N}(0, E_S N_0/4)$, $Y_1 \sim \mathcal{N}(0, E_S N_0/4)$, $X_2 \sim \mathcal{N}(0, E_S N_0/4)$ and $Y_2 \sim \mathcal{N}(0, E_S N_0/4)$ are mutually *i.i.d* Gaussian distributions. Further, $G \sim \mathcal{G}(\nu, 1)$ follows the PDF given in (85). When conditioned on G , both C_1 and C_2 follow Gaussian distributions, and hence, $\Phi \triangleq \arg(C_2 C_1^*)$ conditioned on G is observed as the phase between two *i.i.d* complex Gaussian distributions. Using [204, Eq. (5)], we have

$$\Pr\{-\phi < \Phi < \phi | G\} = 1 - \frac{1}{2\pi} \int_{-(\pi - \phi)}^{\pi - \phi} e^{-\frac{\gamma}{2} h(\phi, \theta)} d\theta, \quad (490)$$

with $h(\phi, \theta) = \sin^2(\phi)/(1 + \cos(\phi) \cos(\theta))$, where γ denotes the instantaneous SNR given by $\gamma = H^2 E_S / N_0$. When s_m is transmitted, a correct decision is made iff $\phi_m - \pi/M < \Phi < \phi_m + \pi/M$ since $\arg(\mathbf{s}_m \mathbf{s}_{m\pm 1}^*) = \pi/M$. With the circularity of complex AWMN noise, we notice that $\Pr\{\phi_m - \pi/M < \Phi < \phi_m + \pi/M\}$ and $\Pr\{-\pi/M < \Phi < \pi/M\}$ are the same. Hence, we can write the probability of making a correct decision as

$$\Pr\{c | H, s_m, G\} = \Pr\{-\pi/M < \Phi < \pi/M\}. \quad (491)$$

Using $\Pr\{e | H, s_m, G\} = 1 - \Pr\{c | H, s_m, G\}$ and (490) and making allowance for the symmetry between the integration

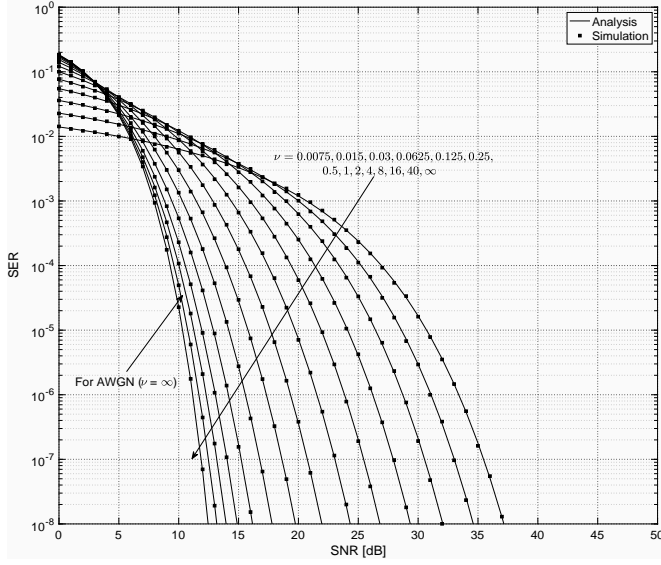
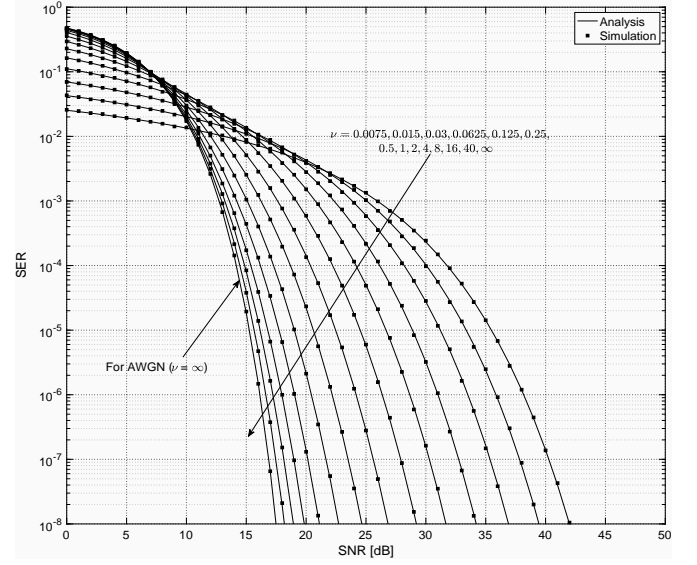
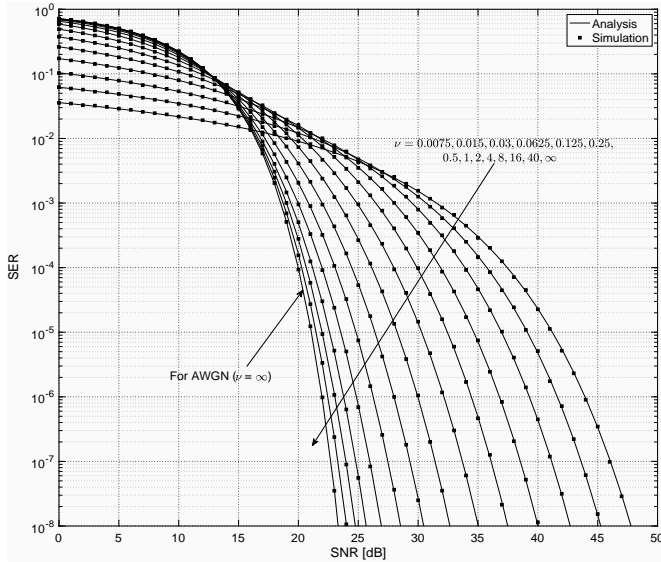
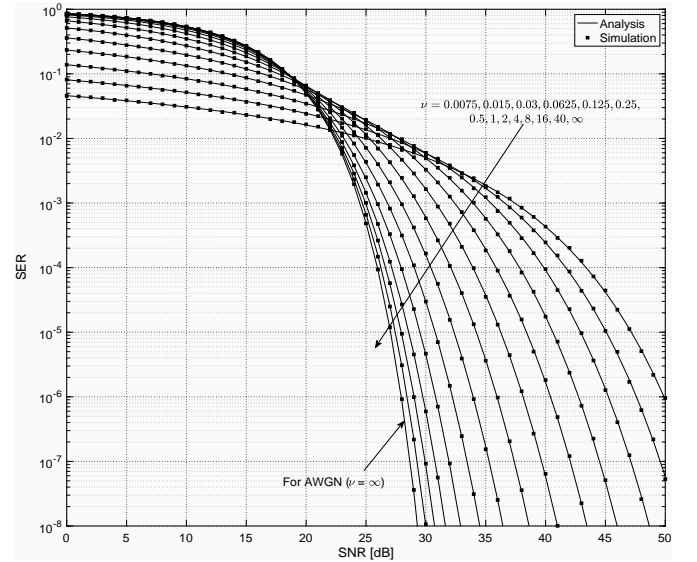

 (a) Modulation level $M = 2$.

 (b) Modulation level $M = 4$.

 (c) Modulation level $M = 8$.

 (d) Modulation level $M = 16$.

Fig. 17: The SER of non-coherent M-DPSK modulation over AWMN channels.

from $-(\pi - \pi/M)$ to zero and the integration from zero to $(\pi - \pi/M)$, we have

$$\Pr\{e | H, s_m, G\} = 1 - \frac{1}{2\pi} \int_{-(\pi-\phi)}^{\pi-\phi} e^{-\frac{2}{\sigma} h(\pi/M, \theta)} d\theta, \quad (492)$$

Noticing $\Pr\{e | H, s_m, G\} = \Pr\{e | H, s_n, G\}$ for all $m \neq n$, we can obtain the probability $\Pr\{e | H, G\}$ as follows

$$\Pr\{e | H, G\} = \sum_{m=1}^M \Pr\{e | H, s_m, G\} \Pr\{s_m\}, \quad (493a)$$

$$= \Pr\{e | H, s_m, G\}. \quad (493b)$$

Hence, the SER $\Pr\{e | H\}$ of non-coherent M-DPSK signaling over complex AWMN channels can be written as $\Pr\{e | H\} = \int_0^\infty \Pr\{e | H, g\} f_G(g) dg$, where substituting both

(85) and (493) results in $\Pr\{e | H\} = \frac{1}{\pi} \int_0^{\pi-\pi/M} I_M(\gamma, \theta) d\theta$, where $I_M(\gamma, \theta)$ is obtained using [148, Eq. (3.478/4)], that is

$$I_M(\gamma, \theta) = \frac{2}{\Gamma(\nu)\lambda_0^\nu} (2\gamma h_M(\pi/M, \theta))^{\nu/2} \times K_\nu\left(\frac{2}{\lambda_0} \sqrt{2\gamma h(\pi/M, \theta)}\right). \quad (494)$$

Finally, using (494) in $\Pr\{e | H\}$ given above yields (487), which completes the proof of Theorem 80. ■

Theorem 81. *The conditional SER of the binary differential phase shift keying (BDPSK) signaling with non-coherent ML detection is given by*

$$\Pr\{e | H\} = \frac{1}{\Gamma(\nu)\lambda_0^\nu} (2\gamma)^{\frac{\nu}{2}} K_\nu\left(\frac{2}{\lambda_0} \sqrt{2\gamma}\right). \quad (495)$$

Proof. The proof is obvious using Theorem 80. ■

For numerical accuracy and analytical validity with respect to SNR, normality and modulation levels, we show in Fig. 17 the conditional SER of non-coherent M-DPSK signaling over complex AWMN channels, where numerical and simulation-based results are in perfect agreement. Further, we also therein acknowledge that the SER performance deteriorates in high-SNR regime while negligibly improves in low-SNR regime when the impulsive nature of the additive noise increases (i.e., the normality ν decreases).

VI. SUMMARY AND CONCLUSIONS

In this article, we introduce McLeish distribution as our first contribution to have a mathematically tractable non-Gaussian noise distribution to model the impulsive effects in signal transmission over communications channels and thereon study the basic statistical principles behind the laws of McLeish distribution ranging from non-Gaussian distribution to Gaussian distribution. As such, we demonstrate the statistical characterization of the McLeish distribution and the sum of the McLeish distributions by deriving their PDF, CDF, C^2DF , MGF and moments for arbitrary parameters. Since complex-valued random noise distributions find wide applications in many areas of reliable transmission, we accomplish the complex extensions, i.e., propose both CCS and CES McLeish distributions, whose real and imaginary parts are jointly McLeish distribution. Further, in this article, for CCS/CES McLeish distributions, we define McLeish’s bivariate Q-function and thereby derive the exact closed-form expressions the PDF, CDF, MGF, and moments. Note that, in the case of multi-dimensional signaling, the multivariate extension of the McLeish distributions becomes attractive for modeling the additive impulsive noise in multi-dimensional communication channels. Accordingly, we also propose both CS and ES multivariate McLeish distributions as the extensions of the standard McLeish distribution to vectors. Their joint PDF, joint CDF, joint C^2DF , joint MGF, and joint moments are thus among our contributions. With the help of these contributions, We treat marginal and conditional distributions of CS/ES multivariate McLeish distributed random vectors. Another contribution we make to multivariate McLeish distributions in this article is just the generalization of CS/ES multivariate McLeish distribution to the CCS/CES multivariate McLeish distribution, where we propose novel closed-form expressions for their joint PDF, CDF, C^2DF , and MGF and benefit from them in the theory of reliable transmission over vector communication channels.

Based on the framework mentioned above, we introduce the complex AWMN channels and show the existence of McLeish noise in modern communication technologies. Accordingly, we consider a signal transmission over complex vector channels, and therein considering the impulsive fluctuations in the total variance of additive noise, we introduce the complex AWMN vector channels, where the impulsive effects are accurately modeled as a CCS/CES multivariate McLeish distributions. This motivates us to consider the optimum receivers (i.e., MAP and ML rules) for coherent signaling over CCS/CES AWMN channels, and specifically propose closed-form expressions for the conditional BER/SER of coherent

signaling. In what follows, closed-form BER/SER expressions for the modulation schemes such as binary keying modulation, M-ASK, M-QAM, and M-PSK are a few of our contributions. Subsequently, we investigate the non-coherent signaling over complex AWMN channels and specifically obtain optimum receivers. Accordingly, we derive the conditional BER/SER for non-coherent orthogonal signaling and DPSK. Thereby, some selected numerical results have shown that these closed-form expressions are in perfect agreement with the simulation-based results.

ACKNOWLEDGMENT

The author would like to thank Dr. Mohamed-Slim Alouini of King Abdullah University of Science and Technology (KAUST) for his, and thanks to Dr. Davut Kavranoglu and Dr. Ibrahim Altunbas of Istanbul Technical University (ITU) for their, and thanks to Dr. Erdal Arıkan and Dr. Sinan Gezici of Bilkent University for their, and thanks to Dr. Oğuz. Kucur of Gebze Technical University (GTU) for his, and thanks to Dr. Murat Uysal of Özyeğin University for his, The author would also like to thank the anonymous reviewers for their instructive and informative comments that strengthened this article.

REFERENCES

- [1] M. K. Simon and M.-S. Alouini, *Digital Communication over Fading Channels*, 2nd ed. John Wiley & Sons, Inc., 2005.
- [2] A. Goldsmith, *Wireless Communications*. Cambridge Univ. Press, 2005.
- [3] J. G. Proakis and M. Salehi, *Digital Communications*, 5th ed. McGraw-Hill, 2008.
- [4] T. S. Rappaport, *Wireless Communications: Principles and Practice*, 2nd ed. Prentice Hall, 2002.
- [5] W. Feller, *An Introduction to Probability Theory and Its Applications*. New York, USA: John Wiley & Sons, 1968.
- [6] P. Billingsley, *Probability and Measure*. John Wiley & Sons, 1979.
- [7] K. J. Kerpez and A. M. Gottlieb, “The error performance of digital subscriber lines in the presence of impulse noise,” *IEEE Transactions on Communications*, vol. 43, no. 5, pp. 1902–1905, 1995.
- [8] N. H. Nedev, *Analysis of the impact of impulse noise in digital subscriber line systems*. University of Edinburgh. College of Science and Engineering. School of, 2003.
- [9] D. Toumpakaris, J. M. Cioffi, and D. Gardan, “Reduced-delay protection of dsl systems against nonstationary disturbances,” *IEEE Transactions on Communications*, vol. 52, no. 11, pp. 1927–1938, 2004.
- [10] T. Y. Al-Naffouri, A. A. Quadeer, and G. Caire, “Impulsive noise estimation and cancellation in dsl using orthogonal clustering,” in *2011 IEEE International Symposium on Information Theory Proceedings*. IEEE, 2011, pp. 2841–2845.
- [11] H. C. Ferreira, L. Lampe, J. Newbury, and T. G. Swart, *Power line communications: Theory and applications for narrow band and broadband communications over power lines*. John Wiley & Sons, 2011.
- [12] B. Han, *Characterization and Emulation of Low-Voltage Power Line Channels for Narrowband and Broadband Communication*. KIT Scientific Publishing, 2017, vol. 14.

- [13] M. Gotz, M. Rapp, and K. Dostert, "Power line channel characteristics and their effect on communication system design," *IEEE Communications Magazine*, vol. 42, no. 4, pp. 78–86, 2004.
- [14] M. Katayama, T. Yamazato, and H. Okada, "A mathematical model of noise in narrowband power line communication systems," *IEEE Journal on Selected Areas in Communications*, vol. 24, no. 7, pp. 1267–1276, 2006.
- [15] B. Han, V. Stoica, C. Kaiser, N. Otterbach, and K. Dostert, "Noise characterization and emulation for low-voltage power line channels across narrowband and broadband," *Digital Signal Processing*, vol. 69, pp. 259–274, 2017.
- [16] H. Meng, Y. L. Guan, and S. Chen, "Modeling and analysis of noise effects on broadband power-line communications," *IEEE Transactions on Power Delivery*, vol. 20, no. 2, pp. 630–637, 2005.
- [17] M. Zimmermann and K. Dostert, "Analysis and modeling of impulsive noise in broad-band powerline communications," *IEEE Transactions on Electromagnetic Compatibility*, vol. 44, no. 1, pp. 249–258, 2002.
- [18] J. Lin, M. Nassar, and B. L. Evans, "Impulsive noise mitigation in powerline communications using sparse bayesian learning," *IEEE Journal on Selected Areas in Communications*, vol. 31, no. 7, pp. 1172–1183, 2013.
- [19] G. M. Wenz, "Acoustic ambient noise in the ocean: Spectra and sources," *The Journal of the Acoustical Society of America*, vol. 34, no. 12, pp. 1936–1956, 1962.
- [20] P. L. Brockett, M. Hinich, and G. R. Wilson, "Nonlinear and non-gaussian ocean noise," *The Journal of the Acoustical Society of America*, vol. 82, no. 4, pp. 1386–1394, 1987.
- [21] D. Middleton, "Channel modeling and threshold signal processing in underwater acoustics: An analytical overview," *IEEE Journal of Oceanic Engineering*, vol. 12, no. 1, pp. 4–28, 1987.
- [22] D. R. Powell and G. R. Wilson, "Class a modeling of ocean acoustic noise processes," in *Topics in non-Gaussian signal processing*. Springer, 1989, pp. 17–28.
- [23] D. W. Stein, "Statistical characteristics of moving acoustic sources in ocean waveguides," *The Journal of the Acoustical Society of America*, vol. 98, no. 3, pp. 1486–1495, 1995.
- [24] F. W. Machell, C. S. Penrod, and G. E. Ellis, "Statistical characteristics of ocean acoustic noise processes," in *Topics in Non-Gaussian Signal Processing*. Springer, 1989, pp. 29–57.
- [25] P. C. Etter, *Underwater acoustic modeling and simulation*. CRC press, 2018.
- [26] D. A. Abraham, "Underwater acoustic signal and noise modeling," in *Underwater Acoustic Signal Processing*. Springer, 2019, pp. 349–456.
- [27] D. Middleton, "Statistical-physical models of urban radio-noise environments-part i: Foundations," *IEEE Transactions on Electromagnetic Compatibility*, no. 2, pp. 38–56, 1972.
- [28] —, "Man-made noise in urban environments and transportation systems: Models and measurements," *IEEE Transactions on Communications*, vol. 21, no. 11, pp. 1232–1241, 1973.
- [29] —, "Statistical-physical models of electromagnetic interference," *IEEE Transactions on Electromagnetic Compatibility*, no. 3, pp. 106–127, 1977.
- [30] D. Middleton and A. Spaulding, *A tutorial review of elements of weak signal detection in non-Gaussian EMI environments*. US Department of Commerce, National Telecommunications and Information, 1986.
- [31] K. L. Blackard, T. S. Rappaport, and C. W. Bostian, "Measurements and models of radio frequency impulsive noise for indoor wireless communications," *IEEE Journal on Selected Areas in Communications*, vol. 11, no. 7, pp. 991–1001, 1993.
- [32] T. K. Blankenship, D. Kriztman, and T. S. Rappaport, "Measurements and simulation of radio frequency impulsive noise in hospitals and clinics," in *1997 IEEE 47th Vehicular Technology Conference. Technology in Motion*, vol. 3. IEEE, 1997, pp. 1942–1946.
- [33] T. K. Blankenship and T. S. Rappaport, "Characteristics of impulsive noise in the 450-mhz band in hospitals and clinics," *IEEE Transactions on Antennas and Propagation*, vol. 46, no. 2, pp. 194–203, 1998.
- [34] M. Flury and J.-y. Boudec, "Interference mitigation by statistical interference modeling in an impulse radio uwb receiver," in *2006 IEEE International Conference on Ultra-Wideband*. IEEE, 2006, pp. 393–398.
- [35] Y. Dhibi and T. Kaiser, "Impulsive noise in UWB systems and its suppression," *Mobile Networks and Applications*, vol. 11, no. 4, pp. 441–449, 2006.
- [36] O. Z. Batur, M. Koca, and G. Dundar, "Measurements of impulsive noise in broad-band wireless communication channels," in *2008 Ph. D. Research in Microelectronics and Electronics*. IEEE, 2008, pp. 233–236.
- [37] J.-W. Moon, T. F. Wong, and J. M. Shea, "Pilot-assisted and blind joint data detection and channel estimation in partial-time jamming," *IEEE Transactions on Communications*, vol. 54, no. 11, pp. 2092–2102, 2006.
- [38] B. Hu and N. C. Beaulieu, "On characterizing multiple access interference in th-uwb systems with impulsive noise models," in *2008 IEEE Radio and Wireless Symposium*. IEEE, 2008, pp. 879–882.
- [39] M. Cheffena, "Industrial wireless communications over the millimeter wave spectrum: opportunities and challenges," *IEEE Communications Magazine*, vol. 54, no. 9, pp. 66–72, 2016.
- [40] L. M. H. Shhab, A. Rizaner, A. H. Ulusoy, and H. Amca, "Impact of impulsive noise on millimeter wave cellular systems performance," in *2017 10th UK-Europe-China Workshop on Millimetre Waves and Terahertz Technologies (UCMMT)*. IEEE, 2017, pp. 1–4.
- [41] N. Iqbal, J. Luo, R. Müller, G. Steinböck, C. Schneider, D. Dupleich, S. Häfner, and R. S. Thomä, "Multipath cluster fading statistics and modeling in millimeter wave radio channels," *IEEE Transactions on Antennas and Propagation*, 2019.
- [42] D. Matolak, A. Kody, S. Kaya, D. DiTomaso, S. Laha, and W. Rayess, "Wireless networks-on-chips: Architecture, wireless channel, and devices," *IEEE Wireless Communications*, vol. 19, no. 5, 2012.
- [43] J. A. Nossek, P. Russer, T. Noll, A. Mezghani, M. T. Ivrlac, M. Korb, F. Mukhtar, H. Yordanov, and J. A. Russer, "Chip-to-chip and on-chip communications," in *Ultra-Wideband Radio Technologies for Communications, Localization and Sensor Applications*. InTech, 2013.
- [44] I. Swarbrick and J. J. Cao, "Chip-to-chip communications," Feb. 16 2016, US Patent 9,264,368.
- [45] R. J. Drost, R. D. Hopkins, R. Ho, and I. E. Sutherland, "Proximity communication," *IEEE Journal of Solid-State Circuits*, vol. 39, no. 9, pp. 1529–1535, 2004.
- [46] T. J. Suzuki and H. Hayakawa, "Non-Gaussianity in a quasiclassical electronic circuit," *Physical Review B*, vol. 95, no. 20, p. 205412, 2017.
- [47] M. W. Thompson and H.-S. Chang, "Coherent detection in Laplace noise," *IEEE Transactions on Aerospace and Electronic Systems*, vol. 30, no. 2, pp. 452–461, 1994.
- [48] C. Gowda, V. Annampedu, and R. Viswanathan, "Diversity combining in antenna array base station receiver for ds/cdma system," in *IEEE International Conference on Communications (ICC 98)*, vol. 3, 1998, pp. 1360–1364.
- [49] Y. Dhibi and T. Kaiser, "On the impulsiveness of multiuser interferences in TH-PPM-UWB systems," *IEEE Transactions on Signal Processing*, vol. 54, no. 7, pp. 2853–2857, 2006.
- [50] J. Fiorina, "A simple IR-UWB receiver adapted to multi-user interferences," in *proceedings of IEEE Global Telecommunications Conference (GLOBECOM'06)*, 2006, pp. 1–4.
- [51] B. Hu and N. C. Beaulieu, "On characterizing multiple access interference in TH-UWB systems with impulsive noise models," in *IEEE Radio and Wireless Symposium (RWS 2008)*, 2008, pp. 879–882.
- [52] N. C. Beaulieu and S. Niranjan, "Uwb receiver designs based on a gaussian-laplacian noise-plus-mai model," *IEEE Transactions on Communications*, vol. 58, no. 3, 2010.
- [53] E. S. Sousa, "Performance of a spread spectrum packet radio network link in a poisson field of interferers," *IEEE Transactions on Information Theory*, vol. 38, no. 6, pp. 1743–1754, 1992.
- [54] J. G. Gonzalez, *Robust techniques for wireless communications in non-Gaussian environments*. University of Delaware, 1997.
- [55] J. Ilow and D. Hatzinakos, "Analytic alpha-stable noise modeling in a poisson field of interferers or scatterers," *IEEE Transactions on Signal Processing*, vol. 46, no. 6, pp. 1601–1611, 1998.
- [56] X. Wang and H. V. Poor, "Robust multiuser detection in non-gaussian channels," *IEEE Transactions on Signal Processing*, vol. 47, no. 2, pp. 289–305, 1999.
- [57] D. Middleton, "Non-gaussian noise models in signal processing for telecommunications: new methods an results for class a and class b noise models," *IEEE Transactions on Information Theory*, vol. 45, no. 4, pp. 1129–1149, 1999.
- [58] J. Mitola, "Cognitive radio—an integrated agent architecture for software defined radio," Ph.D. dissertation, Royal Institute of Technology (KTH), 2000.
- [59] S. Haykin *et al.*, "Cognitive radio: Brain-empowered wireless communications," *IEEE Journal on Selected Areas in Communications*, vol. 23, no. 2, pp. 201–220, 2005.
- [60] W. Hu, D. Willkomm, M. Abusubaih, J. Gross, G. Vlantis, M. Gerla, and A. Wolisz, "Dynamic frequency hopping communities for efficient ieee 802.22 operation," *IEEE Communications Magazine*, vol. 45, no. 5, pp. 80–87, 2007.

- [61] A. J. Goldsmith, S. A. Jafar, I. Maric, and S. Srinivasa, "Breaking spectrum gridlock with cognitive radios: An information theoretic perspective." *Proceedings of the IEEE*, vol. 97, no. 5, pp. 894–914, 2009.
- [62] E. Hossain, D. Niyato, and Z. Han, *Dynamic spectrum access and management in cognitive radio networks*. Cambridge university press, 2009.
- [63] B. Wang and K. R. Liu, "Advances in cognitive radio networks: A survey," *IEEE Journal of Selected Topics in Signal Processing*, vol. 5, no. 1, pp. 5–23, 2011.
- [64] I. F. Akyildiz, W.-Y. Lee, M. C. Vuran, and S. Mohanty, "Next generation/dynamic spectrum access/cognitive radio wireless networks: A survey," *Computer networks*, vol. 50, no. 13, pp. 2127–2159, 2006.
- [65] D. Willkomm, J. Gross, and A. Wolisz, "Reliable link maintenance in cognitive radio systems," in *First IEEE International Symposium on New Frontiers in Dynamic Spectrum Access Networks, 2005. DySPAN 2005*. IEEE, 2005, pp. 371–378.
- [66] Y.-C. Liang, Y. Zeng, E. Peh, and A. T. Hoang, "Sensing-throughput tradeoff for cognitive radio networks," in *2007 IEEE International Conference on Communications*. IEEE, 2007, pp. 5330–5335.
- [67] S. Geirhofer, L. Tong, and B. M. Sadler, "Dynamic spectrum access in the time domain: Modeling and exploiting white space," *IEEE Communications Magazine*, vol. 45, no. 5, pp. 66–72, 2007.
- [68] S. A. Jafar and S. Srinivasa, "Capacity limits of cognitive radio with distributed and dynamic spectral activity," *IEEE Journal on Selected Areas in Communications*, vol. 25, no. 3, pp. 529–537, 2007.
- [69] E. Jakeman, "On the statistics of K-distributed noise," *Journal of Physics A: Mathematical and General*, vol. 13, no. 1, p. 31, 1980.
- [70] R. C. Dorf, *Broadcasting and optical communication technology*, 3rd ed. CRC Press, 2006.
- [71] A. Kamboj, R. K. Mallik, M. Agrawal, and R. Schober, "Diversity combining in FSO systems in presence of non-Gaussian noise," in *proceedings of IEEE International Conference on Signal Processing and Communications (SPCOM 2012)*, 2012, pp. 1–5.
- [72] E. Vanin, G. Jacobsen, and A. Berntson, "Nonlinear phase noise separation method for on-off keying transmission system modeling with non-gaussian noise generation in optical fibers," *Optics letters*, vol. 32, no. 12, pp. 1740–1742, 2007.
- [73] J. Witzens, J. Müller, and A. Moscoso-Mártir, "Modification of level dependent ase-signal beat noise by optical and electrical filtering in optically preamplified direct detection receivers," *IEEE Photonics Journal*, vol. 10, no. 1, pp. 1–16, 2018.
- [74] B. Chan and J. Conradi, "On the non-gaussian noise in erbium-doped fiber amplifiers," *Journal of lightwave technology*, vol. 15, no. 4, pp. 680–687, 1997.
- [75] D. Marcuse, "Derivation of analytical expressions for the bit-error probability in lightwave systems with optical amplifiers," *Journal of Lightwave Technology*, vol. 8, no. 12, pp. 1816–1823, 1990.
- [76] P. A. Humblet and M. Azizoglu, "On the bit error rate of lightwave systems with optical amplifiers," *Journal of lightwave technology*, vol. 9, no. 11, pp. 1576–1582, 1991.
- [77] D. Marcuse, "Calculation of bit-error probability for a lightwave system with optical amplifiers and post-detection gaussian noise," *Journal of Lightwave Technology*, vol. 9, no. 4, pp. 505–513, 1991.
- [78] J.-S. Lee and C.-S. Shim, "Bit-error-rate analysis of optically preamplified receivers using an eigenfunction expansion method in optical frequency domain," *Journal of lightwave technology*, vol. 12, no. 7, pp. 1224–1229, 1994.
- [79] S. Bi, C. K. Ho, and R. Zhang, "Wireless powered communication: Opportunities and challenges," *IEEE Communications Magazine*, vol. 53, no. 4, pp. 117–125, 2015.
- [80] X. Lu, P. Wang, D. Niyato, D. I. Kim, and Z. Han, "Wireless networks with rf energy harvesting: A contemporary survey," *IEEE Communications Surveys and Tutorials*, vol. 17, no. 2, pp. 757–789, 2015.
- [81] I. Krikidis, S. Timotheou, S. Nikolaou, G. Zheng, D. W. K. Ng, and R. Schober, "Simultaneous wireless information and power transfer in modern communication systems," *IEEE Communications Magazine*, vol. 52, no. 11, pp. 104–110, 2014.
- [82] L. Mohjazi, S. Muhaidat, M. Dianati, M. Al-Qutayri, and N. Al-Dhahir, "Performance analysis of swipt relaying systems in the presence of impulsive noise," *IEEE Access*, vol. 6, pp. 71 662–71 677, 2018.
- [83] L. Mohjazi, "Analysis and optimisation of swipt networks." Ph.D. dissertation, University of Surrey, 2018.
- [84] I. Shomorony and A. S. Avestimehr, "Is gaussian noise the worst-case additive noise in wireless networks?" in *2012 IEEE International Symposium on Information Theory Proceedings*. IEEE, 2012, pp. 214–218.
- [85] —, "Worst-case additive noise in wireless networks," *IEEE Transactions on Information Theory*, vol. 59, no. 6, pp. 3833–3847, 2013.
- [86] A. Lapidoth, "Nearest neighbor decoding for additive non-gaussian noise channels," *IEEE Transactions on Information Theory*, vol. 42, no. 5, pp. 1520–1529, 1996.
- [87] S. M. Kay, *Statistical Signal Processing, Volume II, Detection Theory*. Prentice Hall New Jersey, 1998.
- [88] M. Ghosh, "Analysis of the effect of impulse noise on multicarrier and single carrier qam systems," *IEEE Transactions on Communications*, vol. 44, no. 2, pp. 145–147, 1996.
- [89] T. Shongwe, H. C. Ferreira, and A. Han Vinck, "Broadband and narrow-band noise modeling in powerline communications," *Wiley Encyclopedia of Electrical and Electronics Engineering*, pp. 1–18, 1999.
- [90] Y. Ma, P. So, and E. Gunawan, "Performance analysis of ofdm systems for broadband power line communications under impulsive noise and multipath effects," *IEEE Transactions on Power Delivery*, vol. 20, no. 2, pp. 674–682, 2005.
- [91] R. Pighi, M. Franceschini, G. Ferrari, and R. Raheli, "Fundamental performance limits of communications systems impaired by impulse noise," *IEEE Transactions on Communications*, vol. 57, no. 1, pp. 171–182, 2009.
- [92] S. P. Herath, N. H. Tran, and T. Le-Ngoc, "On optimal input distribution and capacity limit of bernoulli-gaussian impulsive noise channels," in *2012 IEEE International Conference on Communications (ICC)*. IEEE, 2012, pp. 3429–3433.
- [93] T. Shongwey, A. H. Vinck, and H. C. Ferreira, "On impulse noise and its models," in *18th IEEE International Symposium on Power Line Communications and its Applications*. IEEE, 2014, pp. 12–17.
- [94] C. Tepedelenlioglu and P. Gao, "On diversity reception over fading channels with impulsive noise," in *IEEE Global Telecommunications Conference, 2004. GLOBECOM'04.*, vol. 6. IEEE, 2004, pp. 3676–3680.
- [95] —, "On diversity reception over fading channels with impulsive noise," *IEEE Transactions on Vehicular Technology*, vol. 54, no. 6, pp. 2037–2047, 2005.
- [96] S. L. Bernstein et al., "Long-range communications at extremely low frequencies," *Proceedings of the IEEE*, vol. 62, no. 3, pp. 292–312, 1974.
- [97] G. Durisi and G. Romano, "On the validity of Gaussian approximation to characterize the multiuser capacity of UWB TH PPM," in *proceedings of IEEE Conference on Ultra Wideband Systems and Technologies.*, 2002, pp. 157–161.
- [98] B. Hu and N. C. Beaulieu, "Accurate evaluation of multiple-access performance in TH-PPM and TH-BPSK UWB systems," *IEEE Transactions on Communications*, vol. 52, no. 10, pp. 1758–1766, 2004.
- [99] Y. Dhibi and T. Kaiser, "Impulsive noise in UWB systems and its suppression," *Mobile Networks and Applications*, vol. 11, no. 4, pp. 441–449, 2006.
- [100] —, "On the impulsiveness of multiuser interferences in TH-PPM-UWB systems," *IEEE Transactions on Signal Processing*, vol. 54, no. 7, pp. 2853–2857, 2006.
- [101] B. Hu and N. C. Beaulieu, "Soft-limiting receiver structures for time-hopping UWB in multiple-access interference," *IEEE Transactions on Vehicular Technology*, vol. 57, no. 2, pp. 810–818, 2008.
- [102] —, "On characterizing multiple access interference in TH-UWB systems with impulsive noise models," in *proceedings of IEEE Radio and Wireless Symposium (RWS'08)*, 2008, pp. 879–882.
- [103] N. C. Beaulieu and D. J. Young, "Designing time-hopping ultrawide bandwidth receivers for multiuser interference environments," *Proceedings of the IEEE*, vol. 97, no. 2, pp. 255–284, 2009.
- [104] M. Chiani and A. Giorgetti, "Coexistence between UWB and narrow-band wireless communication systems," *Proceedings of the IEEE*, vol. 97, no. 2, pp. 231–254, 2009.
- [105] S. Jiang and N. C. Beaulieu, "BER of antipodal signaling in Laplace noise," in *proceedings of IEEE Biennial Symposium on Communications (QBSC'10)*, 2010, pp. 110–113.
- [106] X. Yang and A. P. Petropulu, "Co-channel interference modeling and analysis in a poisson field of interferers in wireless communications," *IEEE Transactions on Signal Processing*, vol. 51, no. 1, pp. 64–76, 2003.
- [107] M. Haenggi et al., "Stochastic geometry and random graphs for the analysis and design of wireless networks," *IEEE Journal on Selected Areas in Communications*, vol. 27, no. 7, 2009.

- [108] C. L. Brown and A. M. Zoubir, "A nonparametric approach to signal detection in impulsive interference," *IEEE Transactions on Signal Processing*, vol. 48, no. 9, pp. 2665–2669, 2000.
- [109] G. A. Tsihrintzis, "Diversity reception in alpha-stable impulsive interference," in *proceedings of IEEE Military Communications Conference (MILCOM'96)*, vol. 3, 1996, pp. 828–832.
- [110] E. E. Kuruoglu, P. J. W. Rayner, and W. J. Fitzgerald, "A near-optimal receiver for detection in alpha-stable distributed noise," in *proc. of IEEE SP Workshop on Statistical Signal and Array Proc.*, 1998, pp. 419–422.
- [111] A. Rajan and C. Tepedelenlioglu, "Diversity combining over Rayleigh fading channels with symmetric alpha-stable noise," *IEEE Transactions on Wireless Communications*, vol. 9, no. 9, pp. 2968–2976, 2010.
- [112] R. Viswanathan and A. Ansari, "Distributed detection of a signal in generalized Gaussian noise," *IEEE Transactions on Acoustics, Speech, and Signal Processing*, vol. 37, no. 5, pp. 775–778, May 1989.
- [113] S. J. Zahabi and A. A. Tadaion, "Local spectrum sensing in non-Gaussian noise," in *proceedings of IEEE International Conference on Telecommunication (ICT'2010), Doha, Qatar*, April 2010, pp. 843–847.
- [114] E. Biglieri, K. Yao, and C. A. Yang, "Fading models from spherically invariant processes," *IEEE Transactions on Wireless Communications*, vol. 14, no. 10, pp. 5526–5538, 2015.
- [115] D. L. McLeish, "A robust alternative to the normal distribution," *Canadian Journal of Stat.*, vol. 10, pp. 89–102, 1982.
- [116] —, "A robust alternative to the normal distribution," Stanford University, CA, Department of Statistics, Tech. Rep., 1982.
- [117] T. J. Kozubowski, M. M. Meerschaert, and K. Podgorski, "Fractional laplace motion," *Advances in applied probability*, vol. 38, no. 2, pp. 451–464, 2006.
- [118] F. J. Molz, T. J. Kozubowski, K. Podgorski, and J. W. Castle, "A generalization of the fractal/facies model," *Hydrogeology journal*, vol. 15, no. 4, pp. 809–816, 2007.
- [119] F. Wu, "Applications of the normal laplace and generalized normal laplace distributions," Ph.D. dissertation, University of Victoria, 2008.
- [120] T. Kozubowski, "Geometric infinite divisibility, stability, and self-similarity: an overview," *Banach Center Publications*, vol. 1, no. 90, pp. 39–65, 2010.
- [121] K. Podgorski and J. Wegener, "Estimation for stochastic models driven by laplace motion," *Communications in Statistics-Theory and Methods*, vol. 40, no. 18, pp. 3281–3302, 2011.
- [122] S. Kotz, T. Kozubowski, and K. Podgorski, *The Laplace Distribution and Generalizations: A Revisit with Applications to Communications, Economics, Engineering, and Finance*. Springer Science & Business Media, 2012.
- [123] C. Schluter and M. Tiede, "Weak convergence to the student and laplace distributions," *Journal of Applied Probability*, vol. 53, no. 1, pp. 121–129, 2016.
- [124] N. L. Johnson, N. Balakrishnan, and S. Kotz, *Continuous Univariate Distributions*, 2nd ed. John Wiley & Sons, 2004, vol. 2.
- [125] M. Subbotin, "On the law of frequency of error," *Matematicheskii Sbornik*, vol. 31, pp. 296–301, 1923.
- [126] R. Zeckhauser and M. Thompson, "Linear regression with non-normal error terms," *Review of Economics and Statistics*, vol. 52, no. 3, pp. 280–286, 1970.
- [127] H. Jakuszenkow, "Estimation of the variance in the generalized laplace distribution with quadratic loss function," *Demonstratio Mathematica*, vol. 3, pp. 581–591, 1979.
- [128] D. Sharma, "On estimating the variance of a generalized laplace distribution," *Metrika*, vol. 31, no. 1, pp. 85–88, 1984.
- [129] J. M. Taylor, "Properties of modelling the error distribution with an extra shape parameter," *Computational statistics & data analysis*, vol. 13, no. 1, pp. 33–46, 1992.
- [130] G. Agro, "Maximum likelihood estimation for the exponential power function parameters," *Communications in Statistics-Simulation and Computation*, vol. 24, no. 2, pp. 523–536, 1995.
- [131] A. Nakamura and T. Matsui, "Acoustic modeling based on a generalized laplacian distribution," in *Sixth European Conference on Speech Communication and Technology*, 1999.
- [132] A. Nakamura, "Acoustic modeling for speech recognition based on a generalized laplacian mixture distribution," *Electronics and Communications in Japan (Part II: Electronics)*, vol. 85, no. 11, pp. 32–42, 2002.
- [133] A. Ayebo and T. J. Kozubowski, "An asymmetric generalization of gaussian and laplace laws," *Journal of Probability and Statistical Science*, vol. 1, no. 2, pp. 187–210, 2003.
- [134] A. Aissa-El-Bey and K. Abed-Meraim, "Blind identification of sparse simo channels using maximum a posteriori approach," in *2008 16th European Signal Processing Conference*. IEEE, 2008, pp. 1–5.
- [135] F. Dubeau and S. El Mashoubi, "The fourier transform of the multidimensional generalized gaussian distribution," *International Journal of Pure and Applied Mathematics*, vol. 67, no. 4, pp. 443–454, 2011.
- [136] K. S. Selim, "Computation of sample mean range of the generalized laplace distribution," *Pakistan Journal of Statistics and Operation Research*, vol. 11, no. 3, pp. 283–298, 2015.
- [137] N. Lassami, A. Aissa-El-Bey, and K. Abed-Meraim, "Adaptive blind identification of sparse simo channels using maximum a posteriori approach," in *Asilomar Conference on Signals, Systems, and Computers*, 2018.
- [138] F. Yilmaz and M.-S. Alouini, "On the bit-error rate of binary phase shift keying over additive white generalized laplacian noise (AWGLN) channels," in *IEEE Signal Processing and Communications Applications Conference (SIU 2018)*, 2018, pp. 1–4.
- [139] O. Marichev and M. Trott, "The ultimate univariate probability distribution explorer," *Wolfram Research Blog*, Feb. 1, 2013. [Online]. Available: <http://blog.wolfram.com/2013/02/01/the-ultimate-univariate-probability-distribution-explorer/>
- [140] J. J. Filliben, A. Heckert, and R. R. Lipman, "McLeish distribution : Dataplot," *National Institute of Standards and Tech. (NIST)*, Apr. 19, 2005. [Online]. Available: <http://www.itl.nist.gov/div898/software/dataplot>
- [141] A. Papoulis, *Probability, Random Variables, and Stochastic Processes*. McGraw Hill, 1991.
- [142] R.-J. Essiambre, G. Kramer, P. J. Winzer, G. J. Foschini, and B. Goebel, "Capacity limits of optical fiber networks," *Journal of Lightwave Technology*, vol. 28, no. 4, pp. 662–701, 2010.
- [143] F. Vacondio, O. Rival, C. Simonneau, E. Grellier, A. Bononi, L. Lorcy, J.-C. Antona, and S. Bigo, "On nonlinear distortions of highly dispersive optical coherent systems," *Optics Express*, vol. 20, no. 2, pp. 1022–1032, 2012.
- [144] C. Häger, "On signal constellations and coding for long-haul fiber-optical systems," Ph.D. dissertation, Department of Signals and Systems, Chalmers University of Technology, 2014.
- [145] D. Zwillinger, *CRC Standard Mathematical Tables and Formulae*, 31st ed. Chapman & Hall/CRC, 2003.
- [146] H. H. Andersen, M. Hojbjerg, D. Sorensen, and P. S. Eriksen, *Linear and graphical models: For the multivariate complex normal distribution*. Springer Science & Business Media, 1995, vol. 101.
- [147] M. Abramowitz and I. A. Stegun, *Handbook of Mathematical Functions with Formulas, Graphs, and Mathematical Tables*, 9th ed. New York, USA: Dover Publications, 1972.
- [148] I. S. Gradshteyn and I. M. Ryzhik, *Table of Integrals, Series, and Products*, 5th ed. San Diego, CA: Academic Press, 1994.
- [149] Wolfram Research, *Mathematica Edition: Version 8.0*. Champaign, Illinois: Wolfram Research, Inc., 2010.
- [150] A. P. Prudnikov, Y. A. Brychkov, and O. I. Marichev, *Integral and Series: Volume 3, More Special Functions*. CRC Press Inc., 1990.
- [151] A. A. Kilbas and M. Saigo, *H-Transforms: Theory and Applications*. CRC Press LLC, 2004.
- [152] F. Yilmaz and M.-S. Alouini, "A novel unified expression for the capacity and bit error probability of wireless communication systems over generalized fading channels," *IEEE Transactions on Communications*, vol. 60, no. 7, pp. 1862–1876, 2012.
- [153] J. W. Craig, "A new, simple and exact result for calculating the probability of error for two-dimensional signal constellations," in *IEEE Military Communications Conference (MILCOM '91)*, vol. 2, Nov. 1991, pp. 571–575.
- [154] M. K. Simon and M.-S. Alouini, "A unified approach to the performance analysis of digital communication over generalized fading channels," *Proceedings of the IEEE*, vol. 86, no. 9, pp. 1860–1877, Sep. 1998.
- [155] M.-S. Alouini and M. K. Simon, "Generic form for average error probability of binary signals over fading channels," *Electronics Letters*, vol. 34, no. 10, pp. 949–950, May 1998.
- [156] M.-S. Alouini and A. J. Goldsmith, "A unified approach for calculating error rates of linearly modulated signals over generalized fading channels," *IEEE Transactions on Communications*, vol. 47, no. 9, pp. 1324–1334, Sep. 1999.
- [157] C. Forbes, M. Evans, N. Hastings, and B. Peacock, *Statistical distributions*, 4th ed. John Wiley & Sons, 2011.
- [158] D. Zwillinger and S. Kokoska, *CRC Standard Probability and Statistics Tables and Formulae*, 31st ed. Boca Raton, FL: Chapman & Hall/CRC, 2000.
- [159] K. Krishnamoorthy, *Handbook of statistical distributions with applications*, 2nd ed. Chapman and Hall/CRC, 2016.

- [160] D. Cafagna, "Fractional calculus: A mathematical tool from the past for present engineers," *IEEE Industrial Electronics Magazine*, vol. 1, no. 2, pp. 35–40, 2007.
- [161] J. Sabatier, O. P. Agrawal, and J. Machado, *Advances in Fractional Calculus: Theoretical Developments and Applications in Physics and Engineering*. Springer, 2007, vol. 4, no. 9.
- [162] M. M. Meerschaert and A. Sikorskii, *Stochastic Models for Fractional calculus*. Walter de Gruyter, 2012, vol. 43.
- [163] C. Walck, "Hand-book on statistical distributions for experimentalists," Particle Physics Group, Fysikum, University of Stockholm, Sweden, Tech. Rep., 1996.
- [164] A. K. Rathie, "A new generalization of generalized hypergeometric functions," *Le Matematiche*, vol. 52, no. 2, pp. 297–310, 1997.
- [165] M. Dishon and G. H. Weiss, "Numerical inversion of mellin and two-sided laplace transforms," *Journal of Computational Physics*, vol. 28, no. 1, pp. 129–132, 1978.
- [166] L. Debnath and D. Bhatta, *Integral transforms and their applications*, 3rd ed. Chapman and Hall/CRC, 2006.
- [167] R. G. Gallager, "Circularly-symmetric gaussian random vectors," preprint, pp. 1–9, 2008.
- [168] N. L. Johnson, N. Balakrishnan, and S. Kotz, *Continuous Univariate Distributions*, 2nd ed. John Wiley & Sons, 2004, vol. 1.
- [169] B. D. Carter and M. D. Springer, "The distribution of products, quotients and powers of independent h-function variates," *SIAM Journal on Applied Mathematics*, vol. 33, no. 4, pp. 542–558, Dec. 1977.
- [170] H. Soury, H. ElSawy, and M.-S. Alouini, "Downlink error rates of half-duplex users in full-duplex networks over a Laplacian inter-user interference limited and EGK fading," *IEEE Transactions on Wireless Communications*, vol. 16, no. 4, pp. 2693–2707, 2017.
- [171] M. K. Simon and D. Divsalar, "Some new twists to problems involving the Gaussian probability integral," *IEEE Transactions on Communications*, vol. 46, no. 2, pp. 200–210, 1998.
- [172] H. H. Andersen, M. Hojbjerg, D. Sorensen, and P. S. Eriksen, *Linear and Graphical Models: for the Multivariate Complex Normal Distribution (Lecture Notes in Statistics)*. Springer, 1995.
- [173] Y. L. Tong, *The Multivariate Normal Distribution (Springer Series in Statistics)*. Springer, 1989.
- [174] K.-T. Fang, S. Kotz, and K. W. Ng, *Symmetric Multivariate and Related Distributions (Chapman & Hall/CRC Monographs on Statistics & Applied Probability)*. Chapman and Hall/CRC, 1989.
- [175] M. Bilodeau and D. Brenner, *Theory of Multivariate Statistics (Springer Texts in Statistics)*. Springer, 1999.
- [176] S. Kotz, N. Balakrishnan, and N. L. Johnson, *Continuous Multivariate Distributions, Volume 1: Models and Applications*, ser. Continuous Multivariate Distributions. Wiley, 2004.
- [177] J. H. Curtiss, "A note on the theory of moment generating functions," *The Annals of Mathematical Statistics*, vol. 13, no. 4, pp. 430–433, 1942.
- [178] D. J. H. Garling, *Inequalities: A journey into linear analysis*. Cambridge University Press, 2007.
- [179] N. J. Higham, *Accuracy and stability of numerical algorithms*. Society for Industrial and Applied Mathematics (SIAM), 2002, vol. 80.
- [180] G. Hammerlin and K.-H. Hoffmann, *Numerical Mathematics*. Springer Science & Business Media, 2012.
- [181] D. W. Allan, "Statistics of atomic frequency standards," *Proceedings of the IEEE*, vol. 54, no. 2, pp. 221–230, 1966.
- [182] F. P. Miller, A. F. Vandome, and M. John, *Allan Variance*. VDM Publishing, 2010.
- [183] L. Galleani and P. Tavella, "The dynamic Allan variance," *IEEE Transactions on Ultrasonics, Ferroelectrics, and Frequency Control*, vol. 56, no. 3, 2009.
- [184] S. Shellhammer and R. Tandra, "Performance of the power detector with noise uncertainty," *IEEE Std. 802.22-06/0134r0*, July 2006.
- [185] H. M. Hall, "A new model for impulsive phenomena: Application to atmospheric-noise communication channels," Stanford Electronics Labs, Stanford University, CA, Tech. Rep., 1966.
- [186] G. L. Hedin, R. A. Janssen, T. I. Smits, and R. F. Lambert, "Approximate prediction of multimodal crest statistics and system reliability for impulsive noise loading," Minnesota University, Minneapolis, Tech. Rep., 1968.
- [187] K. Yao, "A representation theorem and its applications to spherically-invariant random processes," *IEEE Transactions on Information Theory*, vol. 19, no. 5, pp. 600–608, 1973.
- [188] M. Scheffler, M. Dressel, M. Jourdan, and H. Adrian, "Extremely slow Drude relaxation of correlated electrons," *Nature*, vol. 438, no. 7071, p. 1135, 2005.
- [189] R. W. Henry, "Random-walk model of thermal noise for students in elementary physics," *American Journal of Physics*, vol. 41, no. 12, pp. 1361–1363, 1973.
- [190] S. Engelberg, *Random signals and noise: A mathematical introduction*. CRC Press, 2006.
- [191] P. Drude, "Zur ionentheorie der metalle," *Physikalische Zeitschrift*, vol. 1, pp. 161–165, 1900.
- [192] J. B. Johnson, "Thermal agitation of electricity in conductors," *Physical review*, vol. 32, no. 1, p. 97, 1928.
- [193] A. I. Khinchin, *Mathematical Foundations of Statistical Mechanics*. Dover Publications, June 1949.
- [194] J. B. Johnson, "Electronic noise: The first two decades," *IEEE Spectrum*, vol. 8, no. 2, pp. 42–46, 1971.
- [195] N. A. Romero, "Johnson noise," *power*, vol. 2, p. 4, 1998.
- [196] V. V. Antsiferov, *Physics of Solid State Lasers*. Cambridge International Science Publishing Ltd., Oct. 2005.
- [197] O. Thierry, *Electron Transport in Nanostructures and Mesoscopic Devices: An Introduction*. Wiley-ISTE, Sep. 2008.
- [198] D. Vasileška, S. M. Goodnick, and G. Klimeck, *Computational Electronics: Semiclassical and Quantum Device Modeling and Simulation*. CRC Press, 2016.
- [199] M. Dresselhaus, G. Dresselhaus, S. B. Cronin, and A. G. Souza Filho, *Solid State Properties*. Springer, 2018.
- [200] M. Müller and D. Schleicher, "How to add a non-integer number of terms, and how to produce unusual infinite summations," *Journal of Computational and Applied Mathematics*, vol. 178, no. 1–2, pp. 347–360, 2005.
- [201] —, "Fractional sums and Euler-like identities," *The Ramanujan Journal*, vol. 21, no. 2, pp. 123–143, 2010.
- [202] T. Abdeljawad, D. Baleanu, F. Jarad, and R. P. Agarwal, "Fractional sums and differences with binomial coefficients," *Discrete Dynamics in Nature and Society*, 2013.
- [203] H. Nyquist, "Thermal agitation of electric charge in conductors," *Physical review*, vol. 32, no. 1, p. 110, 1928.
- [204] R. F. Pawula, "A new formula for mpsk symbol error probability," *IEEE Communications Letters*, vol. 2, no. 10, pp. 271–272, 1998.



Ferkan Yilmaz (SM'2004–M'2009) received the B.Sc. degree in electronics and communications engineering from Yıldız Technical University, Turkey, in 1997. He was ranked the first among all undergraduate students who graduated from the Department of Electronics and Communication Engineering (ECE), and the second among all undergraduate students who graduated in 1997 from Yıldız Technical University. He received his M.Sc. degree in the field of electronics and communications from Istanbul Technical University, Turkey, in 2002, and

the Ph.D. degree in field of wireless communications from Gebze Institute of Technology (GYTE) in 2009. He was awarded for the best Ph.D. Thesis.

From 1998 to 2003, he worked as a researcher for National Research Institute of Electronics and Cryptology, TÜBİTAK, Turkey. Dr. Yilmaz is the recipient of *The 1999 Achievement Award* from TÜBİTAK.

From 2003 to 2008, he worked as a senior Telecommunications Engineer for Vodafone Technology, Turkey. In November 2008, he was invited by Prof. Dr. M.-S. Alouini to work as a visitor researcher at Texas A&M University (Qatar), and from August 2009 till November 2012, worked as a post-doctoral fellow at King Abdullah University of Science and Technology (KAUST). Between November 2012 and April 2015, he joined as a Senior Telecommunications expert in the Location-based Service Solutions group, Vodafone Technology, and therein developed positioning algorithms and achieved the implementation and assessment of indoor/outdoor location-aware applications. In 2015, he was with KAUST as a Remote Consultant working on optical communications.

In 2016, Dr. Yilmaz joined to the Department of Computer Engineering at Yıldız Technical University. He has been currently working as a Assistant Professor and also engaged in *Alpharabius Solutions* and *Tachyonic Solutions* startup companies. He served as a TPC member for several IEEE conferences and is a regular reviewer for various IEEE journals. His research interests focus on wireless communication theory (i.e. diversity techniques, cooperative communications, spatial modulation, fading channels), signal processing, stochastic random processes, statistical learning theory, and machine learning and data mining (big data, data analytics).